



**This electronic thesis or dissertation has been  
downloaded from Explore Bristol Research,  
<http://research-information.bristol.ac.uk>**

*Author:*

**Hampton-O'Neil, Lea**

*Title:*

**Investigating the formation of erythroblastic islands**

**General rights**

Access to the thesis is subject to the Creative Commons Attribution - NonCommercial-No Derivatives 4.0 International Public License. A copy of this may be found at <https://creativecommons.org/licenses/by-nc-nd/4.0/legalcode>. This license sets out your rights and the restrictions that apply to your access to the thesis so it is important you read this before proceeding.

**Take down policy**

Some pages of this thesis may have been removed for copyright restrictions prior to having it been deposited in Explore Bristol Research. However, if you have discovered material within the thesis that you consider to be unlawful e.g. breaches of copyright (either yours or that of a third party) or any other law, including but not limited to those relating to patent, trademark, confidentiality, data protection, obscenity, defamation, libel, then please contact [collections-metadata@bristol.ac.uk](mailto:collections-metadata@bristol.ac.uk) and include the following information in your message:

- Your contact details
- Bibliographic details for the item, including a URL
- An outline nature of the complaint

Your claim will be investigated and, where appropriate, the item in question will be removed from public view as soon as possible.

# **INVESTIGATING THE FORMATION OF ERYTHROBLASTIC ISLANDS**

**Lea Alice Hampton-O'Neil**

University of Bristol

School of Biochemistry

University Walk

Bristol

UK

January 2019

A dissertation submitted to the University of Bristol in accordance with the  
requirements of the degree of Doctor of Philosophy in the Faculty of Biomedical  
Sciences

Word count: 42 001

## Abstract

Erythropoiesis is one of the most efficient cellular processes in the human body producing approximately 2.5 million red blood cells every second. In humans, this process occurs in the bone marrow on a highly specialised niche called the erythroblastic island. This niche is comprised of a central macrophage surrounded by developing erythroblasts. The central macrophage is known to play an important role in erythropoiesis, but it is unknown how the differentiating erythroblast is initially attracted to the macrophage to form an island. The Eph receptor family is involved in contact inhibition of locomotion which controls how cells react when they initially encounter other cells, leading to adhesion or repulsion. We set out to explore the importance of the Eph receptor family in erythroblastic island formation.

The first objective of this project was to create an assay and imaging pipeline to study the initial contact between macrophages and erythroblasts. Image analysis demonstrated we can observe long-lasting interactions as the macrophages bind one or more erythroblasts. Once this was successfully completed, this methodology was used to dissect the contribution different receptors made at the surface of the two cell types to island formation. We confirmed that human VCAM1<sup>+</sup> and VCAM<sup>-</sup> bone marrow macrophages, and *in vitro* cultured macrophages are ephrin-B2 positive, whereas differentiating human erythroblasts express EphB4, EphB6 and EphA4. Furthermore, we detected a rise in integrin activation on erythroblasts at the stage at which the cells would bind, which is independent of Eph receptor presence. The application of a specific active integrin inhibitory peptide disrupted island formation illustrating the known importance of integrins. We next showed that specific inhibitory peptides or shRNA depletion of EphB4 also cause a significant reduction in the ability of macrophages to interact with erythroblasts. Bone marrow macrophages were also affected by EphB6 depletion illustrating a subtle difference between macrophage type. This study demonstrates for the first time that EphB expression on erythroblasts, independently from integrins, facilitates the initial recognition and subsequent interaction with macrophages.

To conclude, we have developed methodology and imaging analysis which enables us to dissect the different roles surface receptors might play within erythroblastic islands. We have shown that EphB receptors and active integrin  $\beta$ 1 are important for the recognition of the two cell types as binding partners, and their presence ensures that if one is lost, some contacts can still occur. This methodology can be used to decorticate the different pathways involved in the formation and function of erythroblastic islands in humans. This understanding could lead to a better yield and quality of erythropoiesis conducted *in vitro*.

# Acknowledgment

I wish I had started writing these at the beginning of my PhD because there were so many people who have been there for me over the years and I don't want to forget anyone. It takes a village to get a PhD.

The first and most important thanks goes to Ash Toye. There are not enough words to explain how grateful I am to have had you as my supervisor. Your enthusiasm and understanding have kept me going these last 3 years. When I couldn't see the big picture anymore, you were always able to help me dream again. Thank you from the bottom of my heart.

The great people of A100 deserve so many thanks. I like to think that no one has more fun than us. I particularly want to thank Tim Satchwell and Marjolein Meinders. You guys have been there for me throughout, reassuring me and making me realise when 8 cells didn't count as a result. I have grown as a scientist and as a person from knowing you guys. Tim, you have been the best and most fun person to sit next to in the office and you always made things feel less world shattering than they were. Thank you! Thank you MJ for being such a good friend throughout. You have seen me cry, you have seen me eat, you have seen me celebrate, you've been there for it all. May there always be Swoon days in the future. Nat Di Bartolo, you are the nicest person and I am so glad you were there for all the fun, I hope it will continue. Steph Pellegrin you are the most generous person I know. You were there from the beginning of my project and you were always there when I had a question, even if you were in the middle of something. Joe Hawksworth, you have listened to me moan so much without ever flinching. Thank you (and thank you for always having a great story). Pedro Moura, thank you for all the lively debates about food and every topic under the sun. Beth Hawley, thank you for making me be more sporty than I actually am! I never thought I could have run a 10k mud run before you. Katy Haydn Smith, thank you for your cheerfulness and making a 3 hour delay at an airport a lot more fun! Charlie Severn, thank you for taking the time to read the paper so many times. I truly appreciate that.

I have to thank the amazing facilities team at the University. Their help, enthusiasm and cheerfulness always brought joy when working with them. To name a few: Andrew Herman, Lorena Sueiro Ballesteros, Stephen Cross, Katie Jepsen...

I want to thank all my Bristol friends. You have all been amazing. The amazing Wellcome Trust 5: Melanie Panagi, Amy Dey, Rob Lees, Sonam Gurung. From Day 1, it's been love at first sight. We've seen it all, the good, the bad, the ugly. I am so glad the Wellcome Trust brought us together.

My housemates over the years: Amy Dey, Helen Hoogewerf-McComb, Sonam Gurung, Maria Gomez, Alex Fletcher-Jones and Rachel Humphries. Thank you for all being you. It has been 3 great years made more special by getting to come home to you guys.

Helen you get a special mention for having been there for me for the last 8 years. I wouldn't have this PhD without you. More than anyone, you know how difficult believing in myself is for me. Your encouragements throughout the years and your ability to always make me laugh are invaluable to me. I know things haven't always been easy but you definitely have made getting through 8 years of Uni better.

I also need to thank my Union friends without whom the world would definitely not be as fun or adventurous: Laura Ho, Jamie Cross, Lauren Canvin, Kitty Flint, Letty Key....

To Steph Wiedemann, Davina Chao and Grace Vance. We are the Cliquest Flickest and the last 4 years have been great with you guys. You helped me stay an undergrad throughout my postgrad. That is one of the best gifts a girl can get.

I would be remiss if I didn't include my parents who are some of the most supportive and amazing parents I know. They always want the best for me and I love them so much. Thank you for loving me too and supporting me throughout.

Finally, I want to thank my examiners for taking the time to read this thesis. I hope you found it as interesting as I found these last three years.

## Declaration

I declare that the work in this dissertation was carried out in accordance with the requirements of the University's Regulations and Code of Practice for Research Degree Programmes and that it has not been submitted for any other academic award. Except where indicated by specific reference in the text, the work is the candidate's own work. Work done in collaboration with, or with the assistance of, others, is indicated as such. Any views expressed in the dissertation are those of the author.

SIGNED: ..... DATE:.....

# Table of Contents

<b>1</b>	<b>Chapter 1 – Introduction .....</b>	<b>1</b>
1.1	Hematopoietic Stem Cells .....	1
1.2	Erythropoiesis.....	4
1.2.1	A multi-stage process.....	4
1.2.2	Bone marrow macrophages and egress .....	6
1.3	The bone marrow niche .....	8
1.3.1	Macrophage/monocyte development.....	8
1.3.2	Erythroblastic islands.....	12
1.4	Eph receptors .....	21
1.4.1	Contact inhibition of locomotion.....	21
1.4.2	The role of Ephs in the bone marrow niche .....	24
1.5	Culture systems.....	24
1.5.1	2D <i>in vitro</i> erythroid culture systems .....	24
1.5.2	Culture systems and disease.....	26
1.5.3	Macrophage cultures .....	27
1.5.4	Immortalised erythroid cell lines .....	28
1.5.5	Methodology for studying erythroblastic islands formation and integrity	
	29	
1.6	Aims.....	31
<b>2</b>	<b>Chapter 2 – Material and Methods .....</b>	<b>33</b>

2.1	Material.....	33
2.1.1	Buffers and solutions.....	33
2.1.2	Antibodies.....	35
2.1.3	Equipment .....	40
2.1.4	RT-PCR primer sequences .....	42
2.1.5	ShRNA Hairpin sequences .....	44
2.1.6	CRISPR gRNA sequences.....	44
2.1.7	EphA4 gene sequencing primers .....	45
2.1.8	Peptide sequences.....	45
2.1.9	ATP inhibitors .....	46
2.2	DNA preparation and RNA preparation.....	46
2.2.1	Transformation.....	46
2.2.2	Minipreps.....	46
2.2.3	Maxipreps.....	46
2.2.4	Reverse Transcription Polymerase Chain Reaction (RT-PCR).....	47
2.2.5	PCR of genomic DNA for sequencing .....	47
2.2.6	Agarose gel electrophoresis .....	47
2.3	Tissue culture.....	48
2.3.1	Primary Peripheral Blood and Bone Marrow Samples.....	48
2.3.2	Mammalian Cell Line Culture .....	52



2.3.3	Calcium phosphate precipitation transfection of HEK293T cells .....	53
2.3.4	Lentiviral transduction of erythroblasts and macrophages .....	53
2.4	Reconstitution of erythroblastic islands .....	54
2.4.1	Method 1 - Tlescan .....	54
2.4.2	Method 2 - Incucyte .....	54
2.4.3	Transmigration assay .....	55
2.5	Imaging and flow cytometry .....	55
2.5.1	Flow Cytometry .....	55
2.5.2	Fluorescent Activated Cell Sorting (FACS) .....	56
2.5.3	Flow Cytometry of macrophage surface receptors .....	56
2.5.4	Receptor Binding flow cytometry assay .....	56
2.5.5	Immunofluorescence .....	57
2.5.6	Electron microscopy .....	57
2.5.7	Cytospin Preparation and Staining .....	58
2.6	Protein biochemistry methods .....	58
2.6.1	Macrophage cell Surface biotinylation for proteomics .....	58
2.6.2	Cell surface biotinylation of red cells and retics .....	58
2.6.3	Band 3 immunoprecipitation .....	59
2.6.4	Proteomics via mass spectrometry .....	59
2.6.5	Western Blotting .....	60

<b>3 Chapter 3 – Development of a high throughput imaging assay to explore macrophage-erythroblast interactions .....</b>	<b>63</b>
3.1 Introduction .....	63
3.2 Results.....	64
3.2.1 Isolation of macrophage-erythroblast cell clusters from human bone marrow 64	
3.2.2 EDTA disturbs macrophage-erythroblast cluster isolation .....	65
3.2.3 Characterizing the central macrophage in bone marrow .....	67
3.2.4 <i>In vitro</i> cultured macrophages share some of the surface markers of central macrophages.....	71
3.2.5 Exploring whether VCAM1 can be induced in <i>in vitro</i> cultured macrophages .....	73
3.2.6 Selecting an assay method for observing macrophage/erythroblast interactions.....	75
3.2.7 Imaging analysis of reconstituted cell clusters.....	77
3.2.8 Optimization of media and culture plates for imaging cell cluster interactions.....	78
3.2.9 Incucyte system facilitates visualisation of the dynamic relationship between erythroblasts and macrophages .....	79
3.2.10 Dexamethasone treatment increases the number of long-lasting erythroblast-macrophage clusters .....	81
3.2.11 Reconstitution of bone marrow erythroblastic islands using incucyte....	83

3.2.12	Lentiviral transduction of macrophages .....	85
3.3	Discussion .....	91
<b>4</b>	<b>Chapter 4 – Characterization of Eph/ephrin and integrin expression in erythroblasts and macrophages .....</b>	<b>97</b>
4.1	Introduction.....	97
4.2	Results .....	98
4.2.1	Confirmation of Eph receptors expression by mRNA and protein .....	98
4.2.2	Proteomics .....	99
4.2.3	EphA4 on native reticulocytes .....	104
4.2.4	EphA4 is selectively retained in the reticulocyte.....	104
4.2.5	Eph ligands expression by macrophages .....	107
4.2.6	Eph receptors are dynamically expressed during erythroid terminal differentiation .....	109
4.2.7	Baseline activation of integrins occurs during the height of EphB4 and EphB6 expression.....	111
4.2.8	Eph receptor knockdown.....	113
4.2.9	Short exposure to EphrinB2 inhibitory peptides inhibits ligand binding	115
4.2.10	EphrinB2 stimulation does not cause the increase in integrin $\beta$ 1 activation	117
4.2.11	Eph receptors are also expressed on the BEL-A immortalised cell line.	119

4.2.12	EphA4 CRISPR .....	119
4.3	Discussion .....	123
4.3.1	BEL-A cells Eph expression .....	125
4.3.2	Integrin $\beta$ 1 activation .....	127
4.3.3	Conclusion .....	127
<b>5</b>	<b>Chapter 5 – Investigating the involvement of specific receptors in erythroblastic island formation .....</b>	<b>129</b>
5.1	Introduction .....	129
5.2	Results.....	130
5.2.1	EphB4 receptor has a role in the adhesion of erythroblasts to macrophages .....	130
5.2.2	The effects of EphB4 and EphB6 specific knockdowns in erythroblasts on macrophage interactions .....	137
5.2.3	Bone marrow macrophages require both EphB4 and EphB6 for erythroblast recognition.....	139
5.2.4	Role of E-cadherin, Akt and ERK.....	143
5.2.5	Integrins are important to the formation of erythroblastic islands, independent of VCAM1 .....	145
5.2.6	Importance of ATP receptors .....	147
5.3	Discussion .....	150
5.3.1	Summary.....	154

<b>6</b>	<b>Chapter 6 – Reticulocyte egress .....</b>	<b>157</b>
6.1	Introduction.....	157
6.2	Results .....	159
6.2.1	Proteomics suggest reticulocytes have some migration machinery .....	159
6.2.2	Reticulocytes form fewer interactions with macrophage .....	162
6.2.3	Exploring the egress of reticulocyte <i>in vivo in mice</i> .....	162
6.2.4	Assessing different migration assays .....	166
6.2.5	Transendothelial migration experiment: endothelial cells added on top of the filter .....	166
6.2.6	Induced BMEC cells with TNF- $\alpha$ and fibronectin let reticulocytes pass without current.....	169
6.2.7	BMECs do not express VCAM1 but produce their own fibronectin .....	170
6.2.8	Live imaging of BMEC.....	172
6.3	Discussion .....	175
<b>7</b>	<b>Chapter 7 - Discussion .....</b>	<b>181</b>
7.1	Creation a reconstitution assay and imaging methodology to explore interactions between macrophages and erythroblasts.....	181
7.2	Chapter 4 and Chapter 5 – The important role of Eph and Integrins .....	183
7.3	Chapter 6 – Mechanism of reticulocyte egress is still unknown.....	185
7.4	The questions raised .....	185
7.4.1	Importance of VCAM1 and integrins .....	185

7.4.2	Dynamics of erythroblastic islands.....	187
7.4.3	Macrophage identity .....	190
7.4.4	Are animal models useful in this conversation? .....	192
7.5	Improvements to the imaging system .....	193
7.6	Summary.....	194
<b>8</b>	<b>Chapter 8 - References .....</b>	<b>197</b>
<b>9</b>	<b>Chapter 9 – Appendices .....</b>	<b>216</b>

# Index of Figures

Figure 1-1 - Hierarchical tree of haematopoiesis .....	3
Figure 1-2 - Histology of differentiation course.....	5
Figure 1-3 - Hypothesis of erythroblastic island formation and migration .....	7
Figure 1-4 - Diagram of known erythroblastic island interactions .....	18
Figure 1-5 - Schematic of the interactions within the Eph/ephrin family .....	23
Figure 1-6 - Diagram of three-phase system .....	27
Figure 1-7 - Diagram of current hypothesis .....	32
Figure 3-1 – Isolation of native erythroblastic islands from bone marrow .....	66
Figure 3-2 – Bone marrow CD14 <sup>+</sup> CD16 <sup>+</sup> cells have two populations, the larger one is positive for resident macrophage markers .....	68
Figure 3-3 - Characterisation of central macrophage of bone marrow human erythroblastic islands .....	70
Figure 3-4 - The dexamethasone-treated macrophages have a similar surface marker profile to bone marrow macrophages .....	72
Figure 3-5 – Induction of VCAM1 in cultured macrophages .....	74
Figure 3-6 - Optimisation of an erythroblastic island reconstitution system .....	76
Figure 3-7 - Incucyte provides insight into the dynamics of the interactions between macrophages and erythroblasts .....	82
Figure 3-8 – M2c-like +Dex macrophages interact with more erythroblasts than -Dex macrophages.....	84
Figure 3-9 - VCAM1 offers a slight advantage for interactions with erythroblasts in bone marrow macrophages .....	86

Figure 3-10 – pXLG3 vector leads to GFP expression in in vitro cultured macrophages without affecting their phenotype .....	88
Figure 3-11 - Creating a shRNA hairpin derived knockdown in primary cultured macrophages .....	90
Figure 4-1 - Identifying the Eph receptors in erythropoiesis .....	100
Figure 4-2 Surface labelled proteins were depleted of a proportion of band 3 .....	102
Figure 4-3 EphA4 is selectively retained in cultured and native reticulocytes but is lost in red blood cells .....	106
Figure 4-4 Cultured and bone marrow macrophages express Eph receptor ligands ..	108
Figure 4-5 Erythroblasts have a dynamic surface expression of ephrins.....	110
Figure 4-6 Proerythroblasts gain integrin $\beta$ 1 activation .....	112
Figure 4-7 Lentiviral shRNA knockdown of EphB4 and EphB6 .....	114
Figure 4-8 Inhibition or removal of EphB receptors does not affect integrin $\beta$ 1 activation .....	116
Figure 4-9 BEL-A immortalized line express multiple Eph receptors including EphA4 which was knocked down using CRISPR-Cas9 .....	118
Figure 4-10 Single cell cloning EphA4 knockdown cells .....	120
Figure 4-11 The BEL-A 4G1 subclone has reduced EphA4 but the reticulocytes still express detectable EphA4 .....	121
Figure 4-12 Sumary diagram of expression of the different proteins discussed in this chapter throughout erythropoiesis.....	128
Figure 5-1 - EphB4 inhibition leads to a loss of contacts but has no effect on macrophage movement .....	131



Figure 5-2 – Final ratio of macrophages to erythroblast during reconstitution assays after the final wash to remove excess erythroblasts .....	134
Figure 5-3 - Control peptides have an effect on the cells after continual addition for 72h before addition to the macrophages.....	136
Figure 5-4 - Loss of EphB4, not EphB6, in erythroblasts impacts cultured macrophage-erythroblast interactions .....	138
Figure 5-5 – The ratio in bone marrow macrophage experiments are similar across experiments. ....	141
Figure 5-6 -Bone marrow macrophages require both EphB4 and EphB6 on erythroblasts for recognition .....	142
Figure 5-7 - Assessing the expression of known EphB effectors .....	144
Figure 5-8 - Integrin $\beta$ 1 plays an important role in the formation of erythroblastic islands .....	146
Figure 5-9 – Incubation with a range of P2X and P2Y receptor inhibitors affect the relationship between macrophages and erythroblasts.....	148
Figure 6-1 - Leukocyte transendothelial migration pathway is present in reticulocytes .....	160
Figure 6-2 - Reticulocytes lose many proteins to mature into red blood cells.....	161
Figure 6-3 – Incucyte experiment exploring reticulocyte interactions with -/+ Dex cultured macrophages .....	163
Figure 6-4 - Reticulocytes egress from mouse bone marrow sections .....	165
Figure 6-5 - Diagram of different migration assays used.....	167
Figure 6-6 - Reticulocytes and RBCs can move across BMEC layers seeded on transwell filters .....	171

Figure 6-7 - BMECs do not express VCAM1 but do produce their own fibronectin ....	173
Figure 6-8 - BMECs do not pulsate in this assay .....	174
Figure 7-1 - Proposed role of Eph receptors and integrins in the erythroblastic island formation.....	189

# Index of Tables

Table 1-1 - Macrophage subtypes arranged by stimuli and surface markers from Roszner<sup>52</sup>. The different roles were identified from Martinez et al.<sup>69</sup> and Kong et al.<sup>70</sup>.

..... 12

Table 2-1 Primary antibodies used in this thesis ..... 39

Table 2-2 - Directly-conjugated antibodies used in this thesis..... 40

Table 2-3 - RT-PCR primers used in this thesis ..... 44

Table 2-4 - shRNA hairpins used in this thesis ..... 44

Table 2-5 - CRISPR gRNA used in this thesis ..... 45

Table 2-6 - Gene sequencing primers used in this thesis ..... 45

Table 2-7 - Peptides used in this thesis..... 45

Table 3-1 - Summary of the different conditions tested for reconstitution..... 80

Table 4-1 - Surface proteomics of erythroblastic timecourse ..... 103

Table 4-2 shows the exclusive proteins found in surface proteomics of reticulocyte after Band 3 removal ..... 105

Table 6-1 shows potential transendothelial migration proteins present in reticulocytes detected by pathway analysis..... 160

Table 6-2 shows cell-cell adhesion proteins present in reticulocytes surfaceome ..... 161

## List of Abbreviations

ACD	Acid citrate dextrose
APC	Allophycocyanin
APS	Ammonium persulphate
ATP	Adenosine triphosphate
BMEC	Bone marrow endothelial cell
BRIC	Bristol Immunocytochemistry Monoclonal Antibody
BSA	Bovine serum albumin
CD	Cluster of differentiation
CDAII	Congenital dyserythropoietic anaemia type II
CIL	Contact inhibition of locomotion
CO <sub>2</sub>	Carbon dioxide
CPD	Citrate-phosphate-dextrose
C-terminal	Carboxy terminal
DAPI	4',6-diamidino-2-phenylindole
Dex	Dexamethasone
DMSO	Dimethylsulfoxide
DNA	deoxyribonucleic acid
E. coli	Escherichia coli
ECM	Extracellular matrix
EDTA	Ethylenedinitro-tetraacetic acid, disodium salt
EGF	Epidermal growth factor
EGTA	Ethylene glycol tetraacetic acid
Emp	Erythroblast macrophage protein
Eph	Erythropoietin-producing hepatocellular carcinoma
EPO	Erythropoietin
EPOR	Erythropoietin receptor
ER	Endoplasmic reticulum
FACS	Fluorescence activated cell sorting
FBS	Fetal bovine serum
FITC	Fluorescein isothiocyanate

GAPDH	Glyceraldehyde-3-phosphate dehydrogenase
GFP	Green fluorescent protein
GLUT1	Glucose transporter 1
GPA	Glycophorin A
HBSS	Hanks balanced salt solution
HEK	Human embryonic kidney
HEPES	4-(2-hydroxyethyl)-1-piperazineethanesulfonic acid
HRP	Horseradish peroxidase
HSC	Haematopoietic stem cell
ICAM	Intracellular adhesion molecule
IF	Immunofluorescence
IFN- $\gamma$	Interferon gamma
IGF-1	Insulin like growth factor-1
IL-3	Interleukin-3
IL-10	Interleukin-10
iPS	Induced pluripotent stem
IMDM	Iscoe's modified dulbecco's medium
KD	Knockdown
LB	Luria-Bertaini
MACS	Magnetic activated cell sorting
M-CSF	Macophage-colony stimulating factor
MerTK	Mer-tyrosine kinase
MFI	Mean fluorescent intensity
Mn <sup>2+</sup>	Manganese
mRNA	Messenger ribonucleic acid
N-terminal	Amino terminal
PBMC	Peripheral blood mononuclear cell
PBS	Phosphate buffered saline
PBSAG	Phosphate buffered saline with 1% BSA and 2% glucose
PE	Phycoerythrin
PFA	Paraformaldehyde

PMSF	Phenylmethanesulfonylfluoride
PS	Phosphatidylserine
PV	Polycythemia Vera
PVDF	Polyvinylidene fluoride
RBC	Red blood cell
SCF	Stem cell factor
SDS	sodium dodecyl sulphate
SDS-PAGE	sodium dodecyl sulphate polyacrylamide gel electrophoresis
SEM	Scanning electron microscopy
shRNA	Short hairpin ribonucleic acid
TBS	Tris buffered saline
TGF- $\beta$	Transforming growth factor beta 1
TNF $\alpha$	Tumour necrosis factor- $\alpha$
VCAM-1	Vascular cell adhesion molecule 1
VEGF	Vascular endothelial growth factor
VLA-4	Very late antigen-4
VLA-5	Very later antigen-5
v/v	Volume/volume
w/w	Weight/volume

## List of Publications

The following publications arose from work presented in this thesis:

Glucocorticoids induce differentiation of monocytes towards macrophages that share functional and phenotypical aspects with erythroblastic island macrophages.

Heideveld E, Hampton-O'Neil LA, Cross SJ, van Alphen FPJ, van den Biggelaar M, Toye AM, van den Akker E.

Haematologica 2018 Mar;103(3):395-405. doi:10.3324/haematol.2017.179341. Epub 2017 Dec 28.

Transduction with BBF2H7/CREB3L2 upregulates SEC23A protein in erythroblasts and partially corrects the hypo-glycosylation phenotype associated with CD41.

Pellegrin, S, Haydn-Smith, KL., Hampton-O'Neil, LA., Hawley, BR., Heesom, KJ., Fermo, E, Bianchi, P, Toye, AM.

British Journal of Haematology. 2018 Mar 14. doi: 10.1111/bjh.15189

Ephrin/Eph receptor interaction facilitates macrophage recognition of differentiating human erythroblasts.

Hampton-O'Neil, LA., Cross, SJ., Severn, CE., Gurung, S., Nobes, CD., Toye, AM.

Submitted to Haematologica

# 1 Chapter 1 – Introduction

## 1.1 Hematopoietic Stem Cells

The bone marrow is an extremely complex tissue composed of many different cells. It is the birthplace of many different lineages, and during the entirety of a human life it is constantly regenerating more blood cells for the body. Incredibly, the bone marrow can produce over  $2 \times 10^{11}$  red blood cells,  $4 \times 10^{11}$  platelets and  $1 \times 10^{10}$  monocytes, T and B cells within one day. This ability to produce so many different types of cells at such an outstanding rate is due to the presence of hematopoietic stem cells (HSCs). These stem cells reside in the endosteal niche near the bone cells<sup>1,2</sup> while differentiating cells are found in another niche in the bone marrow. The endosteal niche is extremely vascularised, with many sinusoids present<sup>1</sup>. These stem cells are helped throughout their life by the presence of stromal cells and a hypoxic environment which enables them to remain quiescent<sup>1,3,4</sup>. A small pool of progenitor clones is located further away from this niche and provides the cells for the production of constitutive blood cells<sup>5,6</sup>. The quiescent cells are only used in the case of emergencies and stress<sup>7</sup>. It is worth noting that a recent study has questioned the validity of this long-standing clonal theory, as they found that all labelled HSCs were contributing to the formation of progenitor cells<sup>8</sup>. A small pool of the HSCs can also be mobilised into circulation to move to other bones<sup>9</sup>. It is this ability that enables scientists to isolate them from blood to study and differentiate them.

Hematopoietic stem cells can undergo both symmetric and asymmetric division to proliferate. This ability ensures that there will always be a proportion of cells which remain stem cells as others start to differentiate into the different lineages (Figure 1-1).



These cells can differentiate into several different branches, such as megakaryocytes, neutrophils, monocytes and erythroblasts<sup>10</sup>. The main way to distinguish hematopoietic stem cells from progenitor cells is by their expression levels of CD34, a stem cell marker with an unknown function<sup>11-13</sup>. As the cells start to lose their ability to self-renew, they lose CD34 expression and become one of two types of progenitors: the common myeloid progenitor or the common lymphoid progenitor cell<sup>14</sup>. The latter is capable of creating the adaptive immune system, while the former leads to the innate immune system, erythrocytes and megakaryocytes<sup>10</sup>. In the case of cells becoming erythroblasts, as the cells become more and more selected, they gain CD36 and, gain and then lose CD61b<sup>15-17</sup>. These markers enable researchers to demarcate the different stages of potency properly. The stem cells' incredible ability to replenish the entire blood cell system make them very important to the body and to the medical community for their ability to renew the bone marrow niche. Therefore, a large amount of research has been done on how to control, isolate and characterise these cells, which are beyond the scope of this project.

.

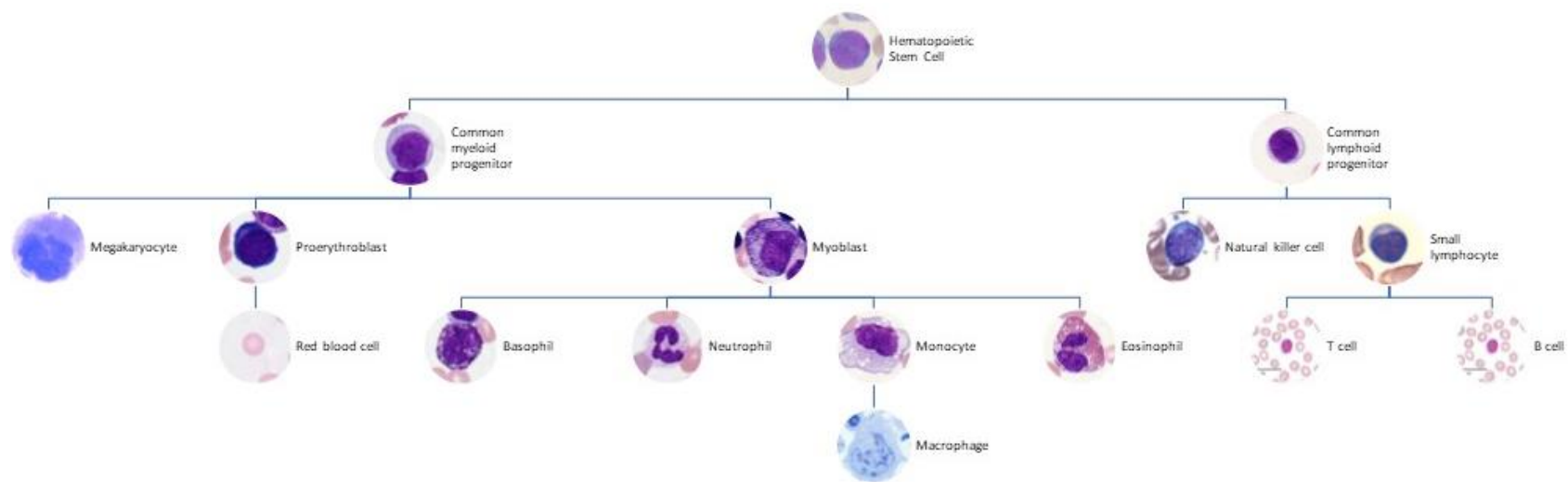


Figure 1-1 - Hierarchical tree of haematopoiesis

Hierarchical tree of haematopoiesis using histological sections, stained with Wright from Yale @histo, histologyguide.com.

## 1.2 Erythropoiesis

### 1.2.1 A multi-stage process

Erythropoiesis is the process whereby haematopoietic stem cells develop into red blood cells. The red blood cells, or erythrocytes, are responsible for carrying oxygen around the body using the haemoglobin they contain. The body makes approximately 2.5 million red blood cells per second<sup>18</sup>, making the erythrocyte the most abundant cell in the body, representing 84% of the total cells<sup>19</sup>. This very efficient process happens in the bone marrow, where the cells are surrounded by a stromal matrix<sup>20</sup>. It is a very dynamic process where the original stem cell undergoes asymmetrical cell division to produce progenitor cells, which then undergo multiple stages of cell division and differentiation. The different stages can be distinguished by the alteration of the cell surface protein markers<sup>21</sup> and distinct cellular morphology, particularly during the terminal differentiation phase. During this final stage, the proerythroblast differentiates, through basophilic erythroblast, polychromatic erythroblast and orthochromatic erythroblast stages until enucleating to form the nascent reticulocyte (Figure 1-2). While the erythroblasts mature, the cells become smaller and lose and gain many proteins<sup>22</sup>. As the cell continues to decrease in size, the nucleus becomes condensed before being expelled, in a step called enucleation. After enucleation, the reticulocyte must exit the bone marrow and enter the bloodstream<sup>23</sup>. During the next 48 hours, the reticulocyte matures in the circulation (and by passage through the spleen), reducing further in size by 20% and remodelling into the recognisable biconcave red blood cell<sup>24–26</sup>. This final phase of

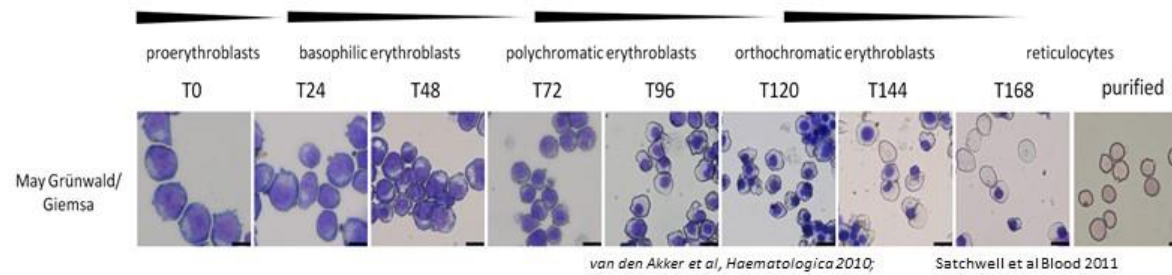


*Figure 1-2 - Histology of differentiation course*

*Representative histology samples of the differentiation course using the three phase system of the Toye laboratory. As the cells differentiate, they become smaller and their nucleus condenses. Towards the end of the differentiation course, the cells will enucleate, leading to reticulocytes. These images are taken from van den Akker et al.(2010) .*

the maturation process whereby reticulocytes become more flexible, lose most of their internal organelles, and become biconcave is not well understood, though it is thought that shear stress<sup>27</sup> and the spleen macrophage play a role<sup>26</sup>. During most of their differentiation in the bone marrow, the erythroblasts are bound to a macrophage, which is discussed in the next section.

### 1.2.2 Bone marrow macrophages and egress

In the bone marrow, the erythroid progenitors are known to interact with a single macrophage on a structure called the erythroblastic island<sup>28</sup>. This interaction is important for the efficiency of the differentiation process, as the inclusion of macrophages in an *in vitro* culture leads to higher proliferation of the progenitors and erythroblasts<sup>17,29–31</sup> and also enhances enucleation<sup>32</sup>. Disruption of macrophage-erythroblast interactions can also have an impact on yield<sup>30</sup>. The balance of erythroblasts to macrophages can have important consequences, as changes can lead to diseases such as polycythaemia vera (PV)<sup>33,34</sup> or  $\beta$ -thalassemia<sup>34</sup>.

As depicted in Figure 1-3, the current view is that erythroblastic islands are formed near the endosteal niche<sup>35,36</sup>. The island then migrates along the oxygen gradient towards the vascular niche<sup>4,35</sup>. As the island migrates, the erythroblasts differentiate, until they enucleate. The central macrophage then phagocytoses the nucleus (also known as a pyrenocyte), which is surrounded by a plasma membrane<sup>37,38</sup>, and the enucleated reticulocyte exits the niche into the sinusoidal vessel<sup>39</sup>.

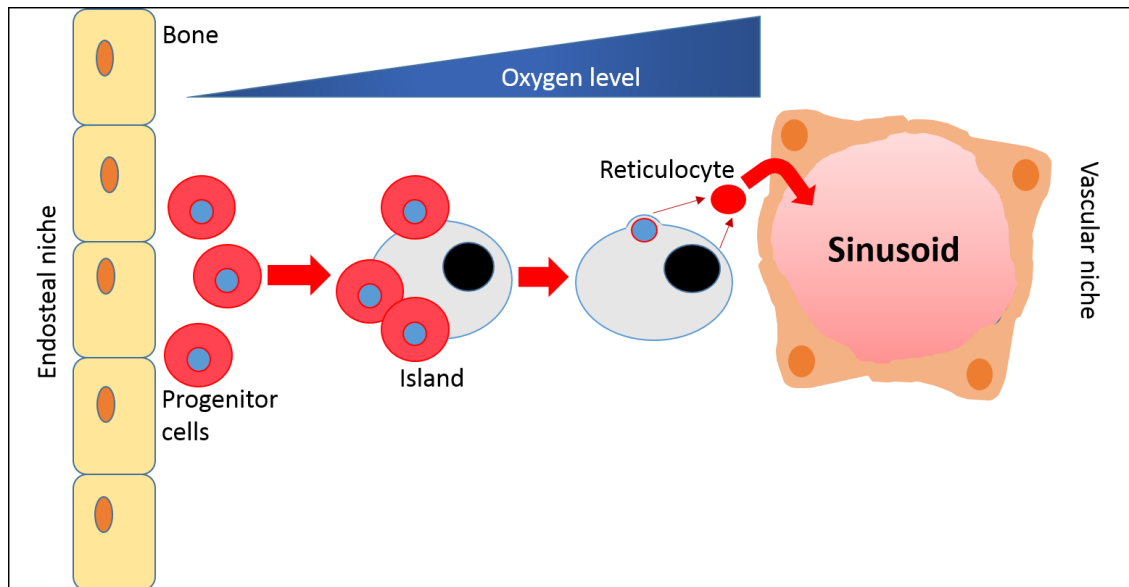


Figure 1-3 - Hypothesis of erythroblastic island formation and migration

Diagram illustrates the hypothesis of erythroblastic island formation and migration. The progenitor cells are thought to bind to the central macrophage nearer to the endosteal niche. Once this has occurred, it has been hypothesised that the erythroblastic island will move along the oxygen gradient to reach the vascular niche. Once enucleation has occurred, the macrophage will phagocytose the pyrenocyte and the reticulocyte will egress into the sinusoid. Adapted from Boulais et al.<sup>40</sup>

Electron microscopy studies<sup>35</sup> suggest that reticulocytes travel solitarily across the endothelial cell layer in the mouse bone marrow. Though, in the same study, some images were obtained that also suggest that the macrophage may be travelling with the reticulocyte into the sinusoid and that the separation only happens once in the blood<sup>35,39</sup>. However, very little is known about the actual mechanisms by which the reticulocyte exits the bone marrow, though several hypotheses have been proposed.

Waugh et al.<sup>41</sup> found that reticulocytes were more rigid than their more mature counterparts. Using endothelial-like pores, they showed that reticulocytes needed more pressure to go through. It is known that the endothelial cells present in the bone marrow are pulsatile<sup>39</sup>. This may create enough pressure to help reticulocytes leave the bone marrow. Furthermore, it is known that when mice are bled, leading to stress erythropoiesis, the endothelial cells lining the sinusoidal vessels stop overlapping, perhaps to allow more space for the reticulocytes to leave<sup>39</sup>. Another possibility, raised by Yokoyama et al.<sup>35</sup> is that the island macrophage itself may help the reticulocyte exit, by travelling as an island or even pushing the reticulocyte through.

### 1.3 The bone marrow niche

#### 1.3.1 Macrophage/monocyte development

Macrophages can originate from two different sources, from the yolk sac or from the bone marrow from the same progenitor cells as the erythroblasts<sup>42</sup>. Most macrophages that respond to inflammatory stimuli are produced in the bone marrow in the form of monocytes<sup>43,44</sup>. These monocytes will then enter the blood circulation to patrol the body. Inflammatory signals will lead to these monocytes entering the site of inflammation through transendothelial migration. Upon being in the site, these

monocytes will differentiate into the appropriate macrophage. The macrophages from the yolk sac often take on the role of tissue resident macrophage, macrophages which remain in one tissue. These cells will often proliferate by self-renewal. Most tissues have resident macrophages, such as the osteoblasts in the bone and Kupffer cells in the liver<sup>45</sup>. It is still debated whether the resident macrophages derive from the yolk sac or are differentiated from monocytes<sup>45–49</sup>. However, there is definite evidence that these cells can exist without the presence of monocytes, indicating that there must be a source of resident macrophages which are not created in the bone marrow<sup>50</sup>.

Although the classification of macrophages is still debated, macrophages are often separated into two categories – M1 and M2. M1 macrophages are described as inflammatory while the M2 macrophages will tend to be nursing cells, helping tissues heal<sup>51</sup>. As can be seen in Table 1-1, the M2 family itself is quite diverse<sup>52</sup>, exhibiting different surface markers and activators (e.g. IL-4 or glucocorticoids (e.g. dexamethasone)). These classifications are based on what will activate these cells<sup>53</sup>. In particular, it was noted that the cytokine GM-CSF would lead to an overly M1 phenotype while M-CSF will ensure an M2 phenotype<sup>54</sup>. The addition of other cytokines and growth factors lead to further differentiation into the subcategories<sup>52</sup>. However, macrophages are quite a heterogeneous population which can adapt to their environment leading to their phenotype being a mix of the different markers assigned to specific categories. For this reason, the M1 and M2 categories are heavily debated in the field.

#### *1.3.1.1 Identifying macrophages using surface markers by flow cytometry*

Many studies on macrophages have concentrated on characterising macrophages using surface antigens and flow cytometry. Therefore, the different categories of



macrophages depicted in Table 1-1 have been identified through the use of specific markers. The main antigen used to detect the monocyte and macrophage population from the rest of the immune cells is the CD14 present at the surface of the cells. This marker is present on macrophages, and is expressed 10 fold lower levels on neutrophils<sup>55</sup>. CD14 is a receptor for bacterial LPS, which has two forms; an anchored version and a soluble version<sup>56</sup>. Due to this ability to be secreted by the cells, this can complicate their identification. This ability is particularly relevant as monocytes are divided by their ability to express CD14 and another marker, CD16. CD16 is an Fc receptor present on most innate immune cells. The co-expression of CD16 alongside CD14 are clear markers for the macrophage and monocyte population. The monocyte population is often divided into three categories: CD14<sup>++</sup>CD16<sup>-</sup>, CD14<sup>+</sup>CD16<sup>++</sup> and CD14<sup>++</sup>CD16<sup>+57</sup>. These three populations have different roles within the body, which are still debated. As monocytes can differentiate into macrophages, it is also important to be able to differentiate between the two cell types. Macrophages are thought to express more CD16 and less CD14 than monocytes<sup>58-60</sup>. However, it can be noted that this would be a very similar phenotype to the CD14<sup>+</sup>CD16<sup>++</sup> phenotype. Therefore, there is a need for more markers to truly differentiate them.

Most markers for macrophages have been discovered after differentiation followed by the activation of monocytes. They are mostly divided into the M1 and M2 categories stated above. It is important to note, however, that macrophages are adaptable and can change their cell surface expression of markers in response to their environment. Therefore, they do not always fit into these discrete categories and the markers we use to differentiate the macrophages are very dependent on their previous environment<sup>42,47</sup>. These markers often describe the role these macrophages will have.

For example, inflammatory macrophages will have more receptors for pathogens, while the M2 macrophages have a broader set of stimuli and functions leading to a wider range of markers (see Table 1-1).

In particular, the M2c phenotype is composed of CD163, CD206 and MerTK<sup>52</sup>. This phenotype is induced by the presence of IL-10, TGF- $\beta$  and glucocorticoids, such as dexamethasone. This phenotype is often referred to as deactivated and they are involved in tissue repair<sup>61</sup>. This type of macrophage, which can be activated both *in vitro* and *in vivo*, is the closest phenotype to the general resident macrophage phenotype (CD163, CD206 and CD209). It is important to note that even within the resident macrophage population, there will be wide differences based on which tissue they belong to<sup>45,47</sup>. CD206 and CD163 are often found co-expressed in both the M2c and resident macrophages<sup>62,63</sup>. The first is a mannose receptor, and the latter is a haemoglobin scavenger receptor. CD163 is not solely in M2 macrophages and therefore, should not be used on its own to identify these cells<sup>64</sup>. Both these markers' roles are not fully understood in the context of macrophages.

Macrophages are known for their capacity to phagocytose debris and whole cells. This capacity is due to many different receptors on their surface. In M2c, the main receptor responsible is Mer tyrosine kinase (MerTK)<sup>65</sup>. This receptor is important for the recognition of phosphatidylserine (PS) on apoptotic cells. These anti-inflammatory cells can, therefore, recognise and phagocytose apoptotic cells when cleaning wounds.

Resident macrophages also have CD209 at their surface. CD209 has been thought to only be present on dendritic cells for a long time. For this reason, it is often used to separate macrophages from dendritic cells. However, several studies have now

confirmed its presence on tissue-resident macrophages<sup>66–68</sup>. Its function, however, remains unknown.

Macrophage type	Activating signals	Flow markers	Roles
M1	LPS, GM-CSF	CD68, CD80, CD86	Initiate immune response, phagocytose microbes
M2a	Fungal infections, IL-4, IL-13	CD163, CD206, Arginase-1, FIZZ1	Pro-fibrotic, interact with T cells
M2b	LPS	CD86, MHC-II	Immune-regulating, interact with B cells, wound healing
M2c	IL-10, TGF-beta, glucocorticoids (e.g. dexamethasone)	CD163, CD206, MerTK	Anti-inflammatory, tissue repair and remodelling
M2d	IL-6, adenosine	VEGF-A	Tumour inhibitor
TAM	Tumour environment, MCSF	CD163, CD68, CD206, VEGF-A	Tumour associated, pro-tumour
Tissue resident M2	Tissue environment, IL-4, IL-10	CD163, CD206, CD209	Tissue-specific, patrols

Table 1-1 - Macrophage subtypes arranged by stimuli and surface markers from Roszner<sup>52</sup>. The different roles were identified from Martinez et al.<sup>69</sup> and Kong et al.<sup>70</sup>.

### 1.3.2 Erythroblastic islands

#### 1.3.2.1 A central macrophage surrounded by erythroblasts

The presence of erythroblastic islands was discovered by Bessis in 1958<sup>71</sup> in the bone marrow and spleen. These islands were composed of a central macrophage surrounded by erythroblasts. The number of erythroblasts vary depending on the species, with 10 in rat femurs to 5-30 in humans<sup>35,72</sup>. It is still unknown whether the erythroblasts around this macrophage are all developmentally the same or if they are at different stages of differentiation. The role of this niche for the erythroblastic island was harder to elucidate due to a lack of techniques. Four main roles have been illuminated.

#### 1.3.2.1.1 Iron

The main role of red blood cells is to carry oxygen around the body. This is done with the help of the molecule haemoglobin, which contains iron to be able to transport this oxygen<sup>73</sup>. For this reason, one of the biggest roles of erythropoiesis is capturing iron for the production of haemoglobin. Iron is captured by transferrin, which is an iron-binding protein found in free circulation in the body. Erythroblasts have a transferrin receptor which enables them to bring this protein into the cell to release its iron<sup>74</sup>. It is also possible for erythroblasts to get their iron from placental ferritin<sup>75</sup>. Upon discovery of the erythroblastic island, Bessis put forward the idea that the main role of macrophages is the transfer of iron to erythroblasts<sup>76</sup>. An *in vitro* study showed that macrophages are capable of secreting ferritin by exocytosis and that nearby erythroblasts can capture it by endocytosis, with the low pH of the erythroblast lysosome leading to a release of the iron into the cytoplasm<sup>77</sup>. The paper claims that in this way, the central macrophage can be a source of iron for the developing erythroblasts. However, as humans exist with no transferrin, and mice deficient in transferrin can have severe cases of anaemia, this points towards a minor role for the macrophage in iron synthesis<sup>78,79</sup>.

#### 1.3.2.1.2 Removal of the expelled nucleus (pyrenocytes)

The second hypothesis put forward by Bessis is that the macrophage played a role in the phagocytosis of the expelled nucleus<sup>76</sup>. Indeed, in the electron microscopy images which identified erythroblastic islands, Bessis found macrophages which had engulfed what looked like the nucleus of the erythroblasts. It is thought that since most adhesion molecules, such as integrins and ICAM4, transfer to the nucleus during enucleation, this enables the nucleus to remain attached to the macrophage to ensure phagocytosis<sup>26</sup>. It has also been found that MerTK is present on the central macrophages<sup>37,65</sup>. This

receptor enables the macrophage to recognise the exposed PS, after it has bound the bridging proteins lactadherin, Gas6 and protein S, on the nucleus and recognise it as an apoptotic cell<sup>26</sup>. In this way, this will lead to the phagocytosis of the nucleus. It is thought that the phagocytosis step happens 10 minutes after expulsion from the nucleus<sup>80</sup>, which is exactly the amount of time it takes for the PS to become exposed at the surface of the cells<sup>81</sup>. It has also been shown that these central macrophages use DNase II to degrade the nuclear DNA. In DNase II-deficient mice, the macrophages could not remove the phagocytosed nuclei and this lead to severe anaemia<sup>82</sup>. Therefore, the removal of these pyrenocytes is an important part of the macrophage's role within the erythroblastic island.

#### 1.3.2.1.3 Proliferation and nutrients

As the central macrophage is present from the beginning of the differentiation process, it has been proposed that macrophages provide the nutrients and the signals necessary to lead to higher proliferation. Removal of macrophages using clodronate liposomes or genetic manipulation leads to a slower recovery from anaemia, demonstrating the importance of macrophages to have enhanced erythropoiesis<sup>33,34</sup>. Furthermore, Heideveld et al.<sup>17</sup> and Rhodes et al.<sup>30</sup> showed that the presence of macrophages in culture with erythroblasts lead to a higher proliferation of the latter. This proliferation could be observed using a transwell assay which stops direct cell interaction, demonstrating the role of secreted factors, as opposed to direct contact<sup>17</sup>. Conditioned media from macrophage cultures was further able to lead to higher yields. Rhodes et al. further showed that this was independent of EPO. Macrophages are also known to secrete several factors, such as IL-10, TGF- $\beta$  and IFN- $\gamma$ , which could all be of importance

in the survival and proliferation of erythroblasts<sup>83,84</sup>. However, the importance of each of these factors remains largely unknown.

#### 1.3.2.1.4 Transport

Finally, studies of erythroblastic islands *in vivo* are difficult due to the opacity of bone marrow and the lack of access. For this reason, most of the positional and functional experiments have been conducted on animals and *in vitro*. It was, however, possible to see in mice bone marrow electron microscope experiments that the erythroblastic islands were dispersed equally throughout the bone marrow<sup>85</sup>. More interestingly, the erythroblastic islands nearer to the endosteal niche were more heavily loaded with early developmental stages, while those closer to the sinusoids, the exit point, had more orthochromatic cells and reticulocytes<sup>35</sup>. It was put forward that these results demonstrated the role of macrophages as a cell transporter, helping differentiating cells move along the oxygen gradient (Figure 1-3). It is also possible that the erythroblasts could be hopping from one macrophage to the next. However, this remains a hypothesis as long as there is a barrier to studying erythroblastic islands *in vivo*.

#### 1.3.2.2 The bone marrow resident macrophage – CD169<sup>+</sup> macrophages

Surprisingly few studies have been conducted on the human bone marrow resident macrophages. Indeed, as it is present at the epicentre of the monocyte/macrophage development, it is quite hard to study and characterise. Several studies in mice have attempted to define the specific phenotype of the macrophages, though their reciprocity in humans has not been shown yet.

With the advent of antibodies, a specific marker for resident macrophages was found in F4/80<sup>86,87</sup>. Indeed, an antibody was raised against these specific macrophages in mice which enabled the identification of these cells. This antibody has proven very useful in

studies to identify erythroblastic islands, illuminating the central macrophage. However, this marker does not have an equivalence in human bone marrow macrophages as F4/80 is specialised to eosinophils in humans<sup>88</sup>.

Chow et al. have shown the presence of CD169<sup>+</sup> macrophages in the bone marrow<sup>89</sup>. To deplete the CD169<sup>+</sup> macrophages, Chow et al created a CD169-DTR mice line so that mice treated with diphtheria toxins lost cells which expressed CD169<sup>+</sup>. This specific depletion of these macrophages in mice led to a major loss of erythroblastic islands in the bone marrow and an early release of erythroblasts into circulation<sup>33</sup>. This loss did not lead to anaemia due to compensatory mechanisms at peripheral sites such as the spleen and the mature red blood cells clearance being delayed. However, when blood-letting was administered to these mice, the animals were no longer able to recover. This study confirmed *in vivo* the role for macrophages to support erythropoiesis, as well as showed that CD169 was a significant marker of these macrophages, as their specific deletion led to a loss of erythroblasts. CD169 is a sialoadhesin, but its exact role in the erythroblastic island has not been elucidated.

MerTK is traditionally found on M2c macrophages<sup>65</sup>. However, it has also found a place in the bone marrow resident macrophage nomenclature as it plays a significant role in erythroblastic island function. As discussed above in Section 1.3.2.1, the macrophage plays an important role in the final stages of erythropoiesis, as it can phagocytose the pyrenocyte. This ability has been discovered to be related to the presence of MerTK receptors<sup>37</sup>. This will be discussed in further detail in section 1.3.2.3.4. However, this important role has led to the inclusion of MerTK in the markers of the bone marrow macrophage<sup>90</sup>. Its presence on M2c macrophages, as well as the other resident

macrophage markers, has led to studies into the interchangeability of these macrophages. It is also important to note that more and more studies show heterogeneity in the phenotypes of the central macrophages, both in their adherence capacities<sup>91</sup> and their surface markers<sup>92</sup>.

The human central macrophage has mainly been described by one paper<sup>72</sup> from 1988, which pointed towards a very immune phenotype CD4+, CD11a+, CD11c+, CD13+, CD14+, CD16+, CD18+, CD31+, CD32+, FcRI+, HLA-DR+, and CD35-, transferrin receptor-negative, and CD11b (weak). Proper markers for the easy identification of human bone marrow resident macrophages are still unknown.

#### *1.3.2.3 Receptors for macrophage-erythroblast interactions*

Macrophages are thought to interact with erythroblasts via cell surface receptors (Figure 1-4). The main receptors implicated to date are integrins  $\alpha 4\beta 1$ , ICAM-4, erythroblastic macrophage receptor (EMP) and ephrins<sup>28,38,93–95</sup>. However, the individual contributions of these proteins to island formation and stability is yet unknown.

##### *1.3.2.3.1 ICAM4*

Several studies have shown that interruption of these interactions has a varying effect on the island formation. The main method used to assess the effect of pathways on the erythroblastic islands is to isolate and count islands flushed out from mice bone marrow or spleens. ICAM-4 was the main receptor identified using this method<sup>93,96</sup>, where the number of islands was reduced in ICAM-4 knockout mice. ICAM-4 is an adhesion protein, whose main binding partners are the integrins, in particular,



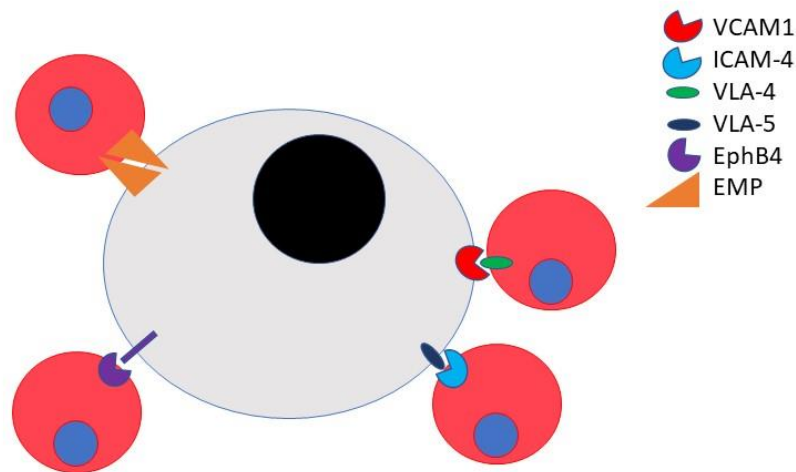


Figure 1-4 - Diagram of known erythroblastic island interactions

Erythroblastic islands are formed of a central macrophage surrounded by differentiating erythroblasts. The interactions are represented in this diagram. All these interactions would be between macrophages and all the erythroblasts.

the integrin complex VLA-5<sup>97</sup>. The disruption of island formation did not exhibit any phenotype in the animals, as they were not anaemic, though this was not tested in stress erythropoiesis conditions. However, the addition of inhibitors did affect the formation of these islands when this was tested *ex vivo*.

#### 1.3.2.3.2 EMP

EMP is a receptor present on both erythroblasts and macrophages, which is believed to interact through homophilic binding<sup>32</sup>. It is mostly thought to be involved in the stimulation of the erythroblast differentiation by the macrophage. Soni et al.<sup>98</sup> showed that when erythroblasts are cultivated with anti-EMP antibodies, they tend to proliferate more and mature faster. Therefore, EMP appears to be more involved in the differentiation process. The same study showed that the loss of EMP also interferes with the enucleation process as its loss leads to high level of nucleated red blood cells. The

loss of EMP did not affect erythroblast and macrophage binding as erythroblastic islands still formed. Despite their ability to bind to macrophages, the erythroblasts are no longer able to differentiate.

#### 1.3.2.3.3 VCAM1

Vascular Cell Adhesion Molecule 1 (VCAM1) is an integrin  $\alpha 4\beta 1$  receptor that is present on mice island macrophages<sup>94</sup>. Using anti-VCAM1 antibodies, it was shown that erythroblasts bind to VCAM1 until they become reticulocytes, at which point they are unable to bind anymore. Furthermore, the presence of anti-VCAM1 antibodies can disrupt island integrity *in vitro*<sup>94</sup>. Therefore, VCAM1 is thought to be important in the formation of islands. However, its importance has recently been questioned as it has been shown using flow cytometry and imaging that VCAM1 is not necessarily at the surface of macrophages within erythroblastic islands in mice<sup>92,99</sup>.

#### 1.3.2.3.4 MerTK

During enucleation, the proteins at the surface of the cells partition in a specific manner between the reticulocyte and the nuclear fraction, the pyrenocyte. In particular, the integrins are thought to partition almost entirely onto the pyrenocyte. The loss of integrin on the reticulocyte would lead to a separation from the macrophage, while the pyrenocyte would be phagocytosed as the integrins at its surface remain bound to the VCAM1 present on the macrophage. It has emerged recently that the integrins present at the surface of the pyrenocyte are inactive<sup>37</sup> and that instead, MerTK receptors on the macrophage bind bridging proteins (lactadhesin, Gas6 and protein S) to exposed PS on the pyrenocyte<sup>26</sup>. PS becomes exposed after the nuclei have detached from the

reticulocyte, due to a drop in ATP<sup>81</sup>. PS is expressed on apoptotic cells, and indicates to the macrophage that they need to be phagocytosed<sup>81</sup>.

#### 1.3.2.3.5 Others

Other integrins, such as integrin  $\beta 3$ , have also been shown to be important as knockout mice show a decrease in erythroblast numbers per island<sup>100</sup>. This result indicates that the cells are no longer able to bind the macrophage as well, leading to loose interactions. Integrin  $\beta 3$  is likely involved in keeping the erythroblasts bound to the macrophage rather than island formation per se, as the number of islands was not reduced in knockout mice.

CD163, as discussed above, is present on M2c and bone marrow resident macrophages. It is known to play a role in clearing haemoglobin complexes as a scavenger receptor<sup>101</sup>. However, it has been shown that the addition of monoclonal antibodies against it leads to the loss of adhesion between erythroblasts and macrophages<sup>102</sup>. Therefore, it may also play an important role in the adhesion of these two cell types. In the same study, CD163 is shown to have a proliferative effect on erythroblasts, as its addition in culture lead to higher proliferation.

The Eph receptor family has been shown to play a role in the erythroblastic island and the bone marrow niche which will be discussed in more detail in section 0<sup>103,104</sup>.

Other receptors or mechanisms could be involved. Indeed, the loss of Stk40, a kinase, in mice leads to severe anaemia and a loss of the ability to form erythroblastic islands<sup>105</sup>. However, the authors of the study show that this loss does not impact the level of any of the currently known interactors. Several receptors are known to be important in the binding and formation of islands, but whether each protein has individual roles or

collaborates together and therefore, can compensate for one another is undetermined. Furthermore, it is still unknown what actually drives occupation of the erythroblast island and then allows the reticulocyte to leave – is it simply based on gradual loss of multiple receptors during maturation or due to the specific spatial-temporal expression of these different proteins?

## 1.4 Eph receptors

Eph receptors are the largest tyrosine kinase receptor family. Both the receptors and their ligands, ephrins, are membrane bound. This family of receptors have a complex signalling capacity, due to their large number of effectors<sup>106</sup> as well as their ability to interact forwards through the Eph receptors, and backwards through the ligands, ephrins<sup>107</sup>. The Eph family have several roles within the body due to this plasticity of signalling, such as proliferation, control of the cytoskeleton, migration of the cells, developmental cell sorting and boundary formation<sup>108–113</sup>. As can be seen in Figure 1-5, ephrins can be divided into two main families: A and B. In most cases, ephrinAs only interact with EphA receptors and vice-versa<sup>114</sup>. EphA4 receptors, however, can also interact ephrinB2<sup>106</sup>.

Ephrins are best known to be involved in neuron development, angiogenesis and tumour metastasis<sup>41,106,114</sup>. One of ephrin's key roles in all these processes is the control of contact inhibition of locomotion, a cellular process that describes the cell behaviour upon cell-cell contact.

### 1.4.1 Contact inhibition of locomotion

Contact inhibition of locomotion (CIL) is an important process in development and collective migration. It ensures that when two cells collide, they will move away from

each other to not collide again. This process involves the two cells recognising each other, disengaging their cytoskeleton and moving in another direction<sup>115</sup>. This pathway enables cells to not move over each other and ensures that cells will grow into a single layer. Indeed, when the cells are grown in a dish or in a tissue, if they are no longer able to avoid a collision, the contact inhibition acts differently making the cells stop moving and also halts the cell cycle. This mechanism ensures that tissues remain a similar size as well as only being a single layer<sup>116,117</sup>. Cancer cells are often devoid of the capacity for these two contact inhibition leading to their capacity for metastasis and evasion of the immune system<sup>118</sup>.

As a research field, contact inhibition of locomotion has not been able to properly establish all the different components required for this reaction. Indeed, multiple pathways have been put forward: Notch, cadherins, nectins and ephrins<sup>114,116,119–122</sup>. It is possible that all of these are involved. The model for CIL involving Eph receptors states that depending on which Eph receptors and ephrins are present at the surface of the cells, this will change the reaction of cells as they come into contact<sup>114</sup>. In most cases, cells will always move away from each other due to the presence of ephrins at the cell surface. However, the Nobes' laboratory has shown that cancer cells can vary in their response to collisions and this is related to the aggressive properties of cancer and level of metastasis. Astin et al.<sup>114</sup> showed that this was directly related to the ratio of ephrinA and ephrinB family present at the cell surface. In fact, if there was more ephrinA present over ephrinB at the surface of the cells, then the cells will not be attracted to each other and will move away. On the other hand, if there is more ephrinB then the cells will be attracted, and this will lead to the cells running into each other and possibly binding. It

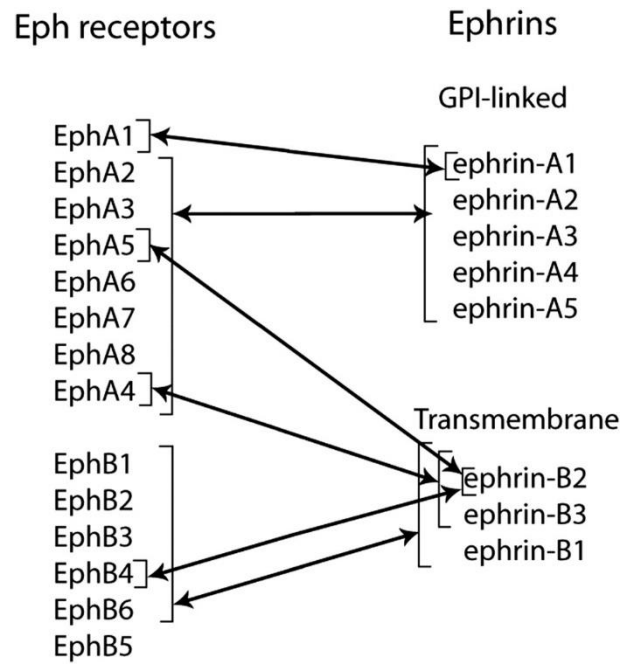


Figure 1-5 - Schematic of the interactions within the Eph/ephrin family

Figure taken from Coulthard et al.<sup>123</sup>. The Eph and ephrin family can be separated into two main families: A and B, where EphA receptors only interact with ephrinA ligands and vice-versa. The exceptions are indicated by the boxes.

is thought that when EphA and ephrinA interact this causes repulsion/movement away, which causes ephrinA to be internalized by the cell expressing the EphA receptor.

#### 1.4.2 The role of Ephs in the bone marrow niche

Recently, several reports have discussed the importance of Eph receptor functions within the bone marrow niche. In mice, one EphB4 ligand, ephrin-B2 is expressed on HSCs and is important for the release of the progenitor cells into the bloodstream <sup>124,125</sup>. EphB4 is also reported to exert control over niche size, as transgenic mice that overexpress EphB4 produce more HSC cells and display a higher bone marrow reconstitution capacity <sup>126,127</sup>. However, the role that Eph receptors play specifically in the erythroid lineage is based primarily upon the demonstration of EphB4 expression on human bone marrow CD34<sup>+</sup> cells, and from the observed increase in erythroblast differentiation upon co-culture with stromal cells overexpressing ephrin-B2 or HSCs overexpressing EphB4 <sup>20,103,104</sup>. More recently, Anselmo et al.<sup>128</sup> proposed a role for EphB1 in the activation of integrins via an agrin-dependent pathway in mice, as they saw a concurrent rise in integrin and EphB1 activation in proerythroblasts after treatment with agrin. They hypothesised that agrin activates EphB1 through binding with dystroglycan receptor binding, which would lead to a rise in integrins, which would facilitate erythroblast binding to macrophages. Whether this observation extends to a human macrophage island context is unknown.

### 1.5 Culture systems

#### 1.5.1 2D *in vitro* erythroid culture systems

The development of erythroid in *in vitro* culture systems has helped the in-depth study of the process of human erythropoiesis in health and disease. The laboratory

methodology used for expansion and differentiation is still less efficient than the body's natural system. One of the ultimate goals of culturing primary cells is their therapeutic potential as the cultured reticulocytes could be used for transfusion. To do this effectively the culture systems need massive gains in efficiency, which could be achieved by more effectively reproducing the process that occurs in the bone marrow.

Multiple culture systems have been proposed and tested over the last 10-15 years<sup>129–144</sup>. These have commonalities but usually exist as two-phase culture systems or three-phase systems utilising erythropoietin (EPO), Stem cell factor (SCF), interleukin-3 (IL-3) and transferrin. The starting material used also varied, as some laboratories have used all the mononuclear cells isolated from peripheral blood<sup>17,141</sup> while others isolate the CD34<sup>+</sup> stem cells to ensure purity of the cells. These attempts have had varying success based on their ability to have a large yield as well as the final cells' ability to enucleate. However, the most recently described systems, which prioritise the production of reticulocytes, have described between 2.5 mL to 10 mL packed reticulocytes<sup>137,138,145,146</sup>

The Toye lab has a variety of methods for the production of reticulocytes, whose use depends on the originating stem cells and what specific outcome is needed, e.g. whether multiple samples from different points of erythropoiesis are needed or whether just retics are required. To do this effectively the lab utilises two separate culture systems; one that incorporates dexamethasone which allows a more synchronous differentiation<sup>141</sup> and another methodology described by Griffiths et al<sup>147</sup> which produces large amounts of reticulocytes, which is used as the basis for a clinical trial called RESTORE, that is currently being prepared in Bristol. In the first phase of the former culture method (Figure 1-6), which is used in this thesis, the cells are primed to



ensure that they survive and proliferate. This phase lasts 3 days (Day 1 to Day 3). The second phase is called the expansion phase. Its purpose is to obtain as many progenitor cells before differentiation starts. Growth factors are added to the media to ensure that they proliferate, such as IGF-1, IL-3 and insulin. Dexamethasone is added to ensure that the cells do not start differentiating early<sup>130,141</sup>. This phase lasts up to 4 days (Day 4 to Day 8). Finally, the third phase is the final differentiation stage, where the cells terminally differentiate. The level of EPO is increased to resemble the one found during stress erythropoiesis. Furthermore, human serum is added which helps the cells differentiate in a yet unknown way. This phase occurs over 7 days and is labelled T0 to T168.

#### 1.5.2 Culture systems and disease

The 2D erythroid culture systems can be used to understand how erythropoiesis is disturbed during disease. For example, the Toye laboratory has used 2D culture systems and PBMCs as a starting material to study the hallmark changes that occur during Hereditary Spherocytosis<sup>148,149</sup> and Congenital Dyserythropoietic Anaemia (type II; CDAIL)<sup>150,151</sup>. CDAIL is a severe type of anaemia due to SEC23B gene mutations<sup>150,152–154</sup> which lead to multinucleated erythroblasts, hyperglycosylated membrane proteins, ER remnants in red blood cells and double plasma membranes on reticulocytes. The culturing system enabled the laboratory to study and characterise the phenotypes at different stages of erythropoiesis in human cells<sup>150</sup>. They found that they could grow patient cells of CDAIL and observe the different proteins expressed at the different stages of erythropoiesis. They found that typical human cells lose Sec23A faster than mice, where Sec23B is kept longer. These results helped explain why the Sec23B knockout mice did not recapitulate the phenotypes seen in humans. SEC23A could have

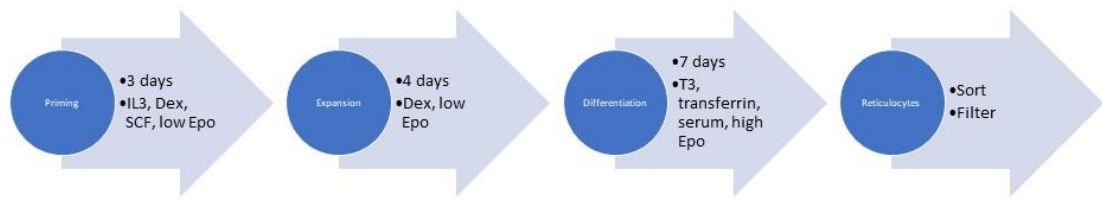


Figure 1-6 - Diagram of three-phase system

Diagram illustrating the three-phase culture system of the Toye laboratory. In the first phase, the cells are primed for 3 days, using cytokines to ensure growth and no differentiation. At day 4, the cells are put in expansion media containing SCF, IL-3, IGF-1. This media ensures that the proerythroblasts proliferate without committing too early. Finally, the cells are put in differentiation media. From this point forward they are named T0 to T164. The media has high EPO and transferrin to ensure that they differentiate. Once enucleation has occurred, the reticulocyte can be purified by FACS or filtering with 5µm filters.

a compensatory role in mice. It is not currently known why Sec23 isoforms are differentially lost in humans.

### 1.5.3 Macrophage cultures

Macrophage are an important part of the inflammatory system. For this reason, many laboratories have developed ways to isolate monocytes from blood<sup>155,156</sup>. These can then be differentiated into macrophages and activated using the different factors highlighted in Table 1-1. Furthermore, cell lines have also been created to study this further, such as THP-1 and U937<sup>157</sup>. Monocytes can be isolated from PBMC using CD14 magnetic beads or by adherence. These cells can then be activated. For example, they can be induced into M2c-like macrophages in the presence of MCSF and dexamethasone for 7 days<sup>17,34</sup>.

#### 1.5.4 Immortalised erythroid cell lines

As part of an effort to study and recapitulate erythropoiesis, numerous attempts have been made to create immortalised cell lines, which theoretically could be grown in unlimited amounts. Most effort has been made around iPS cells<sup>158–163</sup>, embryonic stem cells<sup>143,164–166</sup> and immortalising CD34<sup>+</sup> cells, such as Hudeps<sup>167–169</sup> and HiDEPs<sup>170</sup>. These cells, even though they can differentiate, have issues executing the full erythroid program and so do not produce reticulocytes. Furthermore, these cells do not express the adult form of haemoglobin. However, these cells have proved to be a useful resource to study the stages of erythropoiesis and its development, for example HiDEPs and HuDEPS were used to study haemoglobin switching<sup>171,172</sup>.

The Frayne and Anstee laboratories in Bristol, used a viral technique to immortalise primary cells from adult donated bone marrow. This led to the creation of the Bristol Erythropoietic Line Adult (BEL-A) cells<sup>173</sup>. These cells are immortalised at the basophilic stage of erythropoiesis. When in the presence of doxycycline, they are capable of expanding indefinitely. However, once the doxycycline is removed, this leads to differentiation. Furthermore, these cells can enucleate at a higher rate than previously immortalised lines (>30%)<sup>135,174,175</sup>. The cells reproduce human terminal erythroid differentiation, producing reticulocytes that have very similar proteomes and deformabilities compared to reticulocytes grown from primary cells<sup>176</sup>.

The advantage of immortalised cell lines such as Hudep<sup>171,177,178</sup> and BEL-A<sup>179</sup> is that they are amenable to genetic manipulation and then these cells can be stored. In this way, it is possible to create large quantities of a particular genetic knockout to study its specific characteristics. In particular, it is possible to use CRISPR to knockout entire genes from

these cells. For example, recently, the Toye and Frayne laboratories collaborated to create a cell line which was devoid of the top problematic 5 blood systems that make transfusion difficult<sup>179</sup>.

#### 1.5.5 Methodology for studying erythroblastic islands formation and integrity

##### 1.5.5.1 *Reconstitution*

As mentioned previously in section 1.2.2, erythroblastic islands are extremely difficult to study. The lack of a plentiful supply of bone marrow has led to workarounds. At first, most information was taken from electron microscopy experiments from bone marrow slices generated from mice<sup>71,76,85,180</sup>. These experiments helped establish the presence of the structures as well as their position within the bone marrow. Knockout mice were created to identify the different receptors important in the function of erythroblastic islands. The phenotype of these mice could be studied, as well as the number of erythroblastic islands found within their bone marrow. To obtain this information, bone marrow was flushed out from mice femur. The cells were then given time to recover and stained before being counted out. Furthermore, many studies let the islands settle, before stripping the erythroblasts, with PBS<sup>30,37,87,93,98,105,128,181–184</sup> or serum-free media<sup>185</sup>. This technique enabled the researchers to add back normal erythroblasts to the macrophages or to add knockout erythroblasts to normal macrophages to test the importance of certain receptors on each cell. The majority of the latter experiments are done with splenic erythroblastic islands as these are much simpler to isolate without disruption. Indeed, the flushing from bone marrow is mechanically disruptive, which might separate the two cell types. Another method used was to add the two cell types together in suspension with antibodies after they have been separated into a single cell

suspension<sup>37,93</sup>. It is worth noting that one paper extracted the macrophage membrane, ran it into a page gel and tested for erythroblast adhesion to the gel<sup>29</sup>. One seminal paper isolated intact erythroblastic islands from human bone marrow<sup>72</sup>. This accomplishment enabled them to characterise the human central macrophages.

Co-culture studies have been used to look at the function of macrophages within the erythroblastic island. The use of transwell assay or conditioned media help understand the contributions from the macrophage. Furthermore, these kinds of studies enabled researchers to test out different types of macrophages. Indeed, Heideveld et al.<sup>17,60</sup> and Falchi et al.<sup>31</sup> showed that CD14<sup>+</sup> cells from peripheral blood could be used to help the erythroblasts proliferate in co-culture. Further co-culture experiments also showed that erythroblasts are capable of loose interactions with dexamethasone-treated CD14<sup>+</sup> cells, while tight interactions led to phagocytosis<sup>31</sup>.

#### *1.5.5.2 Imaging*

The interaction between the cells has been studied mainly through fixed images, as the erythroblastic islands are often studied via cytopins, flow cytometry or fluorescence imagery. Several papers have started studying the interactions between the cells using scanning electron microscopy (SEM)<sup>91,186</sup>. These studies have shown different phenotypes for the central macrophages, as some are extremely flat and adherent while others are more rounded<sup>91</sup>. SEM was also able to show the presence of nanotubes between the cells which were thought to possibly be a way for the cells to communicate and exchange nutrients with each other<sup>186</sup>.

Finally, the interactions between the cells have seldom been imaged over time. Indeed, only three papers have currently used long-term imaging to characterise the different

interactions between the cells. In 1992, one study was presented at a conference showing the first videos of isolated mice islands<sup>80</sup>. Several years later, Falchi et al.<sup>31</sup> showed the interactions between monocyte-derived macrophages and erythroblasts using imaging, showing that there were loose interactions. Recently, a paper showed that macrophages showed motility and moved towards erythroblasts when in the right media<sup>187</sup>. These studies indicate that there is still more to be learned of the erythroblast-macrophage interaction while it is studied dynamically.

## 1.6 Aims

This project will investigate how the central macrophage and proerythroblasts are initially attracted and then detach once the cells have enucleated. To do this, a novel methodology will have to be designed to study the interactions between the human erythroblasts and macrophages over time. In particular, the human central macrophage will need to be identified to reproduce the results found in mice. Finding a way to probe the interactions between the cells will provide a way to study the receptors involved in the formation of erythroblastic island, such as the role of the Eph family.

As can be observed in Figure 1-7, we hypothesise that the Eph receptors could be involved in this process; we propose that proerythroblasts would have a higher level of EphB receptors than EphA at their surface, leading them to be attracted when they meet a macrophage in the hematopoietic niche. The cells would then bind via other receptors. As the erythroid cells differentiate, however, their surface composition changes and the EphA family may become the most abundant receptors present at the surface of the cells, leading to the cells being able to detach through repulsion after enucleation.

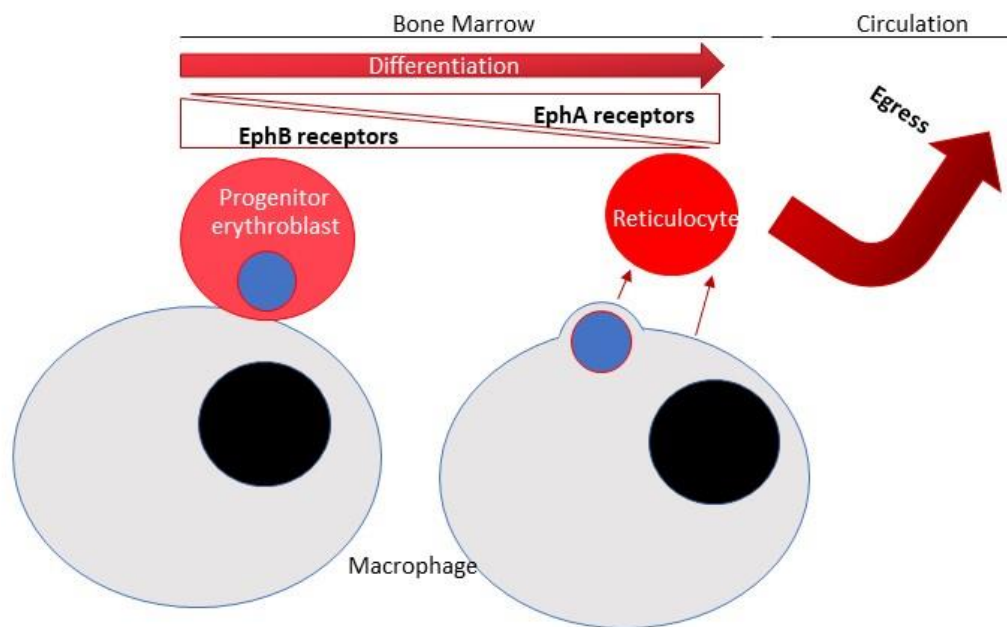


Figure 1-7 - Diagram of current hypothesis

Summary diagram of hypothesis on CIL involvement in erythroblastic island development. As the erythroblast differentiates into a reticulocyte, it loses its EphB4 and EphB6 and does not completely lose its EphA4 receptor leading to the reticulocyte being able to egress into circulation.

Therefore, this project will characterise the contribution of the Eph receptors in the different aspects of macrophage-erythroblast interaction and reticulocyte egress. To achieve this, an assay will be developed to interrogate the process of how human bone marrow erythroblastic islands interactions occur, and also a separate assay to mimic transendothelial migration to study the mechanisms reticulocytes use to egress the bone marrow.

## 2 Chapter 2 – Material and Methods

### 2.1 Material

#### 2.1.1 Buffers and solutions

All chemicals are from Sigma unless otherwise stated.

**Electrophoresis Running Buffer:** 120 mM Trizma (Tris-base), 0.96 mM glycine, 0.5% (w/v) sodium dodecyl sulfate (SDS).

**Fluorescence Activated Cell Sorting (FACS) Buffer:** 2% (v/v) fetal calf serum (FCS; GIBCO), 25 mM HEPES (4-(2-hydroxyethyl)-1piperazineethanesulfonic acid) in phosphate buffered saline (PBS).

**2x HEPES Buffered Saline (HBS):** 0.28 M NaCl, 1.5 M Na<sub>2</sub>HPO<sub>4</sub>, 0.05 M HEPES, [pH7.05].

**Hoechst:** 0.5% (v/v) Hoechst in PBS with 4% bovine serum albumin (BSA) and 2 mg/mL Glucose (PBSAG)

**Imaging media:** Iscove's Medium Dulbecco's Medium (IMDM), 3% Human Serum, 10 U/mL erythropoietin, 1 mg/mL holotransferrin

**Integrin Activating Buffer:** Hanks Buffered Saline Solution (HBSS), Glucose, 4% BSA, 2 mg/mL Mn<sup>2+</sup>

**Liquid Nitrogen Cell Storage solution:** 10% (v/v) dimethylsulfoxide (DMSO), 50% (v/v) fetal bovine serum (FBS) (Life Technologies) in phosphate buffered saline (PBS)

**Magnetic Activated Cell Sorting (MACS) Buffer:** 0.5% (w/v) BSA, 0.6% (v/v) citrate-phosphate-dextrose in PBS.



**Media from Rhodes et al.:** IMDM, 1%BSA, 30% FCS, 0.1 mM  $\alpha$ -thioglycerol (Sigma), 4 U/mL erythropoietin

**Mowiol:** 25% (v/v) glycerol, 3.2 M Mowiol 4-88, 100mM Tris(hydroxymethyl)aminomethane-hydrochloride (Tris-HCl), 2.5% (w/v) 1,4-diazabicyclo-[2.2.2]octane (DABCO) [pH 8.5]

**NP-40 Lysis Buffer:** 20 mM Tris-HCl) [pH 8.0], 137 mM NaCl, 10 mM ethylenediaminetetraacetic acid (EDTA), 100 mM NaF, 1% (v/v) Nonidet P-40, 10% (v/v) glycerol, 10 mM sodium orthovanadate ( $\text{Na}_3\text{VO}_4$ ), 2 mM phenylmethylsulfonyl fluoride (PMSF), 1% (v/v) protease inhibitor cocktail set V (Calbiochem).

**Phosphate Buffered Saline (PBS):** 3.2 mM  $\text{Na}_2\text{HPO}_4$ , 0.5 mM  $\text{KH}_2\text{PO}_4$ , 1.3 mM KCl, 135 mM NaCl, [pH7.4].

**Red Cell Lysis Buffer:** 155 mM  $\text{NH}_4\text{Cl}$ , 0.137 mM EDTA, 1mM  $\text{KHCO}_3$  [pH7.5].

**SDS PAGE Sample Buffer:** 50 mM Tris [pH8], 12% (w/v) glycerol, 10% SDS, 2 mM EDTA, 10%  $\beta$  mercaptoethanol, 2 mM PMSF.

**Semi dry blotting transfer Buffer:** 39 mM Glycine, 48 mM Tris-base, 1.3 mM SDS in 20% methanol.

**Soerensen (SBS) Buffer:** 14.7 mM  $\text{KH}_2\text{PO}_4$ , 2 mM  $\text{Na}_2\text{HPO}_4$  with 120 mM Sorbitol [pH7.8]

**Stripping Buffer:** 20 mM SDS and 24.7 mM TrisBase [pH 6.7]

**Tris-acetate-EDTA (TAE):** 40 mM TrisBase, 20 mM acetic acid and 1 mM EDTA.

**Tris Buffered Saline (TBS) Tween:** 25 mM Tris-base, 0.15 M NaCl, 0.02% TWEEN-20 (Sigma), [pH7.7].

## 2.1.2 Antibodies

### 2.1.2.1 Primary antibodies

International Blood Group Reference Laboratory (IBGRL) provided many monoclonal antibodies created using mice hybridoma. The culture supernatant can then be used neat or diluted in experiments.

Antibody name	Protein target	Species	Type	Source	Use
AKT	Akt	Rabbit	Polyclonal	Cell Signalling Technology	WB (1:1000)
Bric 256	GPA	Mouse	Monoclonal	IBGRL	IF (1:2)
Bric 273	Protein 4.2	Mouse	Monoclonal	IBGRL	WB (1:1000)
Bric 170	Band 3/Anion exchanger 1	Mouse	Monoclonal	IBGRL	IP (neat)
Cas 9	Cas 9	Mouse	Monoclonal	Biolegend	WB (1:500)
E-Cadherin	E-Cadherin	Rabbit	Polyclonal	Cell Signalling Technology	WB (1:1000)
EphA4	EphA4	Rabbit	Polyclonal	Abcam	WB (1:500)

EphA4	EphA4	Rabbit	Polyclonal	Proteintech	Flow (1:50)
EphA4	EphA4	Mouse	Monoclonal	Santa Cruz	WB (1:1000)
EphA4	EphA4	Rabbit	Polyclonal	Gift from Prof David Wilkinson	WB (1:200)
EphA4 (ab5389)	EphA4	Rabbit	Polyclonal	Abcam	WB (1:500)
EphA4 (ab5396)	EphA4	Rabbit	Polyclonal	Abcam	WB (1:500)
EphA5	EphA5	Rabbit	Polyclonal	Santa Cruz	WB (1:500)
EphA5	EphA5	Rabbit	Polyclonal	Abcam	WB (1:500)
EphB1	EphB1	Goat	Polyclonal	Santa Cruz	WB (1:500)
EphB1	EphB1	Mouse	Monoclonal	Santa Cruz	WB (1:500)
EphB4	EphB4	Rabbit	Polyclonal	Novus	WB (1:500)

EphB6	EphB6	Mouse	Monoclonal	Abnova	WB (1:500)
EphrinA1	EphrinA1	Rabbit	Polyclonal	Santa Cruz	WB (1:1000)
EphrinB2	EphrinB2	Rabbit	Polyclonal	Novus	WB (1:1000)
Erk	Erk	Mouse	Monoclonal	Sigma	WB (1:1000)
GAPDH	GAPDH	Rabbit	Polyclonal	Santa Cruz	WB (1:1000), Flow (1:50)
GFP	GFP	Mouse	Monoclonal	Roche	WB (1:2000)
HUTS-21	Integrin $\beta$ 1 (Active)	Mouse	Monoclonal	BD Pharmingen	Flow (1:50)
Integrin $\beta$ 1	Integrin $\beta$ 1	Rabbit	Monoclonal	Abcam	Flow (1:50)
Integrin $\beta$ 1	Integrin $\beta$ 1	Mouse	Monoclonal	IBGRL, NHSBT Filton	WB (1:1000)

Macrophage	Calprotectin	Mouse	Monoclonal	Abcam	IF (1:800)
Phospho AKT	Serine 473 on Akt	Rabbit	Polyclonal	Cell Signaling Technology	WB (1:250)
Phospho Erk	Phosphothreonine ERK-1&2	Mouse	Monoclonal	Sigma	WB (1:1000)
Sec23A	Sec23A	Rabbit	Polyclonal	In house	WB (1:500)
Sec23B	Sec23B	Rabbit	Polyclonal	In house	WB (1:500)
VCAM1	VCAM1	Mouse	Monoclonal	Santa Cruz	Flow (1:50)
YNTU	Band 3	Rabbit	Polyclonal	In house	WB (1:1000)
CREB3L2	CREB3L2/BBF2H7	Rabbit	Polyclonal	Proteintech	WB (1:500)
IgG		Human		Jackson ImmunoResearch	Flow
IgG2a		Mouse		BD Pharmingen	Flow

IgG1		Mouse		BioLegend	Flow
------	--	-------	--	-----------	------

Table 2-1 Primary antibodies used in this thesis

### 2.1.2.2 Directly-conjugated antibodies

Antibody target	Species	Fluorophore	Isotype	Source	Dilution
CD14	Mouse	Pacific Blue	IgG2a	BD Pharmingen	1:150
CD16	Mouse	FITC	IgG2a	BioLegend	1:100
CD34	Mouse	VioBlue	IgG2a	Miltenyi Biotec	1:20
CD36	Mouse	PE	IgG2a	Miltenyi Biotec	1:20
CD61	Mouse	APC-Vio770	IgG1	Miltenyi Biotec	1:20
CD106	Mouse	PE	IgG1	BioLegend	1:100
CD163	Mouse	PE	IgG1	Miltenyi Biotec	1:100
CD169	Mouse	APC	IgG1	Miltenyi Biotec	1:100
CD209	Mouse	PE	IgG1	AbD Serotec	1:100
CD206	Mouse	APC	IgG1	BD Pharmingen	1:100
CD235a (GPA)	Human	APC	IgG1	Miltenyi Biotec	1:20
Isotype IgG1	Mouse	APC-Vio770		Miltenyi Biotec	
Isotype IgG1	Mouse	APC		BD Pharmingen	
Isotype IgG1	Mouse	PE		BioLegend	
Isotype IgG2a	Mouse	FITC		BioLegend	

Isotype IgG2a	Mouse	VioBlue		Miltenyi Biotec	
Isotype IgG2a	Mouse	PE		Miltenyi Biotec	

Table 2-2 - Directly-conjugated antibodies used in this thesis

### 2.1.2.3 Secondary antibodies

HRP-conjugated rabbit anti-mouse, swine anti-rabbit, rabbit anti-goat (DAKO) for immunoblotting.

Alexa-488™, Alexa594™ or Alexa647™ conjugated goat anti-mouse or anti-rabbit (Life Technologies) or Goat anti-human IgG+IgM 647 (Jackson ImmunoResearch).

APC or PE-conjugated anti-mouse IgG from BioLegend. PE-conjugated anti-rabbit IgG from BioLegend.

EphrinB2-Fc, ephrin-A1-Fc, EphB4-Fc and VCAM1-Fc constructs came from R&D systems.

### 2.1.3 Equipment

#### 2.1.3.1 Confocal Microscopy

Leica SP5 confocal microscope (63X oil immersion lens 1.4NA) in the Wolfson Bioimaging Facility, University of Bristol.

#### 2.1.3.2 Widefield Microscopy

Olympus IX81, 63x oil immersion lens (NA 0.17), coupled with the Olympus soft imaging solutions MT20, a heater from Okolab and a Camera from Hamamatsu C11440 (Toye laboratory).

Leica DMI6000 inverted epifluorescence microscope coupled with Leica LASX live cell imaging workstation with Leica DFC365FX monochrome CCD camera (1392x1040 6.45µm pixels, 8 or 12 bit, 21 fps full frame) in the Wolfson Bioimaging Facility.

#### *2.1.3.3 Tissue Culture microscope*

Olympus CK2 10x objective (Toye laboratory)

Incucyte Zoom (Essen BioSciences) in the Wolfson Bioimaging Facility

#### *2.1.3.4 Cytospin Microscope*

Olympus CX31 coupled with the Olympus soft imaging solutions LC20 (Toye laboratory).

#### *2.1.3.5 Flow Cytometers*

MACSQuant VYB flow cytometer (Miltenyi Biotech, Toye laboratory). Cell sorter used was a BD Influx

BD Influx Cell Sorter (BD Biosciences) within the University of Bristol Flow cytometry facility run by Dr Andrew Herman.

#### *2.1.3.6 Mass Spectrometers*

Thermo Scientific Orbitrap Fusion Tribrid Mass Spectrometer with up-stream Ultimate 3000 nano-LC system and Thermo Scientific LTQ-Orbitrap Velos Mass Spectrometer with up-stream Ultimate 3000 nano-LC system in the Proteomics Facility at the University of Bristol run by Dr Kate Heesom.

#### *2.1.3.7 Centrifuges*

Centrifuge 5415 R from Eppendorf, centrifuge 5804 from Eppendorf and Rotina 380R from Hettich zentrifugen



#### 2.1.4 RT-PCR primer sequences

Name	Sequence	Length	mRNA coverage
EphA1 Forward	AGACCTTAAAAGACACATCCCC	490 lgt	4 exons
EphA1 Reverse	ACCTCCCACATCACAATCCC		
EphA2 Forward	TTGGCTTCTTTATCCACCGC	226 lgt	3 exons
EphA2 Reverse	TTGTACACCTCCCCAACTC		
EphA3 Forward	ATGTTTCCAGACACGGTACC	269 lgt	2 exons
EphA3 Reverse	CCATCTTCCTGAGTAGAACTGTGAGG		
EphA4 Forward	ACAGACAAACAGAGGAGAGAC	265 lgt	3 exons
EphA4 Reverse	CCAGATCACGATGCACATAG		
EphA5 Forward	CCTTCTGTGGTACGACACTTG	221 lgt	2 exons
EphA5 Reverse	GGTCTGCACACTTGACAGGTG		
EphA6 Forward	CCG CTG TTG GCG GAT TCA CTC	490 lgt	5 exons
EphA6 Reverse	AGGAAGCTGGGGCAAACGCCTCCAC		

EphA7 Forward	TCAACATCAACCAAACCACAG	553 lgt	4 exons
EphA7 Reverse	CCATAACCAGCAGCAGTAAAAG		
EphA8 Forward	ATG GAG GTG GAG ACC GGG AAA C	218 lgt	3 exons
EphA8 Reverse	TGA TGC AGA GGC AGG AAG ACA G		
EphB1 Forward*	TTC ACT TCA GCC AGC GAC	590 lgt	3 exons
EphB1 Reverse*	TTT CCC TCC TCT CCT TCC C		
EphB1 Forward 2	CTTTGACCCTCCAGAAGTGG	202 lgt	2 exons
EphB1 Reverse 2	CTCCACATTGTCGTCACAGC		
EphB2 Forward	ATGGCGCCCCTCTCCTCTGGCATCA	328 lgt	3 exons
EphB2 Reverse	ACCGCTTGGTTCTTCCCGTG		
EphB3 Forward*	GCA TCG CCT CCA CAG TGA CC	226 lgt	3 exons
EphB3 Reverse*	ACG AAG ACA AGC CCA GCT GTA		
EphB3 Forward 2	CGGTCCCAGATTACACAACC	148 lgt	2 exons

EphB3 Reverse 2	CCAATACGGAGCAGGTCTTC		
EphB4 Forward	TTCGGCCAGGAACATCACAG	200 lgt	3 exons
EphB4 Reverse	CCGATGAGATACTGTCCGTG		
EphB6 Forward	TACCTGTCCAGCTTTGCC	224 lgt	2 exons
EphB6 Reverse	TCTCCATAACTCATCACTTCCC		

Table 2-3 - RT-PCR primers used in this thesis

#### 2.1.5 ShRNA Hairpin sequences

Hairpins were purchased from Dharmacon in the plko.1 plasmid.

	Clone ID	Mature AntiSense Sequence
EphA4 1	TRCN0000010153	ATGGATGATGGTGCTGCTTGG
EphA4 2	TRCN0000010161	TTTGATATCTGTGTTCTGTC
EphA4 3	TRCN0000010164	TAAATACTTCATCCCAGACCC
EphA4 4	TRCN0000010165	TTTATAGAACACACGGACTGA
EphB4 3	TRCN0000001774	AATGTCACCCACTTCAGATCA
EphB6 2	TRCN0000002017	TTGAGGAAGTGTCTGGAAATA

Table 2-4 - shRNA hairpins used in this thesis

#### 2.1.6 CRISPR gRNA sequences

Guide sequences were designed by the Broad Institute and purchased from Genscript.

Guide sequences were chosen within the first or second exons.

Name	Vector	gRNA Sequence
------	--------	---------------

EphA4 CRISPR Guide 3	pLentiCRISPR v2	ACCTCGTGACCTGTGACCG
EphA4 CRISPR Guide 4	pLentiCRISPR v2	GTAGTGGACCCCACTTCCAC

Table 2-5 - CRISPR gRNA used in this thesis

### 2.1.7 EphA4 gene sequencing primers

Primers were designed to be around the CRISPR guide sequences to check for mutations.

Name	Sequence
EphA4 Forward	CGGCCCTGGGAAGTAGAATC
EphA4 Reverse	AAGTGCTCTGATGTCCAGCC

Table 2-6 - Gene sequencing primers used in this thesis

### 2.1.8 Peptide sequences

The following biotinylated inhibitory peptides and controls were synthesized by Cambridge Peptides UK.

Name	Sequence	Purity
Integrin $\alpha$ 4 (EIL)	EILDVPSTGSGSK(Bio)	96.130 and 90.997%
EphB4 (TNYL)	TNYLFSPNGPIARAWGSGSK(Bio)	97.205% and 96.199%
EphB4 Control (DYP)	DYPSMAMYSPSVGSGSK(Bio)	83.563% and 91.083%
Pan-EphB receptor (THW)	THWCHLLNCAALGSGSK(Bio)	96.988%
EphB4 Scrambled control (LFTA)	LFTAPRAYIPWSNNGSGSK(Bio)	94.261%

Table 2-7 - Peptides used in this thesis

### 2.1.9 ATP inhibitors

A74 was kindly gifted by Dr. Young, NF449 and MRS2578 were purchased from Tocris Bioscience and BX430 was purchased from Sigma.

## 2.2 DNA preparation and RNA preparation

### 2.2.1 Transformation

50  $\mu$ l of competent NEB 10  $\beta$  E. coli cells (New England BioLabs (NEB), Herts UK) were thawed on ice for 10 minutes before transferring to an ice cold tube containing between 1 pg to 100 ng plasmid DNA. The mixture was incubated on ice for 30 minutes, subjected to heat-shock for 30 seconds at 42°C, and then incubated on ice for a further 5 minutes. 200  $\mu$ l Luria Broth (LB) prewarmed to 37°C, was then added and placed in an orbital shaking incubator (250rpm) at 37°C for an hour. 100 $\mu$ l of the transformed E. Coli in LB mixture was spread onto pre-warmed selection plates and incubate overnight at 37°C.

### 2.2.2 Minipreps

5 mL of LB with the appropriate antibiotic was inoculated with a single bacterial colony and grown overnight in the shaking incubator (250rpm) at 37°C. DNA was typically isolated from 3 mL of the overnight culture using the Qiagen Spin Miniprep Kit (Qiagen), according to the manufacturer's instructions. Isolated DNA was eluted in deionised water (dH<sub>2</sub>O) and stored at -20°C. The concentration of purified DNA was measured using a NanoDrop ND-1000 spectrophotometer (Labtech International).

### 2.2.3 Maxipreps

5 mL of LB was inoculated with a single bacterial colony in the presence of the appropriate antibiotic for 8 hours at 37°C in a shaking incubator (250rpm). This starter culture was then diluted 1 in 1000 into 250 mL LB containing appropriate antibiotics and

incubated overnight in a shaking incubator (200rpm) at 37°C. Bacteria were harvested from the media by centrifugation at 6,000g for 30 minutes at 4°C. DNA was isolated using the Qiagen Plasmid Maxi (Endo-Free) Kit (Qiagen), according to the manufacturer's instructions. DNA was eluted in dH<sub>2</sub>O and stored at -20°C. The concentration of purified DNA was measured using a NanoDrop ND-1000 spectrophotometer (Labtech International).

#### 2.2.4 Reverse Transcription Polymerase Chain Reaction (RT-PCR)

RNA was extracted using the Quick-RNA Microprep (Zymo research) from 1x10<sup>6</sup> cells at the indicated timepoints. cDNA was synthesised from 100 ng DNase-treated RNA using Superscript III (Invitrogen). Realtime PCR was performed using 1 µl of cDNA using Fast Cycling PCR kit (Quiagen). The DNA was then visualised using an agarose gel.

#### 2.2.5 PCR of genomic DNA for sequencing

1x10<sup>5</sup> BEL-A cells' DNA was isolated following manufacturer's instructions using the DNeasy Blood and Tissue kit (Qiagen). 500 ng of DNA was used to perform PCR to expand the EphA4 piece with Q5 Mastermix (NEB). The product from the PCR was purified with the Qiaquick PCR purification kit (Qiagen) and sent to Eurofins for sequencing with the original Forward primer used to create the PCR product.

#### 2.2.6 Agarose gel electrophoresis

2% (w/v) agarose was added to 1xTAE buffer and heated up using a microwave. 0.5 µM ethidium bromide (Sigma) was added to the TAE. The agarose was added to a gel mould with a comb. After the gel set, DNA was added to the holes created by the comb. Quick-load purple 100bp DNA ladder (NEB) was used alongside the DNA samples to assess the

size of DNA bands. The gel was electrophoresed at 120 volts for 25 minutes and then visualised using Gel Doc EZ System (Biorad).

## 2.3 Tissue culture

### 2.3.1 Primary Peripheral Blood and Bone Marrow Samples

#### 2.3.1.1 *Ethical Approval*

Blood was obtained from healthy blood donors and written informed consent was given in accordance with the Declaration of Helsinki. In the majority of cases the blood was obtained from anonymous waste platelet apheresis cones (Apheresis Unit - Southmead Hospital and Non-Clinical Issue, NHSBT Bristol). Ethics approval for all experimental protocols was granted by Bristol Research Ethics committee (REC number 12/SW/0199) and all methods were carried out in accordance with approved protocols and guidelines.

Bone marrow aspirate samples from hip replacements, from which macrophage were isolated and analysed, were provided by Dr Micheal Whitehouse, University of Bristol and provided with informed consent for research use and used under Bristol Research Ethics Committee approval (REC 12/SW/0199).

#### 2.3.1.2 *Isolation of Peripheral Blood Mononuclear Cells*

Waste peripheral blood mononuclear cells' (PBMNCs) erythrocytes were isolated from healthy donors following platelet apheresis (NHSBT, Filton). The peripheral blood sample was mixed with 0.6% v/v citrate dextrose solution (ACD; Sigma), diluted 1:1 with Hanks balanced salt solution (HBSS; Sigma) plus 0.6% v/v ACD and layered over 25 mL Histopaque 1077 (Sigma). After centrifugation at 400g, RT, 35 min (Hettich Zentrifugen, Rotina 380R, 1754 rotor) the interface mononuclear cell layer was collected, washed 3 times in HBSS and any remaining erythrocytes lysed in 12 mL Red Cell Lysis Buffer, while

incubating on ice for 10 minutes. Cells were washed 2 times in HBSS and counted using a haemocytometer and Trypan Blue solution (Sigma) to distinguish between live and dead cells.

#### *2.3.1.3 Isolation of bone marrow mononuclear cells*

Bone marrow aspirate samples from which macrophage were isolated and analysed were provided by Dr Micheal Whitehouse, University of Bristol and provided with informed consent for research use. Cells were washed out of universal sample tube with HBSS (Sigma) containing 0.6% acid citrate dextrose (ACD) to remove the heparin coated beads (included to prevent coagulation). The red pulp was macerated onto a 70 µm filter. Cells were washed once more with Hanks and 0.6% ACD; cells were centrifuged at 300g between washes. Red cells were lysed using red cell lysis buffer for 10 minutes on ice, cells were washed again in Hanks with ACD, counted and frozen down in Liquid Nitrogen Cell Storage solution at -80°C in a Mr. Frosty (Nalgene).

#### *2.3.1.4 CD34<sup>+</sup> isolation from PBMCs and culture*

MACS CD34<sup>+</sup> isolation was performed on the PBMC cells according to the instructions for the direct CD34<sup>+</sup> progenitor cell isolation kit (Miltenyi Biotech). Briefly, the PBMC cells were resuspended in MACs Buffer with CD34<sup>+</sup> beads for 30 minutes at 4°C. The cells were then washed and passed through a magnetic column and washed 3 times. The cells were then eluted from the column by removing the magnet. The isolated CD34<sup>+</sup> cells were counted and plated at a density of 1x10<sup>6</sup> cells/mL in primary medium composed of Iscove's medium (Biochrom; Source Bioscience UK Ltd) supplemented with 3 U/mL erythropoietin (Bristol Royal Infirmary), 100 ng/mL Stem Cell Factor (SCF, Miltenyi Biotech), 1 µM dexamethasone (Sigma), 40 ng/mL insulin-like growth factor-1



(IGF-1, R&D Systems), 0.5% v/v cholesterol-rich lipids (Sigma), 1 ng/mL IL-3 (R&D Systems) and 100 units/mL penicillin and 100 µg/mL streptomycin. The cells were incubated at 37°C in 5% CO<sub>2</sub> in primary media until Day 3 of culture<sup>141</sup>.

#### *2.3.1.5 Expansion culture of erythroid progenitors and erythroblasts*

On Day 3, the culture CD34<sup>+</sup> progenitors/erythroblasts were counted and reseeded in expansion media. A base Biochrom media composed of Iscove's medium (Source Bioscience UK Ltd) supplemented with 10 µg/mL insulin (Sigma), 3 U/mL heparin (Sigma), 200 µg/mL holotransferrin (Sigma), 3% v/v heat deactivated human, male AB Serum (Sigma), 2% v/v Foetal Bovine Calf Serum (Life Technologies) was in turn supplemented with 3 U/mL erythropoietin (Bristol Royal Infirmary), 100 ng/mL stem cell factor (SCF, Miltenyi Biotech), 1 µM dexamethasone (Sigma), 40 ng/mL insulin-like growth factor-1 (IGF-1, R&D Systems), 0.5% v/v cholesterol-rich lipids (Sigma) and 100 units/mL penicillin and 100 µg/mL streptomycin (Sigma) to give expansion media. The cells are put at 0.5x10<sup>6</sup> cells/mL, with media topped up every day to ensure the cells stay at this density.

The final phase of erythropoiesis, terminal erythroid differentiation, was induced in the erythroblasts on Day 7 of culture by first washing the cells in PBS three times to dilute the dexamethasone out of the culture and then reseeding the cells in differentiation media. This final phase media consisted of the base Biochrom media supplemented with 10 U/mL erythropoietin (Bristol Royal Infirmary), 10 µg/mL insulin (Sigma), 1 mg/mL holotransferrin (Sanquin), 3% v/v human, male AB Serum (Sigma), 1 µM T3 thyroid hormone (Sigma), 40 ng/mL insulin-like growth factor-1 (IGF-1, R&D Systems), 0.5% v/v cholesterol-rich lipids (Sigma) and 100 units/mL penicillin and 100 µg/mL streptomycin

(Sigma). During this phase, cells were maintained at a density of between 2 and  $4 \times 10^6$  cells/mL by daily counting and partial media changes, where cells were centrifuged at 300g for 5 minutes, half of the media was removed and then the cells were resuspended in the amount necessary to be at the right dilution. Reticulocytes were filtered at T168 through a 5  $\mu$ m filter (Pall).

#### *2.3.1.6 Macrophage culture*

PBMC cells isolated as detailed above (section 2.3.1.2) were resuspended at a density of  $3 \times 10^6$ /mL in RPMI supplemented with 100 units/mL penicillin, 10% Foetal Bovine Calf Serum and 25 ng/mL M-CSF, +/- 1  $\mu$ M dexamethasone. The media was changed every third day, and macrophage selection conducted either by adhesion selection, or where stated, the CD14<sup>+</sup> cells are isolated using a CD14 bead isolation kit (Miltenyi), keeping only the cells which stayed adhered to the plate. The macrophages were considered mature at Day 7. To perform flow cytometry, the cells are scraped off the plate with a cell scraper (Corning) before being counted with Countess II Automated Cell Counter (Invitrogen).

#### *2.3.1.7 Sanquin macrophage and erythroblast cell culture protocol*

From Heideveld et al.<sup>60</sup>. CD14 and CD34 MicroBeads (Miltenyi Biotec; Bergisch Gladbach, Germany) were used for cell isolation from peripheral blood. CD14<sup>+</sup> monocytes were cultured at  $1.5-3 \times 10^6$  cells/well (CASY<sup>®</sup> Model TCC, Schärfe System GmbH; Reutlingen, Germany) in a 12-well plate as described<sup>17</sup>. CD34<sup>+</sup> cells were differentiated towards erythroblasts<sup>17</sup>, with the addition of 1ng/ml IL-3 (R&D systems; Abingdon, UK) at the start of culture. Media was replenished every two days. After 8-10 days, cells were differentiated towards reticulocytes by removing dexamethasone,

increased EPO (10 U/mL, ProSpec; East Brunswick, NJ) and addition of heparin (5 U/mL, LEO Pharma B.V.; Breda, The Netherlands), 5% pooled AB+ plasma and holotransferrin (700 µg/mL, Sanquin; Amsterdam, The Netherlands). Every other day, half the media was replenished. For co-culture experiments, CD14+ cells were differentiated with (GCmacrophages) or without dexamethasone for three days and co-cultured with erythroblasts (day 8-10 of culture; ratio 1:1.5) or more differentiated erythroid cells (day 6 of differentiation; ratio 1:4) for 24 hours. Informed consent was given in accordance with the Declaration of Helsinki and Dutch national and Sanquin internal ethic boards.

### 2.3.2 Mammalian Cell Line Culture

#### 2.3.2.1 *HeLa and HEK293T cell culture*

HEK293T and HeLa cells were cultured in Dulbecco's Modified Eagle Serum (DMEM) with 4mM GlutaMAX (GIBCO, Life Technologies) containing 10% (v/v) FCS, penicillin (100 units/mL) and streptomycin (100 µg/mL) and incubated in 5% CO<sub>2</sub> at 37°C. Cells were incubated with 0.25% Trypsin-EDTA (1X), Phenol Red (GIBCO, Life Technologies) for 5 minutes to dissociate the cells to facilitate passaging for cell culture passage or harvesting for western blotting.

#### 2.3.2.2 *Bone Marrow Endothelial Cells cell culture*

Bone Marrow Endothelial Cells (BMEC) cells were a kind gift from Dr. Jim Middleton (Dental School, Bristol University). BMEC cells were cultured in DMEM-F12 (Lonza) containing 10% FCS, penicillin (100 units/mL) and streptomycin (100 µg/mL) and incubated in 5% CO<sub>2</sub> at 37°C. Cells were incubated with 0.25% Trypsin-EDTA (1X), Phenol

Red (GIBCO, Life Technologies) for 5 minutes to dissociate the cells to facilitate cell culture passage or harvesting.

#### 2.3.3 Calcium phosphate precipitation transfection of HEK293T cells

HEK293T cells were grown to 50% confluency in DMEM media supplemented with 10% (v/v) FCS before transfection. In a separate tube, the lentiviral packaging vectors pMO2.VSVG (5 µg) and pPAX (15 µg) and 20 µg of cDNA or shRNA plasmid vector were mixed with 500 µl of CaCl<sub>2</sub> (0.25 M), and then 500µl of 2x HEPES buffered saline (HBS). The HBS was added dropwise while vortexing, before being allowed to precipitate for 30 minutes at room temperature. The precipitate was then added dropwise to the HEK293T dish and left for 18 hours at 5% CO<sub>2</sub> at 37°C, at which point the media was removed and replaced with fresh media. The cells were then incubated for 48 hours at 5% CO<sub>2</sub> at 37°C. The virus was then concentrated using 1 volume of Lenti-X Concentrator (Clontech) to 3 volumes of the supernatant, and then mixed by inversion. After incubation at 4°C centrifuge for 45 minutes the Lenti-X Concentrator-virus mix was centrifuged at 1,500g at 4°C. The supernatant was discarded, and the pellet gently resuspended in 100 µl Biochrom media. Virus was either snap frozen and stored at -80°C or used immediately.

#### 2.3.4 Lentiviral transduction of erythroblasts and macrophages

50-100 µl of concentrated virus was used to transduce 0.5-1 x 10<sup>6</sup> CD34<sup>+</sup> cells or 1x10<sup>6</sup> CD14<sup>+</sup> cells in the presence of 8 µg/mL polybrene (Sigma), and then incubated for 24 hours at 5% CO<sub>2</sub> at 37°C before washing the cells two times with PBS and adding fresh media. To select for successfully virally-transduced cells for the pLKO knockdowns, 1

µg/mL puromycin was added 24 hours after the virus had been washed off and 1 µg/mL puromycin was maintained in the culture media until the cells began to differentiate.

## 2.4 Reconstitution of erythroblastic islands

### 2.4.1 Method 1 - Tiescan

The frozen bone marrow mononuclear cells were thawed and washed twice with PBSAG. CD14<sup>+</sup> isolation was then performed according to the instructions for the direct CD14<sup>+</sup> cell isolation kit (Miltenyi Biotec). The cells were counted and resuspended in 500µl PBSAG. CD14-Pacific Blue, CD106-PE and CD169-APC are added to the cells for 30 minutes at 4°C in the dark. The cells are then washed 2x in PBSAG. The cells populations were then sorted using a BD Influx Cell Sorter into sorting buffer. The cells were then resuspended in imaging media and left to adhere overnight as indicated in the figure legends. The next day, day 6 erythroblasts were added at a ratio of 10:1 and left to adhere overnight in imaging media. The excess cells were then removed by gentle pipetting. The imaging disk (MaTek) was then imaged on a widefield Leica DMI6000.

### 2.4.2 Method 2 - Incucyte

The macrophages were cultured for 7 days, as in Section 2.3.1.6, in a 24 well plate (Corning; cannot currently be done in a 12 well plate). At day 7, the cells were labelled following manufacturer's instructions with Cell Tracker Green CFMDA (Thermo Fischer). When bone marrow macrophages were used, the cells were isolated as in section 2.3.1.3 and the Cell Tracker CFMD label added immediately after isolation. The media with Cell Tracker is then removed and replaced with imaging media. Day 6 erythroblasts were then added to the macrophages at a ratio of 10:1. In the case of inhibitor experiments, after inhibitors were applied the excess erythroblasts were removed the

following day by gentle washes and new media was added. For the receptor knockdown experiments, the day 6 erythroblasts were added at a ratio of 2:1 to the macrophages the day of the imaging. The plate was then put in the Incucyte (Essen BioScience) to image every hour at 20x at 36 points per well.

#### 2.4.3 Transmigration assay

250 000 BMECs were seeded on each (fibronectin-coated if indicated (Santa Cruz)) 3µm pore size inserts in 500 µl media (800 µl in the bottom chamber) with FBS in 24 well plates. When cells were seeded on the bottom of the insert, the cells were left to adhered for 1h at 37°C before the insert was inverted. These were left overnight at 5% CO<sub>2</sub>, 37°C. Where indicated, 10 ng/mL TNF-α (R&D systems) was added to the cell media for 24 hours. Finally, 250 000 reticulocytes were added on top in IMDM media and 100% serum was put on the bottom and left overnight. The cells were counted using the MacsQuant Flow Cytometer.

### 2.5 Imaging and flow cytometry

#### 2.5.1 Flow Cytometry

Fresh cells or paraformaldehyde fixed cells ( $5-20 \times 10^4$ ) were labelled for 45 minutes at room temperature with primary antibodies. The cells were then washed twice and resuspended in the corresponding secondary antibody for 30 minutes at 4°C. The cells are then washed twice more. In the case of directly conjugated antibodies, the cells were labelled for 30 minutes at 4°C. The cells were then washed twice before processing on the MacsQuant.

### 2.5.2 Fluorescent Activated Cell Sorting (FACS)

Erythroblasts were first labelled with specific antibodies and then washed once with PBSAG before being resuspended in sterile FACS buffer on ice. Sorted cells were then collected into sterile 10% FCS.

### 2.5.3 Flow Cytometry of macrophage surface receptors

Adherent macrophages were lifted from tissue culture plastic by scraping with a cell scraper. Fresh cells were labelled with specific antibodies (see figure legends). Cells were auto-labelled with propidium iodide (Miltenyi Biotec) to label dead cells before measurement to a final concentration of 1 µg/mL (wt/vol).

### 2.5.4 Receptor Binding flow cytometry assay

All ephrin-Fc constructs and VCAM1-Fc construct came from R&D systems. Human IgG (Jackson ImmunoResearch) was used in ephrin-Fc binding experiments as a control. Goat anti-human IgG+IgM 647 (Jackson ImmunoResearch) was used to precluster the ephrin constructs. The antibody used to detect active integrin was mouse anti-human CD29 from BD Pharmingen with its isotype control.  $0.2 \times 10^5$  cells were washed in PBSAG. The ephrin construct was pre-clustered with anti-Fc human secondary at a ratio of 5:1 for 55 minutes. The clustered antibodies are then added to the cells for 30 minutes at 4°C in the dark. For VCAM-Fc binding, the cells were pre-activated with HanksAG with 2 µg/mL Manganese. The VCAM construct was then added to the cells for 45 minutes at room temperature. The cells were washed 2 times in HanksAG. The secondary was then added to the cells for 30 minutes at 4°C in the dark and then the cells washed twice in HanksAG/PBSAG. In inhibitory experiments, peptide inhibitors were added first 15 minutes before the addition of ephrin construct, and then the CD29 antibody 15 mins

after the ephrin construct. The CD29 antibody was then left for 45 minutes on the cells at 4°C in the dark. The cells were washed 2 times in PBSAG. The secondary against CD29 was then added for 30 minutes at 4°C in the dark. The cells were washed twice again. The cells were then visualized by MacsQuantVYB (Miltenyi). All data were analysed using FlowJo version vX.0.06 (FlowJo, Ashland, OR).

#### 2.5.5 Immunofluorescence

Cells for imaging were fixed in 1% paraformaldehyde in 1% PBSA (late erythroblasts and reticulocytes were fixed using 1% paraformaldehyde with 0.0075% glutaraldehyde in 1% PBSAG and 2 mg/mL glucose) and allowed to lay down or were cytopspun onto poly-L-lysine. Cells were then permeabilised using 0.05% Triton X-100 (Fluka) for 5 minutes at room temperature and washed twice in PBS. Coverslips were then blocked with PBSAG for 1 hour. Slides were washed 3 times with PBSAG before incubating with primary antibody (primary antibody is as stated in figure legends) for 1 hour, again washed 3 times with PBSAG and incubated with the relevant secondary antibody for 1 hour. Slides were washed 3 times in PBSAG. All steps are carried out at room temperature. Finally, coverslips and slides were washed and mounted using Mowiol and allowed to dry at room temperature.

#### 2.5.6 Electron microscopy

From Agbani et al.<sup>188</sup> The carotid artery was carefully excised and added to 2.5% glutaraldehyde in 0.1 mol/L sodium cacodylate buffer for 1 h. The tissue was post-fixed with 1% osmium tetroxide in sodium cacodylate buffer for 1 h, stained with 3% uranyl acetate in deionised water for 30 min and dehydrated through a graded series of ethanol (70%, 80%, 90%, 96%) followed by three washes in 100% ethanol. The ethanol



was replaced with propylene oxide prior to incubation in a 1:1 mixture of propylene oxide and Epon for 24 h. The propylene oxide was left to evaporate for 3 h before the tissue was added to fresh Epon which was hardened for 72 h at 60°C. The artery was sectioned at a thickness of 70 nm.

#### 2.5.7 Cytospin Preparation and Staining

To analyse cell morphology,  $5-10 \times 10^4$  cells were resuspended in 100  $\mu$ L PBS and cytocentrifuged onto slides at 350g for 5 minutes (Thermo Scientific, Cytospin 4) before fixation in methanol for 15 minutes and staining with MayGrünwald's (VWR Chemicals) and Giemsa (Merck Millipore) stains according to manufacturer's instructions.

### 2.6 Protein biochemistry methods

#### 2.6.1 Macrophage cell Surface biotinylation for proteomics

Cells were biotinylated as previously described<sup>189</sup>, briefly cells were washed twice in borate buffer before incubating with 1mg/mL EZ-Link™ Biotin (Thermo Scientific) for 1 hour with mixing by gentle rocking on ice. Keeping cells on ice, cells were washed once in borate buffer and twice in glycine quench buffer. Cells were lysed in NP40 lysis buffer on ice for 5 minutes; nuclear pellet was removed by centrifugation at 4°C with supernatant added to a fresh tube and snap frozen and either used for immunoprecipitation straight away or stored at -80°C before immunoprecipitation.

#### 2.6.2 Cell surface biotinylation of red cells and retics

$15 \times 10^6$  cells were washed once in SBS buffer and then resuspended in 2mg/mL EZ-Link-NHS-Biotinylation in SBS buffer. The cells were incubated on ice for 30 minutes, washed twice in Hanks buffer with BSA. The cells were then pelleted using centrifugation and then lysed using NP-40 buffer. Cells were lysed in NP40 lysis buffer on ice for 5 minutes;

nuclear pellet was removed by centrifugation at 4°C with supernatant added to a fresh tube and snap frozen and either used for immunoprecipitation straight away or stored at -80°C before immunoprecipitation.

### 2.6.3 Band 3 immunoprecipitation

Protein G beads were washed with NP-40 buffer then incubated with 4% BSA and Bric170 antibody for 45 minutes at room temperature. The beads were then resuspended with cell lysates at 4°C for 1h. The beads are then washed 3 times with NP-40 buffer and purged beads after the final wash. The supernatant is then resuspended with streptavidin beads for 45 minutes at 4°C. The streptavidin beads were washed 3 times with NP-40 buffer and then purged. The beads were then processed for proteomics, in Section 2.6.4

### 2.6.4 Proteomics via mass spectrometry

Cell pellets or purged streptavidin beads were fractionated by 1D SDS-PAGE until the dye front had moved approximately 2 cm into the separating gel. Gel lanes were cut into 2 equal portions and in-gel digested with trypsin. Extracted peptides were subjected to Nano LC mass spectrometry. The raw data files were processed using Proteome Discoverer software v1.4 (Thermo Scientific) and searched against the UniProt Human database release version 57.3 (126385 entries) using the SEQUEST (Ver. 28 Reverse. 13) algorithm. Peptide precursor mass tolerance was set at 10ppm, and MS/MS tolerance was set at 0.8 Da. Search criteria included carbamidomethylation of cysteine (+57.0214) as a fixed modification and oxidation of methionine (+15.9949) as a variable modification. Searches were performed with full tryptic digestion, and a maximum of 1 missed cleavage was allowed. The Reverse database search option was

enabled, and all peptide data was filtered to satisfy false discovery rate (FDR) of 5%. The Proteome Discoverer software generates a Reverse “decoy” database from the same protein database used for the search and any peptides passing the initial filtering parameters that were derived from this decoy database are defined as false positive identifications. The minimum cross-correlation factor (Xcorr) filter was readjusted for each individual charge state separately to optimally meet the predetermined target FDR of 5% based on the number of random false positive matches from the Reverse decoy database. Thus, each data set has its own passing parameters

#### 2.6.5 Western Blotting

All cells for lysis were first pelleted by centrifugation for 5 minutes at 300g. Samples were then resuspended at  $1 \times 10^6$  cells/10  $\mu$ l in NP-40 lysis buffer. Cells were then incubated on ice for 10 minutes prior to centrifugation for 10 minutes, 15871g at 4°C to remove nuclei. For cultured erythroblast lysates during terminal differentiation (t=0 to t=168h), the equivalent of  $1 \times 10^6$  cells was loaded per lane. Separation of proteins by sodium dodecyl polyacrylamide gel electrophoresis (SDS-PAGE) was performed using a BioRad Mini PROTEAN® Tetra gel electrophoresis system. Resolving gels of varying dilutions were prepared using a stock solution of 30% (w/v) acrylamide (Severn Biotech), Tris-HCL (pH8.8, final concentration 0.4M) and SDS (final concentration 0.1%). Gel polymerisation was initiated by the addition of 0.4 N,N,N,N- tetramethylene-diamine (TEMED) and 0.1% ammonium persulphate (APS). The stacking gel placed on top of the resolving gel was made using 5% (w/v) acrylamide, 0.13M Tris-HCL (pH6.8), 0.1% (w/v) SDS, 0.1% (w/v) APS and 0.1% TEMED. Sample buffer (50mM Tris-base pH8, 12% (w/v) glycerol, 10% SDS, 2mM EDTA, 10%  $\beta$ -mercaptoethanol) was used to load lysed cells onto the gel after incubation at 95°C for 30 seconds. A prestained protein

standard – PageRuler (NEB) was run alongside the samples. Electrophoresis commenced at 80 Volts in running buffer (190mM glycine, 25mM Tris-base, 0.1% (w/v) SDS) until all the loading dye was observed to have completely entered the stacking gel and then the voltage was increased to 90-120 Volts.

Once resolved the proteins were transferred to polyvinylidene fluoride membrane (PVDF, Millipore Immobilon-P) which in turn was sandwiched between 3MM Whatman paper pre-soaked in transfer buffer (39mM Glycine, 48mM Tris-base, 1.3mM SDS in 20% methanol). PVDF membrane was presoaked in methanol (2 minutes) and transfer buffer (2 minutes). The proteins were transferred using a semi-dry blotter TE77 PWR (Amersham) set at 45mA per gel for a minimum of 90 minutes. Western blots were blocked 30 minutes at room temperature using a 5% milk solution made using Tris-buffered saline with TWEEN (TBST; 25mM Tris, 0.15M NaCl, 0.02% TWEEN-20 (Sigma), pH 7.7). All washes and antibody incubations were generally carried out at room temperature (although for convenience sometimes primary antibody step was carried out at 4°C overnight) with gentle rocking. 5% milk solution was used to dilute primary antibodies to the required concentration. Diluted primary antibodies were then added to the membrane and left to incubate for 1 hour followed by four 5 minute washes of the membrane in TBST. Diluted secondary antibody conjugated to horseradish peroxidase was then incubated with the membrane for 1 hour and the wash step repeated. Secondary antibody was detected by using Amersham ECL Western blotting reagents (GE Healthcare). Membranes are exposed to Hyperfilm (Amersham Biosciences) and developed using an AGFA Curix 60 developer or a GE Healthcare Amersham Imager 600.



### 3 Chapter 3 – Development of a high throughput imaging assay to explore macrophage-erythroblast interactions

#### 3.1 Introduction

As previously discussed (Section 1.5.5), there is currently no established model system for observing how the cellular interactions within human erythroblastic islands occur over time. Several methodologies have been used to assess the importance of different receptors within these islands. Multiple studies<sup>30,37,87,93,98,105,128,181–184</sup> have successfully reconstituted islands by introducing macrophages and erythroid cells together to recapitulate the relationship between the cells. These papers allowed native mice spleen and bone marrow erythroblastic islands to settle on coverslips, and then used a buffer without calcium and magnesium to strip the erythroblasts off the macrophage. The stripping process works by interfering with the adhesion proteins and leading the macrophages to retract their protrusions<sup>87</sup>. The use of serum-free media also leads to detachment of macrophage from erythroblasts<sup>185</sup>. Erythroblasts from different mice genotypes can then be added back to explore their ability to bind to the macrophage<sup>30,37,87,93,98,105,128,181–184</sup>. This technique enabled researchers to establish whether, for example, in the mice bone marrow, the formation of erythroblastic islands was impacted by the lack of ICAM4, an adhesion protein, in erythroblasts or macrophages<sup>93</sup>. The individually isolated cell types can also be added together in suspension in the presence of receptor-specific antibodies for immunofluorescence<sup>37,93</sup>. In all these assays, the cells were fixed immediately after reconstitution, and therefore, the researchers could not analyse the interactions over time.

Studies have also employed electron microscopy to gain an understanding of the placement of these cells<sup>28,35,39,190–193</sup>. In these experiments, the cells were fixed for analysis, and therefore, could not facilitate analysis of the interactions over time. As yet, no studies have adequately investigated the dynamics of the interactions between macrophages and erythroblasts over time.

As discussed in Section 1.3.2.2, there is much interest in the central macrophage. As the isolation of intact islands is difficult, many aspects remain unknown, such as is there one single specific central macrophage or are there many macrophages that can interact with erythroblasts? Seu et al.<sup>92</sup> recently showed that there was heterogeneity within mice bone marrow. The development of an assay to look at macrophage-erythroblast interactions would help not only better establish the receptors necessary at the surface of the macrophage, but also facilitate characterisation.

In this chapter, we will explore different isolation and reconstitution techniques with the goal of developing a human macrophage-erythroblast reconstitution system that enables a more in-depth exploration of the interaction between macrophages and erythroblasts.

## 3.2 Results

### 3.2.1 Isolation of macrophage-erythroblast cell clusters from human bone marrow

To better understand the interactions between erythroblasts and macrophages, we decided first to explore whether it was possible to isolate intact erythroblastic islands from human bone marrow aspirate samples. To do this, the methodology described by Lee et al.<sup>72</sup> was initially followed. This methodology gently resuspends the bone marrow aspirate in HBSS, and then a slow centrifugation step is used to isolate the larger

cells clusters, while single cells remain in the supernatant. This enabled us to isolate clusters of cells reminiscent of erythroblastic islands (Figure 3-1A). Immunofluorescence confirmed the presence of a central macrophage, and many of the surrounding cells labelled positive for the erythroid-specific membrane protein Band 3 (Figure 3-1B). It was possible to live image these cell clusters for several minutes (Supplementary Video 1 and 2). The time-lapse movies demonstrated that the interactions between the cells were stable compared to the surrounding red blood cells that are very mobile and subject to Brownian motion. We also observed that the central macrophage had dynamic membrane extensions which wrapped around the erythroblasts (see interaction with enucleating cell indicated in Figure 3-1A and shown in time-lapse). These early experiments convinced us that it would be possible to monitor cell behaviour using time-lapse imaging.

### 3.2.2 EDTA disturbs macrophage-erythroblast cluster isolation

During the start of the project, it was observed that one critical component in the bone marrow isolation is the anticoagulant agent used by the surgeon during the donation. Bone marrow samples collected in heparin consistently had intact cell clusters visible immediately after isolation, whereas cell clusters were not recovered from EDTA samples unless the cells were left to bind together for one hour on ice after the low-speed centrifugation step. Weatherall et al.<sup>72</sup> used 30% serum-rich media in their isolation protocol. Therefore, we incubated the sample which had been in EDTA-containing buffer after being washed, in 30% serum media for one hour in an attempt to rescue the clustering phenotype. Although clusters were observed, confocal analysis showed that these clusters consist mainly of macrophages (Figure 3-1C). Since heparin treated samples consistently gave intact cell clusters of macrophages and



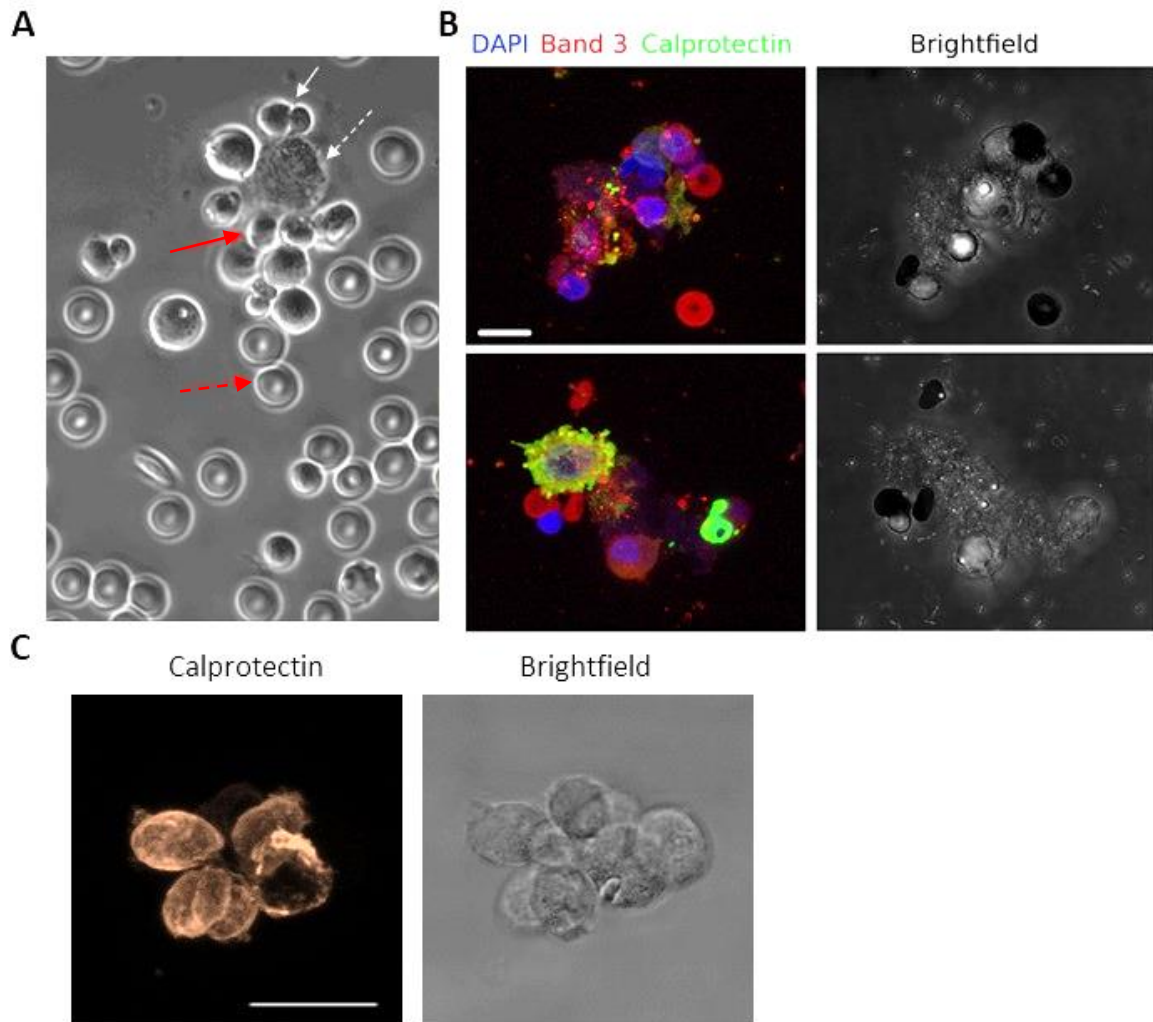


*Figure 3-1 – Isolation of native erythroblastic islands from bone marrow*

*A - Image from timelapse movie of an isolated erythroblastic island captured using Olympus CellR wide-field imaging system using 63x lens. White arrow indicates an enucleating erythroblast. Fragmented white arrow points to the macrophage. Red arrow shows erythroblasts, and the fragmented red arrow shows an example of a red blood cell. B – Paraformaldehyde fixed isolated bone marrow erythroblastic islands were immunostained for Band 3, Calprotectin and Hoechst. Band 3 indicates all cells belonging to the erythroid lineage. Calprotectin stains macrophage and Hoechst stains the nuclei. Scale bar represents 50  $\mu\text{m}$ . C – Bone marrow isolated cells from EDTA buffer after 1 hour on ice in 30% serum-rich media were stained with calprotectin, which labels macrophages. Scale bar represents 10  $\mu\text{m}$ .*

erythroblasts, all future experiments were conducted only on bone marrow samples collected with heparin beads.

### 3.2.3 Characterizing the central macrophage in bone marrow

In the human bone marrow, there are multiple populations of monocytes and macrophages<sup>42</sup>. Typically, mature macrophages would be expected to be CD14<sup>+</sup>CD16<sup>+194,195</sup>. Using these surface markers on our bone marrow aspirate samples, it was observed that these cells represent about 0.2-0.8% of the total bone marrow population (Figure 3-2A). Due to the small size of this macrophage population, the CD14<sup>+</sup> cells were isolated using magnetic beads to facilitate analysis before a panel of different surface markers were applied.

The majority of the macrophage population isolated were observed to be CD14<sup>+</sup>CD16<sup>-</sup>. The small percentage of cells which were CD16<sup>+</sup>, were also 40-70% positive for CD169, an essential marker of the macrophages involved in the hematopoietic niche (Figure 2B)<sup>33</sup>. Confirmation of the CD169 marker on the CD14<sup>+</sup>CD16<sup>+</sup> population is suggestive that the dual positive CD14<sup>+</sup>CD16<sup>+</sup> population is the bone marrow resident population. We further showed that these cells were positive for the other M2 macrophage markers in the test. As discussed in the Section 1.3.1.1, CD163 and CD206 are key markers for M2 macrophages, which are not involved in pro-inflammatory signalling<sup>52</sup>. Figure 3-2B shows that 30-70% of the bone marrow resident population is positive for both CD163 and CD206.

Interestingly the bone marrow macrophage population is also positive for CD209, as this marker is generally specific for dendritic cells. However, it has been reported<sup>66</sup> that

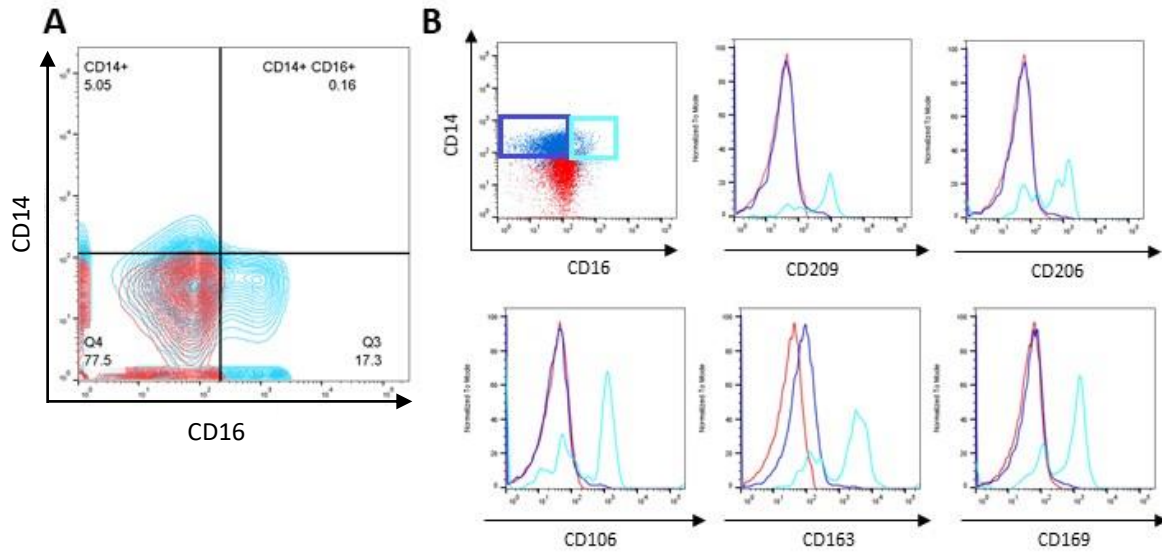


Figure 3-2 – Bone marrow CD14<sup>+</sup> CD16<sup>+</sup> cells have two populations, the larger one is positive for resident macrophage markers

A – Representative contour plot of whole human bone marrow population (n=2). IgG control is in red, and the CD14 and CD16 probed bone marrow cells are in blue. Percentages in each quarter represent the cell population expressing that particular surface marker. B – Representative histogram plots of human bone marrow CD14<sup>+</sup> isolated cells (n=3). CD14<sup>+</sup>CD16<sup>-</sup> population are labelled dark blue. CD14<sup>+</sup>CD16<sup>+</sup> population in light blue. The cells were probed for CD14, CD16, CD206, CD209, CD106, CD163 and CD169.

some tissue-specific macrophages can express this surface marker (e.g. Schwann cells), and our results are the first, to our knowledge, to show that human bone marrow resident macrophages are members of this group. The remaining 30% of the cells which are CD16<sup>+</sup> might be the atypical monocytes<sup>57</sup>, mentioned in Section 1.3.1, as they do not have the other markers for mature macrophages.

According to the literature <sup>94</sup>, mice erythroblastic island macrophages are also positive for VCAM1 (CD106) at their surface. Flow cytometry suggests 40-70% of the human resident macrophage population is also positive for CD106 (Figure 3-3C). Importantly, the larger group of immature CD14 cells (CD14<sup>+</sup>CD16<sup>-</sup>), in bone marrow were not positive for any of the markers tested (CD106, CD169, CD206, CD163 and CD209). This population of cells is probably the monocyte population which is generated from the HSCs.

We next compared these isolated bone marrow macrophages to those which were found within the freshly isolated cell clusters. The collected clusters were disrupted into a single cell population and subjected to flow cytometry. Unfortunately, due to the large numbers of red blood cells present in the samples, the percentage of macrophages which could be detected was extremely low. This made the characterisation difficult with this technique. Only a very small percentage was CD14<sup>+</sup>, with almost none which were CD16<sup>+</sup> (Figure 3-3A). We could observe in Figure 3-3B that both the CD14<sup>+</sup>CD16<sup>-</sup> and CD14<sup>+</sup>CD16<sup>+</sup> populations were slightly positive for the markers tested in this immunofluorescence test (CD106, CD169, CD206, CD163 and CD209).

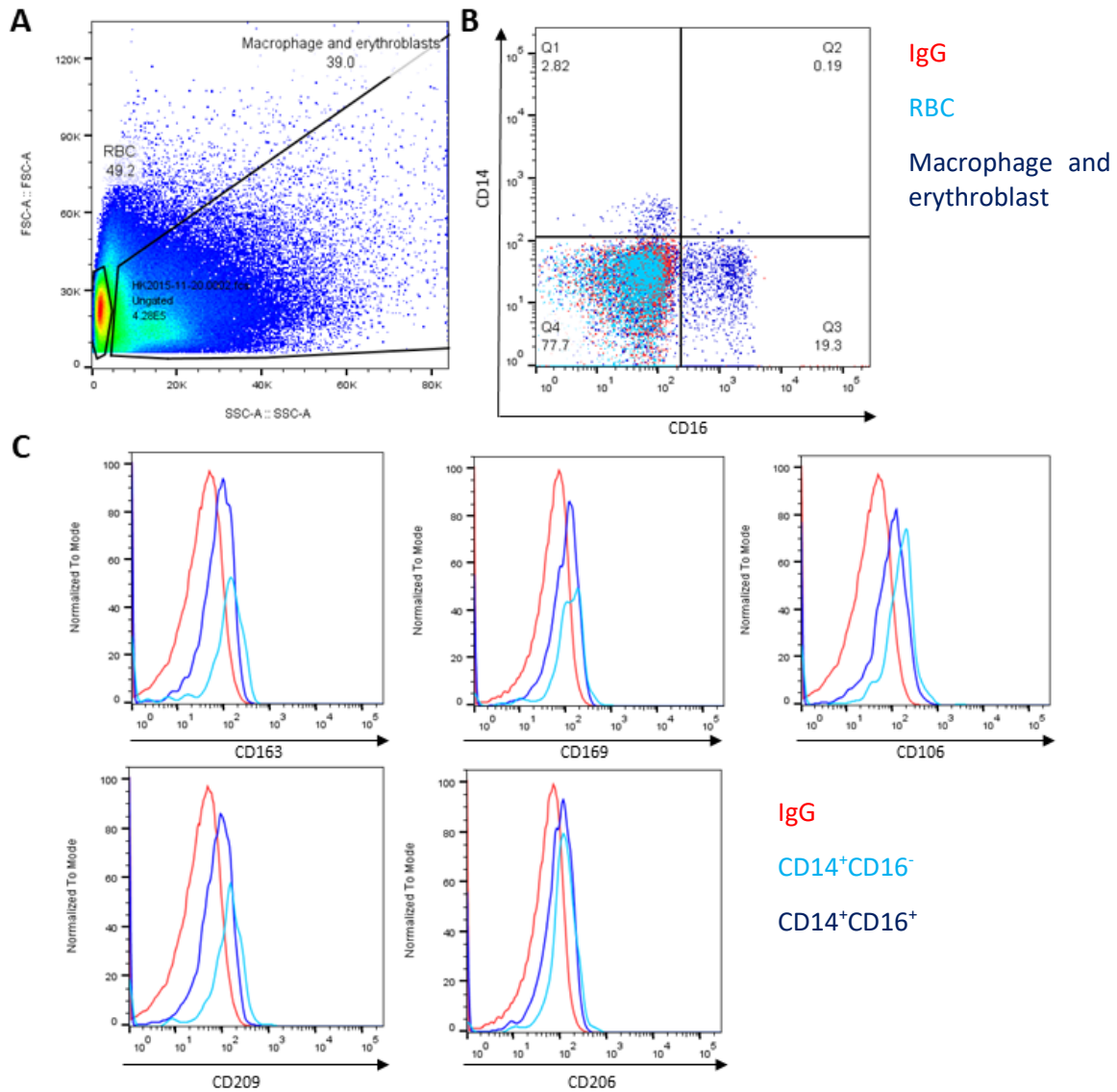


Figure 3-3 - Characterisation of central macrophage of bone marrow human erythroblastic islands

A – Representative dot plot of the whole isolate from a human erythroblastic island isolation (n=2). Gates are drawn to represent the red blood cells (RBC) fraction and the macrophage and erythroblast fraction. B – Representative dot plot of the whole isolate from a human erythroblastic islands isolation (n=2). IgG control is in red, the macrophage and erythroblast fraction probed for CD14 and CD16 are in dark blue, and the red blood cells are in light blue. The percentages in the quarters represent those of the macrophage-erythroblast fraction. C – Representative histogram plot of the macrophage-erythroblast fraction probed for CD206, CD209, CD106, CD163 and CD169 (n=2). IgG control is in red, the CD14<sup>+</sup>CD16<sup>-</sup> cells are labelled dark blue, and the CD14<sup>+</sup>CD16<sup>+</sup> cells are labelled light blue.

#### 3.2.4 *In vitro* cultured macrophages share some of the surface markers of central macrophages

The bone marrow macrophages were next compared to the macrophages grown using *in vitro* culture from immature monocytes. This is because it is hard for us to secure a reliable supply of bone marrow macrophages, and it would be more convenient if we could use macrophages cultured specifically for this purpose. Immature monocytes were isolated from peripheral blood by Percoll gradient centrifugation and then selected by adhesion or using CD14 magnetic beads. These cells were then cultured in the presence of M-CSF as described by Ramos et al.<sup>34</sup>. The macrophages could then be cultured with or without dexamethasone. Dexamethasone is a glucocorticoid which is known to lead to M2c-like macrophages, which are close to resident macrophages in profile<sup>90</sup>, as introduced in Section 1.3.1.1. The dexamethasone untreated and treated are indicated as -Dex or +Dex macrophages respectively. The -Dex macrophages tended to exhibit a more fibroblast-like shape while +Dex macrophages are more rounded and adhere less well (Figure 3-4A and B).

After seven days of differentiation in the presence of M-CSF, Figure 3-4C shows that similar to bone marrow macrophages by flow cytometry +Dex macrophages express CD163, CD169, CD206 and CD209, but they lack VCAM1 expression. The -Dex cells, had a lower MFI for both CD163 and CD169 and a larger portion were CD14-. Therefore, *in vitro* cultured macrophages treated with dexamethasone can exhibit many of the

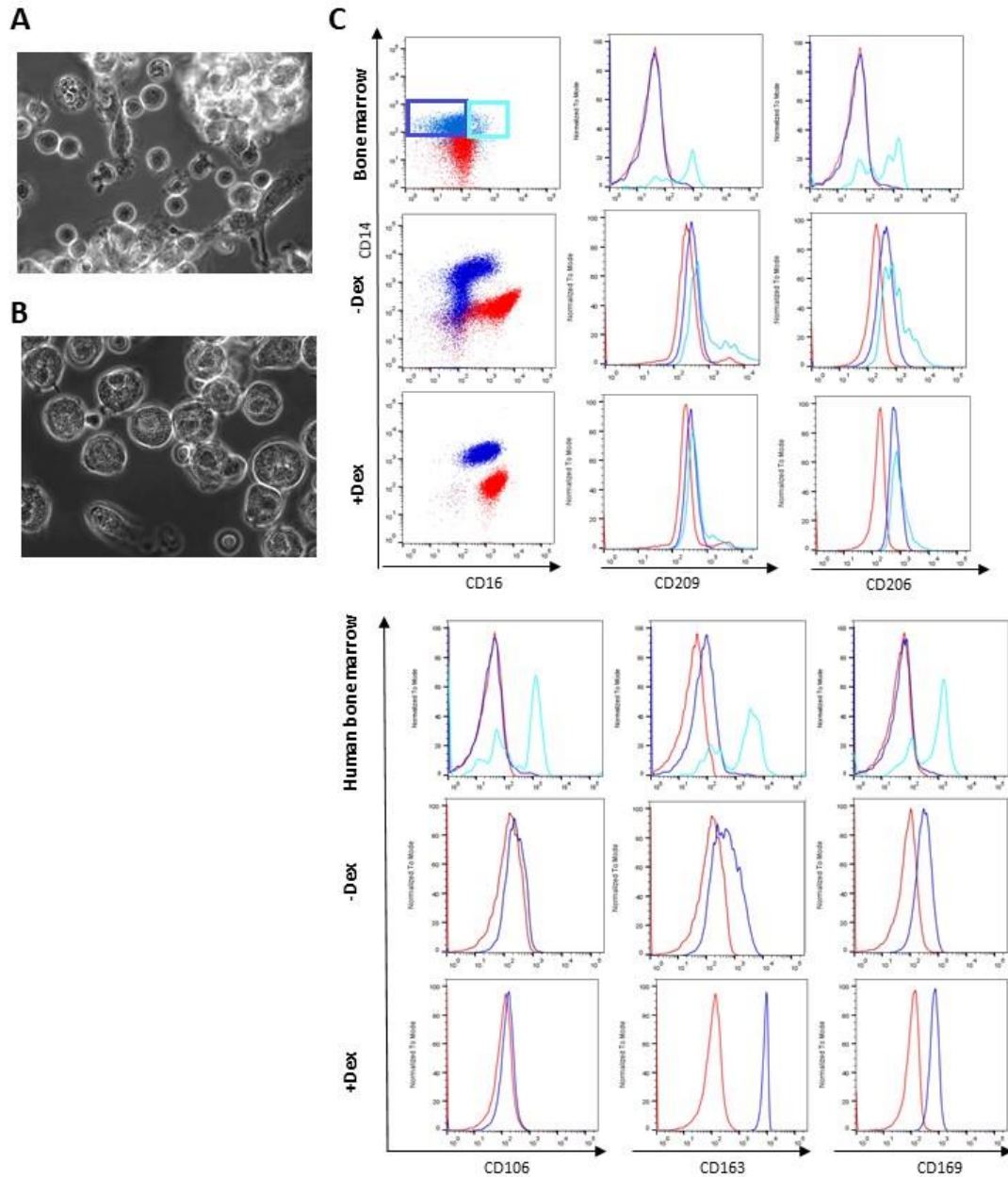


Figure 3-4 - The dexamethasone-treated macrophages have a similar surface marker profile to bone marrow macrophages

A – Representative image of -Dex macrophages taken on Olympus CellR wide-field imaging system using 63x lens on day 7. Most -Dex macrophages take on a fibroblastic shape. Images were taken by Dr. Severn. B – Representative image of +Dex macrophages taken on Olympus CellR widefield imaging system using 63x lens on day 7. The +Dex macrophages are small and round. Images were taken by Dr. Severn. C – Representative histogram plots of human bone marrow CD14<sup>+</sup> isolated cells (from Figure 3-3) and in vitro macrophages cultured with and without dexamethasone (-Dex and +Dex, n=5). CD14<sup>+</sup>CD16<sup>-</sup> population are labelled dark blue. CD14<sup>+</sup>CD16<sup>+</sup> population in light blue. The cells were probed for CD14, CD16, CD206, CD209, CD106, CD163 and CD169.

surface marker profiles of central bone marrow macrophages, but they do not express VCAM1.

### 3.2.5 Exploring whether VCAM1 can be induced in *in vitro* cultured macrophages

The next step was to determine whether it is possible to induce VCAM1 in cultured macrophage. In literature, VCAM1 is reported to be induced in endothelial cells using insulin<sup>196</sup>, epidermal growth factor (EGF)<sup>197</sup> and vascular endothelial growth factor (VEGF)<sup>198</sup>. The *in vitro* cultured macrophages (differentiated from CD14<sup>+</sup> monocytes for seven days) were exposed to these factors for up to 24 hours before checking surface markers by flow cytometry. Additionally, insulin was added to the EGF and VEGF conditions. However, there was no induction of VCAM1 in macrophages after exposition to EGF or VEGF in the presence or absence of insulin (Figure 3-5A and B).

We hypothesised that as the central macrophages would be exposed to the erythroblasts within the niche, it might be possible that the same signals, such as erythropoietin, would help make these cells acquire the resident macrophage phenotype. Macrophages grown in RPMI for 7 and 14 days were next exposed to erythroblast differentiation media for four days. Surprisingly, this treatment led to the loss of CD14 expression at the surface (Figure 3-5C). The cells had either changed cell type, or CD14 had been proteolytically removed. The small number of CD14<sup>+</sup> cells did express more VCAM1 than before. However, since this is a small population, several other surface markers need to be employed to confirm this is an actual macrophage population (such as CD163). Therefore, attempts to induce VCAM1 expression were largely unsuccessful.



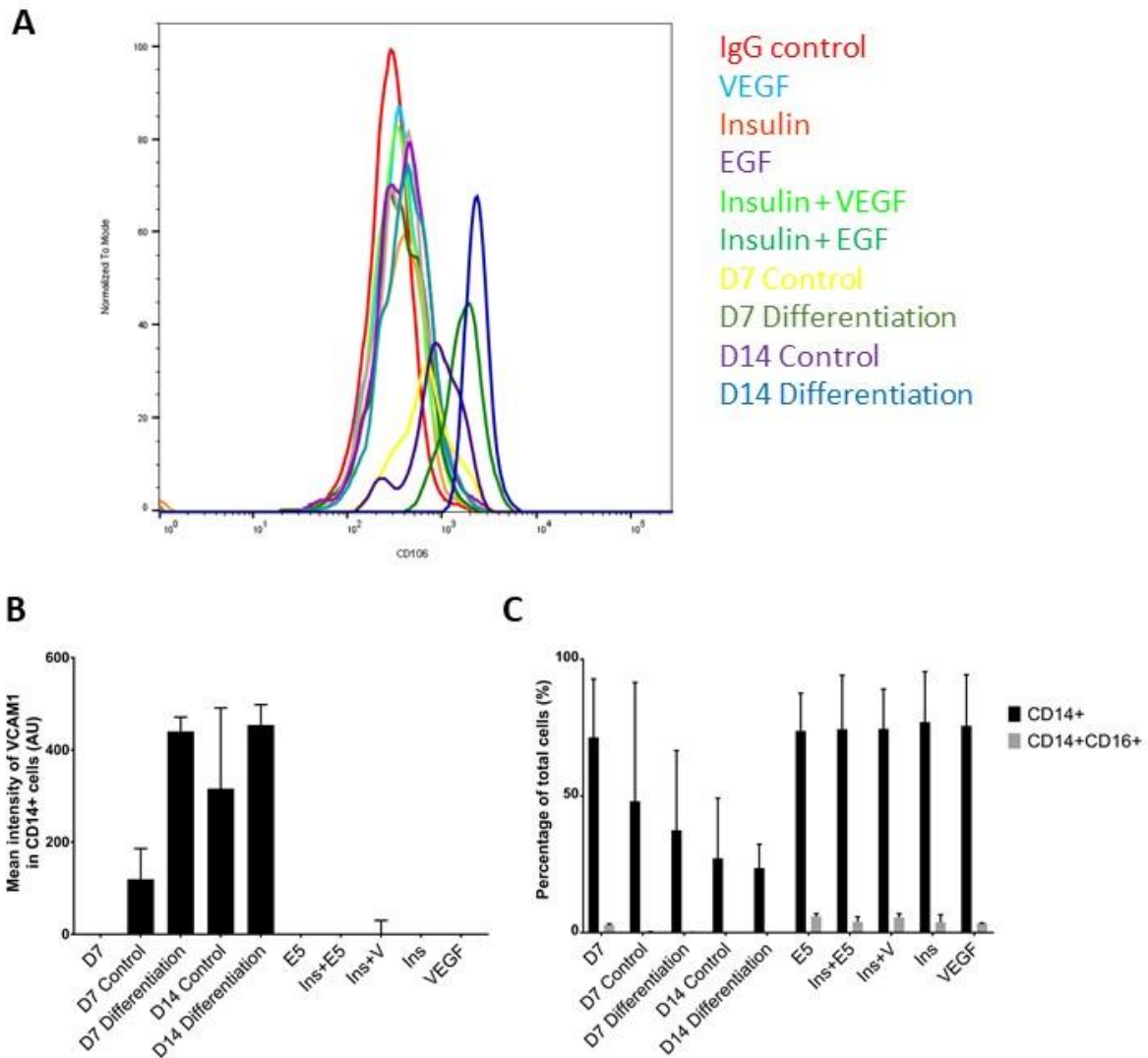


Figure 3-5 – Induction of VCAM1 in cultured macrophages

A - Representative histogram plot of the different conditions (n=3). The cells were probed for CD106 (VCAM1). D7 Control are macrophages which have been treated for 11 days in macrophage culture media. D7 differentiation are macrophages which have been treated for 7 days in macrophage media and 4 days in differentiation media. D14 Control are macrophages which have been treated for 18 days in macrophage media. D14 Differentiation are macrophages which have been treated for 14 days in macrophage media and 4 days in differentiation media. B – Quantification of the flow cytometry mean fluorescence of intensity of VCAM1 in each condition (n=3). E5 is EGF treatment, Ins is insulin treatment, and V is VEGF treatment. C – Quantification of the flow cytometry for the percentage of CD14<sup>+</sup> cells in each condition (n=3). E5 is EGF treatment, Ins is insulin treatment, and V is VEGF treatment.

### 3.2.6 Selecting an assay method for observing macrophage/erythroblast interactions

The next step was to determine the best conditions to observe the cell types and determine whether they interacted together to form cell clusters. Since access to bone marrow was limited, we developed an assay which would model the interaction using cells isolated from two separate sources- *in vitro* cultured and bone marrow. Initially, bone marrow macrophages only were used. These were isolated from the mononuclear fraction from human bone marrow using CD14<sup>+</sup> magnetic beads. The selected cells were then sorted for the CD14<sup>+</sup>VCAM1<sup>+</sup> cells (Figure 3-6A). We confirmed by flow cytometry and sorting that the VCAM<sup>+</sup> cells are also CD169<sup>+</sup> as described previously<sup>33</sup>. The erythroblasts were separately generated by *in vitro* culture of CD34<sup>+</sup> cells isolated from blood donor peripheral. The intention being that by using cultured erythroblasts, we could eventually utilise modified cells to test the importance of different receptors. Several papers had previously reported reconstitution of erythroblast islands, and we initially tested these reported methods before optimising further. Using conditions described by Lee et al.<sup>93</sup>, we attempted to reconstitute islands by resuspending the cells together on ice for 15 minutes in reconstitution buffer (IMDM with sodium citrate, 20% FCS, EGTA, Mg<sup>2+</sup>). No clusters were observed. However, we did observe clusters using conditions described by Rhodes et al.<sup>30</sup>. Briefly, the macrophages were left to adhere overnight in cluster media (IMDM with 1% BSA, 30% FCS and  $\alpha$ -thioglycerol). The erythroblasts were added the next day when they had reached day 6, which is the time in culture when the cells are losing their stem cell features and are erythroid progenitors. The cells were added at a ratio of 10:1 to ensure that there would be approximately between 5 and 10 erythroblasts around the macrophage at this stage<sup>72,199</sup>. The following day, the excess erythroblasts (which have not bound to the

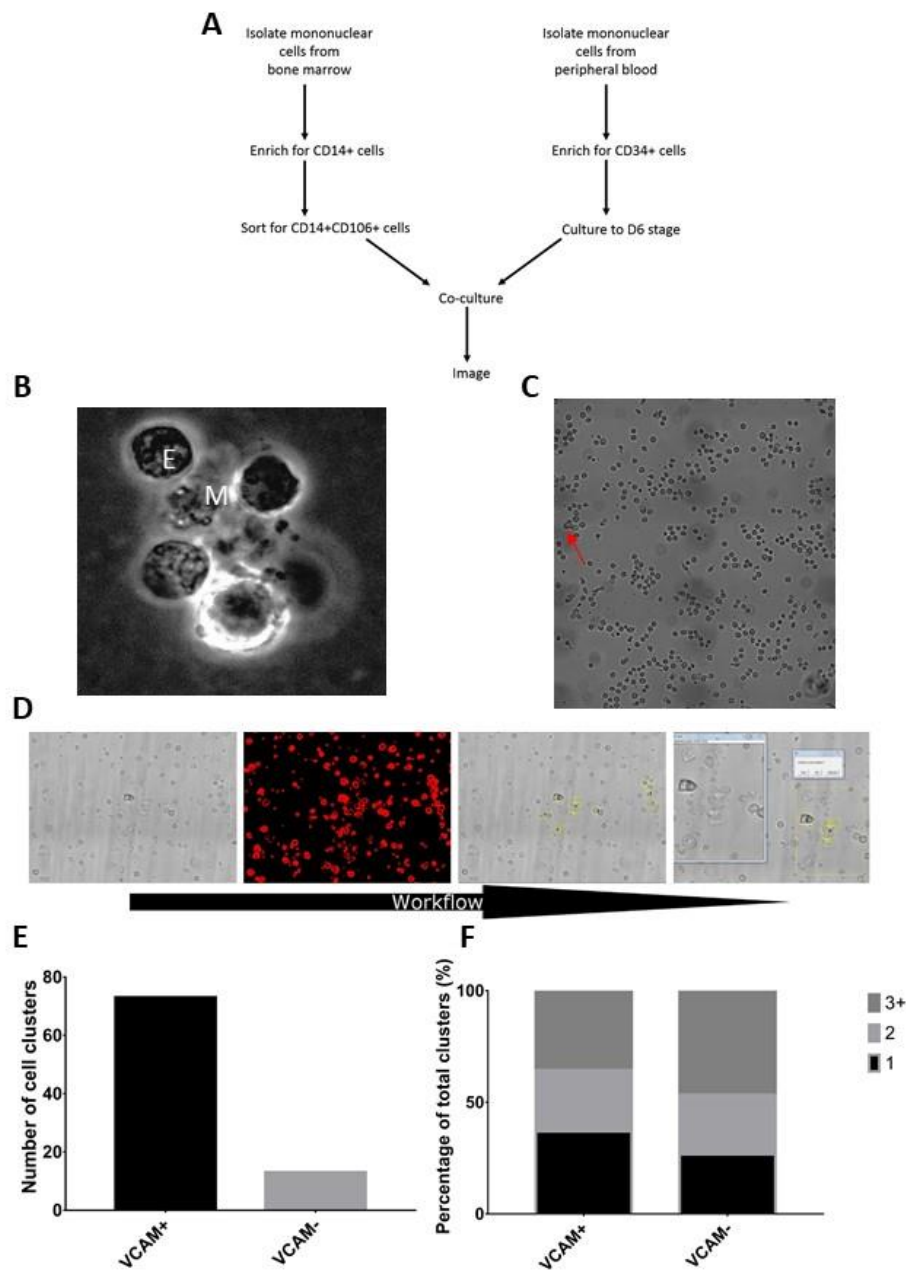


Figure 3-6 - Optimisation of an erythroblastic island reconstitution system

A – Workflow for island reconstitution. B – Representative widefield brightfield image of a cluster in a VCAM positive dish. M is for the central macrophage and E for erythroblasts. C – Representative widefield brightfield image of a tilescan of cells in an island reconstitution. This image shows that the majority of the cells are alone. The only cluster is represented with a red arrow. D – Fiji workflow which puts a mask and thresholds the image, then selects the largest objects and enables the user to confirm the object is a cluster. E – Graph showing the number of clusters detected in one run of a tilescan experiment. F – Graph showing the percentage of clusters with 1, 2 or 3+ cells around the central cell in a cluster.

macrophage) were removed by gentle pipetting. At this point, the plates were imaged on a Leica DMI6000 widefield microscope, using tilescan imaging. It was necessary to use tilescan imaging due to the scarcity of clusters that could be observed in our initial experiments (before optimisation of the conditions). Figure 3-6C shows that the majority of the cells present on the plate were solitary. However, intermittent clusters of cells were observed. As can be observed in Figure 3-6B, these clusters were reminiscent of the morphology of the cell clusters isolated from bone marrow with a single central cell and several smaller cells surrounding it.

### 3.2.7 Imaging analysis of reconstituted cell clusters

As the numbers of cell clusters observed initially were sparse, tilescans were conducted using the entire imaging plate to enable quantification. We quickly realised that assessment of the number of clusters on a whole plate tilescan would require automation of our imaging analysis. To facilitate the counting of clusters in each imaging plate, an analysis program was developed to detect the cell clusters. In the first iteration of the analysis in Fiji (Image J) the clusters were found by creating a mask and thresholding the image (Figure 3-6D). The program selected the largest objects in the image and showed these to the user to decide whether this was a cell cluster. Unfortunately, the program does not remove human bias. However, it does help find the clusters on the tilescan faster to be able to quantify how many cells were bound to the central macrophage, the number of clusters and differences under different conditions.

Using this image analysis program, we found that VCAM<sup>+</sup> cells were capable of forming clusters, while VCAM<sup>-</sup> macrophages formed fewer clusters (Figure 3-6E). Both

macrophage cell types lead to similar numbers of erythroblasts bound to the cells (Figure 3-6F). However, this version of the reconstitution assay did not provide a high enough number of clusters and did not provide a way to analyse the dynamics of the system.

### 3.2.8 Optimization of media and culture plates for imaging cell cluster interactions

We next built on the tilescan imaging system to improve conditions for cluster formation and imaging. The conditions tested included three different media, the use of different materials in the plates as well as the use of adhesion molecules. To be able to image the cells over several days, the cells needed media propitious to their binding, as well as their survival. A range of different reconstitution media had previously been reported in the literature<sup>30,72,93</sup>. The media used by Lee et al.<sup>93</sup> was initially tested on the cells, but unfortunately no cell clusters were observed when this media was used in our conditions. The cell binding was also tested in the presence of the media from Rhodes et al.<sup>30</sup>. In this media, clusters were observed, but unfortunately, after further analysis, there was increased cell death after longer incubation times. We knew that our *in vitro* cultured cells survive in erythropoiesis differentiation media (IMDM with Erythropoietin, Holotransferrin and Human serum). Therefore, we tested the survival of the clusters in this media. Fortunately, the cells remained clustered in this media, and importantly, we observed less cell death than with the other media. It is important to note, however, that these macrophages lose some CD14 expression in the media used for imaging over time (see Figure 3-4B) but enough cells still retain CD14 to analyse the interactions. This raises the necessity to interrogate the phenotype of the macrophages at the end of the assay.

Furthermore, during the stage where the excess erythroblasts were removed by washing on glass coverslips, we observed that clusters were often disturbed and potentially lost. Different culture plates with different treatments were tested to help preserve the cell clusters. Poly-L-lysine treatment of coverslips was also trialled to help promote adherence, but it did not encourage cluster formation. We moved to culturing the cells on plastic cell culture 24-well plates from Corning. The move to plastic plates dramatically improved cluster retention. All of these conditions are summarised in Table 3-1.

### 3.2.9 Incucyte system facilitates visualisation of the dynamic relationship between erythroblasts and macrophages

The move to plastic imaging plates led us to trial the incucyte imaging system which can image through plastic and allows the monitoring of cell behaviour over time in 24 different wells simultaneously. The incucyte is an imaging tool which is placed in an incubator at 37°C and can image over several days without changing the cell conditions. At this point, bone marrow samples were not available, so instead, we used the macrophages grown *in vitro*. As indicated earlier, the +Dex macrophages have a very similar phenotype to the ones found in bone marrow. Therefore, we used these cells to test the imaging. It was also observed from the tilescans that it was difficult to identify macrophages. To enable us to discriminate macrophages from erythroblasts, the macrophages were pre-treated with Celltracker dye which can enter the cells, to be turned into a fluorescent signal which cannot exit the cell and is present over several days. The combination of the cell labelling and the incucyte microscope system gave us the opportunity for the first time to monitor dynamic cell interactions over time to observe different behaviours of the cell clusters. For example, some of the observed

PLATE	MEDIA
Glass bottom 3 cm dish	RPMI + 10% FCS
Glass bottom 24 well plate	RPMI + 30% FCS
Glass coverslips	IMDM + 30% FCS
Poly-L-lysine treated coverslips	IMDM, 3.5% sodium citrate, 20% FCS, 2 mM Mn <sup>+2</sup> , 2 mM EGTA (Lee et al. <sup>93</sup> )
12 well plastic plate	IMDM, 1% deionized bovine serum albumin, 30% FCS, 0.1 mM $\alpha$ -thioglycerol, and 4 U/mL recombinant human EPO (Rhodes et al. <sup>30</sup> )
24 well plastic plate	IMDM with Erythropoietin, Holotransferrin and Human serum

*Table 3-1 - Summary of the different conditions tested for reconstitution*

interactions between the macrophages (labelled in green with the Cell Tracker dye) and the erythroblasts were short-term (Figure 3-7A and B) while others were prolonged, lasting several days (Figure 3-7C and D). The macrophages were observed to migrate around the well with clusters of erythroblasts attached in Figure 3-7E. These images confirm that there is a dynamic interaction between the +Dex macrophages and the Day 6 erythroblasts. Importantly, we did not observe any clusters visible as soon as the imaging begins, with all links forming during the imaging.

Working with Dr. Stephen Cross (Wolfson Imaging Facility, School of Biochemistry), an automated Fiji algorithm was created that tracked the individual movement of macrophages and assessed how many erythroblasts were in contact with each macrophage at every timepoint. We can use this imaging platform to quantify how long the macrophages interact with erythroblasts for and whether they accumulate cells. The data generated by the algorithm has produced many outliers. In the total cell population, most macrophages will have no interaction or transient interactions with erythroblasts. Therefore, the ones which have long interactions will be the outliers that will need to be compared, and our data will not be normally distributed, with a larger slant towards no interaction. For this reason, all the statistical analysis was done with this in mind, using non-parametric tests such as the Kruskal-Wallis method.

#### 3.2.10 Dexamethasone treatment increases the number of long-lasting erythroblast-macrophage clusters

The development of this Incucyte imaging technique led to a collaboration with the van den Akker laboratory (Sanquin Blood Supply, the Netherlands) to use our reconstitution assay and their culture method to grow macrophages resembling bone marrow



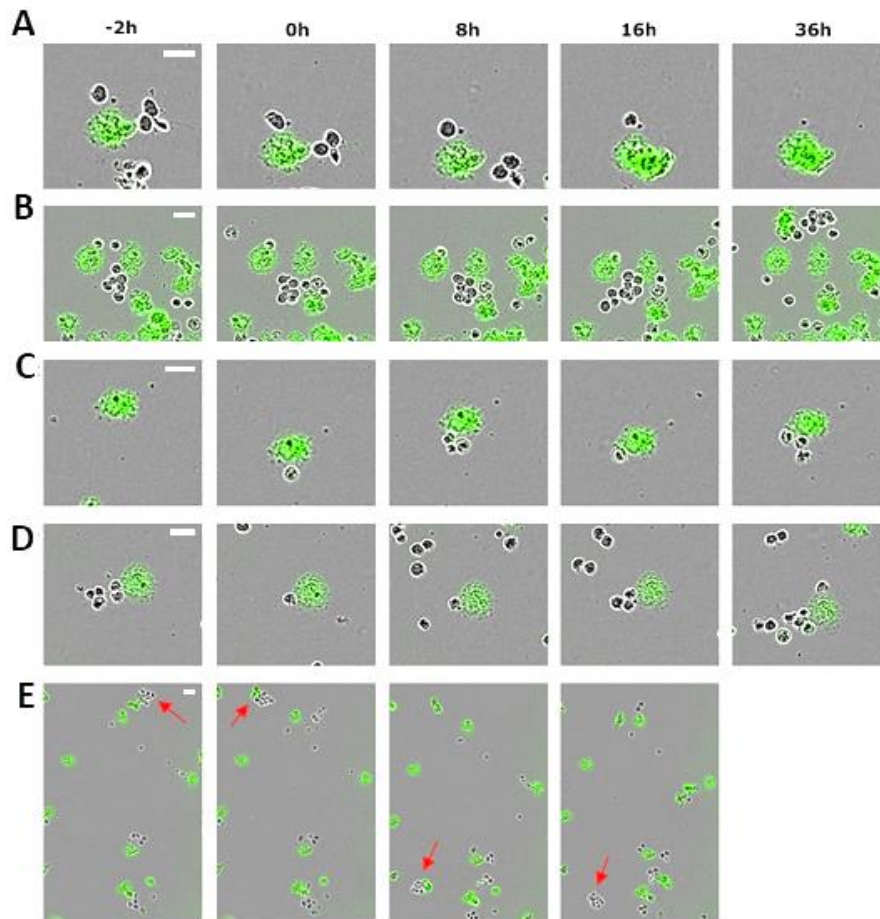


*Figure 3-7 - Incucyte provides insight into the dynamics of the interactions between macrophages and erythroblasts*

*A to E show examples of - +Dex macrophages (labelled with Cell Tracker green) grown from PBMC selected by adherence. The erythroblasts were added at a ratio of 10:1. The excess erythroblasts were gently removed by washing with media after 16 hours incubation. The cells were imaged every hour. There are examples of cells binding each other either in a transient (A, B and E) or non-transient manner (C and D). The arrow in red indicates a macrophage which moves with the erythroblastic cells until it detaches from them. The time indicated is in relation to the cells binding for the first time*

macrophages. They had also shown with their macrophages that they could observe erythroblastic island-like structures using cytopins, and our imaging pipeline provided an opportunity to test the dynamics of their culture system. A PhD student from the laboratory of Emile van den Akker (Sanquin Blood supply, Amsterdam) Esther Heideveld visited the laboratory to work collaboratively. They were able to grow macrophages from CD14<sup>+</sup> with EPO, SCF, lipids and dexamethasone, called GC-macrophages. They observed that these macrophages were CD163<sup>+</sup>, CD169<sup>+</sup> and Mer-TK<sup>+</sup>, and could significantly increase erythroid yield<sup>17</sup>. This differentiation was due to the dexamethasone. For this reason, their macrophages were very similar in morphology and immunoprofile to +Dex macrophages cultured using our methodology. Further, they showed that these macrophages were capable of phagocytosing nuclei.

Using our algorithm, we showed that the macrophages grown in the presence of dexamethasone could interact with more cells and more often than those grown without (Figure 3-8C and D). In both conditions, approximately 25% of these interactions last longer than 2 hours. Strikingly, as observed in Figure 3-8A and B, the dexamethasone-treated macrophages are more mobile than the -Dex macrophages, which stay immobile. This observation suggests that the +Dex macrophages are more mobile and interact with more erythroblasts. Importantly, our data also shows that once the -Dex macrophages contact an erythroblast, there is the same probability of these cells interacting for an extended period.

### 3.2.11 Reconstitution of bone marrow erythroblastic islands using incucyte

We needed to test whether this system would also work for native macrophages isolated from bone marrow. Therefore, using the same sorting method as previously

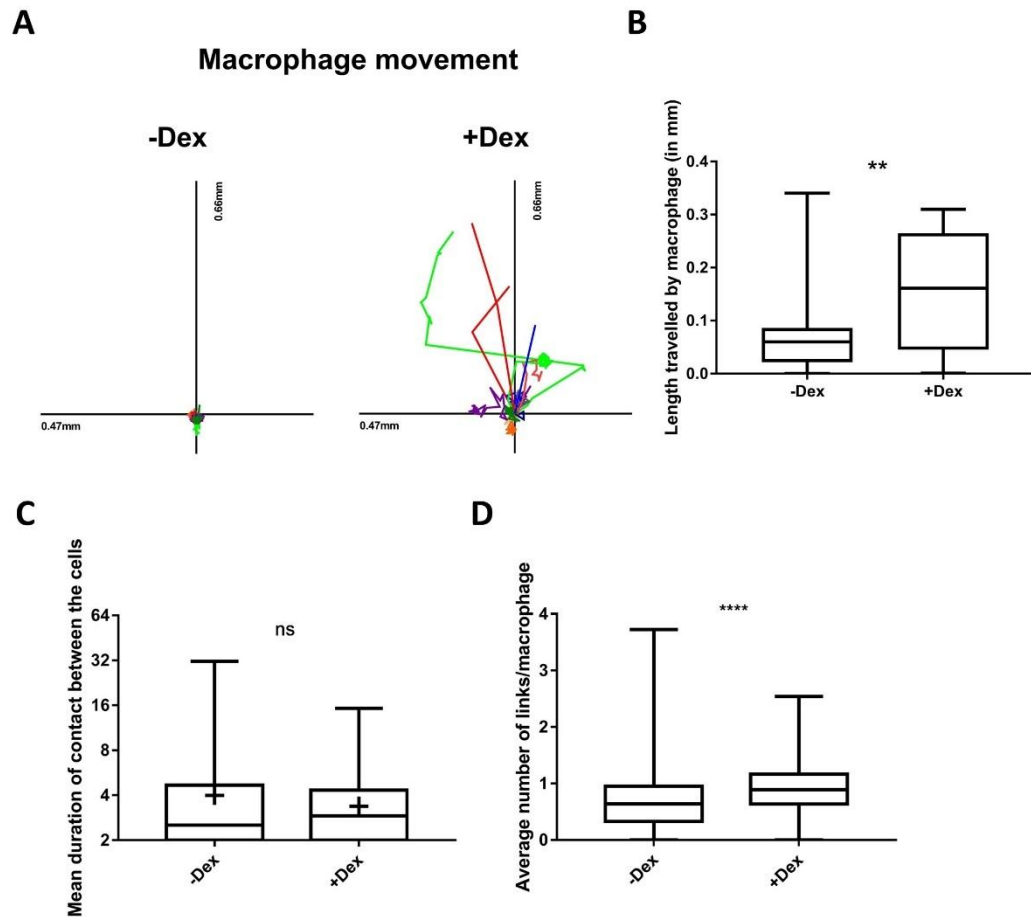


Figure 3-8 – M2c-like +Dex macrophages interact with more erythroblasts than -Dex macrophages

A – Scaled cell-displacement vector diagrams of macrophage movement for 20 randomly selected macrophages for both -Dex and +Dex conditions. B – Mean plot of total path length for 68 randomly selected macrophages from -Dex and 21 from +Dex conditions. Welch's *t* test was conducted on this data. (\*\* ( $p < 0.01$ )). C – Min to max boxplot showing the mean duration of links between macrophages and erythroblasts. The y-axis is a log<sub>2</sub> scale. D – Min to max boxplot showing the average number of links between macrophages and erythroblasts. C and D – Kruskal-Wallis test was performed on 457 macrophages for -Dex and 184 for +Dex ( $n=3$ ; ns ( $p > 0.05$ ); \*\*\*\* ( $p < 0.0001$ )).

described (section 3.2.6), we tested whether the CD14<sup>+</sup>VCAM1<sup>+</sup> cells were better at binding than the VCAM1<sup>-</sup> cells, as most of the literature suggests that VCAM1 is necessary for this interaction to occur<sup>37,94,200,201</sup>. Figure 3-9A shows that we are able to observe clusters between native macrophage and cultured erythroblasts using our reconstitution system. Figure 3-7A demonstrates that under the conditions of the assay, VCAM1<sup>+</sup> bone marrow macrophages can establish long-lasting interactions with multiple erythroblasts, as 50% of their interactions lasts over 2h (Figure 3-9B). VCAM1<sup>-</sup> bone marrow macrophages have 50% of contacts lasting more than 1h compared to 75% of VCAM1<sup>+</sup> cells (Figure 3-9B). Furthermore, VCAM1<sup>-</sup> cells form statistically fewer links ( $p < 0.0001$ ; Figure 3-9C). These macrophages are highly motile as witnessed with the +Dex macrophages (Figure 3-9D). Importantly, as observed for +Dex macrophages in Section 3.2.10 above, a lack of VCAM1 does not stop macrophage interactions with erythroblasts, but its presence denotes a macrophage with a subtly enhanced erythroblast binding ability (Figure 3-9C and D).

### 3.2.12 Lentiviral transduction of macrophages

The full investigation of island interactions requires the ability to manipulate protein expression to explore the involvement of specific proteins within cell clusters. Lentiviral transduction of CD34<sup>+</sup> or erythroblasts is already an established technique used in the Toye laboratory<sup>202</sup>, so the efficiency of lentivirus transduction on macrophages was first explored using two lentiviral vectors available in the lab (pLVX-GFP<sup>203</sup> and pXLG3-GFP), which have a soluble version of GFP as a reporter molecule. CD14 cells were first isolated by magnetic beads from peripheral blood, and these were transduced before they were allowed to differentiate. Figure 3-10A and 10B show that a transduction efficiency of between 30-90% was achieved using pXLG3 but less than 10% with pLVX.

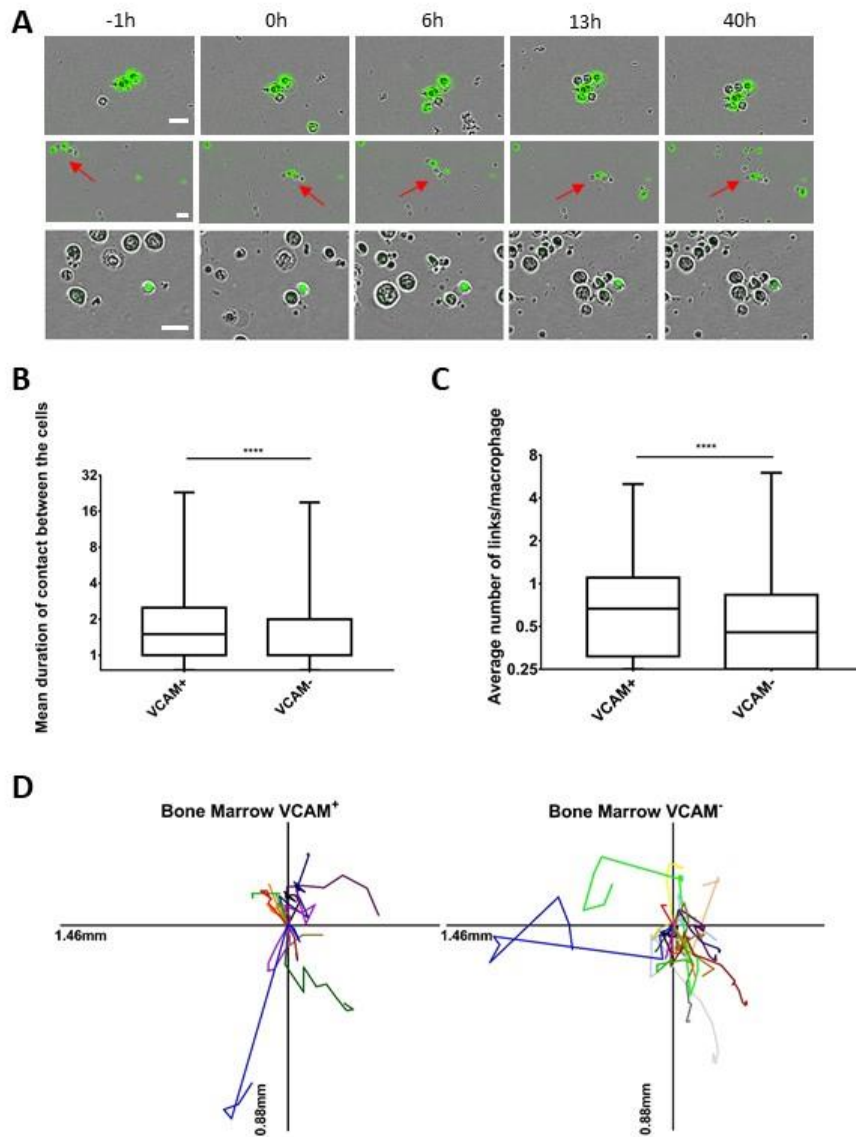
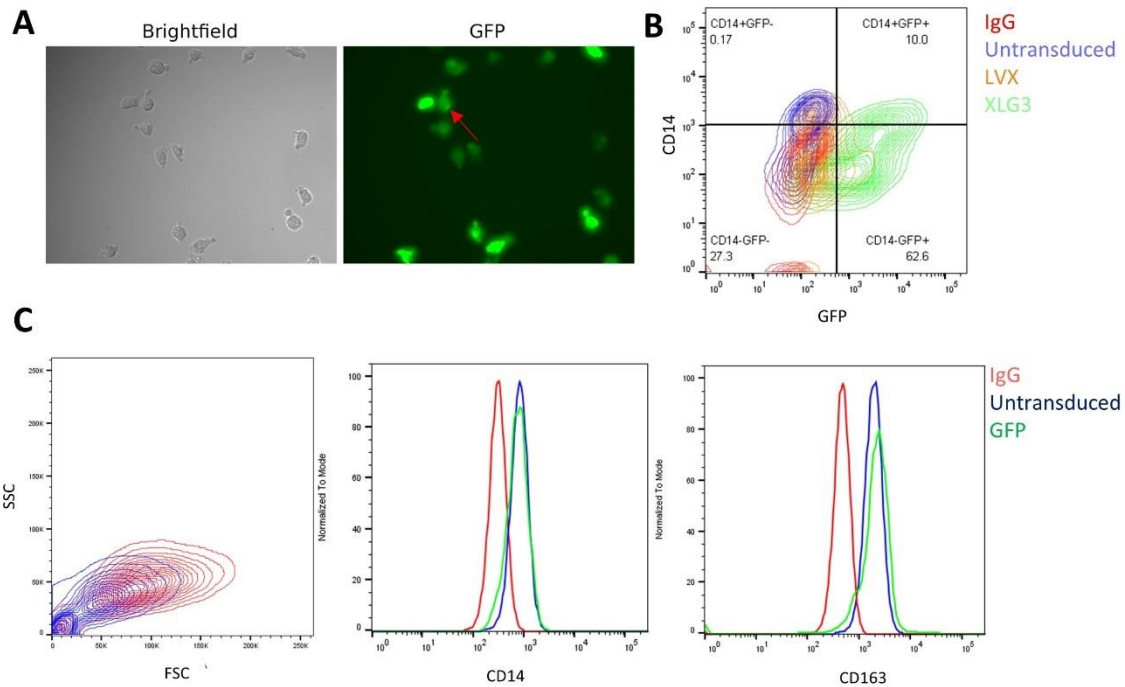


Figure 3-9 - VCAM1 offers a slight advantage for interactions with erythroblasts in bone marrow macrophages

A - Bone marrow macrophages (labelled with Cell Tracker green) were sorted for the CD14<sup>+</sup>CD106<sup>+</sup> cells. The erythroblasts were added at a ratio of 10:1. The excess erythroblasts were gently removed by washing 16 hours after. The cells were imaged every hour. These are examples of cells binding each other in a long-lasting manner. The arrow in red indicates a group of macrophage and erythroblasts moving along together. Scale bar in all images represents 20  $\mu$ m. B- Min to max boxplot showing the mean duration of links between bone marrow macrophages and erythroblasts. C - Min to max boxplot showing the average number of links between bone marrow macrophages and erythroblasts. The y-axis is a log2 scale. B and C Kruskal-Wallis test was performed on 1123 macrophages for scrambled VCAM<sup>+</sup> cells, 779 for scrambled VCAM<sup>-</sup> cells (\*\*\*\* ( $p < 0.0001$ )) from 2 separate experiments from the same donor. The y-axis is a log2 scale. D - Scaled cell-displacement vector diagrams of macrophage movement for 11 randomly selected VCAM<sup>+</sup> macrophages and 20 VCAM<sup>-</sup>.

In some cells, the GFP fluorescence was entirely cytoplasmic, but in some cells, it is localised to vesicle-like structures (Figure 3-10A). The GFP was expressed throughout macrophage differentiation and remained at the same level of transduction after five further days when measured by flow cytometry. The flow data, on day 7, shows that the GFP<sup>+</sup> cells were smaller in size than the control. These cells, however, still maintain expression of CD14 and CD163 (Figure 3-10C). Therefore, based on this work, this shows it is possible to transduce macrophages with exogenous proteins using lentivirus.

Next, we wanted to establish whether it was possible to use shRNA to knock out endogenous proteins. To do this, the CD14<sup>+</sup> selected cells were transduced with CD44 shRNA (previously shown to knockdown CD44 on erythroblasts, (Dr Tim Satchwell University of Bristol) or CD163 shRNA to test if it is possible to downregulate these macrophage surface proteins. This assay was done using a different lentiviral plasmid called pLKO.1, which has been used previously successfully in *in vitro* cultured erythroblasts produced from CD34<sup>+</sup> cells to knock down proteins. The transduced cells were smaller than the control, and more cells detached from the tissue culture plastic, but there was no indication of increased death in these samples with 90% of cells being propidium iodide negative. As can be observed in Figure 3-11A, on Day 4, only the untransduced control has a CD14<sup>+</sup> population. By Day 8, the CD44 shRNA cells have joined the untransduced cells. However, the CD163 shRNA cells have not all managed to become CD14<sup>+</sup>. Figure 3-11B shows that the CD44 shRNA did lead to a small loss of CD44 at the surface of the cells, while Figure 3-11C shows that any virus leads to a severe loss of CD163, as the scrambled control also led to a complete loss of the surface marker. This technique proved very difficult and inefficient.



*Figure 3-10 – pXLG3 vector leads to GFP expression in in vitro cultured macrophages without affecting their phenotype*

*A – Representative widefield image of pXLG3-GFP transduced macrophages at day 7 (n=2). The CD14+ cells were transduced at day 1 and grown in macrophage differentiation media in the presence of dexamethasone. Red arrows indicate a cell where the GFP is in vesicles. B – Representative contour plot of the different transduced cells at day 7 probed for CD14 (n=2). IgG control is in red; untransduced cells are in blue, pLVX-GFP macrophages are in orange and pXLG3-GFP macrophages are in green. C – Representative contour plot and histogram plot of the pXLG3-GFP macrophages and untransduced cells probed with CD14 and CD163 (n=2). IgG control is in red and GFP is in blue. Untransduced is in orange.*

Therefore, since our attempts at lentiviral knockdowns were unsuccessful for the chosen targets, it was decided for the purpose of this thesis, that knockdowns would be done on erythroblasts, which already have a robust, established methodology in the laboratory.



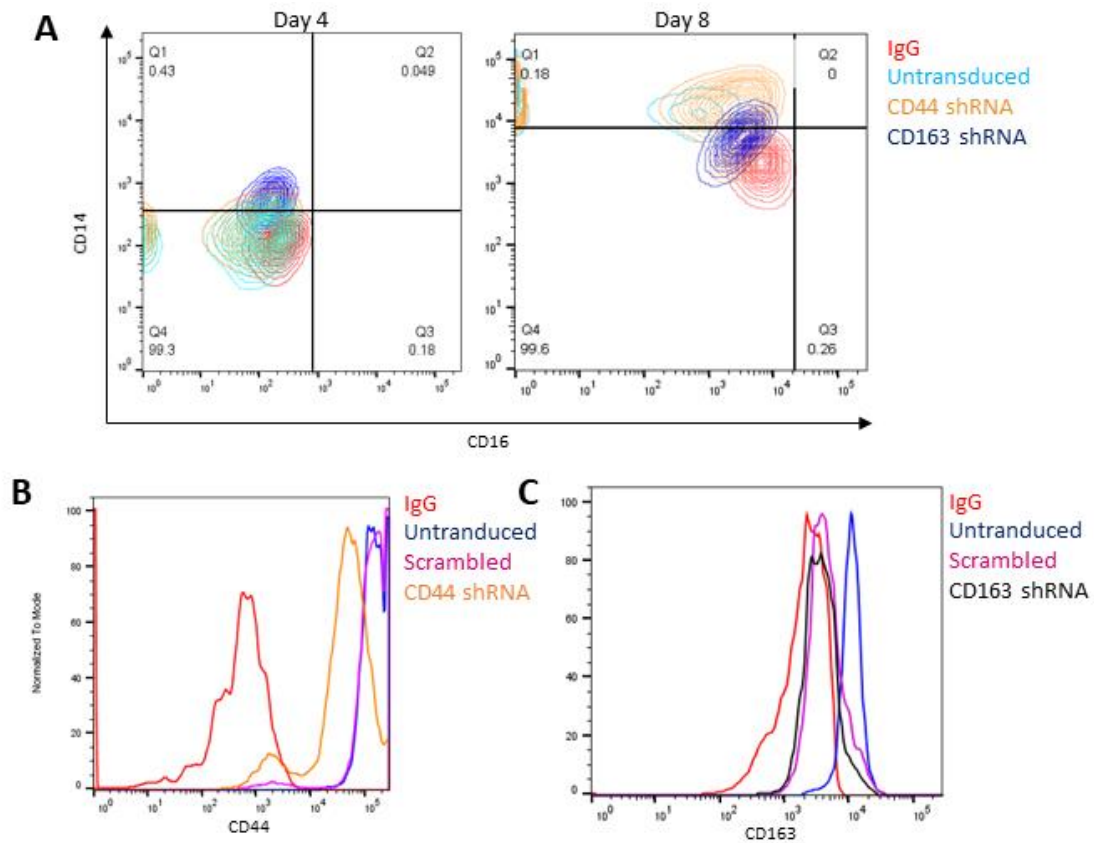


Figure 3-11 - Creating a shRNA hairpin derived knockdown in primary cultured macrophages

A – Representative contour plot of different conditions of macrophages transduced for a knockdown at day 4 and day 7 of differentiation (n=2). IgG control is in red; untransduced cells are in light blue, CD44 shRNA transduced cells are in orange and CD163 shRNA transduced cells are in dark blue. The cells were probed for CD14 and CD16. B – Representative histogram plot of transduced cells probed for CD44. IgG control is in red; untransduced cells are in blue, scrambled transduced cells are in pink and CD44 shRNA transduced cells are in orange (n=2). C – Representative histogram plot of transduced cells probed for CD163 (n=2). IgG control is in red; untransduced cells are in blue, scrambled transduced cells are in pink, and CD163 shRNA transduced cells are in black.

### 3.3 Discussion

The work in this chapter has successfully developed a human primary cell macrophage-erythroblast reconstitution culture system which allows the assembly of macrophage-erythroblast clusters which are reminiscent of erythroblastic islands- with a single macrophage surrounded by a variable number of erythroblasts. This system has shown that a number of different macrophages are able of interacting with erythroblasts to form clusters, including different macrophages sorted from bone marrow and *in vitro* cultured macrophages. This work has also described an imaging pipeline based around the incucyte system which will allow the detailed exploration of the macrophage-erythroblast interaction.

The identity of the central macrophage has been the subject of study for many years with a focus more on the mouse central macrophage<sup>30,33,87</sup>. In this chapter, we observed that the central macrophage was positive for all the resident macrophage traits (CD163, CD169, CD106 and CD206). However, the CD14<sup>+</sup>CD16<sup>+</sup> which would be the mature population was small. This was also observed independently at Sanquin Blood supply and reported by Heideveld et al.<sup>60</sup> who found that adult bone marrow CD163<sup>+</sup> macrophages expressed less CD16 than foetal liver macrophages. This confirms our results which show that the bone marrow macrophages express low CD16. They find that the CD163<sup>+</sup> macrophages, on average, represent 0.5% of the bone marrow cells. This confirms our findings that the macrophage fraction of the bone marrow is quite small and that the cells which have an erythroblastic support role are very poorly represented. Furthermore, they also found that VCAM1 is highly, but variably, expressed in bone marrow macrophages but not foetal liver macrophage. As with Seu

et al.<sup>92</sup>, we found that there was heterogeneity in the bone marrow macrophage population as not all mature macrophages expressed the different markers tested.

The tilescons experiment described in Figure 3-5, first gave us confidence that we were isolating the correct cells from the bone marrow as the VCAM1<sup>+</sup> cells were found to be in a much higher number of clusters than the VCAM1<sup>-</sup> cells. These clusters were very reminiscent of those observed after isolation of native erythroblastic islands. However, further experiments showed that human bias increased the effect VCAM1 has on cluster formation, as the difference was more pronounced in the tilescon analysis than the automated incucyte analysis. Furthermore, this allowed us to define the best conditions which enable these cell types to interact and survive. By the simple addition of cell labelling the macrophages using CellTracker dyes, we were then able to discern this population from the erythroblast population to remove any doubt in calling clusters actual macrophage-erythroblast clusters rather than just cellular clusters. The application of this culture system to the incucyte system allowed us to undertake a real-time assessment of the interactions between macrophages and erythroblasts for the first time.

It is important to note that the plasma membrane of macrophages can turn over in the space of one hour<sup>204</sup> and that tissue macrophages react to their environment<sup>52,61</sup>. Therefore, the media and cytokines the bone marrow macrophages are exposed to could change their phenotype, and they might lose their resident macrophage markers and functionalities. The formation of these clusters in our conditions indicates that we have not dramatically disrupted their phenotype, but there may be subtle differences. In future work, it would be important to test if they have changed their surface markers

after prolonged exposure to media and erythroblasts or utilise proteomics as conducted by Heideveld et al<sup>60</sup> or our own surfaceome methodology.

The observation that EDTA and PBS without calcium and magnesium are important for the relationship between erythroblasts and macrophages demonstrate a role for these ions in the maintenance of erythroblastic islands. In particular, an examination of the literature points to an essential role for calcium as washes with PBS can affect the link between the cells<sup>30,37,87,93,98,105,128,181–184</sup>. This is thought to be through the integrins. Integrins are known to have a divalent cation binding site, MIDAS, which is where  $Mn^{2+}$  ions bind and lead to a conformation change<sup>205</sup>. It is, therefore, possible that calcium is important for the role of integrins in erythroblastic islands. The other adhesion molecules which are calcium-dependent (cadherins and selectins)<sup>206</sup> have barely been studied as the role of cadherins has only been shown in one paper<sup>207</sup>, and selectins have not been shown to be present in erythroblastic islands. In our experiments, PBS did not only strip the erythroblasts from the macrophages; it tended to wash most cells away. It is pointed out by one paper<sup>87</sup> that it is necessary to be very gentle with the washes in PBS to not also disrupt the binding of the macrophages to the plate. It is possible that the washes done in this study were too harsh for the cell clusters. However, several different techniques were tested to mitigate this such as blotting and dipping, to no avail. These results indicate the necessity to study other molecules than integrins.

Unfortunately, the algorithm created with Stephen Cross does not give us the capacity yet to follow each erythroblast as the current frame speed leads to movements from the erythroblasts that are too big. Therefore, it is impossible to follow the interaction of a known macrophage with a known erythroblast through this algorithm. To be able

to have this level of scrutiny, the imaging frequency would have to be increased. With the current specifications from the incucyte, and given the need to maximise the number of conditions tested per experiment, this is not yet possible. Furthermore, it would be useful to test if the algorithm is detecting real interactions by testing the binding of erythroblasts to neutrophils, for example.

This assay has enabled us to visualise the interactions between human macrophages and erythroblasts *in vitro*. The use of different macrophages from different sources demonstrated that many of these interactions are transient (at least under the conditions of the assay), with 50% of interactions lasting less than 2 hours, in both +Dex macrophages and bone marrow macrophages. However, the VCAM1<sup>+</sup> bone marrow macrophages have more cells bound than the +Dex cells and the -Dex cells. This result indicates that VCAM1<sup>+</sup> would be more important for retention/formation than initial binding. This is interesting as these cells have a different expression of VCAM1 at their surface. These subtle changes in surface protein between the different macrophage types used in our experiments leave us to question whether the association of active integrins with VCAM1 on erythroblasts is responsible for the binding observed in VCAM1<sup>+</sup> cells. The evidence presented here could point towards a VCAM1-independent interaction for integrins in erythroblastic island formation, or perhaps associations are more promiscuous than anticipated.

These data have demonstrated that multiple types of macrophages can interact with erythroblasts. For example, this assay enabled us to look at the motility of macrophages. There was quite a large difference between the macrophages, as -Dex macrophages did not migrate while both +Dex macrophages and bone marrow macrophages were

extremely motile. Although a large number of mature macrophages in the human bone marrow are VCAM1<sup>+</sup>, indicating a preference for this phenotype in cell cluster formation, the ability for VCAM1<sup>-</sup> macrophages to form interactions with erythroblasts indicates a flexibility in terms of the type of macrophages which can participate in erythroblastic island formation which may be important during stress erythropoiesis. Therefore, perhaps in the bone marrow the interaction can be made more stable or be prioritised with VCAM1<sup>+</sup> cells. One consideration for future work would be to overexpress proteins such as VCAM1 at the surface of macrophages. This may be possible as the overexpression vector the Toye lab uses pXLG3 plasmid was fairly efficient at transducing macrophages.

To determine whether VCAM1 is important for erythroblastic islands and therefore erythropoiesis *in vivo*, one model that can be used is mice. However, the knockout of VCAM1 leads to premature death which means we cannot study the effect on erythropoiesis. One laboratory has managed to create a mouse which targeted VCAM1<sup>-</sup> solely within its bone marrow using an ER-intrabody system (iER-VCAM1 mice)<sup>208</sup>. Direct correspondence with the laboratory has led us to understand that they do not detect any observable effect on erythropoiesis as the mice have a normal haematocrit. However, it would be interesting in the future to look at the effect of VCAM1 loss on stress erythropoiesis by blood-letting these mice. Furthermore, it would be of interest to look at the bone marrow and observe if this loss affects the number or composition of the erythroblastic island, or whether the islands exist in the absence of VCAM1 with other, surrogate, macrophages as our data here would suggest.

In summary, this work has enabled us to reconstitute the interactions between human macrophages and erythroblasts and image the dynamics between these two very different cell types for the first time. This provides a means of characterising the importance of individual molecular interactions involved in this key relationship. This reconstitution assay and imaging pipeline are exploited further in the remaining chapters of this thesis.

## 4 Chapter 4 – Characterization of Eph/ephrin and integrin expression in erythroblasts and macrophages

### 4.1 Introduction

The importance of Eph receptor function within the bone marrow niche has been explored previously in the literature, but the emphasis has largely been on mice studies. In mice, the EphB4 ligand, ephrin-B2, which is expressed on HSCs, was found to be important for the release of the progenitor cells into the bloodstream as it enabled the HSCs to interact with the sinusoidal endothelial cells<sup>124,125</sup>. EphB4 is also reported to exert control over niche size, as transgenic mice that overexpress EphB4 produce more HSC cells and display a higher bone marrow reconstitution capacity<sup>126,127</sup>. However, the role that Eph receptors specifically play in the erythroid lineage is based primarily upon the demonstration of EphB4 expression on human bone marrow CD34<sup>+</sup> cells and from the observed increase in CFU-E formation upon co-culture with stromal cells overexpressing ephrin-B2 or HSCs overexpressing EphB4<sup>20,103,104</sup>. The expression profile and roles of Eph/ephrins in the human bone marrow is largely unstudied.

Eph receptors are known to interact with integrins as they can influence the migration of cells. In particular, during haematopoiesis, stimulated EphB4 increased the adhesion of hematopoietic cell lines UT-7/GM and K562 to fibronectin<sup>209</sup> and stimulation of EphB1 on P19 cells increased binding to fibronectin<sup>210</sup>. It is known that VLA-4 (Integrin  $\alpha 4\beta 1$  complex) and VLA-5 (Integrin  $\alpha 5\beta 1$  complex) are present on erythroblasts<sup>94,211,212</sup>. The VLA-4 complex is important for the formation of the erythroblastic island<sup>94</sup>, while the VLA-5 has been shown to be activated by EphB1 stimulation in mouse



erythroblasts<sup>128</sup>. In the latter case, EphB1 was reported to be activated on erythroblasts by agrin (a proteoglycan which can bind dystroglycan) in mouse bone marrow. Activated EphB1 was shown to activate the VLA-5 complex in these cells, and the authors postulated that this would help the erythroblasts bind to the macrophages. Although this paper demonstrated the presence of EphB1 at the early stages of differentiation in mice, it did not go on to explore the expression during different stages of erythropoiesis. Therefore, it is important to establish whether one of the roles of Eph receptors on human erythroblasts is to activate the integrins necessary for adhesion to macrophages and the stroma throughout erythropoiesis.

This chapter will set out to determine the definitive Eph family expression profile during human erythropoiesis and on human macrophages. It will also establish whether Eph receptor activation is important for activating integrins in erythroblasts.

## 4.2 Results

### 4.2.1 Confirmation of Eph receptors expression by mRNA and protein

To determine which receptors were expressed during erythroblast differentiation, RT-PCR was performed on mRNA isolated from multiple *in vitro* cultured differentiation courses. As shown in Figure 4-1A, the RNA for Eph receptors (EphA1, EphA2, EphA3, EphA6, EphA7, EphA8 and EphB2) was not detected during erythropoiesis. HEK293, OVCAR 3 and HeLa cells were used as positive controls<sup>213,214</sup> (data not shown). For each sample, a negative control, where the isolated RNA has not been processed into cDNA, was also performed to confirm the absence of genomic DNA contamination. Surprisingly, the negative controls were positive for EphB1, and EphB3 using primers indicated with a star in the Materials and Methods and the bands were of the incorrect

size. When new EphB1 and EphB3 primers were selected<sup>215</sup>, no bands were observed in the negative control and the erythropoiesis samples (see Figure 4-1A and B).

The RT-PCR shown in Figure 4-1A confirms the presence of mRNA expression of EphB4 and EphA4 at day 6 and T0 (erythroid progenitors and the first day of terminal differentiation respectively). The Western blotting confirmed this result for EphB4 (Figure 4-1C), while EphA4 expression persisted to the later terminal differentiation stages but at diminished levels. EphB6 RNA was also detected. Western Blotting (Figure 4-1A and C) showed that EphB6 is present during day 6 and T0, but similarly to EphB4, is lost at the RNA and protein level from T72 onwards. Unlike for mice<sup>128</sup>, no EphB1 was detected in either the RNA or protein level in most repeats (Figure 4-1A and B; n=2 out of 3). The donor in which EphB1 was detected with a mouse antibody, which was also positive in the HeLa negative control, was negative with the other EphB1 antibody suggesting that it was a nonspecific band (Figure 4-1D). A similar result was found with EphA5 which was not detected in most samples (Figure 4-1E; n=2 out of 3): except for a single mRNA sample at T72 and a single protein sample in reticulocytes. Finally, we also detected the ligand for EphB4 and EphB6, ephrinB2, on the erythroblasts during differentiation. The ligand is present until T72.

#### 4.2.2 Proteomics

To further understand what proteins might be present at the surface of the erythroblasts a surface proteomics assay was conducted. The proteins at the surface of the differentiating erythroblasts taken from Day 6, T0, T72 and reticulocytes were surface biotinylated using EZ-Link Sulfo-NHS Biotin (Thermo). Initial tests did not detect any Eph peptides. We speculated that this was due to the higher abundance of other

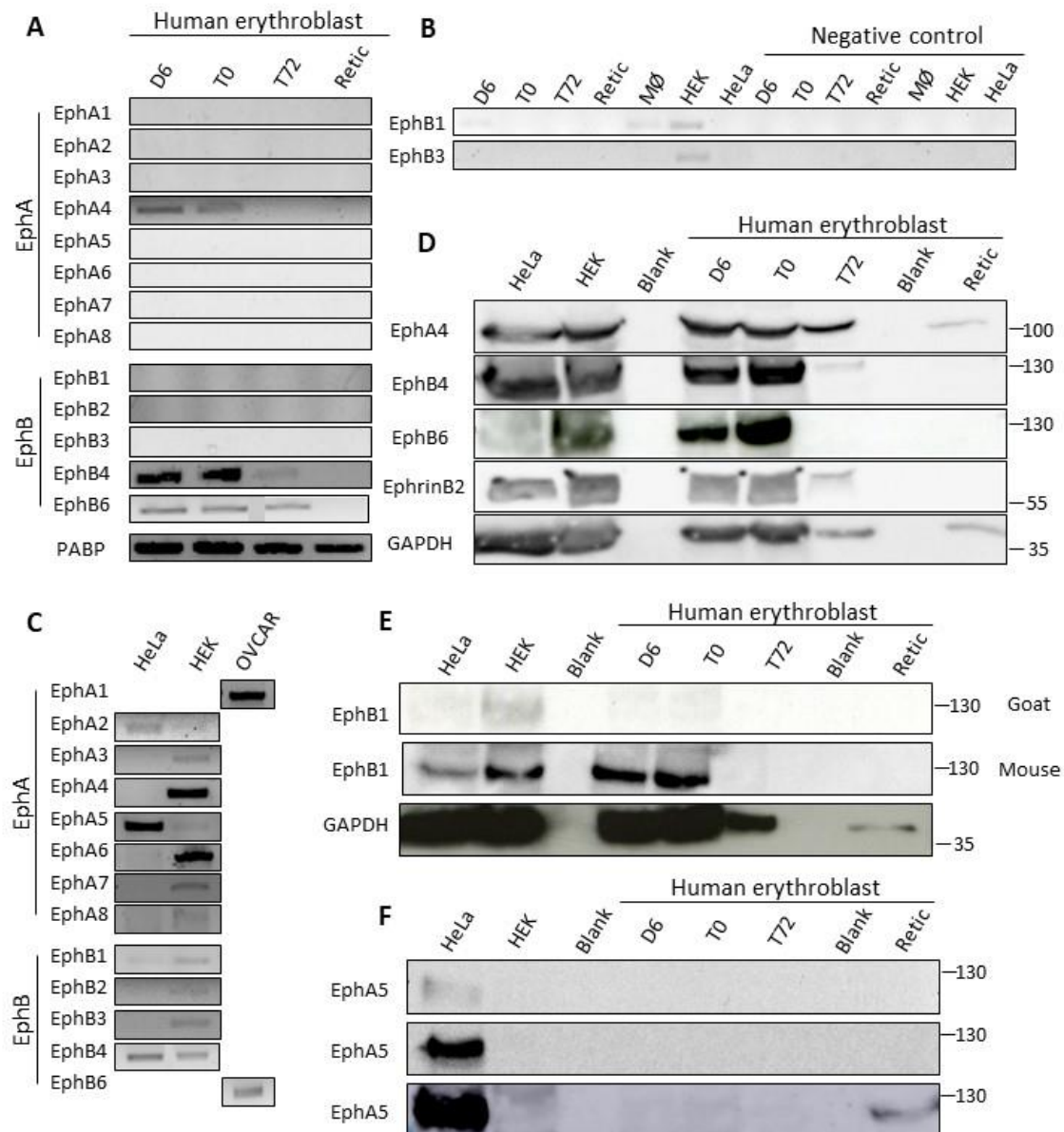


Figure 4-1 - Identifying the Eph receptors in erythropoiesis

A - Representative DNA gels showing the PCR products from an erythroblast differentiation course using primers against EphA1-8 and EphB1-6 (n=3). For each sample, a negative control was also performed to confirm the absence of genomic DNA contamination. HEK293, OVCAR 3 and HeLa cells were used as positive controls as shown in C. B - Representative DNA gels showing the PCR products from an erythroblast differentiation using the new primers against EphB1 and EphB3 with their negative control. C - Representative DNA gels showing the PCR products of the positive controls for A. D - Lysates from erythroblast differentiation course were blotted for EphB4, EphB6, EphA4, EphA5, EphA6, ephrin-B2 and GAPDH. This is a representative blot (n=3). E - Lysates from one erythroblast differentiation course were blotted with two different EphB1 antibodies and GAPDH. F - Lysates from three erythroblast differentiation course were blotted for EphA5. D, E and F - All lanes were loaded with  $1 \times 10^6$  cells.

erythroid peptides, for example band 3 and band 3 associated proteins which are highly abundant in the cell membrane<sup>216</sup>. We added a step after biotinylation and the cell lysis, where a proportion of band 3 (and therefore band 3 associated proteins) was reduced by conducting three consecutive immunoprecipitations (IP) with the aim of increasing the sensitivity of the proteomics analysis for less abundant surface proteins. It should be noted that the entirety of Band 3 was not removed from the samples (Figure 4-2) and therefore, we would expect to still detect Band 3 and its binding partners within our samples.

As can be observed in Table 4-1, the EphB receptors were detected during the early stages of differentiation but are quickly lost by T72. At low stringency (FDR  $p < 0.05$ ) peptides corresponding to EphA4 and EphA8 receptors proteins were detected but at a lower abundance compared to EphB. After more stringent filtering of the data, using a higher confidence threshold (FDR  $p < 0.01$ ), only EphB6, ephrinB1 and EphA4 had unique hits. Due to the redundancy of the Eph receptors' sequence, many peptide sequences identified to one receptor are common to other EphB receptors. Therefore, we cannot rule out that other Eph receptors may be present at the cell surface. It is also notable that in some of the proteomic runs (n=3 of 10), no Eph receptors were detected. Eph receptors are membrane proteins, and it is well known that it is more difficult to detect hydrophobic membrane proteins by using mass spectrometry<sup>217</sup>. These results show that this technique enables the visualisation of rarer proteins within the erythroblastic surface. However, comparisons of the reticulocyte surface data with other 4 high stringency available reticulocyte proteomes<sup>176,218–220</sup> showed that the majority of the proteins detected using the surface labelling are already detected. Only 16 were newly

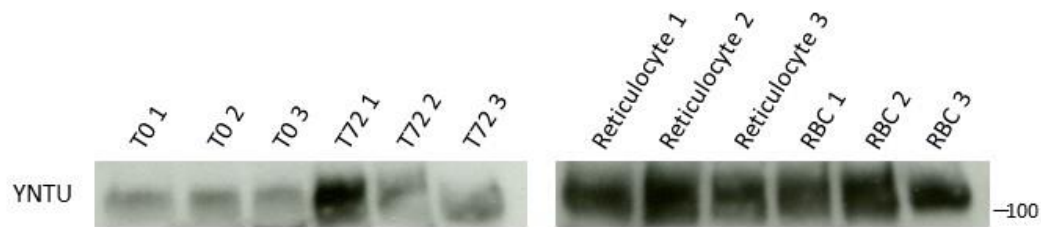


Figure 4-2 Surface labelled proteins were depleted of a proportion of band 3

Biotinylated lysates of differentiation courses were partially depleted of band 3 to increase proteomics sensitivity. After elution from streptavidin beads the sample was depleted of Band 3 by using Bric170 bound Protein G beads 3 separate times on the lysates. Both panels show the amount of Band 3 captured by the beads, to illustrate the depletion, using a polyclonal antibody for Band 3 C-terminal YNTU antibody. The final Band 3 pulldown is still saturated in reticulocyte and red blood cell samples, suggesting that some will still be present in these samples.

Accession	Description	D6	D6	T0	T0	T72	T72	Retic	Retic	Retic	Identity coverage peptide
P54764	Ephrin type-A receptor 4							1			100% EphA4
A0A087WYP8	Ephrin type-B receptor 6 (Fragment)	3									3 peptides 100% EphB6
O15197	Ephrin type-B receptor 6	13	4		1						8 peptides 100% EphB6 5 are shared between 3 to 5 Eph including EphB4 and EphA4
P98172	Ephrin-B1	4				3	2				5 peptides shared between 2 ephrinB including ephrinB2
Accession	Description	D6	D6	T0	T0	T72	T72	Retic	Retic	Retic	
P54764	Ephrin type-A receptor 4							1			
P29322	Ephrin type-A receptor 8	2	1		2	1	1				3 peptides shared between 3 to 7 Eph including EphB4 and EphA4
A0A087WYP8	Ephrin type-B receptor 6 (Fragment)	3									
O15197	Ephrin type-B receptor 6	14	4		1		1				
D6RDV5	Ephrin-A5						1				1 peptide shared between 6 ephrin including ephrinB2
P98172	Ephrin-B1	4				3	3				

Table 4-1 - Surface proteomics of erythroblastic timecourse

Table representing the abundance of peptides found in each samples for Eph receptors and their ligands, ephrins. The top of the table represents the peptides with a high level of confidence while those in the bottom of the table are those with a medium level of confidence.

detected and described in Table 4-2. A similar analysis needs to be conducted on the other stages of erythropoiesis.

#### 4.2.3 EphA4 on native reticulocytes

To ensure that the presence of EphA4 is not an unanticipated artefact of *in vitro* erythroid culture, we isolated native reticulocytes from peripheral blood by using CD71 magnetic beads as CD71 is present on reticulocytes but not red blood cells. Figure 4-3A shows that by western blot EphA4 is expressed in CD71<sup>+</sup> cells but not CD71<sup>-</sup> cells. Furthermore, we were later able to show the same thing by flow cytometry (Figure 4-3C).

#### 4.2.4 EphA4 is selectively retained in the reticulocyte

Using FACS sorted *in vitro* derived reticulocytes and nuclei using Hoechst samples kindly provided by Dr. Amanda Bell (Toye lab, University of Bristol), we confirmed that EphA4 restricts to the reticulocyte during enucleation, similar to protein 4.2, whereas the majority of integrin  $\beta$ 1 is preferentially lost with the nucleus <sup>22</sup> ( see Figure 4-3B; n=2). This suggests that the EphA4 that remains is preferentially retained in the reticulocyte, similar to other erythroid proteins that are known to preferentially partition to the human reticulocyte<sup>22</sup>. EphA4 could be used as a novel marker for reticulocytes as it is exclusive to reticulocytes compared to red blood cells

<b>GENE NAME</b>	<b>PROTEIN NAME</b>
<b>CD163L1</b>	CD163 molecule like 1(CD163L1)
<b>CSF2RB</b>	colony stimulating factor 2 receptor $\beta$ common subunit(CSF2RB)
<b>DISP1</b>	dispatched RND transporter family member 1(DISP1)
<b>EMP3</b>	epithelial membrane protein 3(EMP3)
<b>EPHA4</b>	Ephrin family-receptor 4 (EPHA4)
<b>FAM186B</b>	family with sequence similarity 186 member B(FAM186B)
<b>HLA-B</b>	major histocompatibility complex, class I, B(HLA-B)
<b>HLA-E</b>	major histocompatibility complex, class I, E(HLA-E)
<b>ITGA4</b>	integrin subunit $\alpha$ 4(ITGA4)
<b>ITGA5</b>	integrin subunit $\alpha$ 5(ITGA5)
<b>NCKAP1L</b>	NCK associated protein 1 like(NCKAP1L)
<b>PATJ</b>	PATJ, crumbs cell polarity complex component(PATJ)
<b>PKD1</b>	polycystin 1, transient receptor potential channel interacting(PKD1)
<b>PLXNA1</b>	plexin A1(PLXNA1)
<b>SLC22A8</b>	solute carrier family 22 member 8(SLC22A8)
<b>TMUB1</b>	transmembrane and ubiquitin like domain containing 1(TMUB1)

*Table 4-2 shows the exclusive proteins found in surface proteomics of reticulocyte after Band 3 removal*



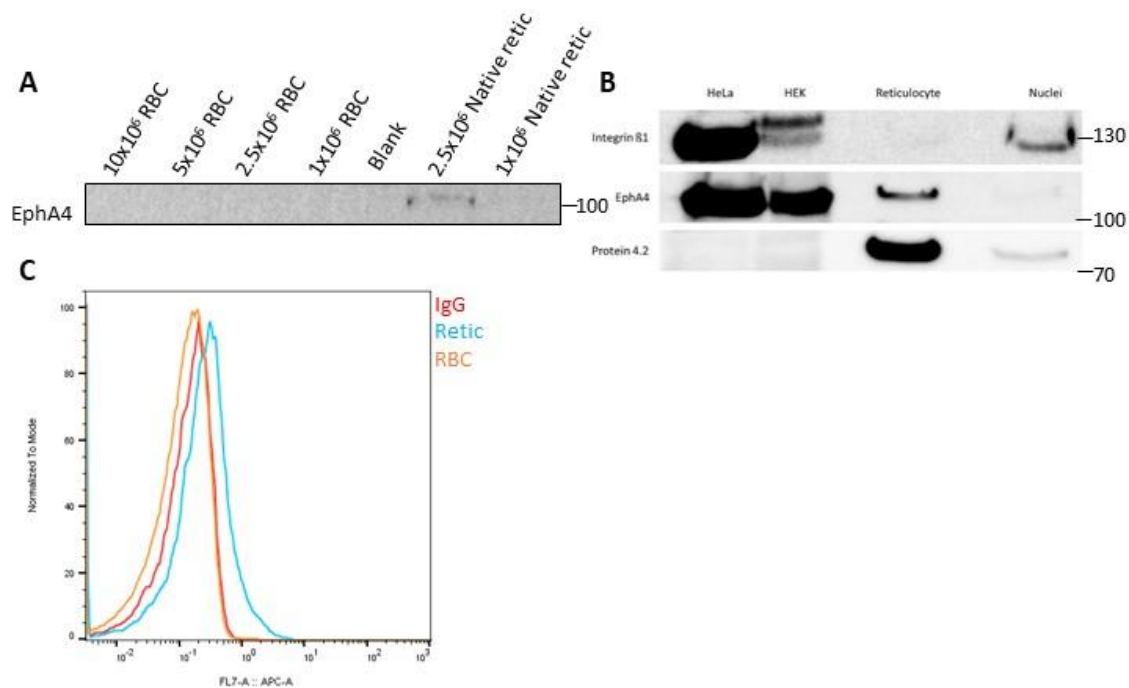


**Figure 4-3** EphA4 is selectively retained in cultured and native reticulocytes but is lost in red blood cells

**A** – Lysates from red blood cells and native reticulocytes were probed for EphA4 (n=2). This shows that EphA4 is present on native reticulocytes but is lost during maturation. **B** – Lysates from HeLa, HEK, and FACS sorted reticulocytes and nuclei were probed for Integrin β1, EphA4 and protein 4.2 (n=2). Integrin β1 was used as a control for nuclei and protein 4.2 as a control for the reticulocyte. EphA4 is selectively retained in the reticulocyte. **A and B** – All lysates were of 1x10<sup>6</sup> cells. **C** - Representative histogram plot of EphA4 expression in reticulocytes and red blood cells (RBC) (n=2). IgG control is in red, Reticulocytes are in light blue and RBC are in orange.

#### 4.2.5 Eph ligands expression by macrophages

Previous unpublished work by Dr. Charlotte Severn (Toye lab, University of Bristol) performed surface biotinylation and proteomics to generate a cultured macrophage “surfaceome” to identify proteins/receptors found at the cell surface (n=3). The only ephrins which were detected by proteomics were ephrinB1 (n=2 of 3) and ephrinB2 (n=2 of 3). EphrinB2 is the most common ligand of EphB4 and EphB6<sup>221</sup> which we detected on erythroblasts, therefore, we confirmed that ephrinB2 was detected on cultured macrophages and bone marrow macrophages (see Figure 4-4A and B). EphrinB2 is expressed at a higher abundance in cultured macrophage in comparison to native macrophages from the bone marrow (Figure 4-4C), and there was no discernible difference between sorted VCAM1<sup>+</sup> and VCAM1<sup>-</sup> macrophages. It is interesting to note that EphA4 is the only EphA receptor which has ephrinB2 as a ligand which is present in both the cultured and bone marrow macrophages.

We further tested whether any other ephrin from the A family were expressed by the macrophages, in particular ephrinA1, as it is one of the main ligands which interacts with EphA4<sup>221</sup> which is expressed on erythroblasts. EphrinA1 is present in these macrophages but at only low levels compared to the levels found in T0 erythroblasts (Figure 4-4D). This low abundance may explain why it was not detected in the cultured macrophage surfaceome proteomic dataset, as well as the macrophage’s ability to turn over its surface rapidly.

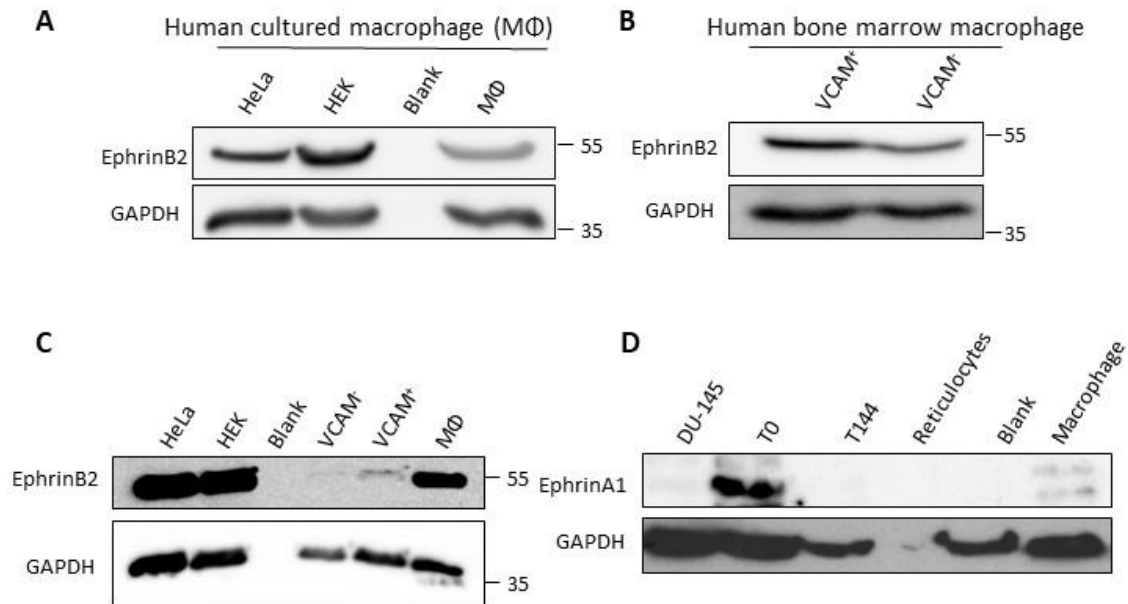


Figure 4-4 Cultured and bone marrow macrophages express Eph receptor ligands

A – Lysates from HEK, HeLa and cultured macrophages with dexamethasone were probed for ephrinB2 and GAPDH (n=3). B – Lysates from human bone marrow macrophages sorted for CD14<sup>+</sup>VCAM1<sup>-</sup> and CD14<sup>+</sup>VCAM1<sup>+</sup> cells probed for ephrinB2 and GAPDH (n=2). C – Lysates from HEK, HeLa, bone marrow sorted and cultured macrophages with dexamethasone were probed for ephrinB2 and GAPDH (n=2). D - Lysates from an erythroblast differentiation course and cultured macrophages with dexamethasone probed for ephrinA1 and GAPDH (n=1). A, B and C – All lysates were the equivalent of  $1 \times 10^6$  cells.

#### 4.2.6 Eph receptors are dynamically expressed during erythroid terminal differentiation

To assess the timeframe in which the Eph receptors are expressed on the surface of erythroblasts during terminal differentiation, a surface binding assay was performed as no flow antibodies are currently reported. EphrinB2 was selected as the ligand used in this experiment as it is known to bind all EphB receptors<sup>222</sup>. Figure 4-4C demonstrates that the erythroblasts bind ephrin-B2 during the expansion phase when cells are CD34<sup>low</sup>/CD36<sup>high</sup> and judged morphologically to be proerythroblasts (Figure 4-5A). Once cells commence terminal differentiation (T0 hours), a steady reduction of ligand binding was observed and by T72 hours all ability to bind ephrin B2 is lost. At T72 hours, the majority of erythroblasts present in culture were beyond the basophilic stage (Figure 4-5B), confirming that EphB receptors are expressed during the early phases of erythroid terminal differentiation. However, no binding of ephrinA1 or EphB4 was observed. We would expect these to bind due to the presence of EphA4 and ephrinB2 on the cells. This implies that these receptors and ligands either may not be in an accessible form or may not be present at the surface of these cells.

Integrins are crucial in cell to cell contact and adhesion with macrophages through the formation of focal adhesion points<sup>93,100,128,223</sup>. We tested whether the appearance of integrins on the erythroblast surface coincided with EphB4 receptor surface expression. To detect the total level of integrins which could bind VCAM1, a surface binding experiment was conducted using VCAM1-Fc and the integrins were pre-activated with manganese to ensure VCAM1-Fc construct would bind. VCAM1-Fc bound throughout erythroblast differentiation with a loss at approximately T144 hours when 50% of the

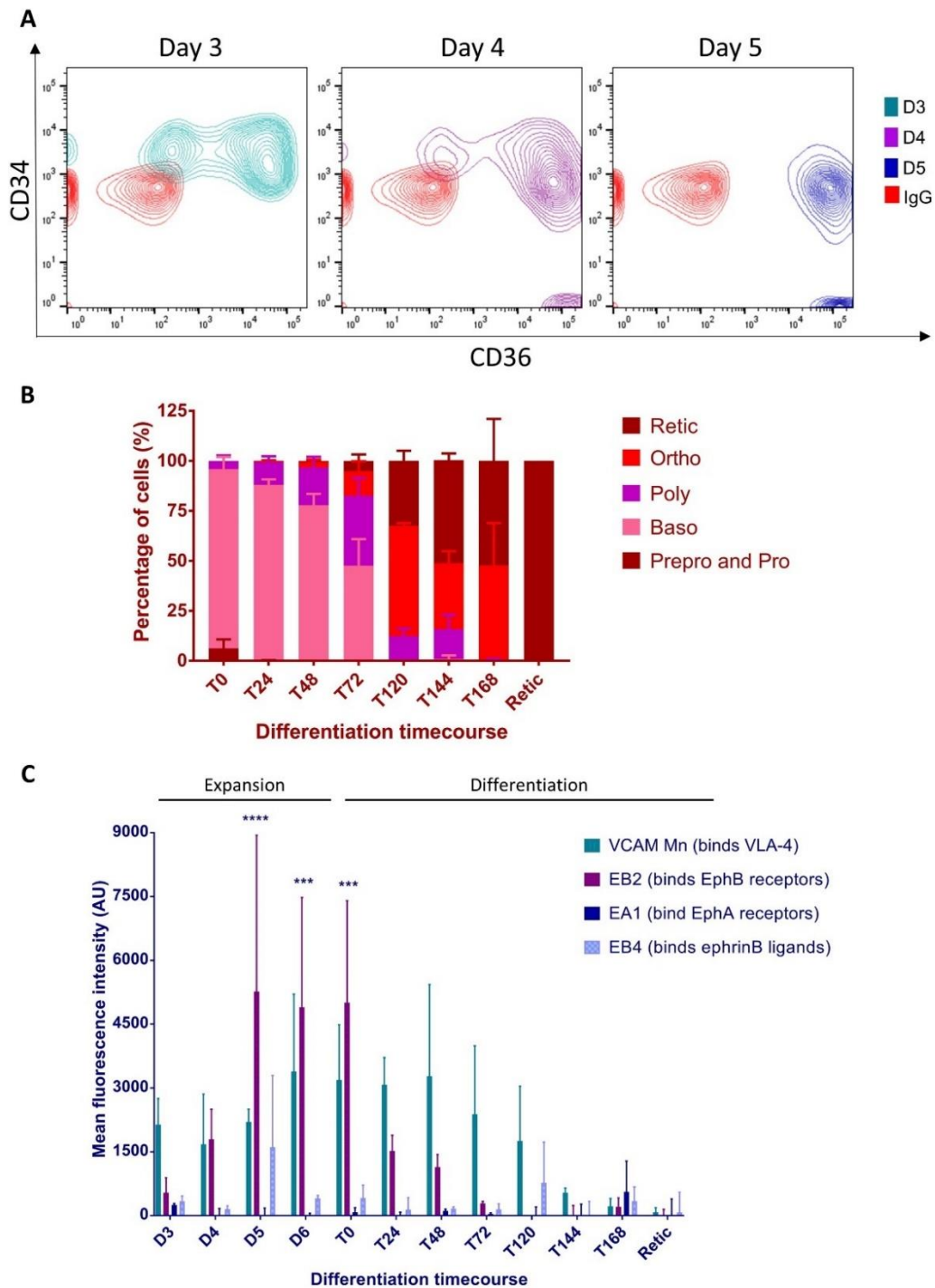


Figure 4-5 Erythroblasts have a dynamic surface expression of ephrins

A - Representative waterfall flow cytometry of the CD34 and CD36 at day 3, day 4 and day 5 of erythropoietic culture ( $n=5$ ). B - Cytospin counts from 6 separate differentiation cultures for the cell types observed in cultures ( $n=6$ ). C - Graph showing the mean fluorescent intensity (MFI) obtained by flow cytometry of the constructs binding to erythroblasts throughout terminal differentiation. EB2 is ephrin-B2-Fc and VCAM Mn is VCAM-Fc with manganese activation. The ephrin constructs were pre-clustered. All points are means for ephrin-Fc constructs ( $n=5$ ) and VCAM ( $n=3$ ). The error bars represent the standard error of the mean. 2way ANOVA was performed as a comparison of binding compared to the IgG control (\*\*\*) ( $p<0.001$ ); \*\*\*\* ( $p<0.0001$ )).

cells were reticulocytes (Figure 4-5C). Manganese treatment was observed to increase cell death and clustering, therefore, flow cytometry analysis was performed only on live single cells during the surface assay by gating on unclustered propidium iodide negative cells.

#### 4.2.7 Baseline activation of integrins occurs during the height of EphB4 and EphB6 expression

We next wanted to establish the level of integrin  $\beta 1$  activation during the stages at which EphB4/B6 become more pronounced at the surface of erythroblasts. To do this, we used an antibody HUTS-21 that specifically recognises the active form of integrin  $\beta 1$ , which is present in both the VLA-4 and VLA-5 complexes. Manganese was used to activate integrins beforehand as a positive control. We detected a marked increase of integrin  $\beta 1$  activation between days 4 and 5 on erythroblasts in the absence of any treatment (representing an increase from 10 to 30% of cells by day 5; Figure 4-6A). The CD36<sup>high</sup>/CD34<sup>low/-</sup> populations displayed this rise in baseline integrin  $\beta 1$  activation (Figure 4-5A). We can see from Figure 4-6B that the cells which have the activation have a higher mean, but this is still relatively small compared to the one found when the integrins are completely activated with manganese. Importantly, we can also confirm that from the VCAM1 binding experiment shown in Figure 4-5C, that the level of total integrin is not altered at this stage of differentiation. To determine the contribution of Eph receptor stimulation on integrin  $\beta 1$  activation, the amount of active form of integrin  $\beta 1$  was monitored in the presence of clustered Ephrin-B2. The addition of ephrinB2 did not have any significant effect on the activation levels of integrin  $\beta 1$  (Figure 4-6A).

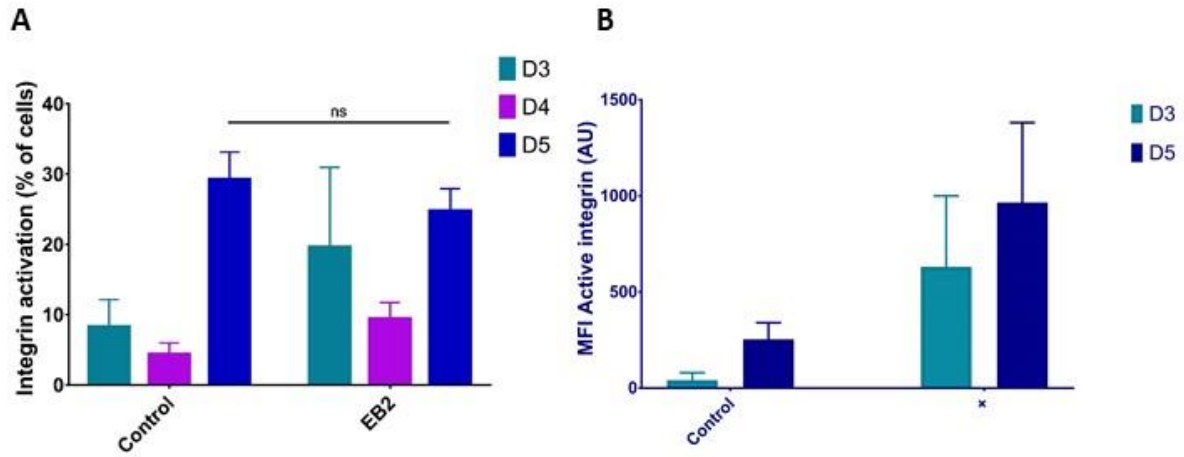


Figure 4-6 Proerythroblasts gain integrin $\beta$ 1 activation

A - Histogram showing the percentage of cells with active integrin obtained by flow cytometry using an antibody that detects the active form of integrin  $\beta$ 1 during three days of expansion of the erythroblasts and after stimulation with ephrinB2 (EB2;  $n=4$ ). Error bars represent standard error of means. B – Histogram showing the mean fluorescence intensity of active integrin through expansion of erythroblasts and after stimulation with manganese (+;  $n=4$ ). Error bars represent standard deviation.

#### 4.2.8 Eph receptor knockdown

To confirm the presence of the specific Eph expression and to study the contribution of the Eph receptors in these cells, EphB4, EphB6 and EphA4 knockdowns were attempted in primary erythroblasts using lentiviral shRNA. Since the EphB4 and EphB6 receptors expression are lost from the cells by T72 (see figure 4-1B), we wanted to ensure that they were knockdown earlier than our current protocol would allow (around T0) and assess the effects on the expanding erythroblasts. To achieve this, the lentivirus transduction protocol was adjusted to add virus to the cells at Day 0, straight after their isolation rather than at Day 3. This meant a higher level of death due to the addition of virus, but also impacted on cell numbers in later experiments. The cells also took longer to respond to puromycin; therefore, puromycin was present for a longer period of time to select for transfected cells.

After amending the lentiviral transduction protocol, EphB4 and EphB6 were successfully knocked down from day 3 onwards (Figure 4-8A; n=6). This was observed using 3 different hairpins (Figure 4-8E and F). However, EphA4 was not knocked down despite testing 4 different hairpins (3 examples are shown in Figure 4-8C and D). Interestingly, the quantification of the western blots in Figure 4-8B suggests that when EphB4 is knockdown, this affects the level of EphB6. On the other hand, when EphB6 is knockdown, there is no change in EphB4 receptor levels. Of particular note is that the cells with reduced EphB4 also exhibited reduced expansion, due to death or loss of proliferation capacity, while EphB6 shRNA cells were not affected. When two different hairpins for EphB6 were combined there was a larger loss of EphB6 as well as a loss of EphB4 (Figure 4-8B). Therefore, some EphB4 can remain on its own when EphB6 is



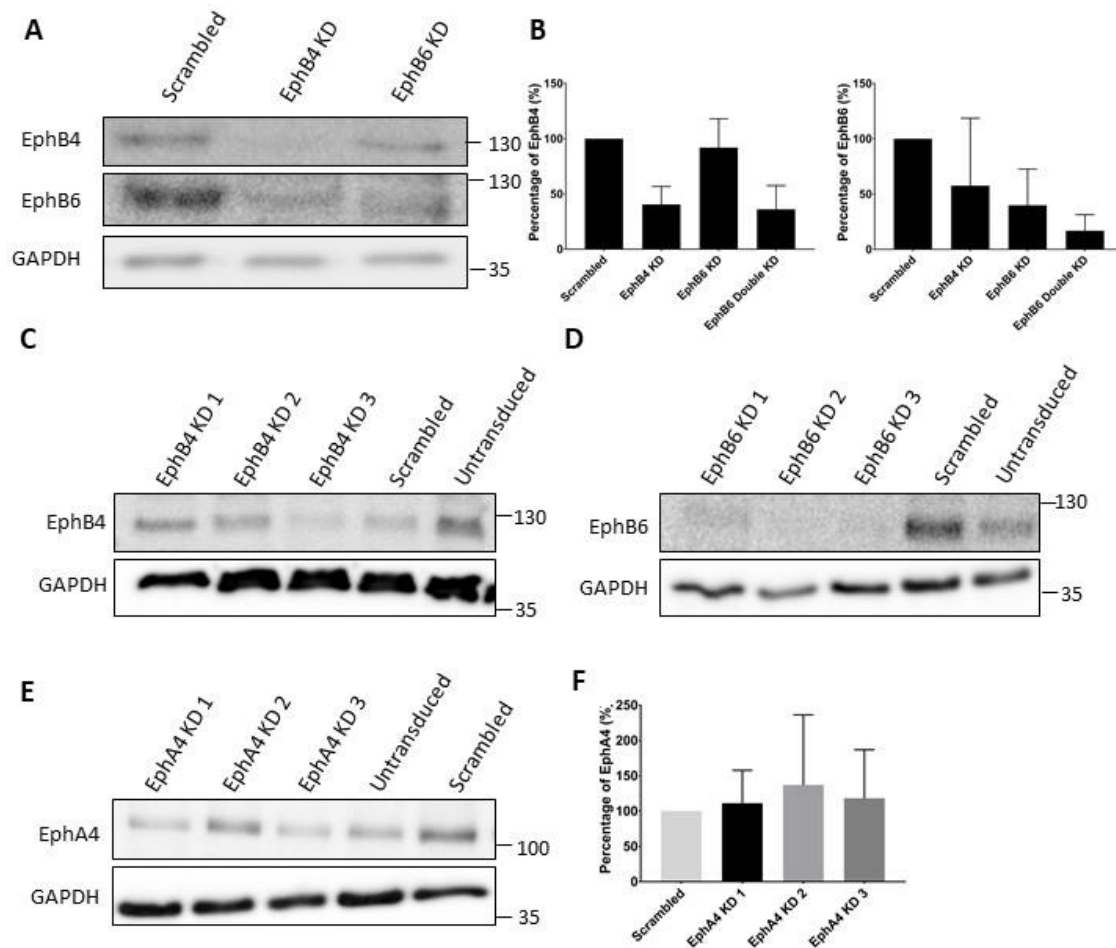


Figure 4-7 Lentiviral shRNA knockdown of EphB4 and EphB6

A – Lysates from day 4 erythroblasts, treated with the indicated shRNA, were blotted for EphB4, EphB6 and GAPDH. This is a representative plot (n=5). Lysates were equivalent of 150 000 cells. B– Quantification of the blots in A and 4 other repeats, normalised to GAPDH (n=5). Left panel shows the standard error of the mean and right panel shows standard deviation. C – Lysates from day 8 erythroblasts, treated with 3 hairpins for EphB4, blotted for EphB4 and GAPDH (n=2). D – Lysates from day 8 erythroblasts, treated with 3 hairpins for EphB6, blotted for EphB6 and GAPDH (n=2). E - Lysates from day 8 erythroblasts, treated with 3 hairpins for EphA4, were blotted for EphA4 and GAPDH (n=3). C, D and E – Lysates were equivalent to 1x10<sup>6</sup> cells. F – Quantification of the blots in E and 1 other repeat, normalised to GAPDH.

removed, but if all of it is removed, then EphB4 is no longer able to be sustained and is lost.

#### 4.2.9 Short exposure to EphrinB2 inhibitory peptides inhibits ligand binding

We next wanted to examine whether the Eph receptors were responsible for the activation of the integrin  $\beta 1$  at the surface of the cells. We hypothesised that the engagement of Eph receptors would result in activated integrins which can then bind the macrophage and solidify the attraction and the tie of the cells to each other. Anselmo et al.<sup>128</sup> hinted towards such a potential mechanism. We further hypothesised that since Day 6 erythroblasts have both ephrinB2 and EphB4/EphB6, the cells could be interacting with each other in culture (and in the bone marrow stem cell niche *in vivo*). Through the Eph receptor-ligand interaction, there could be activation of integrin which would help prime the cells for when they contact the macrophages.

To test the impact of the loss of Eph activation, we first added specific EphB4 receptor inhibitors and a pan-Eph receptor inhibitor. These inhibitors were described by Koolpe et al.<sup>224</sup>. The EphB4 receptor inhibitor (TNYL-RAW peptide) competes with the ephrinB2 binding but does not activate the receptor. The pan-EphB receptor inhibitor (THW peptide) is a peptide capable of binding all the EphB receptors, and therefore blocking all interactions with ephrin ligands. As a control, we used a peptide used in a study testing EphA2 peptides<sup>225</sup> (DYP) which used this peptide as a control as it should not bind any Eph receptors.

In a competition assay, it was observed from Figure 4-8A, that the TNYL-RAW inhibitor had a significant effect on ephrinB2 binding to the cells, indicating that the ligands mostly bind the EphB4 receptor rather than the EphB6 receptor. However, this could

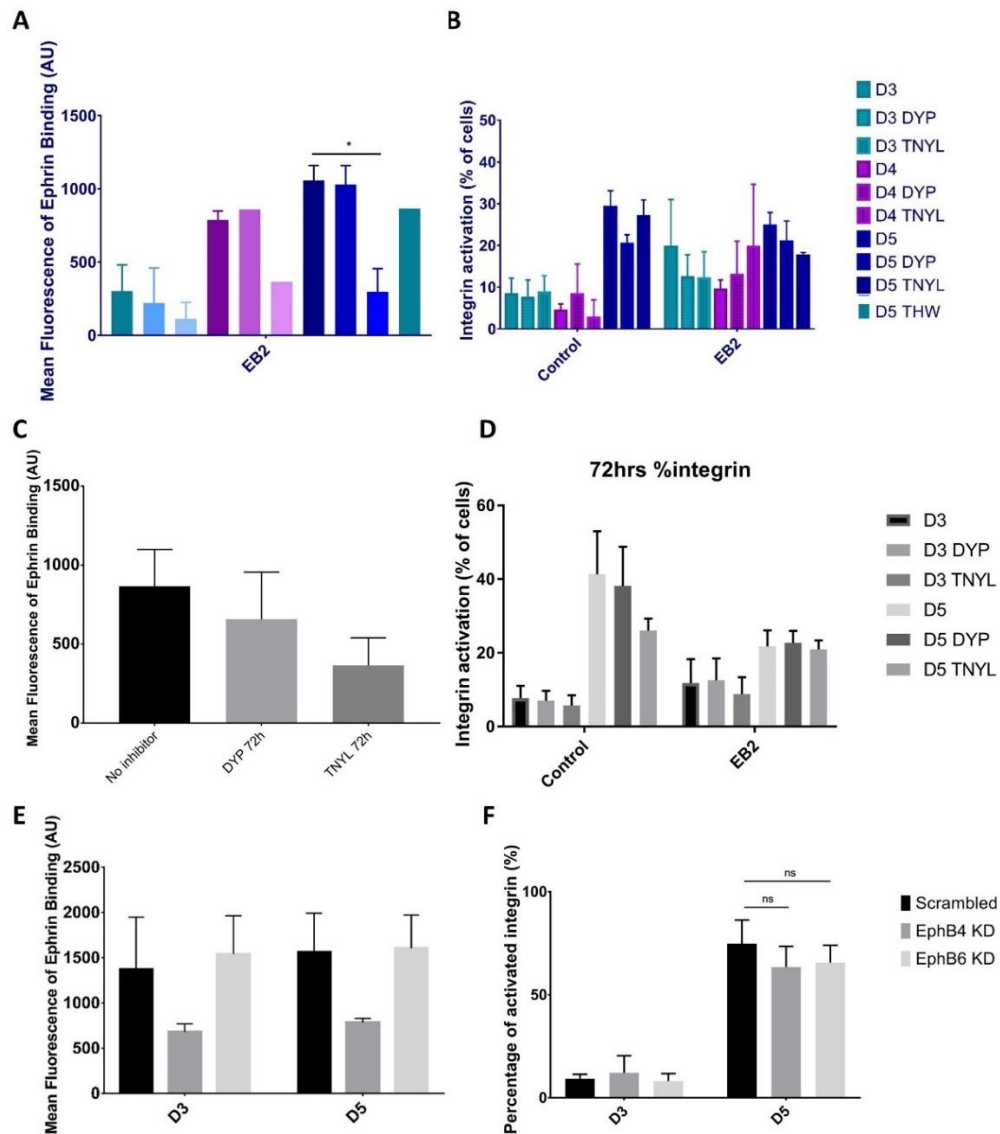


Figure 4-8 Inhibition or removal of EphB receptors does not affect integrin ̢1 activation

A - Graph shows the mean fluorescence value obtained by flow cytometry of the ephrin-B2 construct binding through three days of expansion of the erythroblasts with different 15-minute treatments (n=3). One-way ANOVA conducted on the data (\* (p<0.05)). B - Graph shows the percentage of cells obtained by flow cytometry expressing the active form of integrin ̢1 through three days of expansion of the erythroblasts with different 15-minute treatments (n=2). DYP is the control peptide; TNYL is a specific EphB4 inhibitory peptide and THW is a pan-EphB inhibitory peptide. The error bars represent the standard error of the mean. C - Graph shows the mean fluorescence intensity obtained by flow cytometry of the ephrinB2 construct binding through three days of expansion of the erythroblasts with treatment added throughout (n=3). B - Graph showing the percentage of cells obtained by flow cytometry expressing the active form of integrin ̢1 through three days of expansion of the erythroblasts with treatment added throughout (n=3). E - Graph shows the mean fluorescence value obtained by flow cytometry of the ephrin-B2 construct binding through three days of expansion of shRNA-treated erythroblasts (n=4). F - Graph shows the percentage of cells obtained by flow cytometry expressing the active form of integrin ̢1 through three days of expansion of shRNA-treated erythroblasts (n=4). The error bars represent the standard error of the mean. Two-way ANOVA conducted on the data (ns (p>0.05)).

also be because we have not saturated the receptors, as only two concentrations of the inhibitor were tested. The inhibition by TNYL-RAW was very rapid, occurring within 15 minutes before ephrinB2 was added to the cells. Importantly, the DYP control had no effect on ephrinB2 binding and surprisingly, the THW peptide did not affect ephrin binding.

#### 4.2.10 EphrinB2 stimulation does not cause the increase in integrin $\beta 1$ activation

The addition of ephrinB2, which would activate the EphB receptors and their effectors, did not have any effect on active integrin  $\beta 1$  (Figure 4-6A). The presence of inhibitors specifically blocked the binding of ephrinB2 (Figure 4-8A and C) but did not significantly affect the rise of integrin activity (Figure 4-8B). The inhibitor was only added for 15 minutes before the ephrinB2 was added. Therefore, it is possible that the cells need sustained inhibition. The inhibitors were also added throughout expansion (Figure 4-8C and D). This treatment did not increase the level of inhibition of ligand binding, the cells capacity to expand, or their ability to exhibit activated integrin on the cell surface. Furthermore, the continued application of control peptide DYP, which did not affect the binding of ephrinB2 (Figure 4-8A), affected the activation of integrin for unknown reasons.

To finally determine whether integrin  $\beta 1$  activation is controlled by EphB receptors, we used the EphB4 or EphB6 shRNA knockdown erythroblasts to explore whether specific removal of Eph impacted on the activation of integrins. The rise in integrin  $\beta 1$  activation was not significantly affected by either knockdown treatment (Figure 4-8E and F). Therefore, although integrin  $\beta 1$  activation is coincident with the appearance of EphB receptors on the surface during erythroblast differentiation, the rise in integrin  $\beta 1$

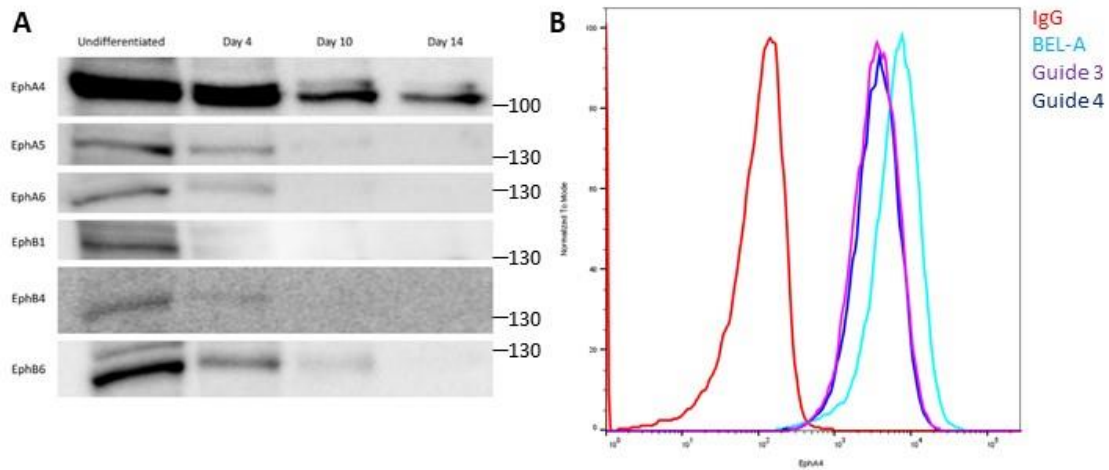


Figure 4-9 BEL-A immortalized line express multiple Eph receptors including EphA4 which was knocked down using CRISPR-Cas9

A – Lysates from expanding and differentiating BEL-A cells were probed for EphA4, EphA5, EphA6, EphB1, EphB4 and EphB6 (n=1).  $1 \times 10^6$  cells were loaded in each well. B – Histogram plot of BEL-A cells, transduced with EphA4 CRISPR guides, probed for EphA4 (n=2). IgG control is in red, untransduced BEL-A cells are in light blue, BEL-A cells transduced with Guide 3 are in purple and BEL-A cells transduced with Guide 4 are in dark blue.

activation is independent of EphB and might rely on or be circumvented by an alternative integrin  $\beta$ 1 activation pathway.

#### 4.2.11 Eph receptors are also expressed on the BEL-A immortalised cell line

We also explored the presence of Eph receptors in the erythroid cell line BEL-A<sup>173</sup> to test if we could use these cells as a model cell to test our hypotheses. Surprisingly, as can be observed in Figure 4-9A, expanding BEL-A cells were positive for all Eph receptors proteins tested. However, once the doxycycline is removed at day 4, the cells only express EphB4, EphB6, and EphA4 similar to normal erythroblasts. In addition, EphA4 was the only receptor which persists until the end of the differentiation course and is detected on reticulocytes.

#### 4.2.12 EphA4 CRISPR

As the EphA4 shRNA did not work on primary cells, and the role of EphA4 needs to be studied in reticulocytes, the recent availability of BEL-A cells gave the opportunity to remove this receptor using CRISPR-Cas9 generated knockouts. To do this, we used two confirmed guides introduced by lentivirus (Figure 4-9B). After selection by puromycin, a large proportion of the cells exhibited a reduction in EphA4, but there were no full knockout clones detected (see Figure 4-9B). These cells were single cell cloned to find the clone with the smallest amount of EphA4 (Figure 4-10A and B). Out of 34 subclones selected, only two subclones had a low amount of EphA4 but, unfortunately, none were a complete knockout. One of the two clones was selected for expansion and sequenced. It had a mutation close to the guide target site which led to a single amino-acid deletion (Figure 4-11A). These cells were differentiated to test whether upon differentiation EphA4 was completely lost as many proteins reduce expression during the terminal

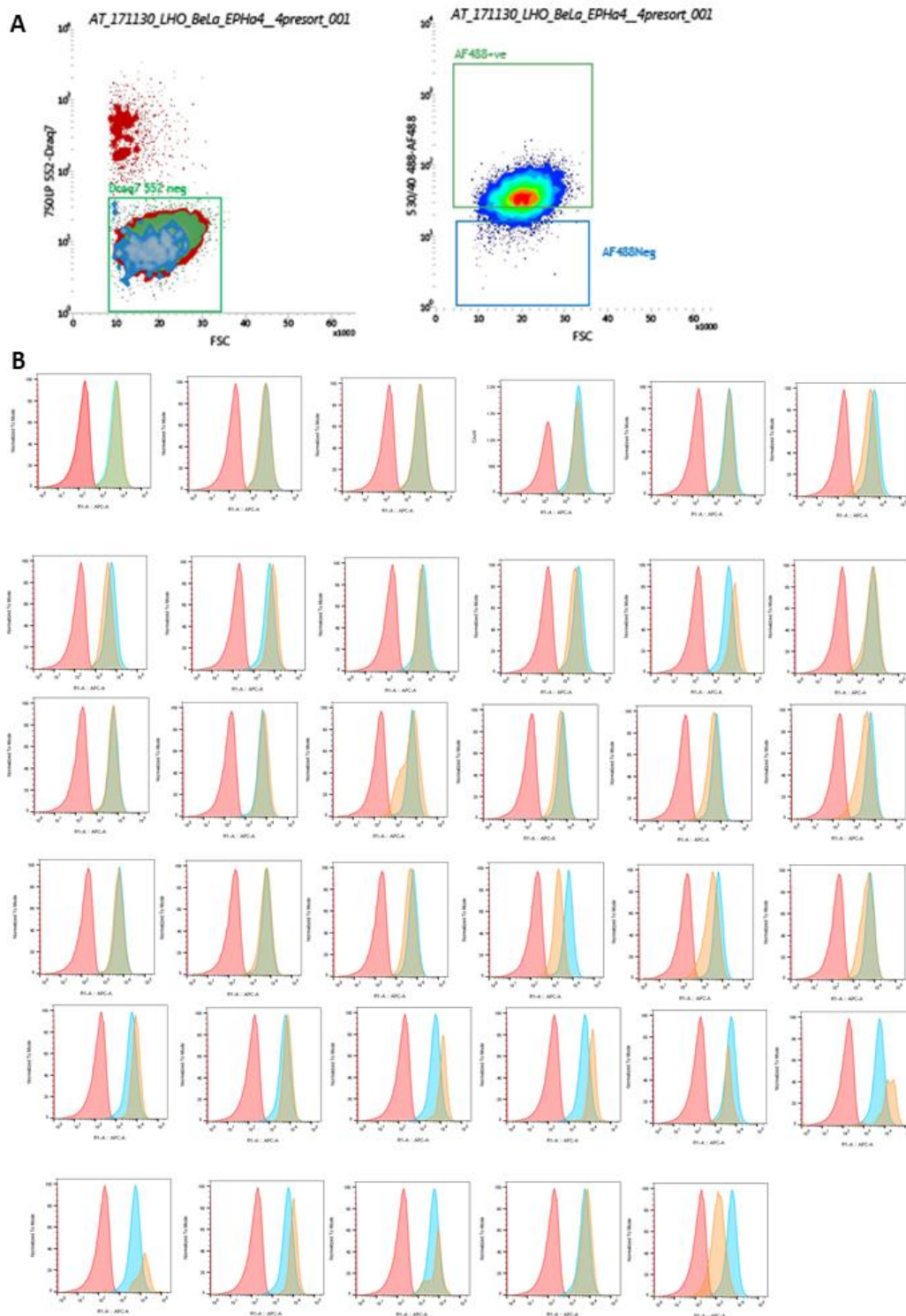


*Figure 4-10 Single cell cloning EphA4 knockdown cells*

*A – Dot plots of the transduced BEL-A cells pre-sort and the gates used for FACS sorting EphA4<sup>+</sup> cells. B – Histogram plot of 36 single-sorted BEL-A cells probed for EphA4. IgG control is in red, BEL-A cells are in blue and transduced cells are in orange.*





differentiation stage. Unfortunately, the cells still retained the EphA4, almost more than the BEL-A cells at the reticulocyte stage (Figure 4-11B and C). At this point, this project was stopped as EphA4 appeared to be important for BEL-A, and possibly, erythroblast survival.

### 4.3 Discussion

In this chapter, we have explored the expression of Eph/ephrins family proteins in erythroblasts and macrophages as these were hypothesised to play an important role in the adhesion of the erythroblastic island.

Using mRNA, western blots and proteomics, we showed that several Eph receptors are present at the surface of the erythroblasts as they differentiate. However, they are only present at the surface of the cells for a specific amount of time. EphB4 and EphB6 have been shown to have a specific spatiotemporal expression profile at the surface of the erythroblasts, and this is detectable in advance of the VLA-4 integrin complex expression which binds VCAM1. The integrin complex increases its presence at the surface of the cells about 24 hours after the EphB4 and EphB6 is at peak binding capacity, and shortly after there is a rise in basal level of integrin  $\beta$ 1 activation. EphB4, EphB6, and EphA4 are the only receptors which are expressed on the surface in the differentiating erythroblasts. Interestingly, these three receptors have been known to cluster together. Truitt et al.<sup>226</sup> showed that when the EphB6 and EphB4 heterodimerize this leads to the cells favouring adhesion after activation by ephrinB2. They also found that in breast cancer cells, EphB6 is downregulated leaving EphB4 on its own, making cells more motile. This fits our hypothesis that the EphB receptors at this stage in the differentiation are important for the adhesion of erythroblasts to macrophages. This result might also help explain the reason why we observe a loss of EphB6 when EphB4 is knockdown but not the contrary when EphB6 is removed. Therefore, the EphB4 and EphB6 receptors may be working together at the surface of the erythroblast. Furthermore, the effect on EphA4, which is also present, was not tested. It would be

interesting to see if this receptor may also play a role as it could also heterodimerize with EphB4 and EphB6<sup>227</sup>.

It is also known that varying levels of ephrin-B2 can influence the function of EphB6<sup>228</sup>. With low levels of stimulation from ephrinB2, EphB6 leads to attraction while high levels lead to repulsion. This might affect the interactions between the erythroblasts and the macrophages. As we saw in Figure 4-3, the cultured macrophages and the bone marrow macrophages have very different levels of ephrinB2, though their surface was not tested. Therefore, this is something that will need to be kept in mind when testing the interactions between these cells as the +Dex macrophages and the bone marrow macrophages interact in very similar ways with erythroblasts. This implies that EphB6 might play quite a minor role. This is evidenced further by its loss upon removal of EphB4 but not vice-versa. It is possible that in our cells, these receptors can heterodimerize and help each other be stable in the membrane. However, only the loss of EphB4 would lead to a complete loss of the complex. EphB4 expression alone would be able to homodimerize and compensate. The role of EphB6 could be dissected further in future work to understand whether it exists in a complex with EphB4 at the surface of the cells.

We also report for the first time that mRNA and western blots showed the presence of EphA4 in these cells, throughout differentiation for the first time but its expression diminished at the later stages of differentiation. The surface proteomics experiments only detected EphA4 in a single proteomics experiment, but it was also detected on the surface by flow cytometry. However, the expression levels may not be significant or functional as binding experiments with ephrinA1 (the most potent binding partners of

EphA4) did not demonstrate any binding at any stage of differentiation. Further, ephrinB2 which can also bind to EphA4 was not able to bind anymore after T72 despite the sustained presence of EphA4. It is possible that too little EphA4 remains at the final stages for ephrinB2 to bind or it is possible that EphA4 is unstable at the cell surface and internalised throughout the differentiation course or presented differently. It would be necessary to check this in further experiments, for example by using immunofluorescence and internalisation assays.

Surprisingly, some of the receptors were observed only in specific donors. For example, EphA5 appeared in the mRNA at T72 and the protein in the reticulocyte in one donor but did not appear in the other two donors tested. This could be attributed to donor variation or non-specific binding. This is particularly interesting with EphB1, which is claimed by Anselmo et al. to be present in mice erythroblasts. However, we only detected EphB1 expression in one of our donor samples. Therefore, this shows the importance of not just extrapolating observations in mice to humans without checking protein expression for these receptors.

#### 4.3.1 BEL-A cells Eph expression

Recently a novel erythroid cell line has been reported that offers an exciting opportunity to manipulate erythroblast protein expression and this was first done recently for certain problematic blood groups<sup>179</sup>. We show that undifferentiated BEL-A cells are not a good model for our system when they are expanding as they express a higher amount of multiple Eph receptors, in particular, EphA receptors. However, once they are induced to differentiate, they regain the specific receptor expression profile we characterised for primary erythroblasts. Therefore, the altered Eph receptors

abundance is due to the characteristics of the expanding cell line. This poses an intriguing question: why do they possess this increased Eph receptor profile? This could be to be able to expand indefinitely. It could also explain why these cells need to be grown at low density, to reduce the chance of differentiation. This could be brought about by the contact inhibition of locomotion, as these cells will migrate away from each other, staying at a low density. It would be interesting to look at the role of the Eph receptors in these cells in the future. If they are the reason they need to be grown at low density, manipulating Eph/ephrin family signalling may provide an opportunity to expand these cells in a more cost-effectively way.

The BEL-A cells have proven very useful in their ability to be genetically manipulated<sup>179</sup>, in particular using CRISPR. They can be efficiently transduced, and many of the cells will have mutations on both alleles around the guide sequence. This poses an interesting question for the CRISPR of EphA4 on BEL-A cells. All of the clones which survived and were sequenced which had mutations only had it on one allele, or it led to a null mutation. In this way, all of the cells had a small loss of EphA4 as shown in Figure 4-8B, but there never was a complete knockout. This implies that removing EphA4 might be affecting the cells survival. It is possible that the complete knockout of EphA4 is fatal to BEL-A cells and even primary cells, as shRNA did not produce a reduction either. Therefore, EphA4 might play a more substantial role than expected in erythropoiesis and it would be important to study this further. It is important to note, however, that removal of EphA4 in mice has not been reported to affect haematopoiesis (personal correspondence with Prof Jing, Wakayama Medical University), though stress erythropoiesis has not been applied to these mice and there may be species differences.

#### 4.3.2 Integrin $\beta$ 1 activation

The rise in basal integrin  $\beta$ 1 activation observed after the appearance of EphB binding capability in differentiating erythroblasts is intriguing. This suggests that the integrins might be activated by the interaction between the EphB receptors and ephrinB2. Since the progenitor cells will have both the receptors and the ligands expression the cells could be interacting with each other in the endosteal niche, or in the dish, leading to a “priming” of the integrins before the cells meet the macrophages. This may also explain why erythroblasts can be grown in culture in the absence of macrophage. However, we observed that Eph receptors do not affect the activation of integrin  $\beta$ 1. There appears to be a correlation between integrin activation and the presence of EphB receptors at the surface of these cells. However, this is not causal. This goes against the findings of Anselmo et al.<sup>128</sup>, pointing to a difference between mice and human cells.

Even though the published control peptide DYP did not affect Eph binding, it does appear to affect the integrin  $\beta$ 1 activation after repeated additions. Therefore, the addition of a peptide in the media can affect the cells. We cannot exclude the fact that it may have secondary binding sites which might affect the integrin. The addition of a peptide might simply interfere with the ability of integrins to bind to the antibody. Therefore, it was important to follow up our inhibitor study with a knockdown of Eph receptors using genetic manipulation.

#### 4.3.3 Conclusion

This work has defined the Eph/ephrin family expression on erythroblasts throughout erythropoiesis for the first time and also confirmed the presence of EphrinB2 on both cultured and bone marrow macrophages. The specific combinations of Ephs/ephrins

and the known role in regulating migration/adhesion is consistent with the idea that these may drive an interaction between the two different cell types and also potentially between themselves (in the case for erythroblasts). The expression patterns of the different proteins are summarized in Figure 4-12. However, lack of effect of Ephs/ephrins on integrin activation suggests they may not play as vital a role given the belief in the field that it is integrins that drive this interaction. The role that Ephs/ephrin family interactions will be tested further in the next chapter by bringing together the high throughput imaging assay in Chapter 3 and the manipulations of EphB4 and EphB6 interaction developed in this chapter.

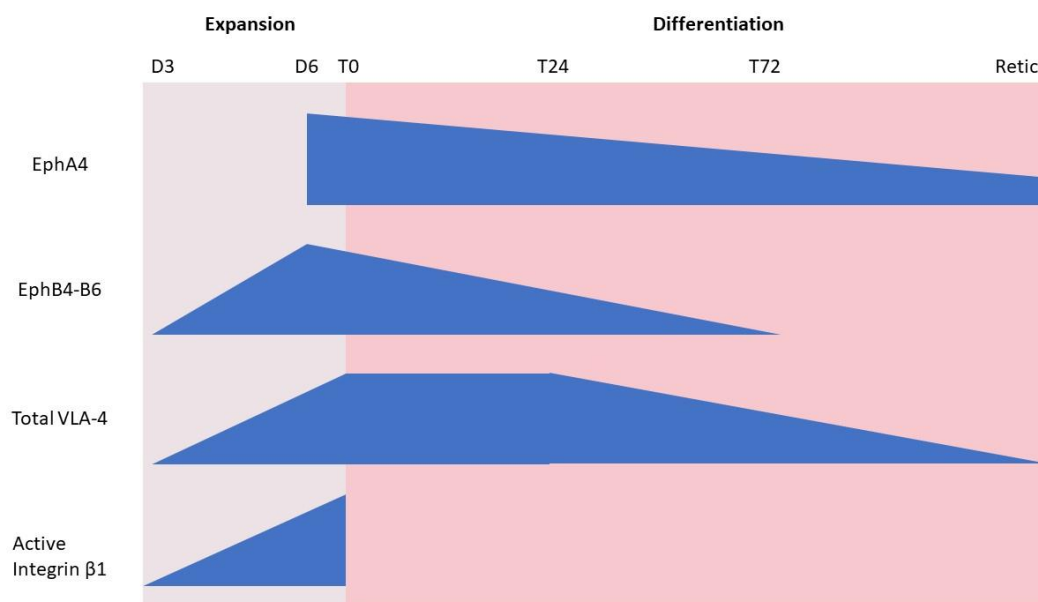


*Figure 4-12 Summary diagram of expression of the different proteins discussed in this chapter throughout erythropoiesis*

*Diagram representing the expression patterns of EphA4, EphB4, EphB6, VLA-4 and active integrin β1 in erythropoiesis.*

*The diagram is based on results found in this chapter but is not to scale.*

## 5 Chapter 5 – Investigating the involvement of specific receptors in erythroblastic island formation

### 5.1 Introduction

Using our reconstitution assay and live imaging assay described in Chapter 3, we were able to distinguish two distinct aspects of erythroblastic island formation or more specifically the interaction between macrophages and erythroblasts. We demonstrated that this methodology could separate the number of connections and the length of time the cells interact. This can inform us on whether receptors are involved in recognition, the binding or stability of this important interaction between these two cells types. The presence of VCAM1 on the macrophages does affect how the two cell types interact with each other. However, cells without VCAM1 on their surface (+Dex macrophages or VCAM1<sup>-</sup> bone marrow macrophages) can still form interactions with erythroblasts. Therefore, our system has improved our understanding of the importance VCAM1 plays in these interactions. The next step is to gauge the roles of a variety of signals.

Given the information we now have about the Eph receptors present and the tools we established in Chapter 4, we can now design experiments to assess the role of the Eph receptors in macrophage-erythroblast interactions in our reconstitution/live cell imaging assay.

In addition to studying the role of ephrins in erythroblastic island formation, we can now also explore the utility of the screening methodology to determine whether the different classes of P2 receptors, which are abundant on the surface of macrophages,



have any involvement in the interaction with erythroblasts or reticulocytes. Immune cells are known to express a range of different purinergic receptors to help direct their migration and activation<sup>229</sup>. The surfaceome work that we undertook on cultured macrophages suggested that p2x7, p2y11 and p2y6 receptors are present in cultured macrophages and that P2X7 was particularly abundant. As inhibitors to the different classes of P2X and P2Y receptors are available, we hypothesised that inhibiting these receptors could affect the interaction with erythroblasts.

This chapter will explore the importance of Eph/Ephrins in the macrophage/erythroblast interaction and also undertake preliminary work to explore whether the P2X and P2Y receptors are involved.

## 5.2 Results

### 5.2.1 EphB4 receptor has a role in the adhesion of erythroblasts to macrophages

Using the macrophage-erythroblast live cell imaging assay described in Chapter 3, we tested the involvement of Eph receptors in erythroblastic island formation. Experiments were performed on +Dex macrophages to optimise the assay as their phenotype is very close to the bone marrow macrophage's. To do this, we used the inhibitors tested in Chapter 4, using DYP as a control and TNYL as a specific EphB4 inhibitor<sup>224</sup>. For the imaging, inhibitors were preincubated with the erythroblasts for 15 minutes before adding to the macrophages, as according to previous reports, after 15 minutes, the inhibitors will have started to have an effect<sup>230,231</sup>. The inhibitor was then replenished the next day when the excess erythroblasts were removed with a gentle media wash. Preliminary data showed that even a single wash in PBS can lead to a loss

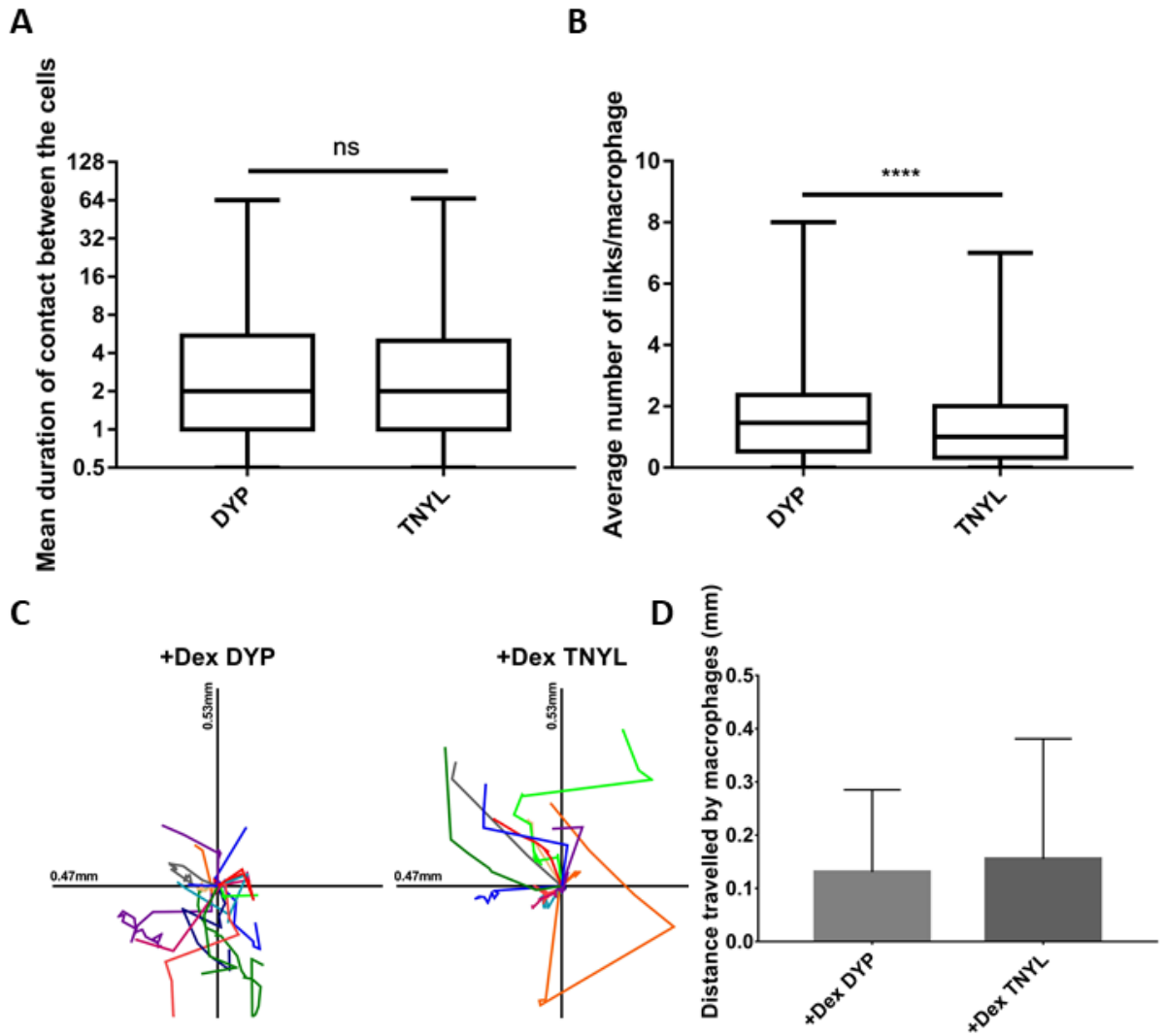


Figure 5-1 - EphB4 inhibition leads to a loss of contacts but has no effect on macrophage movement

A - Min to max boxplot showing the mean duration of links between macrophages and erythroblasts over 72 hours. The inhibitor was added 15 minutes before the cell types were introduced together. B – Min to max boxplot showing the average number of links between macrophages and erythroblasts over 72 hours. The inhibitor was added 15 minutes before the cell types were introduced together. A and B - Kruskal-Wallis test was performed on 2038 macrophages for +Dex TNYL and 2444 for +Dex control DYP ( $n=3$ ; ns ( $p>0.05$ ), \*\*\*\*( $p<0.0001$ )). The y axis is a log2 scale. C - Scaled cell-displacement vector diagrams of macrophage movement for 18 randomly selected macrophages from the control DYP and 13 from the TNYL condition. D - Mean plot of total path length for 82 randomly selected macrophages from DYP and 46 from TNYL conditions.

of inhibition of ephrinB2 from the EphB4 inhibitor, which is why the inhibitor was added again after the excess erythroblasts were removed. Figure 5-1A and B shows that the addition of the EphB4 inhibitor statistically changes the average number of interactions the macrophages have but not the mean duration of these contacts. The TNYL treated cells lose the majority of their links. This is in comparison to the cells treated with the DYP control peptide which made a higher number of links.

From Chapter 4, we know that the addition of the EphB4 inhibitor affects 50% of ephrinB2 binding. These results indicate that inhibiting 50% of EphB4 is enough to cause a significant effect in the interaction between the two cell types and this has affected the recognition. Furthermore, the movement of the macrophages has not been changed by the addition of the inhibitors as we can observe that the +Dex macrophages still exhibit a high level of movement in the well (Figure 5-1C). The length of these pathways is the same in Figure 5-1D, though it seems like the macrophages treated with TNYL might settle less at the end of the imaging, possibly because they are still looking for a contact.

During optimization of the imaging assay, we noticed several parameters which could influence the behaviour of the cells and skew the results. To ensure we had the right set up, we tested out several of these parameters. One crucial parameter that influences the data generated by the incucyte experiments is the cell numbers present in each experiment. Further analysis of the inhibitor experiments found that the macrophage-erythroblast ratio impacted on the efficacy of the inhibitor and the observed behaviours. In all experiments with inhibitors, the total number of erythroblasts present after the excess erythroblasts were removed was approximately

60 000 cells in a 24-well plate (Figure 5-2). When the macrophages were present at lower quantities than the erythroblasts, TNYL would lead to a reduction in mean duration and links. However, when the macrophage number equalled or surpassed that of the erythroblasts (n=1 out of 4), the presence of inhibitor did not show any effect compared to the DYP control on the average number of links. It is possible that due to the high numbers of macrophages, the chances of meeting was increased, and therefore, the number of links could not be decreased, but once the contacts formed, they were bound for a shorter period of time. For this reason, the rest of the experiments kept to a ratio where there are more erythroblasts than macrophages, near a ratio of approximately 2:1 (see figure 5-2).

The second parameter which could have an effect on the results was the length of time the erythroblasts were stimulated with the inhibitors for before being added to the macrophages. As described in chapter 4, the erythroblasts go through a large change in adherence properties from Day 4 onwards, as there is a sudden gain in integrin activation and ability to bind ephrinB2. For this reason, the inhibitors were tested on erythroblasts from Day 3 onwards to ensure that this change could not occur before addition to the macrophages. However, we do know from Chapter 4 that this exposure to inhibitor peptide did not affect the activation of integrins.

We wanted to check if continued application of peptide could still affect the formation assay. Surprisingly, despite the lack of effect on binding, the prolonged exposure of the cells with multiple control peptide doses before addition to the macrophages affected the results in the assay. The behaviour of erythroblasts treated

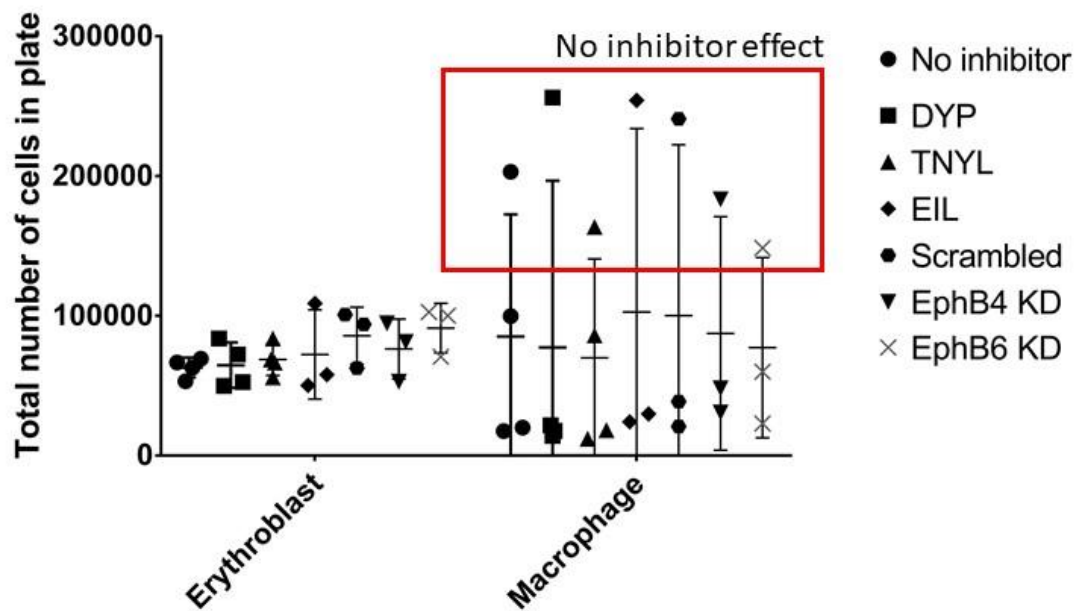


Figure 5-2 – Final ratio of macrophages to erythroblast during reconstitution assays after the final wash to remove excess erythroblasts

Graph representing the maximal total number of cells in each well in each experiment after the excess erythroblasts are removed, separating between erythroblasts and macrophages (n=4). On average, the erythroblasts were at a ratio of 2:1 to the macrophages. This shows the cells numbers are consistent between the different experiments undertaken.

with DYP for 72 hours were no longer similar to non-treated cells. As can be observed in Figure 5-3A and B, they lost the ability to contact the macrophages for a long period of time. This experiment was only conducted once, however, since its effect was so significant on the control, it was felt that this methodology could not be used. This experiment did highlight that the peptides could affect the binding of erythroblasts simply by being present for a longer period of time. Due to the cells being affected by the continual addition of peptides before addition to the macrophage, the cells, in future experiments, were only exposed to inhibitors 15 minutes before addition to the macrophages.

As highlighted in Chapter 4, the peptide DYP also affected the integrin activation. Furthermore, the sequence for DYP was unrelated to the tested peptides, and therefore, might not be reliably testing for the secondary effect of the inhibitory peptide. We generated a scrambled peptide control for the TNYL peptide to test whether this control would be more appropriate. This peptide, LFTA, however, affected the mean duration of contacts between macrophages and erythroblasts and the average number of links (Figure 5-3C and D) after addition for only 15 minutes before addition to the macrophages. When this peptide is put through BLAST, it corresponds to other proteins, so this might explain its effect. It was not used as a control further and in the future, a new scrambled control should be used.

Although the TNYL inhibition experiments have proven to affect the behaviour of macrophages, they were strongly dependent on the experimental setup. Further, these experiments did not test for the specific role of EphB6. For this reason, we needed to

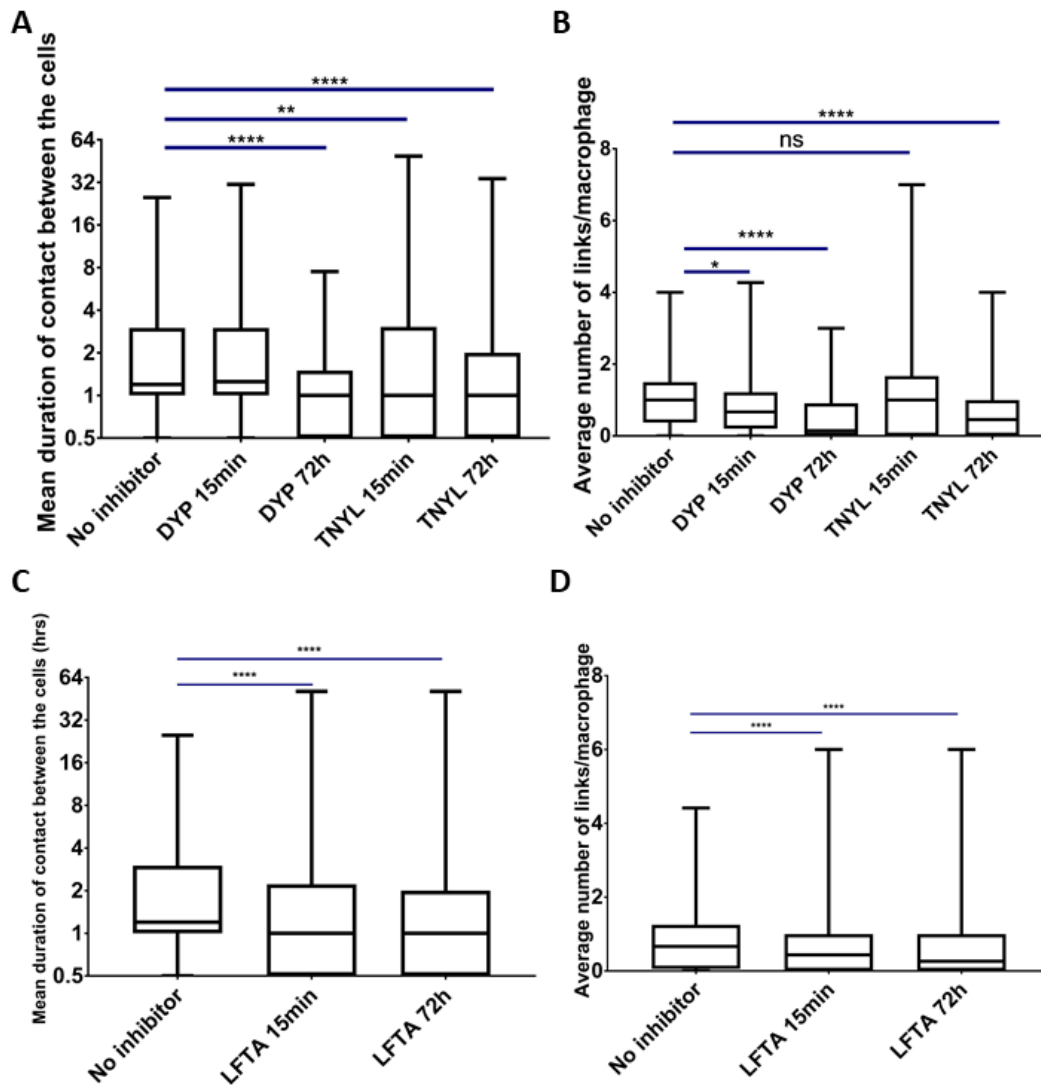


Figure 5-3 - Control peptides have an effect on the cells after continual addition for 72h before addition to the macrophages

A – Min to max boxplot of the mean duration of contact between erythroblasts and macrophages. B – Min to max boxplot of the average number of links. A and B - The erythroblasts were either stimulated for 15 minutes or 72 hours with the peptides before addition to the macrophages. Kruskal-Wallis test was performed on 820 macrophages for No inhibitors, 1120 macrophages for DYP 15 minutes, 683 macrophages for DYP 72 hours, 1361 macrophages for TNYL 15 minutes, 758 macrophages for TNYL 72 hours ( $n=2$ ; \* ( $p<0.01$ ), \*\*\*\* ( $p<0.0001$ )). The y axis is a log2 scale.

C – Min to max boxplot of the mean duration of contact between erythroblasts and macrophages. D – Min to max boxplot of the average number of links. C and D - The erythroblasts were either stimulated for 15 minutes or 72 hours with the peptides before addition to the macrophages. Kruskal-Wallis test was performed on 820 macrophages for No inhibitors, 1077 macrophages for LFTA 15 minutes and 902 macrophages for DYP 72 hours ( $n=2$ ; \*\*\*\* ( $p<0.0001$ )). The y axis is a log2 scale.

use an alternative method to demonstrate the role of specific Eph receptors within this system.

#### 5.2.2 The effects of EphB4 and EphB6 specific knockdowns in erythroblasts on macrophage interactions

We next wanted to determine whether specific EphB4 and EphB6 knockdowns on erythroblasts can also impact macrophage interactions. However, as noted in Chapter 4, the cells which had EphB4 knocked down proliferated less, reducing the numbers of cell available for experiments. To accommodate this, the erythroblasts were added to the macrophage on the same day as imaging at a ratio of 2:1 rather than 10:1. This is the cell ratio that was found to be optimal in the incucyte after the removal of the excess cells in other experiments. This ensured that even with the smaller cell number at the start, this setup was comparable across experiments.

When EphB knockdown erythroblasts were added to macrophages (Figure 5-4A and B), only erythroblasts with EphB4 depletion caused a loss of both average number of links (scrambled control median of 0.43 vs EphB4 KD median of 0.26) and the mean duration of these contacts between cultured macrophages and erythroblasts (75% last longer than 1h in scrambled control vs 50% in EphB4 KD on average). The loss of EphB6 did not lead to any differences in mean duration to the scrambled control (Figure 5-4A) in cultured macrophages; therefore, confirming the EphB4 peptide inhibitor result.

The shRNA for EphB6 does not have the same effect as EphB4 shRNA on the other's capacity to be expressed. EphB6 often led to either no change in EphB4 or increase in its expression. Interestingly, as can be observed in Figure 5-4B, EphB6 knockdown leads to a statistically higher number of contacts (median of 0.43 vs 0.57;  $p < 0.0001$ );



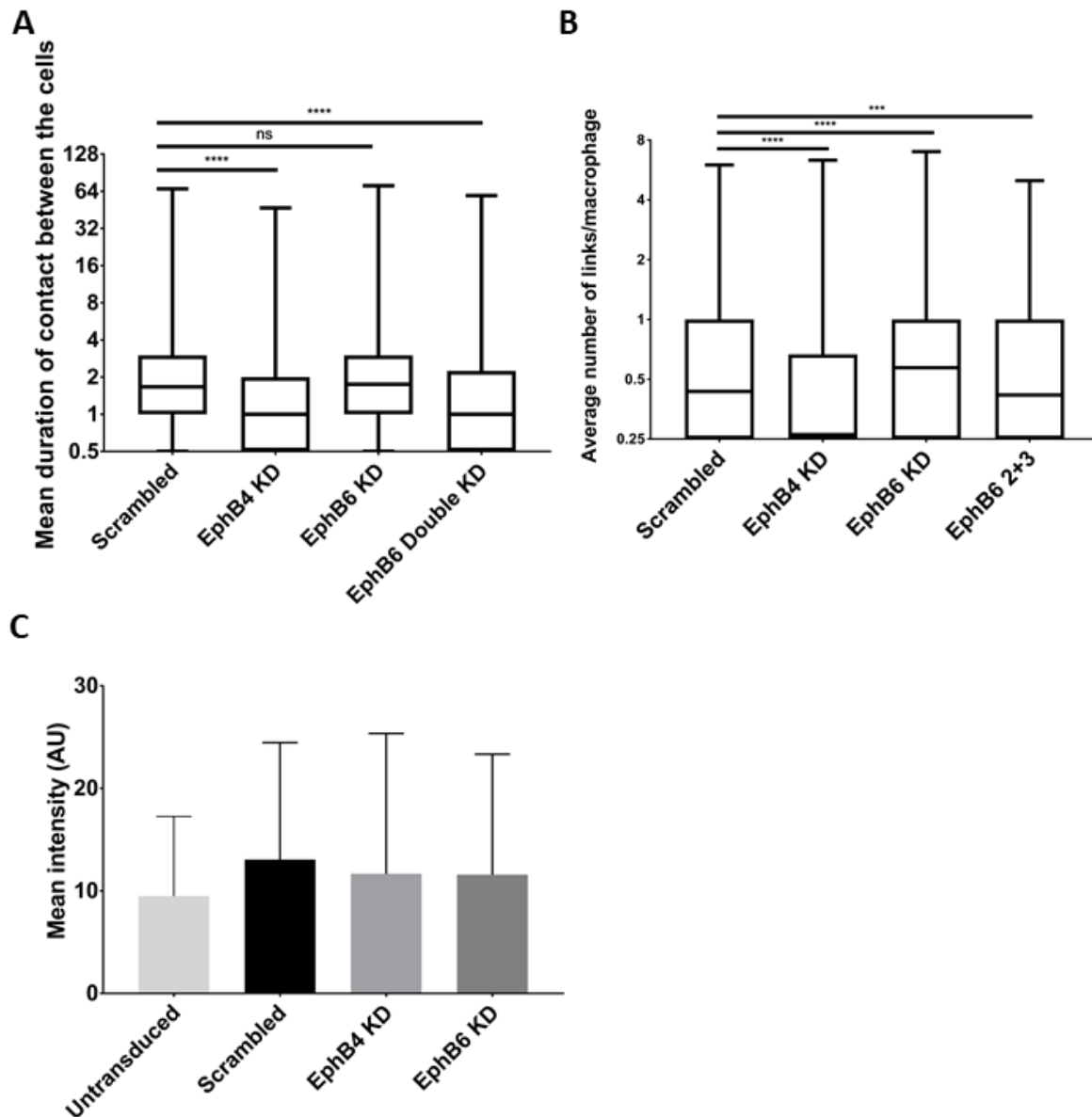


Figure 5-4 - Loss of EphB4, not EphB6, in erythroblasts impacts cultured macrophage-erythroblast interactions

A - Min to max boxplot showing the mean duration of links between cultured +Dex macrophages and erythroblasts.

B - Min to max boxplot showing the average number of links between +Dex macrophages and erythroblasts. A and B

- Kruskal-Wallis test was performed on 5023 macrophages for Scrambled, 6060 for EphB4 KD, 3467 for EphB6 KD (n=3; ns (p>0.05), \*\*\*\* (p<0.0001)). The y axis is a log2 scale. C – Histogram of mean intensity of the erythroblasts

in contact with the +Dex macrophages. The erythroblasts will have a varying level of fluorescent intensity dependent on their state of living (or NucDead 488 uptake). In this experiment, 337 scrambled erythroblasts were analysed, 485

EphB4 shRNA erythroblasts, 527 EphB6 shRNA erythroblasts and 849 untransduced erythroblasts.

indicating that the sole presence of EphB4 is enough to have a higher number of long-lasting contacts with macrophages. When two different shRNAs for EphB6 were used on the cells, this led to a loss of EphB4 at the same time as the loss of EphB6. In these situations, the effect on binding is the same as observed with the EphB4 shRNA cells. It should be noted that we observed that the knockdown experiments are less sensitive to the ratio of macrophages to erythroblasts, than the inhibitor experiments.

Importantly, it was observed that the EphB4 knockdown cells also have a higher level of cell death and macrophages are known to phagocytose dead and dying cells<sup>232</sup>. This enhanced cell death may affect how the macrophages react to the cells. For this reason, a preliminary experiment was conducted using a live cell death marker, NucDead 488, during imaging. This assay required dual colour analysis. Dr Stephen Cross from the Department of Biochemistry Wolfson Imaging facilities was able to update the software to include the analysis of these cells. We observed in Figure 5-4C that the macrophages in each condition deal with a similar number of dying cells. This implies that in the EphB4 condition in which there are fewer interactions, more of the remaining interactions are with dead cells than erythroblasts. Therefore, the difference between the scrambled control and EphB4 knockdown conditions are actually far greater because it is masked by the interaction with dead cells.

### 5.2.3 Bone marrow macrophages require both EphB4 and EphB6 for erythroblast recognition

To test the importance of Eph receptors in the context of bone marrow macrophages, shRNA cells were added to VCAM<sup>+</sup> and VCAM<sup>-</sup> cells and the cell interactions monitored by live cell imaging. Image analysis showed that the ratio of erythroblasts to

macrophages used was close to that achieved using cultured macrophages, though there was more erythroblasts because some macrophages died during processing (Figure 5-5). The results with VCAM1<sup>+</sup> and VCAM<sup>-</sup> cells reproduced those observed using +Dex cultured macrophages with the loss of EphB4 impacting on erythroblast association, as 50% of the low number of EphB4 cells' contact lasted less than 1h while 75% of Scrambled cell contacts were longer than 1h (Figure 5-6A and B). However, unlike +Dex cultured macrophages the loss of EphB6 also significantly affected the initiation of associations between bone marrow macrophages and erythroblasts. There was 50% marked reduction in the number of average contacts per cells with the EphB6 shRNA cells. This loss is accompanied by a small decrease in length of contact as well. Therefore, EphB6 is equally important as EphB4 in erythroblastic island reconstitutions using bone marrow macrophages (Figure 5-6A and B). These results confirm the importance of EphB receptors for the recognition of erythroblasts as binding partners by macrophages.

Interestingly, the VCAM<sup>-</sup> cells were also affected by the loss of either EphB receptor. Loss of either EphB4 and EphB6 led to a significant loss in mean duration with 75% of contact being less than 1h for EphB4 shRNA cells and 50% less with EphB6 shRNA while 75% of contacts are longer than 1h with VCAM<sup>-</sup> cells. Similarly, the number of links is decreased significantly. As the trend continues, this points towards a shared system of binding recognition between the different macrophages in the bone marrow. The VCAM<sup>-</sup> cells were more sensitive compared to the VCAM<sup>+</sup> cells when it comes to the effect of EphB6 shRNA on contacts.

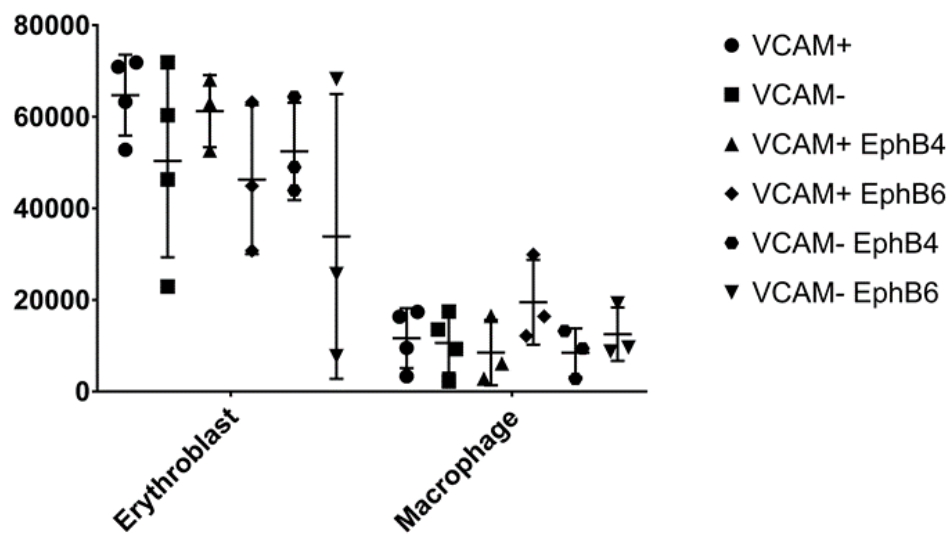


Figure 5-5 – The ratio in bone marrow macrophage experiments are similar across experiments.

Graph representing the maximal total number of cells in each well in each experiment after the excess erythroblasts are removed, separating between erythroblasts and macrophages (n=4). On average, the erythroblasts were at a ratio of 3:1 to the macrophages.

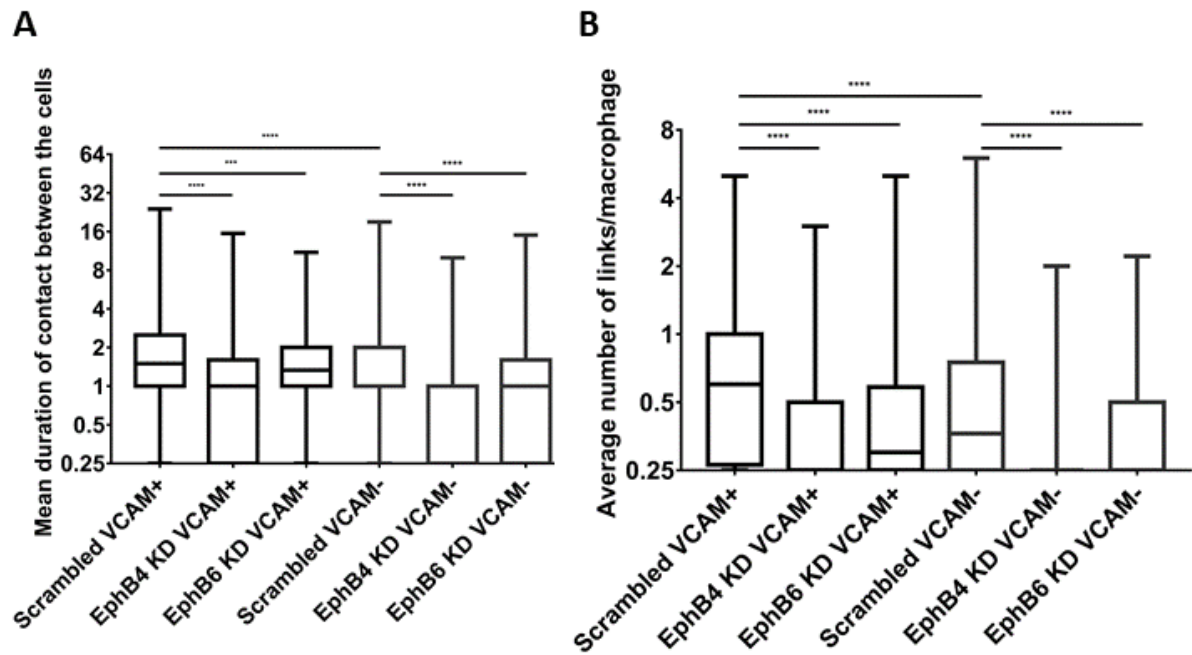


Figure 5-6 -Bone marrow macrophages require both EphB4 and EphB6 on erythroblasts for recognition

A - Min to max boxplot showing the mean duration of links between bone marrow macrophages and erythroblasts. B - Min to max boxplot showing the average number of links between bone marrow macrophages and erythroblasts. A and B - Kruskal-Wallis test was performed on 1332 macrophages for scrambled VCAM+ cells, 875 for EphB4 KD VCAM+ cells, 854 for EphB6 KD VCAM+ cells, 963 for scrambled VCAM- cells, 164 for EphB4 KD VCAM- and 714 for EphB6 KD VCAM- (\*\*\*( $p < 0.001$ ), \*\*\*\*( $p < 0.0001$ )) from 2 separate experiments from the same donor but using different donor erythroblasts. The y axis is a log2 scale.

#### 5.2.4 Role of E-cadherin, Akt and ERK

To better understand the role Eph receptors play in the erythroblastic island formation, the pathways involved were tested. As was discussed in Chapter 4, the EphB receptors are most likely not responsible for the rise in integrin activation, consequently the Eph binding must be acting on the cell through a different mechanism. Eph receptors are known to regulate the presence of E-cadherin at the surface of cells<sup>233</sup>. E-cadherin can help create adhesion points between cells, in a calcium dependent manner. Therefore, we looked at the effect of the shRNA for EphB receptors on the total presence of E-cadherin.

Interestingly, upon reduction of EphB4 or EphB6, there is a marked decrease in E-cadherin (Figure 5-7A). Quantification of the western blots in Figure 5-7B suggests the loss is more pronounced in EphB6 shRNA cells than EphB4 shRNA cells. As EphB6 shRNA erythroblasts are able to bind +Dex cells, this points to a separate mechanism of adhesion control. However, it is possible that the loss of total E-cadherin expression does not correlate to a loss of surface E-cadherin. This would need to be tested further in future experiments.

We wanted to test if the removal of the EphB receptors affected the main effectors of Eph receptors: Akt and Erk<sup>234</sup>. These kinases are mainly known for their role in proliferation and survival. As EphB4 leads to a higher death count, this would be relevant to discover if this is through the loss of these systems. Furthermore, these two pathways are known to be involved in the regulation of the cytoskeleton. These experiments were conducted after incubation with the TNYL inhibitor and its control DYP for 15 minutes. As can be observed in Figure 5-7C, there was no noticeable change

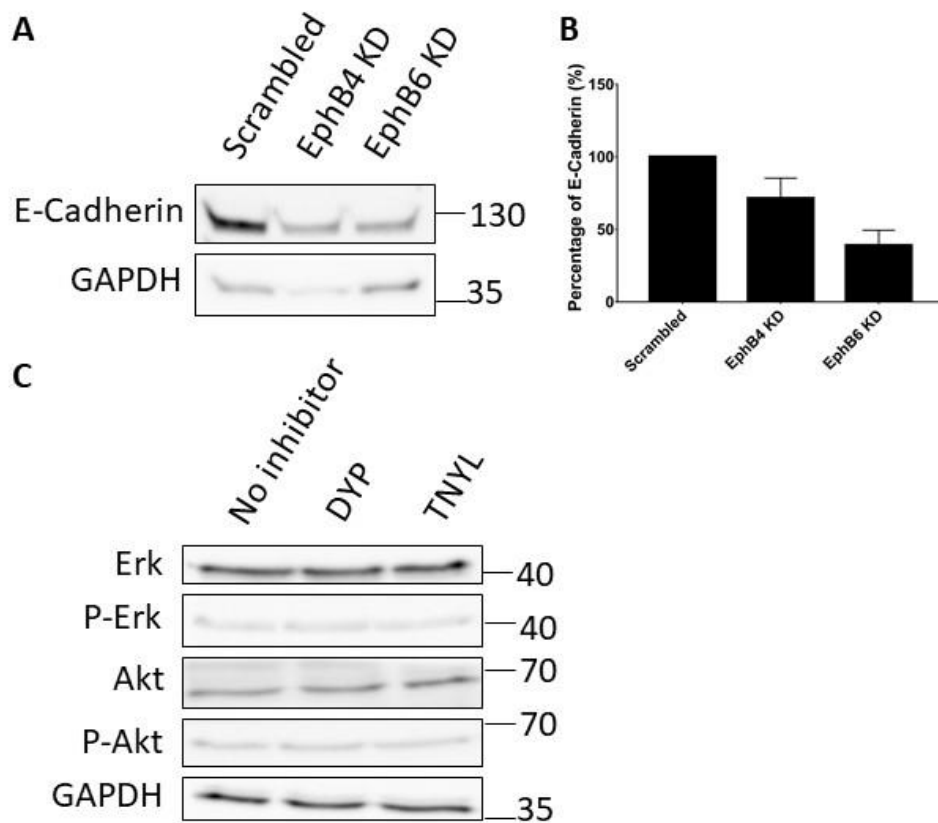


Figure 5-7 - Assessing the expression of known EphB effectors

A – Representative blot of lysates of scrambled transduced, EphB4 shRNA transduced and EphB6 shRNA transduced day 6 erythroblasts were probed for E-cadherin and GAPDH (n=3). The lysates used were equivalent of 100 000 cells.

B – Quantification of the western blots shown (n=3). The standard deviation is represented in this graph. C – Lysates of cells treated with or without inhibitors for 15 minutes were blotted for Erk, phosphor-Erk, Akt, phospho-Akt and GAPDH.  $1 \times 10^6$  cells were in each lysate (n=1).

in the level of total or phosphorylated Akt or Erk after the inhibitory treatment. This was conducted on only one experiment and so more repeats would be needed to assess this fully.

#### 5.2.5 Integrins are important to the formation of erythroblastic islands, independent of VCAM1

For a long time, the dogma in the erythropoiesis field has been that VCAM1 was an important part of the erythroblastic island. However, our experiments and those of others<sup>92,99</sup> have shown that it might not be a necessary element of these structures. However, it is worth noting that the integrins still exhibit a raised profile on the erythroblasts during differentiation, and many integrins have been shown to be present on erythroblasts during differentiation. To test if the integrins might be playing a role independent of VCAM1, a peptide against integrins, EIL, was introduced in the formation assay. This peptide was created from a fragment of fibronectin which binds and locks the integrin  $\beta 1$  into the active form. Its presence in the formation assay led to a loss in mean duration (75% of cells have contacts which last less than 1h compared to 75% which last more) and an average number of links in +Dex cells (Figure 5-8A and B). As the +Dex macrophages do not possess VCAM1, EIL must be inhibiting the binding of a different receptor on the macrophage, responsible for the binding between the cells. However, the fact that EIL also affects the number of links indicates that the integrins play an important part in the recognition as well. This would need to be tested further with bone marrow cells, to truly know that the macrophages were not influenced by the environment in to expressing VCAM1.



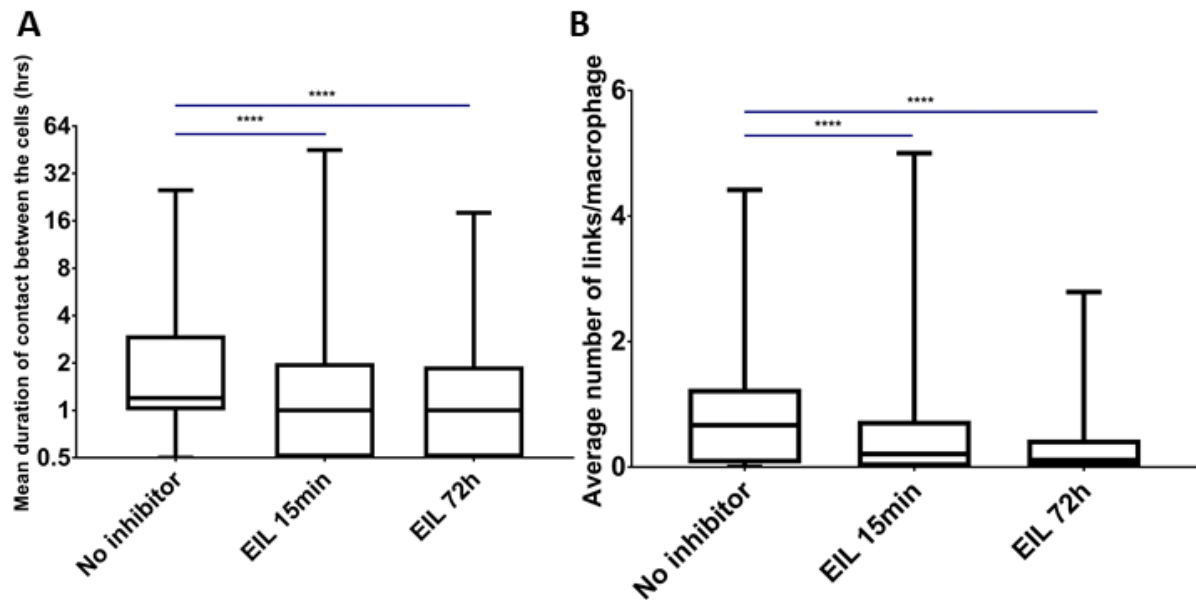


Figure 5-8 - Integrin  $\beta 1$  plays an important role in the formation of erythroblastic islands

A – Min to max boxplot of mean duration of contacts between erythroblasts and macrophages. B – Min to Max boxplot of average number of links between erythroblasts and macrophages. A and B –The EIL inhibitor was either applied for 15 minutes or 72 hours. Kruskal-Wallis test was performed on 820 cells with no inhibitors, 1848 macrophages with EIL for 15 minutes and 585 macrophages with EIL for 72 hours ( $n=2$ , \*\*\*\* ( $p<0.0001$ )). The y axis is a log2 scale.

### 5.2.6 Importance of ATP receptors

As discussed in Chapter 4, surface proteomics were conducted on macrophages to establish the proteins at the surface of macrophages. As expected, one of the most abundant receptors class on macrophages are ATP receptors, and p2x7, p2y11 and p2y6 were all detected. The P2 receptors respond to ATP or UTP and this leads to the activation of a G protein in the case of P2Y receptors<sup>235</sup> or the opening of ion channels in the case of P2X receptors<sup>236</sup>. Reticulocytes are reported to release ATP under certain circumstances<sup>237</sup>. We therefore decided to test whether these receptors were involved the formation of erythroblastic islands using inhibitors.

In collaboration with Dr Young (Cardiff University), we screened known inhibitors against different ATP receptors, both known to be present and not present at the surface of the macrophages. None of the inhibitors affected significantly the mean duration of the interactions (Figure 5-9A), however, the presence of BX430 (a p2x4 antagonist) and MRS2578 (a p2y6 antagonist) affected the number of interactions between the two cell types. Interestingly, BX430 caused an increase in links while MRS2578 caused a significant decrease in contacts (Figure 5-9B). These inhibitors did not have a large effect on the movement of the macrophages, though they do all seem to have less wide-ranging movements compared to the control macrophages.

However, when we put A74 (a p2x7 antagonist), which does not affect the +Dex cells, onto bone marrow cells, we saw in Figure 5-9D that this had a large effect on the bone marrow cells as well (over 75% of contacts are less than 2 hours with the inhibitors compared to 50% of contacts lasting over 2 hours without inhibitor). This also affected the VCAM<sup>+</sup> cells which have 75% of contacts lasting less than 1 hour with the inhibitor.

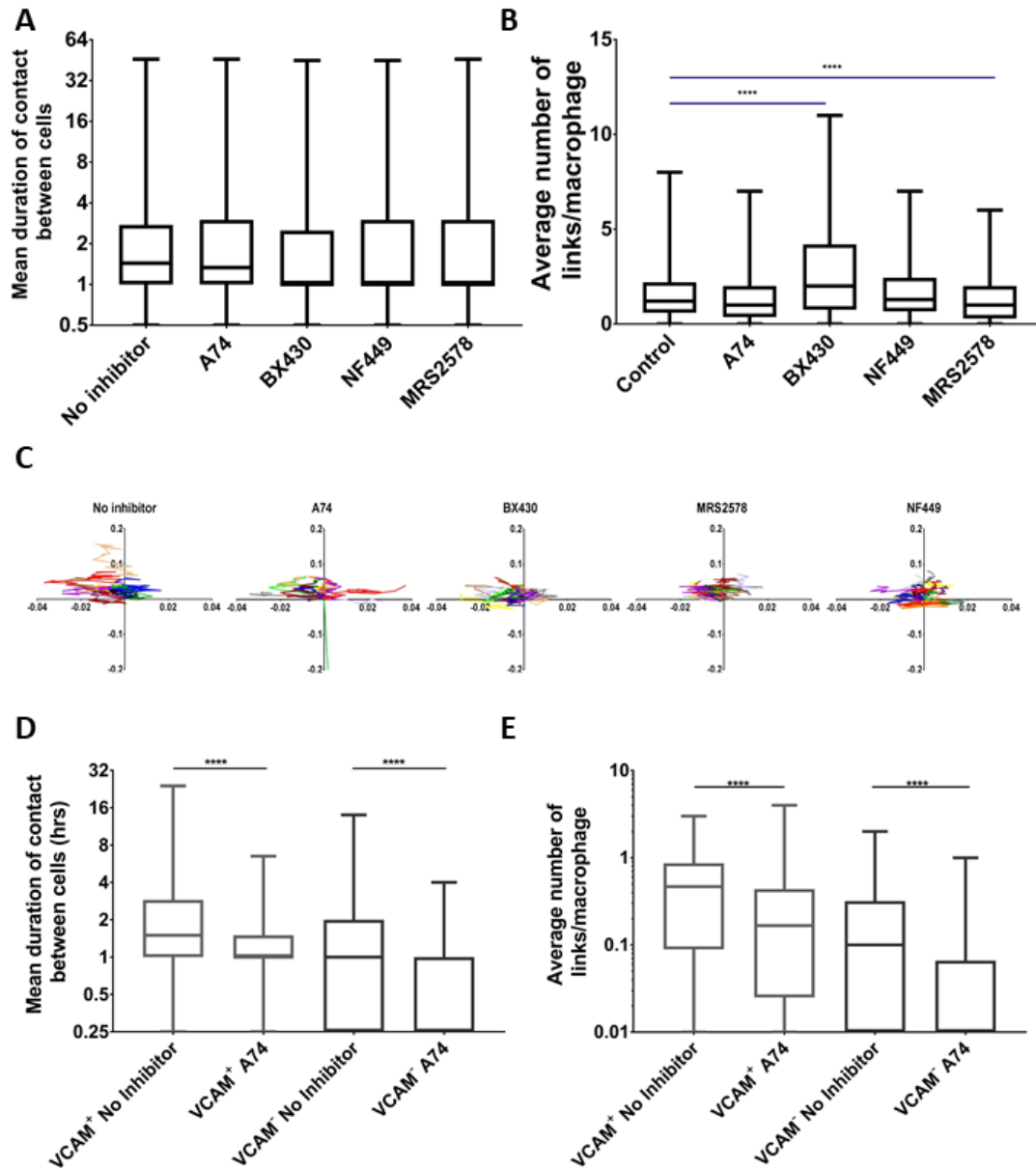


Figure 5-9 – Incubation with a range of P2X and P2Y receptor inhibitors affect the relationship between macrophages and erythroblasts

A – Min to max boxplot of mean duration of contacts between erythroblasts and +Dex macrophages. B – Min to Max boxplot of average number of links between erythroblasts and +Dex macrophages. A and B –The inhibitors were applied for 15 minutes. Kruskal-Wallis test was performed on 891 cells with no inhibitors, 1026 macrophages with A74, 763 macrophages with BX430, 908 macrophages with NF449 and 864 macrophages with MRS2578 ( $n=2$ , \*\*\*\* ( $p<0.0001$ )). The y axis is a log2 scale. C - Scaled cell-displacement vector diagrams of macrophage movement for 20 randomly selected macrophages for each condition. D - Min to max boxplot of mean duration of contacts between erythroblasts and macrophages. E – Min to Max boxplot of average number of links between erythroblasts and macrophages. D and E –The inhibitors were applied for 15 minutes. Kruskal-Wallis test was performed on 213 VCAM<sup>+</sup> cells with no inhibitors, 291 VCAM<sup>+</sup> macrophages with A74, 188 VCAM<sup>-</sup> macrophages with no inhibitor and 215 VCAM<sup>-</sup> macrophages with A74 and 864 macrophages with MRS2578 ( $n=1$ , \*\*\*\* ( $p<0.0001$ )). The y axis is a log2 scale.

As can be observed in Figure 5-9E, the average number of links was also affected significantly ( $p < 0.0001$ ). Therefore, this illustrates that there are important differences between the +Dex cells and the bone marrow cells. Furthermore, these results point towards an interesting role for ATP or its metabolites in the interactions between erythroblasts and macrophages.

### 5.3 Discussion

This work has begun to generate evidence that the Eph receptors have a role in the adhesion of erythroblasts to macrophages, but importantly do not affect the migration of the macrophages. In particular, loss of EphB4 binding abrogates the macrophage interaction with erythroblasts in both cultured and bone marrow derived macrophages. As almost all long-lasting interactions are abolished, this indicates that the Eph receptors were responsible for the initial recognition of the erythroblasts as objects to bind to by the macrophage. It is interesting that simply inhibiting the binding of EphB4 can have such a large effect on the interaction between the cells. This questions the necessity of the EphB6 receptor in certain conditions. However, it is possible that if these receptors heterodimerize, the activation or inactivation of EphB4 is enough to also influence the EphB6 signal input on the cell, but not vice versa.

It is important to note that since the loss of EphB4 is accompanied by the loss of EphB6 and that the sole presence of EphB4 does not impact the binding, we cannot distinguish between a scenario where it is the loss of both proteins that is disruptive, or simply EphB4 which leads to the loss of binding. One way to determine this would be to rescue EphB4 or EphB6 expression individually in the knockdown erythroblasts. This would enable us to test the singular role of each receptor in the binding to macrophages. However, these results do indicate that the presence of EphB6 at the surface of these cells is dependent on the presence of EphB4 and not vice-versa. This implies that these receptors will heterodimerize to help with the stability of EphB6 at the surface and so, overexpression of one will be likely accompanied by the partner protein.

The inhibitor experiments have shown that it is possible to interrogate the system rapidly (15mins) by simply adding peptide inhibitors. However, the effect of the control DYP after prolonged and repeated additions on integrins does raise the question of whether adding peptides causes unanticipated side effects on these cells that are hard to control. DYP does not affect ephrinB2 binding or the ability of macrophages to interact with erythroblasts when added in right before the experiment, but when it is present for a long time it affects the cells. The simple presence of peptides in the media for a long period of time affects the interactions with macrophages. This shows that the cells are quite sensitive to their environment and that they need to be in the right condition to ensure that they will be able to interact with the macrophages.

Eph receptors are known to have a role in the regulation of the cytoskeleton of cells and the cytoskeleton might be a good indication of whether cells are actively changing their morphology to be able to bind to the cells. Observation of the cytoskeleton by live cell imaging would help understand whether the binding is an active process rather than an act of coincidence. Therefore, it would be of interest to add actin labels such as SiRActin<sup>238</sup> to the macrophages or erythroblasts to study these changes. Furthermore, these could also be added in the case of inhibitors and knockdown cells, giving us the opportunity to study whether the inhibitors are stopping the reaction at the level of the cytoskeleton or at the binding level, such as changing the level of a binding partner.

It has previously been shown by Frenette et al.<sup>99</sup> and ourselves<sup>60</sup> that VCAM1 does not have a central role in the binding of erythroblasts to macrophages. However, the removal of the VLA-4 complex by binding to fibronectin does remove the ability of erythroblasts to bind to macrophages. The integrins play an important role in the

binding of these cells to each other. However, VCAM1 does not need to be present in the macrophage to lead to this binding. It is possible other adhesion molecules might be involved as we know that EDTA can affect the binding of the cells. E-Cadherin was observed as reduced in the presence of EphB4 and EphB6 shRNA. However, it was reduced more in the presence of EphB6 shRNA. It is unlikely to be a binding partner in the erythroblast-macrophage interaction. It might be of interest to look at other cadherins and the selectins which are known to be affected by the presence of EDTA. This could be investigated globally by doing comparative proteomics.

The work in this study was unsuccessful in uncovering the mechanisms through which Eph receptors might be able to affect the interactions with macrophages. However, Eph receptors, like tyrosine kinase receptors, can interact with a wide variety of signalling pathways. Even though Akt and Erk are some of the major signalling pathways for migration, it is possible that the Eph receptors within the erythroblasts are instead acting on pathways such as Stat3 or FAK which are both known to lead to cell migration and adhesion through the Eph receptors<sup>239,240</sup>. Furthermore, ephrins can signal in a process called backwards signalling. Therefore, it would also be necessary to study the effect of these contacts within the macrophages in the future.

The results with the different ATP receptors inform us that different types of ATP or other metabolites might influence or help tailor the macrophage erythroblast interaction. In particular, it was observed that inhibitors BX430 and MRS2578, p2y6 and p2x4 respectively, influenced the interaction between macrophages and erythroblasts. P2y6 responds to UDP and p2x4 responds to extremely low ATP concentrations<sup>241,242</sup> and had opposing effects. This suggests that the energy metabolism or state around the

cell may be sensed by macrophages. ATP is an extremely important part of the erythrocyte life. It is known that when erythrocytes lyse, they release a large amount of ATP. Some reports even show that erythrocytes can release ATP when they go through veins, through shear stress<sup>243</sup>. The amount of ATP released leads to macrophages in the spleen knowing when to clear the cells. There is a theory that spleen macrophages recognise which erythrocyte to remove from the bloodstream by the amount of PS at the surface of the cells. PS flips to the surface of the cells when ATP is released, due to an ATP-dependent translocase enzyme<sup>38</sup>. Another theory for the removal of erythrocyte from the bloodstream is that CR1-mediated ATP release from the erythrocyte stimulates phagocytosis and engages the cell towards the sinusoids of the spleen to go through clearance<sup>244</sup>. Because ATP is important for the relationship between erythrocytes and macrophages at the end of their life, it is possible that it is important in the initial stages. We know that the macrophages have tendrils around the erythroblasts, and therefore, could put stress on the cells. It is still unknown whether erythroblasts would release ATP during differentiation.

However, it is worth noting that p2x4 was not found in the macrophage proteomics or the erythroblast proteomics, consequently the inhibitor may be having a secondary effect. However, just like with the Eph/ephrin family, there is a lot of overlap between the different members of the family. Peptide analysis shows that some of the fragments found in macrophages could correspond to both P2X7 and P2X4. Furthermore, these results point towards the fact that the +Dex macrophage system is less sensitive than the bone marrow system. The +Dex macrophages were not as affected by the A74 as the bone marrow macrophages. Therefore, the similitude between +Dex macrophages and bone marrow macrophages we looked at do not show the whole picture of what



defines these macrophages and their capabilities. More work is needed to better understand the contribution of p2xy receptors and ATP or its metabolites in the macrophage-erythroblast interaction.

### 5.3.1 Summary

We have shown with these results that our imaging assay can provide a powerful screening method to test the contributions proteins make during erythroblastic island formation. Furthermore, the analysis programme separates two factors within binding. The length and the number of adhesions made can inform us about the different capacities/activities of the protein. A protein which induces a loss of length of contact is one which affects the binding, while a protein which affects the number of links will be one which affects the recognition of the cells with each other or the ability of the binding to become long-term. In this study, we were able to show the different roles of VCAM1, EphB4, EphB6, integrins and ATP metabolites within erythroblastic island formation, though more work is needed to confirm the latter results. Therefore, it is possible to screen the role of many receptors at the same time, while also separating their different functions within a complex system and over time. It will be interesting to use this assay to study diseases which are linked to the macrophage-erythroblast interaction such as in Polycythaemia Vera, as the bone marrow macrophages have been implicated in the disease's pathology<sup>33,34</sup>.

These results also indicate that a variety of macrophages exist which can interact with erythroblasts but also the fact that they can do this with varying ability and through utilising different mechanisms. The bone marrow itself has a wide variety of monocytes and macrophages within it. As was discussed in Chapter 3, there are 5% of CD14<sup>+</sup> cells

in the bone marrow, and the resident macrophages represent a very small part of this percentage. This gives the opportunity for the body to have several cells be able to help erythroblasts differentiate. Furthermore, rather intriguingly, it indicates that there is inherent flexibility in the system and so the body has a chance for backup macrophages which can help in emergencies, such as during stress erythropoiesis.



## 6 Chapter 6 – Reticulocyte egress

### 6.1 Introduction

The majority of the cells that are manufactured in the bone marrow will at some point egress from their origin. The numerous types of immune cells that are produced in the bone marrow need to mobilise to the bloodstream to ensure that the entire body is protected<sup>245</sup>. It is also known that a proportion of hematopoietic stem cells can leave the bone marrow to re-home themselves in other bones<sup>246</sup>. Over 2 million reticulocytes are made per second in the bone marrow, and these must enter the bloodstream to complete their final stages of maturation. However, reticulocytes are more rigid compared to red blood cells<sup>41</sup>. Furthermore, they are believed to have lost all their adhesive properties<sup>176</sup>, such as integrins because this facilitates their detachment from macrophage and departure into the bloodstream<sup>247</sup>. However, there remains a debate over how the reticulocyte can traverse the endothelial layer which forms a barrier at the sinusoid.

Mel et al. in 1977 indicate that in the bone marrow there are two types of reticulocytes: a motile fraction (25% of the reticulocytes) which has just expelled its nuclei and cannot be found in the blood, and a more mature non-motile fraction which has taken the typical red blood cell shape. This study also suggests that the reticulocyte which would travel through the endothelial layer into the bloodstream is the more mature, non-motile form. Chamberlain and Lichtman showed, in 1978, that the endothelial cells had areas where they were thinner or had perforations, which they called pores. They showed that granulocytes and reticulocytes exit through these pores in preference over other locations in the endothelial cells. They propose that this is a passive process for

the endothelial cells, with the granulocytes and the reticulocytes creating a pit at the point of egress, which becomes a pore and the migrating cells moving actively through the endothelial cells. On the other hand, Waugh et al.<sup>249</sup> propose in their study in 1986 that it is the hydraulic pressure from either side of the pore which would lead to the movement of the reticulocyte within the bloodstream. However, this experiment was not conducted in the presence of endothelial cells. Furthermore, Dabrowski et al. showed in 1981 that changing the pressure within a femur, by electrostimulating the muscle, increased the number of reticulocytes leaving the bone marrow. Therefore, pressure plays an important role in the reticulocyte egress. It has also been suggested that the pulsation from the endothelial cells themselves would be enough to cause the pressure for the reticulocytes to travel across the layer<sup>39</sup>.

Most of the molecular relationship between reticulocytes and endothelial cells studied have been in the context of sickle cell anaemia. In the case of an anaemic crisis, the reticulocyte will start to bind the endothelial cells. The sickle reticulocyte was shown to express a higher amount of integrin  $\alpha 4$  and CD36<sup>251</sup>. This led to these cells being able to bind the VCAM1 present on endothelial cells. However, this is known to be the case with only red blood cells from sickle individuals, as normal red blood cells will not bind the endothelial layer at all<sup>252</sup>. These experiments are conducted on the apical side of the endothelial layer rather than the basal side.

This final chapter will explore, using a range of experiments, whether the reticulocyte plays an active or passive role in their passage through the endothelial layer and whether they possess the molecular means to interact with endothelial cells.

## 6.2 Results

### 6.2.1 Proteomics suggest reticulocytes have some migration machinery

The proteomics data gained in Chapter 4 was used to compare the surface proteomics of reticulocytes and red blood cells to detect if there are receptors or adhesion molecules which might contribute any reticulocyte movement. It has long been believed in the field that all the majority of integrins were lost with the nuclei after enucleation<sup>247,253</sup>. However, we found in our data that reticulocytes still express a small amount of integrin  $\alpha$ -4 and  $\alpha$ -X as well as integrin  $\beta$ 1 (Figure 6-2), which has been shown previously in the laboratory<sup>22</sup>. These are completely lost in red blood cells, as these cells should not adhere to the blood vessel walls.

When the reticulocyte data was subjected to DAVID pathway analysis, one of the top pathways which are present in reticulocytes is transendothelial migration (Table 6-1). Many of the cytoskeletal regulators and cytosolic proteins involved in binding are detected within the surface of the reticulocyte, probably as they are pulldown in signalling complexes (Figure 6-1). This pathway is absent once the cells have matured into red blood cells (Figure 6-2). The presence of these proteins is a potential indication of the possibility of migration as the cells have some of the necessary machinery. Furthermore, many of the proteins present are also responsible for cell-cell adhesion (Table 6-2). Therefore, future experiments could test the role of these proteins using knockdowns, if a suitable assay system can be perfected for monitoring reticulocyte migration. However, preliminary images of native reticulocytes do not show any motile activity.

NAME	ACCESSION NUMBER	RETIC 1	RETIC 2	RETIC 3
F11R	D3DVF0	2	4	3
GNAI2	P04899		2	
GNAI3	P08754		1	
RAP1B	P61224	1	3	1
INTEGRIN $\alpha$ 4	P13612	8	1	9
INTEGRIN $\beta$ 1	P05556	6	4	11
MYOSIN LIGHT CHAIN 12A	P19105	1	1	
RAC1	P63000	1	3	1
RAC2	P15153		2	
VAV2	P52735		1	

Table 6-1 shows potential transendothelial migration proteins present in reticulocytes detected by pathway analysis.

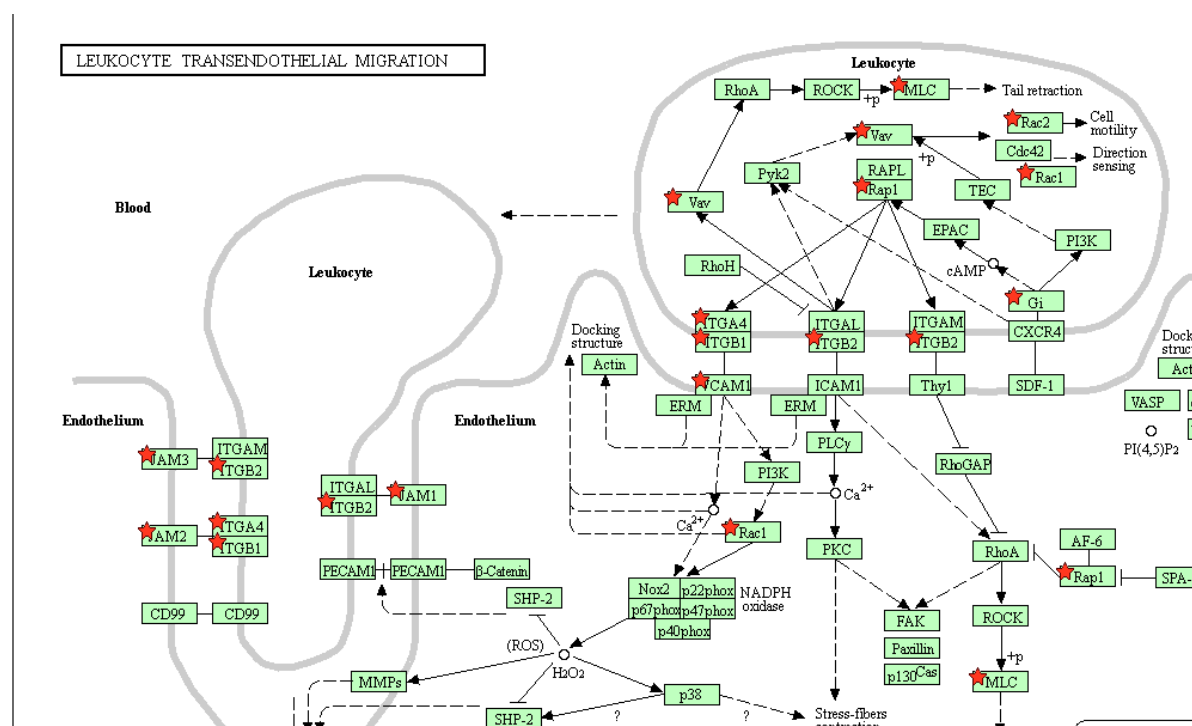


Figure 6-1 - Leukocyte transendothelial migration pathway is present in reticulocytes

Image generated by DAVID (accessed 12/09/2018). Red stars represent the main proteins affected by the presence of proteins in Table 6-1.

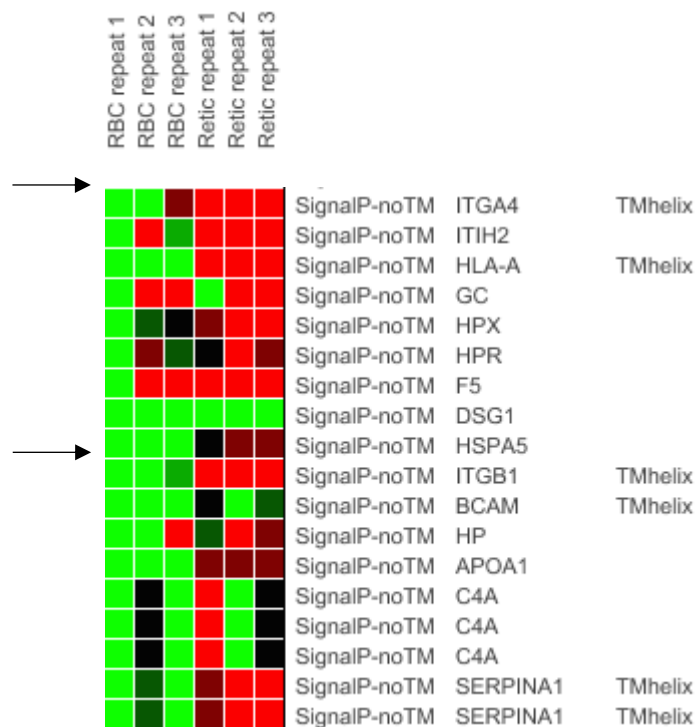


Figure 6-2 - Reticulocytes lose many proteins to mature into red blood cells

Small portion of eat map of red blood cells versus reticulocyte surface proteomics using GI Tools. Red is a gain while green is a loss. Red blood cells are the first three sample. TMhelix represent the proteins which possess a transmembrane helix. The SignalP represents the proteins with a signaling peptide.

ID	GENE NAME
F5H6T1	ARP2 actin related protein 2 homolog(ACTR2)
Q14344	G protein subunit $\alpha$ 13(GNA13)
J3KS60	Rho GDP dissociation inhibitor $\alpha$ (ARHGDI A)
O15144	actin related protein 2/3 complex subunit 2(ARPC2)
B1AK87	capping actin protein of muscle Z-line $\beta$ subunit(CAPZB)
P31146	coronin 1A(CORO1A)
Q9NP10	insulin like growth factor 1(IGF1)
B4E0K5	mitogen-activated protein kinase 14(MAPK14)
P26038	moesin(MSN)
P63000	ras-related C3 botulinum toxin substrate 1 (rho family, small GTP binding protein Rac1)(RAC1)
Q9Y490	talin 1(TLN1)
P10599	thioredoxin(TXN)
F5H7S3	tropomyosin 1 ( $\alpha$ )(TPM1)
A0A087WWU8	tropomyosin 3(TPM3)
P68371	tubulin $\beta$ 4B class IVb(TUBB4B)
P07437	tubulin $\beta$ class I(TUBB)
E9PRD9	vanin 2(VNN2)

Table 6-2 shows cell-cell adhesion proteins present in reticulocytes surfaceome



### 6.2.2 Reticulocytes form fewer interactions with macrophage

In the bone marrow, it is possible to find reticulocytes still attached to erythroblastic islands<sup>35</sup>. Therefore, we wanted to test our system to look at the interactions between macrophages and reticulocytes. A mix of reticulocytes and orthochromatic erythroblasts were added to macrophages and imaged using the incucyte imaging system. Surprisingly, as can be observed in Figure 6-3, the reticulocytes did not interact with the +Dex macrophages as much as the -Dex macrophages. Furthermore, these interactions were of a similar duration to the ones witnessed with Day 6 erythroblasts. It was not possible to visualise enucleating orthochromatic erythroblasts in the assay in this form, likely due to the time period used for incucyte imaging.

### 6.2.3 Exploring the egress of reticulocyte *in vivo in mice*

To start looking at the reticulocyte egress, at first, the idea was to look at the bone marrow of mice and observe cells egressing into the sinusoid. In collaboration with Dr Ed Brown from Prof. Alastair Poole's laboratory (University of Bristol) electron microscopy images of mice bone marrow were produced using normal mice. The samples were fixed in a manner that ensured that the cells were not affected too much during the fixing phase by not perfusing the mice and fixing the femurs before isolating the bone marrow. This ensured that the cells were fixed in their natural state as described in Agbani et al.<sup>254</sup>. The first electron microscopy images of the bone marrow led us to realise how many cells the bone marrow contained and to observe that there is a variety of cell types present at the edges of sinusoids (Figure 6-4). Without any cell labelling, it is not possible to discern any of the

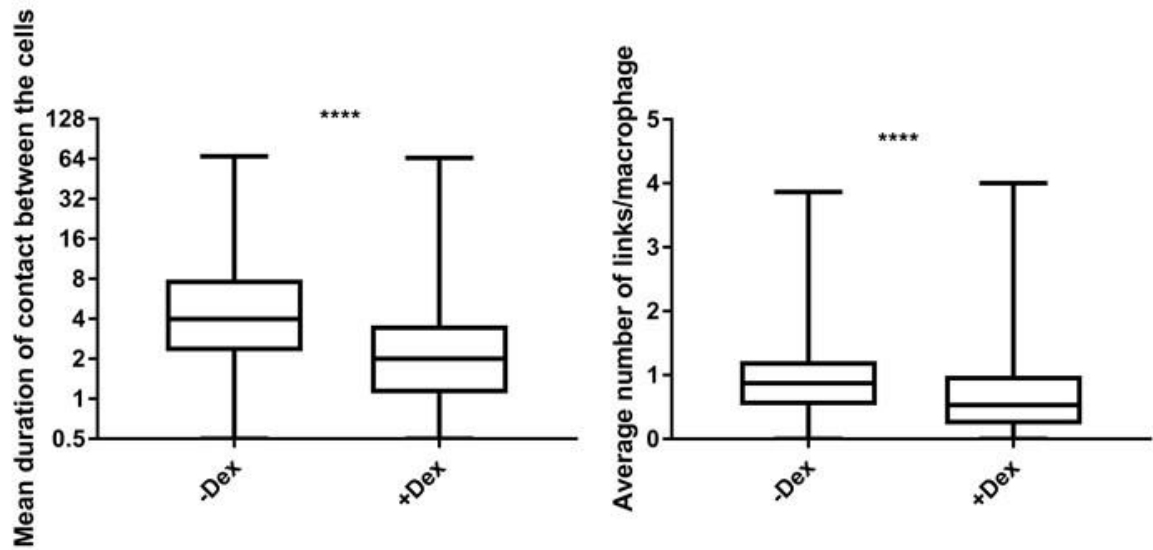
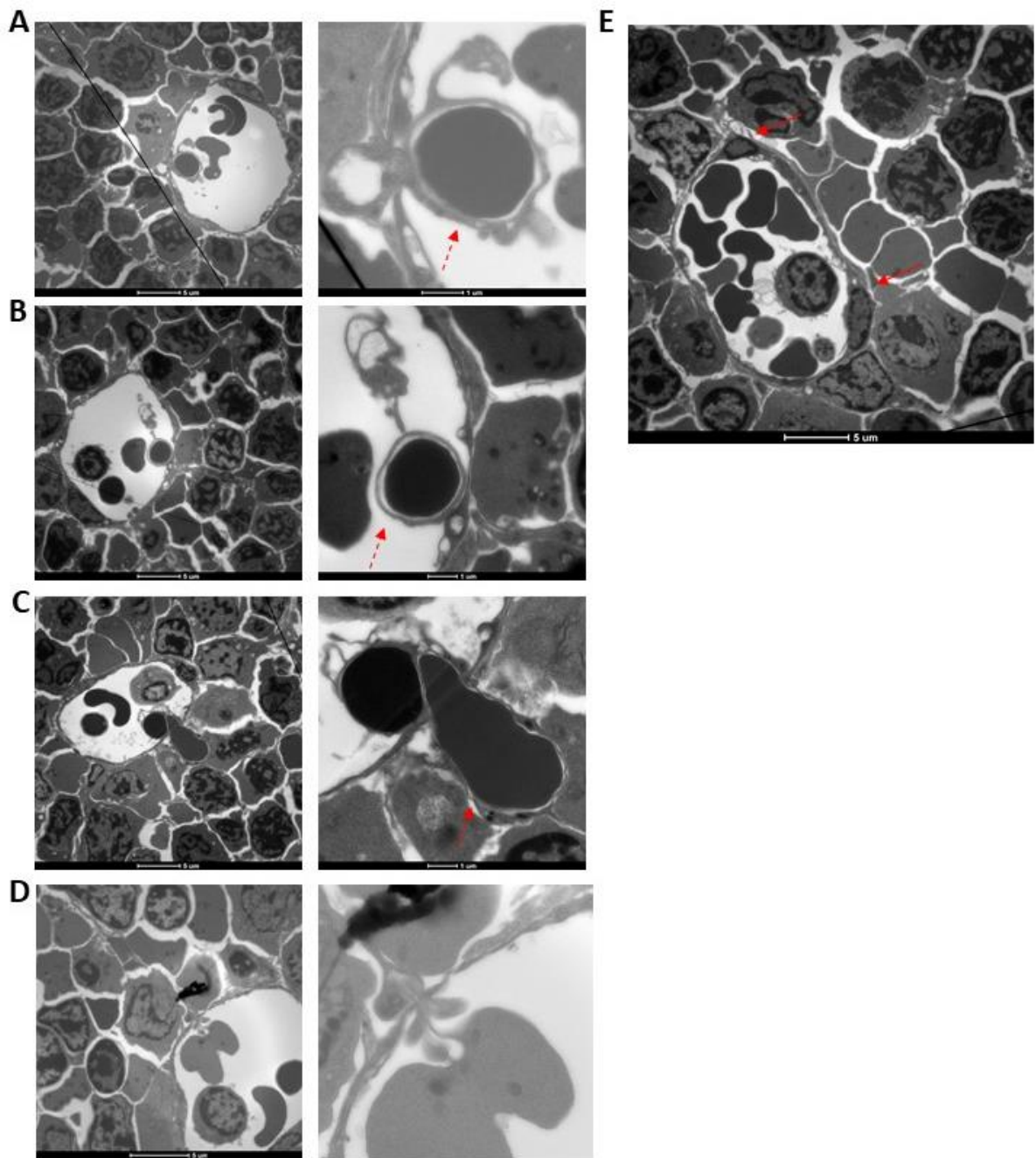


Figure 6-3 – Incucyte experiment exploring reticulocyte interactions with +/- Dex cultured macrophages

A – Min to max plot of the mean duration of contact between reticulocytes and macrophages. B – Min to max plot of the average number of links between reticulocytes and macrophages. A and B – Kruskal-Wallis test was performed on 213 macrophages for -Dex macrophages and 345 macrophages for +Dex macrophages (\*\*\*\* ( $p < 0.0001$ )). The y-axis is log2 scale.

characteristics of these different cells. Furthermore, these were thin sections. Therefore, it is hard to know if a cell possesses a nucleus, one of the main ways of differentiating reticulocytes from other cells. It is possible, however, to discern the darker colour of these cells, suggesting they contain a high level of haemoglobin. Haemoglobin, as discussed in Section 1.3.2.1.1, has a high level of iron which as a metal would be detected by electron microscopy<sup>255</sup>. In many sinusoids, it is possible to detect that there are very dark cells. These are probably red blood cells. It is also possible to observe lighter cells with a nucleus within the sinusoids. These are likely circulating immune cells.

Around the sinusoid, there is a thin layer of endothelial cells, with some sinusoids consisting of one endothelial cell with long tendrils. As can be observed in Figure 6-4E (indicated with red arrows), when there is more than one cell forming the sinusoid barrier, these cells overlap over quite a long distance (around 5-15  $\mu\text{m}$ ). Surprisingly, when observing dark cells, believed to be reticulocytes, exiting into the sinusoid, they are all surrounded by a layer of endothelial cells as if they are engulfed by the cells. A reticulocyte, which is presumably starting to egress appears caught between two layers of endothelial cells (Figure 6-4A, B and C, dotted arrow). Some reticulocytes were also observed to be fully within the sinusoid with membrane surrounding them. Only egress of reticulocytes was observed in the sections examined, and we were not able to compare it to the egress of immune cells within these available samples. Therefore, in these mouse bone marrow samples, the reticulocytes exit in a mechanism resembling transcellular transendothelial migration.



*Figure 6-4 - Reticulocytes egress from mouse bone marrow sections*

*Selection of representative EM images taken using a FEI Technai 12 electron microscope from non-perfused mice femur bone marrow in resin. The slides were stained with  $\text{OsO}_4$ . The red arrows point towards the end of overlaps of endothelial cells. The red dotted arrow highlights examples of endothelial membrane surrounding reticulocytes. Mice bone marrow electron microscopy samples were kindly provided by Dr. Ed Brown and Prof. Alastair Poole. A to D – Scale bar in the left panel is 5  $\mu\text{m}$  and 1  $\mu\text{m}$  in the right panel.*

#### 6.2.4 Assessing different migration assays

The next step was to determine whether we could design experiments to reproduce this phenomenon *in vitro*. We attempted two different methods to study reticulocyte migration; a methylcellulose assay, based on the one described in Bahnson's patent<sup>256</sup>, and a transendothelial migration assay (Figure 6-5A and B). Both the methylcellulose assays and transendothelial migration assays ran into the issue that reticulocytes and red blood cells are small, dense, flexible cells which can pass through most filters and cannot be suspended into 3D cultures.

Setting up the methylcellulose assay did not lead to fruitful results, as the methylcellulose could not maintain a gradient for more than 20 minutes. Therefore, we decided not to use this assay.

Furthermore, we could not use a transwell assay with no endothelial cells as the reticulocytes could pass through a 3  $\mu$ m filter using gravity alone.

#### 6.2.5 Transendothelial migration experiment: endothelial cells added on top of the filter

Therefore, we utilised an assay involving bone marrow endothelial cells, generously provided by Dr. Middleton (Dental School, University of Bristol). In the first instance, 250 000 bone marrow endothelial cells (BMEC) were added to the top surface of a 3  $\mu$ m transwell filter, which was then transferred into a well on a 24 well tissue culture plastic plate. As the reticulocytes would need to egress towards the bloodstream, it was assumed in this experiment that human serum would contain the chemoattractant necessary for reticulocyte egress. The well was either exposed to 800  $\mu$ L of human serum, or IMDM media without serum as a control in the bottom well.

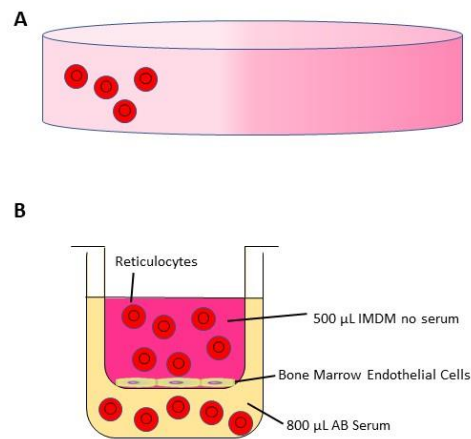


*Figure 6-5 - Diagram of different migration assays used*

*A – Diagram of methylcellulose assay. The reticulocytes are placed in the methylcellulose with no chemoattractant to visualise if they move towards the methylcellulose layer containing the chemoattractant gradient. B – Diagram of transendothelial migration assay. BMECs are placed either over or under a 3  $\mu$ m filter. These cells can be activated with  $TNF-\alpha$ . The labelled reticulocytes and RBCs are then added in the top chamber in media without serum. We can count how many cells have then moved towards the bottom chamber containing serum or serum using flow cytometry.*

Reticulocytes were added to the top of the filter suspended in 500  $\mu$ L of IMDM media with no serum. Red blood cells were also used as a negative control as it was expected that they should not be able to go through the BMEC layer and therefore would indicate a leak.

This assay demonstrated that a proportion of reticulocytes are able to go through the layer immediately in any condition after approximately 1 minute, though less in the presence of serum (Figure 6-6A). However, the wells that included serum in the lower chamber showed a steady increase of reticulocytes in the lower chamber over time, while the ones using media only showed no more increase in reticulocytes after 1 minute. It is possible that the more flexible and mature reticulocytes can simply go through the BMEC layer with no help, using gravity. However, the less flexible ones may require a signal such as serum to make them start migrating through the BMEC layer. However, it is also possible that the viscosity of the serum could affect the speed of egress and could explain the temporal delay.

The BMEC layer integrity was checked by immunofluorescence to ensure that there were no obvious holes/leaks in the filter. When this experiment was repeated for longer time points (Figure 6-6B), it can be observed that more cells exit towards the serum, but there still is egress with no serum present into the bottom chamber. However, red blood cells were also capable of egressing despite the lack of leak detected by immunofluorescence.

#### 6.2.6 Induced BMEC cells with TNF- $\alpha$ and fibronectin let reticulocytes pass without current

Additionally, preliminary unpublished results acquired by Dr Frances Spring at Filton NHSBT (personal correspondence) indicate that reticulocyte migration might be observed when the BMECs are grown on the bottom of the well rather than the top surface. This is thought to be more representative of the situation found in the bone marrow as the cells would be going from the basal side to the apical side to egress. Furthermore, in this case the BMECs were exposed to fibronectin and TNF- $\alpha$  to ensure that they expressed VCAM1, a protein known to be important in transendothelial migration for cell-cell contact<sup>257</sup>.

We also decided to grow the BMECs on the bottom layer of the filter to test if this changed the reticulocyte behaviour. Some BMECs were grown with fibronectin and others were exposed to TNF- $\alpha$  for 24 hours after the cells had grown for 24 hours. Others were exposed to both. Red blood cells were used as a control to ensure that the VCAM1 layer was not leaky as red blood cells are not expected to migrate through the sinusoid membrane. The reticulocytes were labelled with CellTracker first to differentiate them from red blood cells so they could be put in the same assay. The assay was tested at first with media without serum. The cells were added to the filter overnight and then counted using flow cytometry. The cells were also added to a filter without BMECs to ensure that the effect measured was due to BMECs and not the presence of the filter. Our first observation from Figure 6-6B was that few reticulocytes were going through the filters in the absence of BMEC, while sometimes red blood cells were capable of going through (but not in every case). The Toye lab uses 3  $\mu$ m transwell filters to routinely isolate reticulocytes from cultures<sup>150</sup> using a specific amount of



media in the top and bottom surfaces. The experiment in Figure 6-6C must not have created a difference in liquids around the filter. Therefore, in this experiment, there is no pressure pushing the reticulocyte to go through the filter as the level between the liquids is equivalent. Despite this, we observed a high count of reticulocytes going through when the BMEC layer was present. Red blood cells were also present in the bottom chamber after the experiment. This would indicate a leak through the BMEC layer, however, as indicated above, even without the BMEC presents, fewer reticulocytes and red blood cells were going through. This suggests an active role for the BMECs for this increased number of reticulocytes within the bottom chamber. The same effect was observed with the other conditions (fibronectin, TNF- $\alpha$  or both) as the reticulocytes were equally passing through the BMEC layer (Figure 6-6C).

Observations with the serum condition were more difficult as the flow cannot discern the cells from the debris floating in the serum. Some results were counted by hand to double check the flow counts. It might be necessary to filter the serum for future experiments.

#### 6.2.7 BMECs do not express VCAM1 but produce their own fibronectin

To ensure the BMEC cells were expressing VCAM1 and to observe the placement of the fibronectin, the filters were fixed after the migration assay with paraformaldehyde. These filters were then probed for the presence of VCAM1 and fibronectin. It can be observed using immunofluorescence shown in Figure 6-7 that the BMECs overlap and cover the entire filter. Interestingly, fibronectin deposition was detected in all samples (except in the condition where both TNF $\alpha$  and fibronectin were used), not only

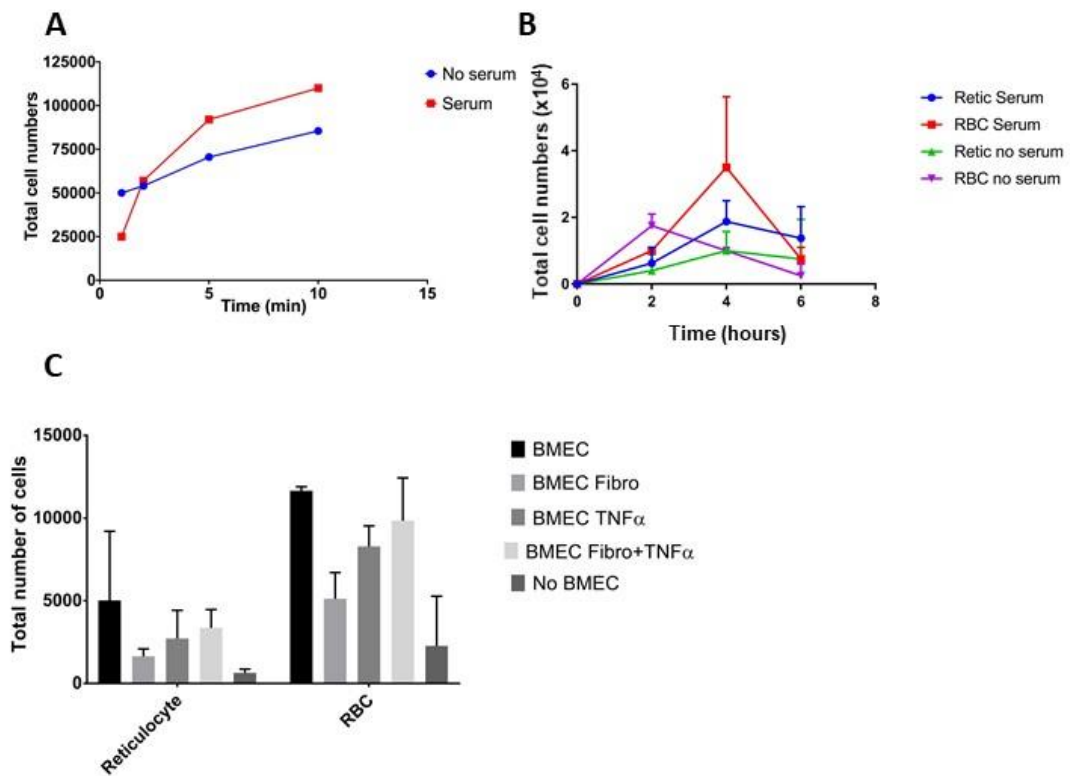


Figure 6-6 - Reticulocytes and RBCs can move across BMEC layers seeded on transwell filters

A – Dot plot of total reticulocyte present in the bottom well over time in serum or media with no serum after 1 to 10 minutes in the presence of BMECs on top (n=2). B – Dot plot of total reticulocytes and red blood cells present in the bottom well over time in serum or media with no serum after 2 to 6 hours in the presence of BMECs on top (n=3). C – Histogram of total number of reticulocytes or RBCs present in the bottom well after 16 hours in the presence of BMECs under different conditions underneath the filter (n=2). Standard deviation is represented.

those where it had been added (Figure 6-7C). Therefore, the cells can lay down their own extracellular matrix (ECM) when they grow on the filter.

Unfortunately, VCAM1 was not detected in any conditions above the background levels found in the secondary only control in this line of BMECs (Figure 6-7B).

#### 6.2.8 Live imaging of BMEC

To study the activity of the BMECs on the filters, the cells grown on filters with TNF- $\alpha$  were put into wells with a glass coverslip at the bottom. Their activity could then be imaged over several minutes to observe their capacity for movement. Aoki et al.<sup>39</sup> suggested that the endothelial cells surrounding the sinusoid were pulsating. Therefore, this might explain why the reticulocytes are capable of more movement in the presence of BMECs, rather than an active movement on the reticulocytes' part.

The BMECs were labelled with CellTracker to visualise their cytoplasm more clearly. In most videos, the cells are not moving or pulsating over the period of 30 minutes, but they do appear to have hole-like structures within their cytoplasm (Figure 6-8). After several minutes of imaging, the cells start retracting from one another. This may be due to light toxicity due to the imaging conditions. This experiment would need repeating, but this preliminary data does not suggest an active pulsating role for this line of BMECs.

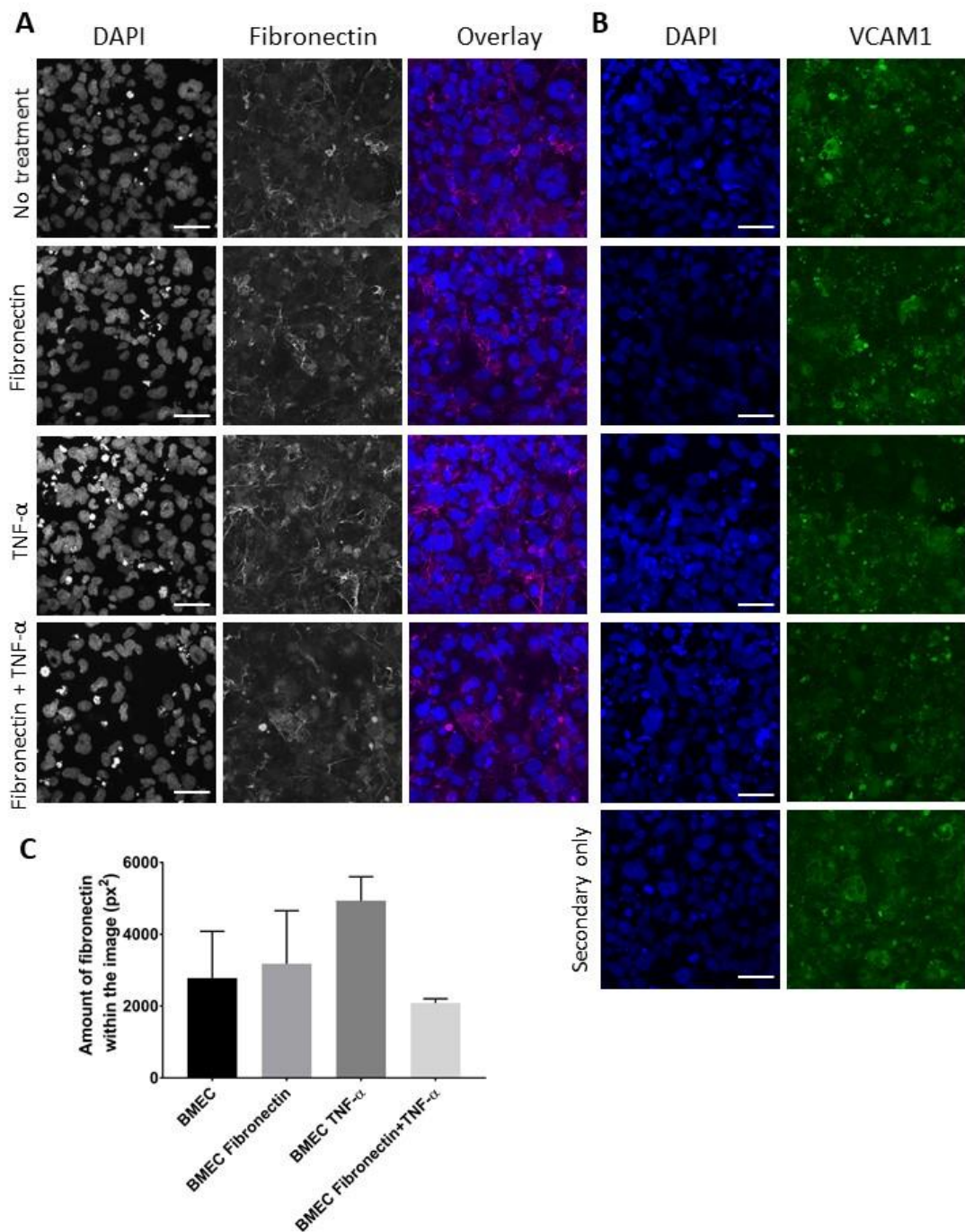
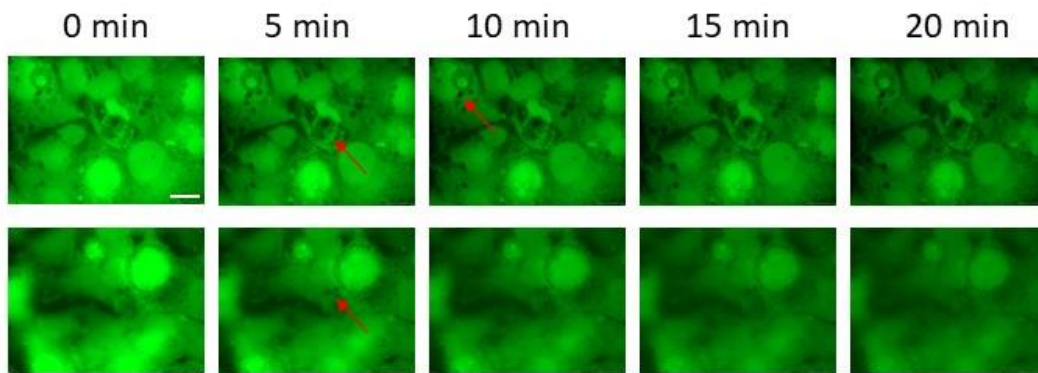


Figure 6-7 - BMECs do not express VCAM1 but do produce their own fibronectin

A and B – Representative images of BMECs after 72hrs culture on the filters. The cells were probed for DAPI and Fibronectin. The cells were placed either on filters with no fibronectin or fibronectin deposited for 1 hour. The cells were then be activated with TNF-α after they had been growing for 48 hours on the filters. The cells were then fixed with paraformaldehyde and probed with fibronectin (A), VCAM1 (B) or DAPI (A and B). C – Quantification of area of fibronectin present in each sample adjusted to the secondary only control using Fiji macro (n=2). Scale bar represents 10μm.



*Figure 6-8 - BMECs do not pulsate in this assay*

*Representative live cell imaging of CellTracker labelled BMECs grown on the bottom of a transwell filter after 72hours imaged through a glass coverslip using Olympus CellR wide-field imaging system using 63x lens. The BMECs were imaged every 20 seconds for 30 minutes. Red arrows indicate examples of holes present within the cytoplasm of the cells. Scale bar represents 50 $\mu$ m.*

### 6.3 Discussion

This chapter has conducted preliminary experiments to start to determine whether reticulocytes are migratory and therefore capable of egress from the bone marrow alone. As these experiments are very preliminary, this discussion will discuss conclusions from the experiments made and potential improvements or considerations that could be incorporated in future experiments.

First, we explored the surface proteomics data, and David pathway analysis suggests that they have some remaining peptides from proteins that are known to be involved in transendothelial migration in leukocytes. This pathway is not present in red blood cells, and so at the very least the cells have some machinery that could be involved in egress, but similarly, due to the low peptide numbers, these may be vestigial expression. We also conducted imaging of native reticulocytes, but surprisingly, no active movement was detected. This may be due to the imaging conditions used or the surface coating on the plates. Interestingly, the cells were still capable of some long-lasting interactions despite the lower amount of integrins on reticulocytes. We looked at the ability of the reticulocytes to traverse 3  $\mu\text{m}$  transwell filters and the relationship between reticulocytes and endothelial cells. We found that reticulocytes could traverse filters better in the presence of endothelial cells than without. Therefore, these very preliminary data point towards a possible migratory capacity in reticulocytes.

The interactions observed between reticulocytes and macrophages are an interesting one. It would be expected that reticulocytes would no longer be able to interact with macrophages, as they will be egressing towards the bloodstream. This continued interaction could be because the reticulocytes are still immature or have produced PS

vesicles which are still able to bind the macrophage. This binding could be part of the reticulocyte maturation process as the macrophage help the reticulocyte detach from its vesicles<sup>220,258</sup>. It is also possible that, as presented by Yokoyama et al.<sup>35</sup> and Dennis Skinner (conference abstract, unpublished), the macrophage remains attached to the reticulocytes and helps them migrate through the BMEC layer. However, the EM images shown in Figure 6-4 suggest that reticulocytes are capable of traversing the BMEC layer on their own in mice. Therefore, the macrophages might simply be there as an aid or this interaction is for another purpose. In the future, cytotracker dye could be added to the erythroblasts to stain for the nucleus. This will enable us to look at whether the macrophages are interacting with orthochromatic cells, reticulocytes or nuclei to be phagocytosed. Furthermore, it might give us some insight on how the relationship evolves pre- and post-enucleation.

One of the most puzzling results from these experiments is the presence of red blood cells in the bottom chamber of the transendothelial migration assay. As red blood cells should not be able to migrate through the BMEC layer, this implies that there is a gap between the cells which enables them to leave. However, there are more red blood cells in the bottom chamber with the BMECs than without any cells on the filter. Therefore, under the conditions used, the BMECs are acting in a currently unknown way which facilitates both retics and red blood cells to cross the filter.

These experiments raise the question of which cells are actively engaged in the process of moving out. It is possible that the BMECs are actively creating a pressure to help the reticulocytes out by pulsating. It could also be that reticulocytes are still capable of migrating with the small number of integrins available. To further study whether the

BMECs were playing an active role within the movement of reticulocytes through the filter, we could fix the BMECs with methanol after they have been activated with TNF- $\alpha$ . The migration assay can then be conducted under these conditions. This would help test whether the BMEC cells are actively helping the reticulocytes leave through a pulsating activity.

It would be interesting to explore EphA4's role in both a release from macrophages as well as their movement through bone marrow endothelial cells. We know that EphA receptors can have a role in making cells move away from each other as well as having an important role in transendothelial migration. However, as was discussed in Chapter 4, it was not possible to remove EphA4 from either BEL-A cells or primary cells. For this reason, in the future, it might be necessary to use small molecules known to block EphA4 activity<sup>259,260</sup> or perhaps use beads coated with EphA4.

As discussed previously (section 6.2.1), integrins are present in small quantities on reticulocytes, and we know from Chapter 4 that the cells do not bind to VCAM1 anymore. The lack of presence of VCAM1 on the BMECs might not affect the egress of the reticulocytes. To test whether VCAM1 would make a difference it would be possible to test the different cytokines used in Chapter 3 on macrophages on the BMECs to induce them to express the adhesion molecule, overexpress VCAM1 or use another source of BMEC. For now, these results point towards another mechanism. A study showed that EPO causes an increase in podocalyxin at the surface of reticulocytes and that there was a faster rate of egress in bone marrows treated with Epo<sup>261</sup>. Therefore, it is possible that the adhesion protein podocalyxin, which can bind L-selectin or integrins on the endothelial cells<sup>262</sup>, would help the reticulocytes navigate along the



cells barriers. Interestingly, one protein which is involved with erythroblast differentiation<sup>36,95,98</sup> has recently been found to have a role in cell migration: the erythroblast-macrophage protein (EMP)<sup>263</sup>. In this study, the macrophages which were transduced with EMP shRNA had abnormal cell motility as the protein played an active role in the regulation of the actin skeleton. This result indicates another interesting avenue for reticulocytes which possibly still express the protein.

The visualisation of the BMEC layer was difficult to interpret as it was not possible to always tell where the cells ended. For this reason, it might be worth it to add the CellTracker to only a portion of the cells to detect the edges more clearly. However, from the current images, the BMECs do not have any visible movement. Therefore, it would be interesting to watch the reticulocytes travel through this layer as the BMECs do not have an active role or creating pressure in this assay. Furthermore, the presence of reticulocytes or macrophages might be necessary for the BMECs to be stimulated. The addition of reticulocytes, macrophage or both would help inform on what factors are necessary for the egress of reticulocytes.

As stress erythropoiesis leads to a higher release of reticulocytes and a thinning of the BMEC overlap in the bone marrow<sup>39</sup>, the addition of the factors released by the body for stress erythropoiesis such as EPO, dexamethasone or SCF-1<sup>264</sup>, could lead to a more striking change in the BMECs which might help visualise the egress of reticulocytes better within this assay.

To conclude, there remain numerous questions around how reticulocytes egress from the bone marrow and we have tried to begin to make models to mimic this but there were many technical issues. The best way to study this phenomenon would be to study

it *in vivo* or to better mimic the bone marrow environment and circulation more effectively *in vitro*.



## 7 Chapter 7 - Discussion

### 7.1 Creation a reconstitution assay and imaging methodology to explore interactions between macrophages and erythroblasts

In Chapter 3, we were able to create a live cell imaging-based assay to investigate the interaction between erythroblasts and macrophages. This methodology built on previous studies which explored the reconstitution of erythroblastic islands as well as the identification of the central macrophages within the island to facilitate isolation. This enabled us to delve into the interactions between the erythroblasts and the macrophages and develop analysis methods. This method has produced new important information as to how these cells interact, with added information on the length of interactions between erythroblasts and macrophages as well as a good method to screen for the molecular pathways involved in this interaction. It facilitates screening for the involvement of receptors in the detection, formation, and stability of erythroblastic island formation.

Other studies looking at erythroblastic island molecular pathways utilised different methods, such as the isolation of islands from mice bone marrow<sup>93,100,265,266</sup>, or use of imaged flow cytometry (i.e. ImageStream) to identify the different receptors present at the surface of both cells within these structures<sup>92</sup>. However, none of these systems can look at the start of the interaction and the formation of these clusters. Our system can separate out the function of different molecules between the formation and the binding role that it may play. Furthermore, the fact that 24 wells can be imaged at the same

time over several days in the incucyte system gives the opportunity to study multiple molecular pathways at the same time, and their effect over a long period of time.

However, it is good science to ask whether this system is actually biologically relevant. We currently can observe using imaging that these erythroblasts can bind the macrophages for a long period of time, reminiscent of the erythroblastic islands found after flushing the bone marrow. In this assay, we have not assessed the effect on erythropoiesis or whether these macrophages have changed phenotype after being in the presence of media and erythroblasts. We do know from Heideveld et al.<sup>60</sup> that the +Dex macrophages are capable of forming larger erythroblastic islands over time as well as help the erythroblasts proliferate and remove pyrenocytes<sup>90</sup>. For this reason, we believe that in this system we are looking at biologically-relevant interactions. In the future, it would be a positive step to improve the system to truly appreciate this fact, as well as being able to confirm our findings *in vivo*.

One more consideration to have is whether the numbers being compared between conditions in this system are biologically relevant, as they are quite small. We can see in all the experiments from the incucyte that we are comparing an average number of links which is below 1 and many lengths of interactions which are below 1 hour. However, it is important to remember that there are many macrophages and not all of them will interact with many erythroblasts. Therefore, if they are in contact with 1 erythroblast for about half of the time, the average link will be 0.5. Any larger number than 1 implies a macrophage which was in contact with a large number of erythroblasts for a long time. Many studies have demonstrated that in the early stages, most macrophages are only in contact with in between 1 to 5 erythroblasts. The numbers we

are looking at should be relevant to the numbers found by other studies, and it is possible to compare these relatively small numbers. Regarding the length of interactions, it is not known how long erythroblasts interact with macrophages in the bone marrow. It is not yet possible to know if the lengths found in this study are comparable to erythroblastic islands in the bone marrow. It will be necessary, in the future, to compare these lengths *in vivo*. However, this new assay system has helped uncover parts of the interaction on which we possess small amounts of information. This new system will hopefully give the haematopoiesis community a chance to study more thoroughly the role of the macrophage within erythropoiesis, and the molecular pathways involved as well as being able to study the role this interaction can play in human disease pathology.

## 7.2 Chapter 4 and Chapter 5 – The important role of Eph and Integrins

These experiments established the expression profile for Eph receptors on erythroblasts throughout development. We have demonstrated that EphB receptors are present at the surface of erythroblasts during terminal differentiation between the proerythroblast and orthochromatic stages and that this temporal expression profile coincides with increased integrin activation. The depletion of EphB4 causes macrophages and erythroblasts to have fewer long-duration contacts, and the removal of EphB4 or its inhibition did not impact on integrin activation. Therefore, loss of EphB4 is sufficient to reduce macrophage recognition of erythroblasts as binding partners, however, not all contacts are abrogated. We hypothesise that as the active integrin is still present, cells can bind spontaneously if they encounter erythroblasts. We also

suggest that ensuring integrins have heightened activation alongside ephrin-B2 binding reinforces recognition.

Contact inhibition of locomotion is thought to be controlled by a ratio of EphB and EphA receptors<sup>114</sup>. Interestingly, we observed that erythroblasts have a high level of EphB and EphA receptors during early stages of differentiation, but lose EphB receptors by the final stages of differentiation while EphA is retained (albeit at lower levels). We hypothesise that Eph receptors contribute to the whole process of differentiation; in the early stages of differentiation, EphB receptor is present in higher amounts than EphA leading to recognition between the cells, supported by the EphB4 inhibition disrupting this interaction. As the cells differentiate, the amount of EphA receptor becomes dominant over EphB tantalisingly suggesting that, once the erythroblast has enucleated to form a reticulocyte, EphA4 may be involved in the separation of the cells. However this will need to be explored in future experiments. In addition to driving interactions, the Eph receptors may play additional supportive roles within the erythroblastic island. It was previously reported that overexpression of EphB4 increases HSC numbers<sup>127</sup>, therefore EphB4 might have a proliferative role within the niche. The silencing of EphB4 led to slower proliferation and some death in our culture. As erythroblasts both express ephrin-B2 and EphB4, the homophilic cell interaction could lead to higher proliferation, as suggested in our model in Figure 7-1. This could explain the ability of erythroblasts to proliferate *in vitro* in the absence of macrophages. Furthermore, it is possible that EphB4 also acts as an erythropoietin receptor<sup>267</sup>, enabling these cells to be more responsive to local concentrations of erythropoietin in media or erythroblastic islands.

### 7.3 Chapter 6 – Mechanism of reticulocyte egress is still unknown

The experiments in Chapter 6 show that *in vitro* experiments to explore the dynamics of reticulocytes and the egress from bone marrow is quite difficult to study, and currently there are no techniques established which help answer the questions around this process. Reticulocytes and their interaction with macrophages have mostly been studied within the macrophage's role in clearance and nuclei phagocytosis, but it is important to know whether macrophages have a central role in the egress of reticulocytes into the bloodstream. This knowledge could help elucidate disease mechanisms as well as the creation of a more efficient methodology to isolate reticulocytes from *in vitro* cultures.

Similarly, the relationship between reticulocytes and endothelial cells remains mostly descriptive as studies have mostly been conducted using electron microscopy on fixed mice bone marrow tissue. For this reason, the dynamics and the molecular pathways have mostly remained inaccessible. New methods will need to be established to be able to answer this question, such as the advance of bone marrow on a chip<sup>268–270</sup>. These devices help to recreate the whole bone marrow with all of its complexities. This would help observe all the dynamics in a system which reproduces the bone marrow more closely.

### 7.4 The questions raised

#### 7.4.1 Importance of VCAM1 and integrins

The general dogma in the field has long stated the importance of VCAM1 being present on macrophages, to interact with the integrins on the erythroblasts, the main adherence proteins present at the surface. However, recent papers have questioned its



importance<sup>92,99</sup>, mirroring our experiments which show that macrophages *in vitro* cultured and isolated from bone marrow without VCAM1, can interact with erythroblasts. However, it was observed that bone marrow macrophages expressing VCAM1 do have more interactions than VCAM1<sup>-</sup> cells. This suggests that the presence of VCAM1 may bind the integrins increasing the amount of adhesions available to the macrophage, helping stabilise the interaction.

The removal of the Eph receptors might still be affecting the VCAM1 binding if this loss affects the integrins  $\alpha$  subunits rather than the  $\beta$  subunits. This would lead to a change in level of the active  $\alpha\beta$  complexes. This might explain why we cannot detect changes in our experiments as only  $\beta$  activation was explored. It would be necessary to look at the  $\alpha$  subunits' presence and activation. However, the fact that macrophages which do not have VCAM1 are capable of interacting with both erythroblasts and reticulocytes point towards a VCAM1-independent role for integrins which has not been investigated. As the EIL peptide, which inhibits binding to the integrin  $\alpha4\beta1$  complex, can disrupt the interactions as well with VCAM1<sup>-</sup> macrophages, there is evidence for this. Other receptors for integrins that might play a role include ICAM4<sup>93</sup>.

Taken together, the experiments in this thesis have shown that Eph receptors are more important to the recognition between erythroblasts and macrophages than VCAM1. This mirrors the results found by Wei and Frenette when they saw that EMP was more important than VCAM1 for the further stages of the interaction<sup>99</sup>. However, we do not fully understand the hierarchy between Eph receptors and the integrins. Our experiments do however demonstrate that both Eph and integrins together are essential for the interaction and recognition of the macrophages to the erythroblasts.

Interestingly, the timing of the presence at the surface are important, as the Eph receptors are present at the same time as a rise in integrin  $\beta 1$  occurs. As discussed in Chapter 4, this coincidence may be important in the binding of erythroblasts to macrophages as the removal of either EphB4, EphB6 (for interaction with bone marrow macrophage) or integrin complexes can affect the binding and the formation of interactions. For this reason, it is possible that there is a coincidence detector within this system which enables macrophages to recognize erythroblasts specifically as ready to bind within the niche. Perhaps, it is the presence of both at the surface of the cells which regulates the binding of erythroblasts to macrophages. For example, it could be the presence of both which leads to the binding, as a recognition pattern, as many cells in the bone marrow will express integrins. It remains unknown what leads to this activation of integrin  $\beta 1$  in humans, as our results do not mirror those found by Anselmo et al, in mice.<sup>128</sup> As illustrated in Figure 7-1, we propose a model of interaction whereby EphB receptors and integrin engagement may act together as a coincidence detector to ensure that the macrophage associates and binds to the differentiating progenitor cell at the appropriate time.

#### 7.4.2 Dynamics of erythroblastic islands.

The use of the incucyte has brought in a new angle for interrogating the relationship between erythroblasts and macrophages. As we saw in Chapter 3 and 5, the incucyte has enabled us to quantify the first interactions between the two cell types as we can measure how long they interact, as well as assessing how many erythroblasts one macrophage can interact with at a time. Furthermore, we can investigate whether macrophages are motile. All of the factors that we can now monitor will help us

understand the importance of different receptors within the system as discussed in section 7.2, but it also raises many questions.

As the macrophages are observed to be motile in both the +Dex macrophages and bone marrow, this raises the question of whether this is something which happens *in vivo*. Yokoyama et al.<sup>35</sup> showed that the erythroblastic islands had different occupancies as they approached the sinusoid. The conclusion was that the macrophages were used to move the erythroblasts closer to the sinusoid as they differentiated. The fact that macrophages are capable of movement is a good indication that in the bone marrow they might be able to provide this service to the erythroblasts, which are less motile.

However, it is also noticeable that the contacts between erythroblasts and macrophages are not all the same length. This might be an artefact of our assay because the erythroblasts are quite a heterogeneous population, and therefore might not be all ready to bind macrophages when they encounter them. Furthermore, the media and 2D structure of the assay might be altering the quality of binding or the phenotypes of the cells enough to lead to this heterogeneous binding time. However, it is also possible that erythroblasts do have a large range of binding time as they instead move from one macrophage to the next in the bone marrow as they differentiate. This would also explain Yokoyama et al.'s results as the occupancy would change as the cells would move along.

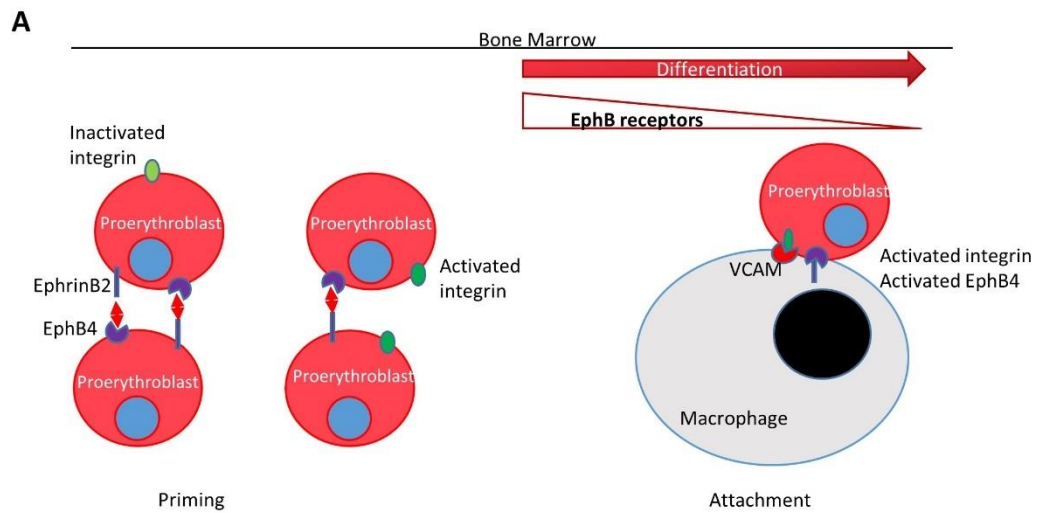


Figure 7-1 - Proposed role of Eph receptors and integrins in the erythroblastic island formation

Summary diagram of the coincidence detection hypothesis. In the later stages of expansion, as the cells become CD36 positive, the cells gain EphB4 and active integrin at their surface. The presence of EphB4 and active integrin helps the cells bind both VCAM positive and negative macrophages..

Furthermore, the relationship between the macrophages and the reticulocytes and the fact that they can still interact poses the question of the fate of the macrophage at the end of the erythroblastic development. The role of the macrophage is often studied in its ability to phagocytose the nuclei<sup>26</sup>. The incucyte assay and other imaging methodologies that may follow will hopefully, in the future, be able to shed more light in this dynamic process. It will be possible to quantify the interactions between all the different components of the system (macrophages, reticulocytes and pyrenocytes), as well as study the different receptors involved. However, it is rarely studied what happens to the macrophages after the separation from the reticulocyte. In our assay, we observe that they are still capable of interacting with reticulocytes. Therefore, it remains possible that they accompany the reticulocytes into the bloodstream. If the erythroblasts move between the macrophages in the bone marrow, it is possible that the occupancy of that macrophage would simply get filled afterwards. Studies *in vivo* and reconstructions of the bone marrow would help understand all of these dynamics further.

Overall, our system has shown that it is important not to forget to study the dynamics of a system when studying cell interactions, as there are many aspects of interactions that occur between cells which might be important or highly biologically relevant.

#### 7.4.3 Macrophage identity

The identity of the central macrophage has long intrigued hematopoietic researchers. While other resident macrophages play more a role of immune defence for a specific organ<sup>52,61</sup>, this central macrophage has more of a nursing role for a specific type of cells. It is possibly also responsible for the secretion of different factors responsible in the

control of HSCs<sup>89,200,271</sup>. One more difficulty is its presence amongst the bone marrow, one of the main sites where monocytes are generated. Some studies have enabled the identification of important receptors at the surface of these macrophages, which enable researchers to identify and isolate them. However, the experiments in this thesis have shown that a varied source of macrophages can interact with erythroblasts. Falchi et al.<sup>31</sup> and Heideveld et al.<sup>17</sup> have shown that +Dex macrophages grown from blood isolations are capable of improving erythropoiesis. Furthermore, Heideveld et al. has shown that these same macrophages can phagocytose the nuclei expelled from the reticulocytes<sup>60</sup>. All of this information points towards the existence of not a single macrophage erythroblast interaction phenotype, but multiple. Recently, a similar finding was found using ImageStream flow cytometry which showed that erythroblastic islands do not always have the same type of central macrophages<sup>92</sup>. All of this evidence points towards the possible existence of a pool of macrophages which can potentially interact and support erythroblasts, but also the existence of a “backup” pool of macrophages which can also step in to help with the function, the VCAM1<sup>+</sup> fraction of the bone marrow, ready to help at any moment.

The identity of the central macrophages has also been studied analogously with the central macrophage present in the spleen. As these macrophages also interact with erythroblasts and reticulocytes, it is understandable that they would be similar. As spleens are easier to isolate from mice, most results have been obtained using these cells. However, some differences remain between the two macrophages. This is particularly observed when a study ablated CD169 macrophages with G-CSF, as it mobilizes them from the bone marrow and found that those in the spleen were not removed and that this site formed erythroblasts as compensation<sup>246</sup>, though another

study's ablation via extended treatment with diphtheria toxins on CD169-DTR did lead to a loss of spleen macrophages<sup>33</sup>. There are stark differences between bone marrow macrophages and spleen macrophages, such as their different reaction to G-CSF, though they both express CD169<sup>26</sup>. Where do these differences come from and what is their purpose?

#### 7.4.4 Are animal models useful in this conversation?

A good portion of the research conducted in the field of erythropoiesis has been carried out in animal models such as mice<sup>92,100,183,200,201,265,272</sup>, rats<sup>35,39,102,190</sup> and zebrafish<sup>273</sup>. These animal models offer an opportunity to easily isolate the cells and study the bone marrow and the erythroblastic islands without disruption. However, more and more studies are showing that there are species differences between humans and animals which would need to be taken into account when studying erythroblastic island function<sup>274</sup>. For example, humans produce a foetal globins not found in mice<sup>275</sup>, or the lack of a phenotype in Sec23B mice<sup>150</sup>.

The research outlined in this thesis has studied the molecular pathways involved with the interactions between human erythroblasts and macrophages. We found, like others, that there are significant differences between our findings and those observed in mice. For example, we were not able to reconstitute erythroblastic islands using the media from Lee et al.<sup>93</sup> or to observe the expression of EphB1 in our human donors as well as the role of Eph receptors on the activation of integrin  $\beta$ 1, unlike Anselmo et al.<sup>128</sup>. These differences in results between species suggest not all observations in animals such as mice are translatable to humans due to species differences.

## 7.5 Improvements to the imaging system

In the future, we would hope to study the different questions posed by this research. One of the main ways to do this would be to continue to improve the incucyte system and the different information we can obtain from it. In particular, we would be interested in studying the level of cell death and tracking the erythroblasts through to their enucleation. These factors would inform us on the interactions the macrophages have with the erythroblasts throughout erythropoiesis as well as possibly giving us more information on how this assay affects erythropoiesis. This system would hopefully also help study further the molecular pathways involved, such as the potential role of P2X and P2Y receptors and ATP or its metabolites, as well as studying the pathology of haematology diseases which may have a macrophage interaction axis such as PV or MDS<sup>33,34</sup>.

Furthermore, the strength of the interaction between the cells could be studied using atomic force microscopy (AFM). There is precedent for studying cell-cell interactions and the forces involved using this technique<sup>276–278</sup>. It would be possible to attach erythroblasts at different stages of terminal differentiation to AFM needles and study the force needed to attach and detach them from macrophages. Moreover, where our experiments have shown that there are minor differences between the different macrophages studied which might affect the interactions, the use of AFM may facilitate a better understanding of these interactions. We do not have a complete portrait of the macrophages within the bone marrow and therefore, performing surface proteomics of bone marrow macrophages fractionated using certain surface receptors (such as



VCAM1) would also provide additional understanding and context to our imaging studies.

Finally, as discussed in Chapter 6, the best way to gain a good understanding of the entire situation between erythroblasts, macrophages and endothelial cells, would be to study the entire bone marrow *in situ*. One of the new ways this could be done is through looking at bone marrow in live mice through decalcified bones. The use of these mice and labelled cells could help explain the dynamics within the bone marrow through intravital imaging. For example, this technique enabled scientists to show that progenitor cells and hematopoietic stem cells have different motilities within the niche itself<sup>279</sup>. Therefore, it is possible to gain valuable information on the dynamics of the different cells within the bone marrow. However, as noted in section 7.4.4, it is necessary to also work with human cells. For this reason, working with systems such as SynVivo<sup>280</sup> or growing bone marrow on chips<sup>281–283</sup> would help scientists study the different interactions while taking into account the complexity of the bone marrow.

## 7.6 Summary

In summary, several studies to date have successfully isolated intact erythroblastic islands from rat spleens<sup>265,272</sup> or human bone marrow<sup>72</sup>. However, the majority have concentrated on determining the phenotype of the central macrophage. Several studies in mice have investigated the impact of receptor removal by knocking out ICAM4 or VCAM1 to determine effects on erythroblastic islands. The phenotypes of these have been surprisingly limited, perhaps because of the presence of multiple interactions compensating for each other. This study is the first example where live imaging of human macrophages and erythroblasts has been used to probe a potential receptor

interaction between the cells over time. This has shown a dependence on EphB interactions for the macrophage and erythroblast interaction for the first time. In more preliminary studies it has also implicated a role for P2X and P2Y receptors in the macrophage-erythroblast associations. We hope this imaging assay can help further delineate the importance of other receptors in the interaction between human erythroblasts and macrophages in future experiments.



## 8 Chapter 8 - References

11. Nombela-Arrieta C, Pivarnik G, Winkel B, et al. Quantitative imaging of haematopoietic stem and progenitor cell localization and hypoxic status in the bone marrow microenvironment. *Nat. Cell Biol.* 2013;15(5):533–543.
2. Morrison SJ, Scadden DT. The bone marrow niche for haematopoietic stem cells. *Nature.* 2014;505(7483):327–334.
3. Wilson A, Laurenti E, Oser G, et al. Hematopoietic Stem Cells Reversibly Switch from Dormancy to Self-Renewal during Homeostasis and Repair. *Cell.* 2008;135(6):1118–1129.
4. Spencer JA, Ferraro F, Roussakis E, et al. Direct measurement of local oxygen concentration in the bone marrow of live animals. *Nature.* 2014;508(7495):269–73.
5. Sun J, Ramos A, Chapman B, et al. Clonal dynamics of native haematopoiesis. *Nature.* 2014;514(7522):322–327.
6. Yamamoto R, Morita Y, Ooehara J, et al. Clonal analysis unveils self-renewing lineage-restricted progenitors generated directly from hematopoietic stem cells. *Cell.* 2013;154(5):1112–1126.
7. Schoedel KB, Morcos MNF, Zerjatke T, et al. The bulk of the hematopoietic stem cell population is dispensable for murine steady-state and stress hematopoiesis. *Blood.* 2016;128(19):2285–2296.
8. Sawai CM, Babovic S, Upadhaya S, et al. Hematopoietic Stem Cells Are the Major Source of Multilineage Hematopoiesis in Adult Animals. *Immunity.* 2016;45(3):597–609.
9. Cavins JA, Scheer SC, Thomas DE, Ferrebee JW. The Recovery of Lethally Irradiated Dogs Given Infusions of Autologous Leukocytes Preserved at -80 C. *Blood.* 1964;23(1):38–43.
10. Mansson R, Zandi S, Bryder D, Sigvardsson M. The road to commitment: Lineage restriction events in hematopoiesis. *Mol. Basis Hematop.* 2009;23–46.
11. Baum CM, Weissman IL, Tsukamoto AS, Buckle AM, Peault B. Isolation of a candidate human hematopoietic stem-cell population. *Proc. Natl. Acad. Sci.* 1992;89(7):2804–2808.
12. Civin CI, Strauss LC, Brovall C, et al. Antigenic analysis of hematopoiesis. III. A hematopoietic progenitor cell surface antigen defined by a monoclonal antibody raised against KG-1a cells. *J. Immunol.* 1984;133(1):157–165.
13. Servida F, Soligo D, Caneva L, et al. Functional and morphological characterization of immunomagnetically selected CD34+ hematopoietic progenitor cells. *Stem Cells.* 1996;14(4):430–8.
14. Lansdorp PM, Sutherland HJ, Eaves CJ. Selective expression of CD45 isoforms on functional subpopulations of CD34+ hemopoietic cells from human bone

- marrow. *J. Exp. Med.* 1990;172(1):363–6.
15. Li J, Hale J, Bhagia P, et al. Isolation and transcriptome analyses of human erythroid progenitors: BFU-E and CFU-E. *Blood*. 2014;124(24):3636–3645.
  16. Severn CE, Macedo H, Eagle MJ, et al. Polyurethane scaffolds seeded with CD34 + cells maintain early stem cells whilst also facilitating prolonged egress of haematopoietic progenitors. *Sci. Rep.* 2016;6:32149.
  17. Heideveld E, Masiello F, Marra M, et al. CD14+ cells from peripheral blood positively regulate hematopoietic stem and progenitor cell survival resulting in increased erythroid yield. *Haematologica*. 2015;
  18. Palis J. Primitive and definitive erythropoiesis in mammals. *Front. Physiol.* 2014;5:3.
  19. Bianconi E, Piovesan A, Facchin F, et al. An estimation of the number of cells in the human body. *Ann. Hum. Biol.* 2013;40(6):463–471.
  20. Suenobu S, Takakura N, Inada T, et al. A role of EphB4 receptor and its ligand, ephrin-B2, in erythropoiesis. *Biochem. Biophys. Res. Commun.* 2002;293(3):1124–31.
  21. Satchwell TJ, Bell AJ, Pellegrin S, et al. Critical band 3 multiprotein complex interactions establish early during human erythropoiesis. *Blood*. 2011;118(1):182–91.
  22. Bell AJ, Satchwell TJ, Heesom KJ, et al. Protein Distribution during Human Erythroblast Enucleation In Vitro. *PLoS One*. 2013;8(4):e60300.
  23. Goltry KL, Patel VP. Specific domains of fibronectin mediate adhesion and migration of early murine erythroid progenitors. *Blood*. 1997;90(1):138–147.
  24. Liu J, Guo X, Mohandas N, Chasis JA, An X. Membrane remodeling during reticulocyte maturation. *Blood*. 2010;115(10):2021–7.
  25. Mel HC, Prenant M, Mohandas N. Reticulocyte Motility and Form: Studies on Maturation and Classification.
  26. Klei TRL, Meinderts SM, van den Berg TK, van Bruggen R. From the cradle to the grave: The role of macrophages in erythropoiesis and erythrophagocytosis. *Front. Immunol.* 2017;8(FEB):73.
  27. Moura PL, Hawley BR, Mankelow TJ, et al. Non-muscle Myosin II drives vesicle loss during human reticulocyte maturation. *Haematologica*. 2018;haematol.2018.199083.
  28. Chasis JA, Mohandas N. Erythroblastic islands: Niches for erythropoiesis. *Blood*. 2008;112:470–478.
  29. Hanspal M, Hanspal JS. The association of erythroblasts with macrophages promotes erythroid proliferation and maturation: a 30-kD heparin-binding protein is involved in this contact. *Blood*. 1994;84(10):3494–504.
  30. Rhodes MM, Kopsombut P, Bondurant MC, Price JO, Koury MJ. Adherence to

- macrophages in erythroblastic islands enhances erythroblast proliferation and increases erythrocyte production by a different mechanism than erythropoietin. *Blood*. 2007;111(3):1700–1708.
31. Falchi M, Varricchio L, Martelli F, et al. Dexamethasone targeted directly to macrophages induces macrophage niches that promote erythroid expansion. *Haematologica*. 2015;100(2):178–187.
  32. Hanspal M, Smockova Y, Uong Q. Molecular identification and functional characterization of a novel protein that mediates the attachment of erythroblasts to macrophages. *Blood*. 1998;92(8):2940–50.
  33. Chow A, Huggins M, Ahmed J, et al. CD169<sup>+</sup> macrophages provide a niche promoting erythropoiesis under homeostasis and stress. *Nat. Med*. 2013;19(March):429–36.
  34. Ramos P, Casu C, Gardenghi S, et al. Macrophages support pathological erythropoiesis in polycythemia vera and  $\beta$ -thalassemia. *Nat. Med*. 2013;19(4):437–445.
  35. Yokoyama T, Etoh T, Kitagawa H, Tsukahara S, Kannan Y. Migration of erythroblastic islands toward the sinusoid as erythroid maturation proceeds in rat bone marrow. *J. Vet. Med. Sci*. 2003;65(4):449–452.
  36. Mao X, Shi X, Liu F, Li G, Hu L. Evaluation of erythroblast macrophage protein related to erythroblastic islands in patients with hematopoietic stem cell transplantation. *Eur. J. Med. Res*. 2013;18(1):9.
  37. Toda S, Segawa K, Nagata S. MerTK-mediated engulfment of pyrenocytes by central macrophages in erythroblastic islands. *Blood*. 2014;123(25):3963–71.
  38. de Back DZ, Kostova EB, van Kraaij M, van den Berg TK, van Bruggen R. Of macrophages and red blood cells; A complex love story. *Front. Physiol*. 2014;5 JAN(January):
  39. Aoki M, Tavassoli M. Dynamics of red cell egress from bone marrow after blood letting. *Br. J. Haematol*. 1981;49(3):337–47.
  40. Boulais PE, Frenette PS. Making sense of hematopoietic stem cell niches. *Blood*. 2015;125(17):2621–9.
  41. Waugh RE. Reticulocyte rigidity and passage through endothelial-like pores. *Blood*. 1991;78(11):3037–42.
  42. Heideveld E, van den Akker E. Digesting the role of bone marrow macrophages on hematopoiesis. *Immunobiology*. 2017;222(6):814–822.
  43. Epelman S, Lavine KJ, Randolph GJ. Origin and Functions of Tissue Macrophages. *Immunity*. 2014;41(1):21–35.
  44. Hettinger J, Richards DM, Hansson J, et al. Origin of monocytes and macrophages in a committed progenitor. *Nat. Immunol*. 2013;14(8):821–830.
  45. Hashimoto D, Chow A, Noizat C, et al. Tissue-resident macrophages self-maintain locally throughout adult life with minimal contribution from circulating

- monocytes. *Immunity*. 2013;38(4):792–804.
46. Hoeffel G, Chen J, Lavin Y, et al. C-Myb<sup>+</sup> Erythro-Myeloid Progenitor-Derived Fetal Monocytes Give Rise to Adult Tissue-Resident Macrophages. *Immunity*. 2015;42(4):665–678.
  47. Lavin Y, Winter D, Blecher-Gonen R, et al. Tissue-resident macrophage enhancer landscapes are shaped by the local microenvironment. *Cell*. 2014;159(6):1312–1326.
  48. Iwatsuki H, Sasaki K, Suda M, Itano C. Origin of the central cells of erythroblastic islands in fetal mouse liver: Ultrahistochemical studies of membrane-bound glycoconjugates. *Histochem. Cell Biol*. 1997;107(6):459–468.
  49. Wang J, Hayashi Y, Yokota A, et al. Expansion of EPOR-negative macrophages besides erythroblasts by elevated EPOR signaling in erythrocytosis mouse models. *Haematologica*. 2018;103(1):69–79.
  50. Kuziel W a, Morgan SJ, Dawson TC, et al. Severe reduction in leukocyte adhesion and monocyte extravasation in mice deficient in CC chemokine receptor 2. *Proc. Natl. Acad. Sci. U. S. A*. 1997;94(22):12053–12058.
  51. Koh TJ, DiPietro LA. Inflammation and wound healing: the role of the macrophage. *Expert Rev. Mol. Med*. 2011;13:e23.
  52. Roszer T. Understanding the mysterious M2 macrophage through activation markers and effector mechanisms. *Mediators Inflamm*. 2015;2015:1–16.
  53. Martinez FO, Gordon S. The M1 and M2 paradigm of macrophage activation: time for reassessment. *F1000Prime Rep*. 2014;6:13.
  54. Verreck FAW, de Boer T, Langenberg DML, et al. Human IL-23-producing type 1 macrophages promote but IL-10-producing type 2 macrophages subvert immunity to (myco)bacteria. *Proc. Natl. Acad. Sci*. 2004;101(13):4560–4565.
  55. Antal-Szalmas P, Van Strijp JAG, Weersink AJL, Verhoef J, Van Kessel KPM. Quantitation of surface CD14 on human monocytes and neutrophils. *J. Leukoc. Biol*. 1997;61(6):721–728.
  56. Shive CL, Jiang W, Anthony DD, Lederman MM. Soluble CD14 is a nonspecific marker of monocyte activation. *AIDS*. 2015;29(10):1263–1265.
  57. Ziegler-Heitbrock L, Ancuta P, Crowe S, et al. Nomenclature of monocytes and dendritic cells in blood. *Blood*. 2010;116(16):e74–e80.
  58. Perussia B, Ravetch J V. FcγRIII (CD16) on human macrophages is a functional product of the FcγRIII-2 gene. *Eur. J. Immunol*. 1991;21(2):425–429.
  59. Nagarajan S, Chesla S, Cobern L, et al. Ligand Binding and Phagocytosis by CD16 (Fc γ Receptor III) Isoforms. *J. Biol. Chem*. 1995;270(43):25762–25770.
  60. Heideveld E, Hampton-O’Neil LA, Cross SJ, et al. Glucocorticoids induce differentiation of monocytes towards macrophages that share functional and phenotypical aspects with erythroblastic island macrophages. *Haematologica*. 2017;haematol.2017.179341.

61. Mills C. M1 and M2 Macrophages: Oracles of Health and Disease. *Crit. Rev. Immunol.* 2012;32(6):463–488.
62. Aron-Wisnewsky J, Tordjman J, Poitou C, et al. Human adipose tissue macrophages: M1 and M2 cell surface markers in subcutaneous and omental depots and after weight loss. *J. Clin. Endocrinol. Metab.* 2009;94(11):4619–4623.
63. Kambara K, Ohashi W, Tomita K, et al. In vivo depletion of CD206+M2 macrophages exaggerates lung injury in endotoxemic mice. *Am. J. Pathol.* 2015;185(1):162–171.
64. Barros MHM, Hauck F, Dreyer JH, Kempkes B, Niedobitek G. Macrophage polarisation: An immunohistochemical approach for identifying M1 and M2 macrophages. *PLoS One.* 2013;8(11):e80908.
65. Zizzo G, Hilliard BA, Monestier M, Cohen PL. Efficient Clearance of Early Apoptotic Cells by Human Macrophages Requires M2c Polarization and MerTK Induction. *J. Immunol.* 2012;189(7):3508–3520.
66. Teles RMB, Krutzik SR, Ochoa MT, et al. Interleukin-4 regulates the expression of CD209 and subsequent uptake of Mycobacterium leprae by Schwann cells in human leprosy. *Infect. Immun.* 2010;78(11):4634–4643.
67. Kämmerer U, Eggert AO, Kapp M, et al. Unique appearance of proliferating antigen-presenting cells expressing DC-SIGN (CD209) in the decidua of early human pregnancy. *Am. J. Pathol.* 2003;162(3):887–896.
68. Preza GC, Tanner K, Elliott J, et al. Antigen-presenting cell candidates for HIV-1 transmission in human distal colonic mucosa defined by CD207 dendritic cells and CD209 macrophages. *AIDS Res. Hum. Retroviruses.* 2014;30(3):241–9.
69. Martinez FO, Gordon S. The M1 and M2 paradigm of macrophage activation: time for reassessment. *F1000Prime Rep.* 2014;6:13.
70. Kong X, Gao J. Macrophage polarization: a key event in the secondary phase of acute spinal cord injury. *J. Cell. Mol. Med.* 2017;21(5):941–954.
71. Bessis M. Erythroblastic island, functional unity of bone marrow. *Rev Hematol.* 1958;13(1):8–11.
72. Lee SH. Isolation and immunocytochemical characterization of human bone marrow stromal macrophages in hemopoietic clusters. *J. Exp. Med.* 1988;168(3):1193–1198.
73. Finch CA. “The role of iron in hemoglobin synthesis.” Conference on Hemoglobin. National Academies Press (US); 1958.
74. Khalil S, Holy M, Grado S, et al. A specialized pathway for erythroid iron delivery through lysosomal trafficking of transferrin receptor 2. *Blood Adv.* 2017;1(15):1181–1194.
75. Vaisman B, Fibach E, Konijn AM. Utilization of intracellular ferritin iron for hemoglobin synthesis in developing human erythroid precursors. *Blood.* 1997;90(2):831–838.



76. BESSIS MC, BRETON-GORIUS J. Iron metabolism in the bone marrow as seen by electron microscopy: a critical review. *Blood*. 1962;19(6):635–63.
77. Leimberg MJ, Prus E, Konijn AM, Fibach E. Macrophages function as a ferritin iron source for cultured human erythroid precursors. *J. Cell. Biochem*. 2008;103(4):1211–1218.
78. Bartnikas TB. Known and potential roles of transferrin in iron biology. *BioMetals*. 2012;25(4):677–686.
79. Korolnek T, Hamza I. Macrophages and iron trafficking at the birth and death of red cells. *Blood*. 2015;125(19):2893–2897.
80. Allen TD, Testa NG. Cellular interactions in erythroblastic islands in long-term bone marrow cultures, as studied by time-lapse video. *Blood Cells*. 1991;17(1):29-38; discussion 39-43.
81. Yoshida H, Kawane K, Koike M, et al. Phosphatidylserine-dependent engulfment by macrophages of nuclei from erythroid precursor cells. *Nature*. 2005;437(7059):754–8.
82. Kawane K, Fukuyama H, Kondoh G, et al. Requirement of DNase II for definitive erythropoiesis in the mouse fetal liver. *Science (80-. )*. 2001;292(5521):1546–1549.
83. Genin M, Clement F, Fattaccioli A, Raes M, Michiels C. M1 and M2 macrophages derived from THP-1 cells differentially modulate the response of cancer cells to etoposide. *BMC Cancer*. 2015;15(1):577.
84. Zermati Y, Fichelson S, Valensi F, et al. Transforming growth factor inhibits erythropoiesis by blocking proliferation and accelerating differentiation of erythroid progenitors. *Exp. Hematol*. 2000;28(8):885–894.
85. Mohandas N, Prenant M. Three-dimensional model of bone marrow. *Blood*. 1978;51(4):633–43.
86. Morris L, Graham CF, Gordon S. Macrophages in haemopoietic and other tissues of the developing mouse detected by the monoclonal antibody F4/80. *Development*. 1991;112(2):517–526.
87. Crocker PR, Gordon S. Isolation and characterization of resident stromal macrophages and hematopoietic cell clusters from mouse bone marrow. *J. Exp. Med*. 1985;162(3):993–1014.
88. Hamann J, Koning N, Pouwels W, et al. EMR1, the human homolog of F4/80, is an eosinophil-specific receptor. *Eur. J. Immunol*. 2007;37(10):2797–2802.
89. Chow A, Lucas D, Hidalgo A, et al. Bone marrow CD169 + macrophages promote the retention of hematopoietic stem and progenitor cells in the mesenchymal stem cell niche. *J. Exp. Med*. 2011;208(2):261–271.
90. E. H, M. VDB, F.P. VA, M. VL, E. VDA. Cultured human macrophages as a model for central macrophages in erythroblastic islands. *Blood*. 2016;128(22):.
91. Yeo JH, McAllan BM, Fraser ST. Scanning Electron Microscopy Reveals Two

Distinct Classes of Erythroblastic Island Isolated from Adult Mammalian Bone Marrow. *Microsc. Microanal.* 2016;1–11.

92. Seu KG, Papoin J, Fessler R, et al. Unraveling macrophage heterogeneity in erythroblastic islands. *Front. Immunol.* 2017;8(SEP):1140.
93. Lee G, Lo A, Short SA, et al. Targeted gene deletion demonstrates that the cell adhesion molecule ICAM-4 is critical for erythroblastic island formation. *Blood.* 2006;108(6):2064–71.
94. Sadahira Y. Very late activation antigen 4-vascular cell adhesion molecule 1 interaction is involved in the formation of erythroblastic islands. *J. Exp. Med.* 1995;181(1):411–415.
95. Soni S, Bala S, Hanspal M. Requirement for erythroblast-macrophage protein (Emp) in definitive erythropoiesis. *Blood Cells, Mol. Dis.* 2008;41(2):141–147.
96. Lee G, Spring FA, Parsons SF, et al. Novel secreted isoform of adhesion molecule ICAM-4: Potential regulator of membrane-associated ICAM-4 interactions. *Blood.* 2003;101(5):1790–1797.
97. Spring FA, Parsons SF, Orllepp S, et al. Intercellular adhesion molecule-4 binds  $\alpha 4\beta 1$  and  $\alpha v$ -family integrins through novel integrin-binding mechanisms. *Blood.* 2001;98(2):458–466.
98. Soni S, Bala S, Gwynn B, et al. Absence of Erythroblast Macrophage Protein (Emp) Leads to Failure of Erythroblast Nuclear Extrusion. *J. Biol. Chem.* 2006;281(29):20181–20189.
99. Wei Q, Frenette PS. Macrophage Erythroblast Attacher (MAEA), but Not VCAM1, Is Required for the Bone Marrow Erythroblastic Niche. *Blood.* 2015;126(23):.
100. Wang Z, Vogel O, Kuhn G, Gassmann M, Vogel J. Decreased stability of erythroblastic islands in integrin  $\beta 3$ -deficient mice. *Physiol. Rep.* 2013;1(2):e00018.
101. Kristiansen M, Graversen JH, Jacobsen C, et al. Identification of the haemoglobin scavenger receptor. *Nature.* 2001;409(6817):198–201.
102. Fabrick BO, Polfliet MMJ, Vloet RPM, et al. The macrophage CD163 surface glycoprotein is an erythroblast adhesion receptor. *Blood.* 2007;109(12):5223–5229.
103. Wang Z, Miura N, Bonelli A, et al. Receptor tyrosine kinase, EphB4 (HTK), accelerates differentiation of select human hematopoietic cells. *Blood.* 2002;99(8):2740–2747.
104. Inada T, Iwama A, Sakano S, et al. Selective expression of the receptor tyrosine kinase, HTK, on human erythroid progenitor cells. *Blood.* 1997;89(8):2757–65.
105. Wang L, Yu H, Cheng H, et al. Deletion of Stk40 impairs definitive erythropoiesis in the mouse fetal liver. *Cell Death Dis.* 2017;8(3):e2722.
106. Pasquale EB. Eph receptors and ephrins in cancer: bidirectional signalling and beyond. *Nat. Rev. Cancer.* 2010;10(3):165–80.

107. Kullander K, Klein R. Mechanisms and functions of Eph and ephrin signalling. *Nat. Rev. Mol. Cell Biol.* 2002;3(7):475–86.
108. Xiao Z, Carrasco R, Kinneer K, et al. EphB4 promotes or suppresses Ras/MEK/ERK pathway in a context-dependent manner: Implications for EphB4 as a cancer target. *Cancer Biol. Ther.* 2012;13(8):630–637.
109. Alfaro D, Muñoz JJ, García-Ceca J, et al. The Eph/ephrinB signal balance determines the pattern of T-cell maturation in the thymus. *Immunol. Cell Biol.* 2011;89(8):844–852.
110. Wang Z, Cohen K, Shao Y, et al. Ephrin receptor, EphB4, regulates ES cell differentiation of primitive mammalian hemangioblasts, blood, cardiomyocytes, and blood vessels. *Blood.* 2004;103(1):100–109.
111. Füller Tim, Korff Thomas, Kilian Adrienne, Dandekar Gudrun, Augustin Hellmut G. Forward EphB4 signaling in endothelial cells controls cellular repulsion and segregation from ephrinB2 positive cells. *J. Cell Sci.* 2013;116:2461–2470.
112. Arthur A, Zannettino A, Panagopoulos R, et al. EphB/ephrin-B interactions mediate human MSC attachment, migration and osteochondral differentiation. *Bone.* 2011;48(3):533–542.
113. Ventrella R, Kaplan N, Getsios S. Asymmetry at cell-cell interfaces direct cell sorting, boundary formation, and tissue morphogenesis. *Exp. Cell Res.* 2017;358(1):58–64.
114. Astin J, Batson J, Kadir S, et al. Competition amongst Eph receptors regulates contact inhibition of locomotion and invasiveness in prostate cancer cells. *Nat. Cell Biol.* 2010;12(12):1194–1204.
115. Kadir S, Astin J, Tahtamouni L. Microtubule remodelling is required for the front–rear polarity switch during contact inhibition of locomotion. *J. Cell Sci.* 2011;124:2642–2653.
116. Carmona-Fontaine C, Matthews HK, Kuriyama S, et al. Contact inhibition of locomotion in vivo controls neural crest directional migration. *Nature.* 2008;456(7224):957–961.
117. Abercrombie M, Heaysman JEM. Observations on the social behaviour of cells in tissue culture. II. “Monolayering” of fibroblasts. *Exp. Cell Res.* 1954;6(2):293–306.
118. Abercrombie M. Contact inhibition and malignancy. *Nature.* 1979;281(5729):259–262.
119. Chen W, Obrink B. Cell-cell contacts mediated by E-cadherin (uvomorulin) restrict invasive behavior of L-cells. *J. Cell Biol.* 1991;114(2):319–327.
120. Takai Y, Miyoshi J, Ikeda W, Ogita H. Nectins and nectin-like molecules: Roles in contact inhibition of cell movement and proliferation. *Nat. Rev. Mol. Cell Biol.* 2008;9(8):603–615.
121. Huttenlocher A, Lakonishok M, Kinder M, et al. Integrin and cadherin synergy regulates contact inhibition of migration and motile activity. *J. Cell Biol.*

- 1998;141(2):515–526.
122. Crouner D, Le Gall M, Gates MA, Giniger E. Notch steers Drosophila ISNb motor axons by regulating the Abl signaling pathway. *Curr. Biol.* 2003;13(11):967–972.
  123. Coulthard MG, Morgan M, Woodruff TM, et al. Eph/ephrin signaling in injury and inflammation. *Am. J. Pathol.* 2012;181(5):1493–1503.
  124. Kwak H, Salvucci O, Weigert R, et al. Sinusoidal ephrin receptor EPHB4 controls hematopoietic progenitor cell mobilization from bone marrow. *J. Clin. Invest.* 2016;126(12):4554–4568.
  125. Okubo T, Yanai N, Obinata M. Stromal cells modulate ephrinB2 expression and transmigration of hematopoietic cells. *Exp. Hematol.* 2006;34(3):330–338.
  126. Tosato G. Ephrin ligands and Eph receptors contribution to hematopoiesis. *Cell. Mol. Life Sci.* 2017;74(18):3377–3394.
  127. Nguyen TM, Arthur A, Panagopoulos R, et al. EphB4 Expressing Stromal Cells Exhibit an Enhanced Capacity for Hematopoietic Stem Cell Maintenance. *Stem Cells.* 2015;33(9):2838–2849.
  128. Anselmo A, Lauranzano E, Soldani C, et al. Identification of a novel agrin-dependent pathway in cell signaling and adhesion within the erythroid niche. *Cell Death Differ.* 2016;23(8):1322–1330.
  129. Neildez-Nguyen TMA, Wajcman H, Marden MC, et al. Human erythroid cells produced ex vivo at large scale differentiate into red blood cells in vivo. *Nat. Biotechnol.* 2002;20(5):467–472.
  130. Migliaccio G, Di Pietro R, Di Giacomo V, et al. In Vitro mass production of human erythroid cells from the blood of normal donors and of thalassemic patients. *Blood Cells, Mol. Dis.* 2002;28(2):169–180.
  131. Baek EJ, Kim H-S, Kim S, et al. In vitro clinical-grade generation of red blood cells from human umbilical cord blood CD34+ cells. *Transfusion.* 2008;
  132. Timmins NE, Athanasas S, Günther M, Buntine P, Nielsen LK. Ultra-high-yield manufacture of red blood cells from hematopoietic stem cells. *Tissue Eng. - Part C Methods.* 2011;
  133. Tirelli V, Ghinassi B, Migliaccio AR, et al. Phenotypic definition of the progenitor cells with erythroid differentiation potential present in human adult blood. *Stem Cells Int.* 2011;2011:1–9.
  134. Boehm D, Murphy WG, Al-Rubeai M. The potential of human peripheral blood derived CD34+ cells for ex vivo red blood cell production. *J. Biotechnol.* 2009;144(2):127–134.
  135. Huang X, Shah S, Wang J, et al. Extensive ex vivo expansion of functional human erythroid precursors established from umbilical cord blood cells by defined factors. *Mol. Ther.* 2014;22(2):451–463.
  136. Lee YT, Kim KS, Byrnes C, et al. A Synthetic Model of Human Beta-Thalassemia Erythropoiesis Using CD34+ Cells from Healthy Adult Donors. *PLoS One.*

- 2013;8(7):e68307.
137. Douay L, Giarratana M-C. Ex vivo generation of human red blood cells: a new advance in stem cell engineering. *Methods Mol. Biol.* 2009;
  138. Giarratana MC, Rouard H, Dumont A, et al. Proof of principle for transfusion of in vitro-generated red blood cells. *Blood.* 2011;
  139. Douay L, Giarratana MC. The cultured red blood cell. A study tool with therapeutic perspectives. *Cell Cycle.* 2005;4(8):999–1000.
  140. Leberbauer C, Boulmé F, Unfried G, et al. Different steroids co-regulate long-term expansion versus terminal differentiation in primary human erythroid progenitors. *Blood.* 2005;105(1):85–94.
  141. van den Akker E, Satchwell TJ, Pellegrin S, Daniels G, Toye AM. The majority of the in vitro erythroid expansion potential resides in CD34 - cells, outweighing the contribution of CD34 + cells and significantly increasing the erythroblast yield from peripheral blood samples. *Haematologica.* 2010;95(9):1594–8.
  142. Miharada K, Hiroyama T, Sudo K, Nagasawa T, Nakamura Y. Efficient enucleation of erythroblasts differentiated in vitro from hematopoietic stem and progenitor cells. *Nat. Biotechnol.* 2006;24(10):1255–1256.
  143. Hiroyama T, Miharada K, Aoki N, et al. Long-lasting in vitro hematopoiesis derived from primate embryonic stem cells. *Exp. Hematol.* 2006;34(6):760–769.
  144. Miharada KI, Hiroyama T, Sudo K, Nagasawa T, Nakamura Y. Refinement of cytokine use in the in vitro expansion of erythroid cells. *Hum. cell Off. J. Hum. Cell Res. Soc.* 2006;19(1):30–37.
  145. Kupzig S, Parsons SF, Curnow E, Anstee DJ, Blair A. Superior survival of ex vivo cultured human reticulocytes following transfusion into mice. *Haematologica.* 2017;102(3):476–483.
  146. Griffiths RE, Kupzig S, Cogan N, et al. Maturing reticulocytes internalize plasma membrane in glycophorin A-containing vesicles that fuse with autophagosomes before exocytosis. *Blood.* 2012;119(26):6296–6306.
  147. Griffiths RE, Kupzig S, Cogan N, et al. Maturing reticulocytes internalize plasma membrane in glycophorin A-containing vesicles that fuse with autophagosomes before exocytosis. *Blood.* 2012;119(26):6296–6306.
  148. van den Akker E, Satchwell TJ, Pellegrin S, et al. Investigating the key membrane protein changes during in vitro erythropoiesis of protein 4.2 (-) cells (mutations Chartres 1 and 2). *Haematologica.* 2010;95(8):1278–1286.
  149. Satchwell TJ, Bell AJ, Hawley BR, et al. Severe Ankyrin-R deficiency results in impaired surface retention and lysosomal degradation of RhAG in human erythroblasts. *Haematologica.* 2016;101(9):1018–1027.
  150. Satchwell TJ, Pellegrin S, Bianchi P, et al. Characteristic phenotypes associated with congenital dyserythropoietic anemia (type II) manifest at different stages of erythropoiesis. *Haematologica.* 2013;98(11):1788–96.

151. Pellegrin S, Haydn-Smith KL, Hampton-O'Neil LA, et al. Transduction with BBF2H7/CREB3L2 upregulates SEC23A protein in erythroblasts and partially corrects the hypo-glycosylation phenotype associated with CD41. *Br. J. Haematol.* 2018;
152. Khoriaty R, Vasievich MP, Jones M, et al. Absence of a Red Blood Cell Phenotype in Mice with Hematopoietic Deficiency of SEC23B. *Mol. Cell. Biol.* 2014;34(19):3721–3734.
153. Punzo F, Bertoli-Avella AM, Scianguetta S, et al. Congenital dyserythropoietic anemia type II: Molecular analysis and expression of the SEC23B Gene. *Orphanet J. Rare Dis.* 2011;6(1):89.
154. Bianchi P, Fermo E, Vercellati C, et al. Congenital Dyserythropoietic Anemia type II (CD41) is caused by mutations in the SEC23B gene. *Hum. Mutat.* 2009;30(9):1292–1298.
155. Menck K, Behme D, Pantke M, et al. Isolation of Human Monocytes by Double Gradient Centrifugation and Their Differentiation to Macrophages in Teflon-coated Cell Culture Bags. *J. Vis. Exp.* 2014;(91):e51554.
156. De Almeida MC, Silva AC, Barral A, Netto MB. A simple method for human peripheral blood monocyte Isolation. *Mem. Inst. Oswaldo Cruz.* 2000;95(2):221–223.
157. Passmore JS, Lukey PT, Ress SR. The human macrophage cell line U937 as an in vitro model for selective evaluation of mycobacterial antigen-specific cytotoxic T-cell function. *Immunology.* 2001;102(2):146–156.
158. Nakamura YN. In Vitro production of transfusable red blood cells. *Vox Sang.* 2009;
159. Dias J, Gumenyuk M, Kang H, et al. Generation of Red Blood Cells from Human Induced Pluripotent Stem Cells. *Stem Cells Dev.* 2011;20(9):1639–1647.
160. Luo Y, Zou P, Zou J, et al. Autophagy regulates ROS-induced cellular senescence via p21 in a p38 MAPK $\alpha$  dependent manner. *Exp. Gerontol.* 2011;46(11):860–867.
161. Kobar L, Yates F, Oudrhiri N, et al. Human induced pluripotent stem cells can reach complete terminal maturation: In vivo and in vitro evidence in the erythropoietic differentiation model. *Haematologica.* 2012;97(12):1795–1803.
162. Chang C-J, Mitra K, Koya M, et al. Production of Embryonic and Fetal-Like Red Blood Cells from Human Induced Pluripotent Stem Cells. *PLoS One.* 2011;6(10):e25761.
163. Hirose SI, Takayama N, Nakamura S, et al. Immortalization of erythroblasts by c-MYC and BCL-XL enables large-scale erythrocyte production from human pluripotent stem cells. *Stem Cell Reports.* 2013;1(6):499–508.
164. Fauzi I, Panoskaltsis N, Mantalaris A. In Vitro Differentiation of Embryonic Stem Cells into Hematopoietic Lineage: Towards Erythroid Progenitor's Production. *Methods Mol. Biol.* 2015;1341:217–234.
165. Lu S-J, Feng Q, Park JS, et al. Biologic properties and enucleation of red blood cells

- from human embryonic stem cells. *Blood*. 2008;112(12):4475–4484.
166. Olsen AL, Stachura DL, Weiss MJ. Designer blood: Creating hematopoietic lineages from embryonic stem cells. *Blood*. 2006;107(4):1265–1275.
  167. Moir-Meyer G, Cheong PL, Olijnik A-A, et al. Robust CRISPR/Cas9 Genome Editing of the HUDEP-2 Erythroid Precursor Line Using Plasmids and Single-Stranded Oligonucleotide Donors. *Methods Protoc*. 2018;1(3):28.
  168. Lessard S, Gatof ES, Beaudoin M, et al. An erythroid-specific ATP2B4 enhancer mediates red blood cell hydration and malaria susceptibility. *J. Clin. Invest*. 2017;127(8):3065–3074.
  169. Canver MC, Smith EC, Sher F, et al. BCL11A enhancer dissection by Cas9-mediated in situ saturating mutagenesis. *Nature*. 2015;527(7577):192–197.
  170. Ghosh A, Garee G, Sweeny EA, Nakamura Y, Stuehr DJ. Hsp90 chaperones hemoglobin maturation in erythroid and nonerythroid cells. *Proc. Natl. Acad. Sci*. 2018;115(6):201717993.
  171. Canver MC, Smith EC, Sher F, et al. BCL11A enhancer dissection by Cas9-mediated in situ saturating mutagenesis. *Nature*. 2015;527(7577):192–197.
  172. Ghosh A, Garee G, Sweeny EA, Nakamura Y, Stuehr DJ. Hsp90 chaperones hemoglobin maturation in erythroid and nonerythroid cells. *Proc. Natl. Acad. Sci*. 2018;115(6):201717993.
  173. Trakarnsanga K, Griffiths RE, Wilson MC, et al. An immortalized adult human erythroid line facilitates sustainable and scalable generation of functional red cells. *Nat. Commun*. 2017;8:14750.
  174. Deezagi A, Abedi-Tashi M. Studying the enucleation process, DNA breakdown and telomerase activity of the K562 cell lines during erythroid differentiation in vitro. *Vitr. Cell. Dev. Biol. - Anim*. 2013;49(2):122–133.
  175. Kurita R, Suda N, Sudo K, et al. Establishment of Immortalized Human Erythroid Progenitor Cell Lines Able to Produce Enucleated Red Blood Cells. *PLoS One*. 2013;8(3):e59890.
  176. Wilson MC, Trakarnsanga K, Heesom KJ, et al. Comparison of the Proteome of Adult and Cord Erythroid Cells, and Changes in the Proteome Following Reticulocyte Maturation. *Mol. Cell. Proteomics*. 2016;15(6):1938–1946.
  177. Moir-Meyer G, Cheong PL, Olijnik A-A, et al. Robust CRISPR/Cas9 Genome Editing of the HUDEP-2 Erythroid Precursor Line Using Plasmids and Single-Stranded Oligonucleotide Donors. *Methods Protoc*. 2018;1(3):28.
  178. Lessard S, Gatof ES, Beaudoin M, et al. An erythroid-specific ATP2B4 enhancer mediates red blood cell hydration and malaria susceptibility. *J. Clin. Invest*. 2017;127(8):3065–3074.
  179. Hawksworth J, Satchwell TJ, Meinders M, et al. Enhancement of red blood cell transfusion compatibility using CRISPR-mediated erythroblast gene editing. *EMBO Mol. Med*. 2018;10(6):e8454.

180. Berman I. The ultrastructure of erythroblastic islands and reticular cells in mouse bone marrow. *J. Ultrastruct. Res.* 1967;17(3):291–313.
181. Iavarone A, King ER, Dai XM, et al. Retinoblastoma promotes definitive erythropoiesis by repressing Id2 in fetal liver macrophages. *Nature.* 2004;432(7020):1040–1045.
182. Tishevskaya N V., Bolotov AA, Lebedeva YE. Dynamics of Erythropoiesis in Erythroblastic Islands in the Bone Marrow in Experimental Benzene-Induced Anemia. *Bull. Exp. Biol. Med.* 2016;161(3):384–387.
183. Sui Z, Nowak RB, Bacconi A, et al. Tropomodulin3-null mice are embryonic lethal with anemia due to impaired erythroid terminal differentiation in the fetal liver. *Blood.* 2014;123(5):758–767.
184. Kusakabe M, Hasegawa K, Hamada M, et al. c-Maf plays a crucial role for the definitive erythropoiesis that accompanies erythroblastic island formation in the fetal liver. *Blood.* 2011;118(5):1374–1385.
185. Zakharov YM, Prenant M. [Technique for isolation and culture of erythroblastic islands and separation of their central macrophage]. *Nouv. Rev. Fr. Hematol.* 1982;24(6):363–7.
186. Yeo JH, Xie V, Campbell I, Fraser S. Interferon regulatory factor-8 (IRF-8) regulates erythroblastic island morphology and function. *Exp. Hematol.* 2015;43(9):S103.
187. Belay E, Hayes BJ, Blau CA, Torok-Storb B. Human cord blood and bone marrow CD34+ cells generate macrophages that support erythroid islands. *PLoS One.* 2017;12(1):e0171096.
188. Agbani EO, Van Den Bosch MTJ, Brown E, et al. Coordinated membrane ballooning and procoagulant spreading in human platelets. *Circulation.* 2015;132(15):1414–1424.
189. Williamson RC, Brown ACN, Mawby WJ, Tøye AM. Human kidney anion exchanger 1 localisation in MDCK cells is controlled by the phosphorylation status of two critical tyrosines. *J. Cell Sci.* 2008;121(Pt 20):3422–32.
190. Muto M. A scanning and transmission electron microscopic study on rat bone marrow sinuses and transmural migration of blood cells. *Arch. Histol. Jpn.* 1976;39(1):51–66.
191. De Bruyn PP, Michelson S, Thomas TB. The migration of blood cells of the bone marrow through the sinusoidal wall. *J. Morphol.* 1971;133(4):417–37.
192. Allen TDD, DEXTER TMM. Ultrastructural aspects of erythropoietic differentiation in long-term bone marrow culture. *Differentiation.* 1982;21(2):86–94.
193. Chamberlain JK, Weiss L, Weed RI. Bone marrow sinus cell packing: a determinant of cell release. *Blood.* 1975;46(1):91–102.
194. Kigerl KA, Gensel JC, Ankeny DP, et al. Identification of Two Distinct Macrophage Subsets with Divergent Effects Causing either Neurotoxicity or Regeneration in the Injured Mouse Spinal Cord. *J. Neurosci.* 2009;29(43):13435–13444.



195. Pilling D, Fan T, Huang D, Kaul B, Gomer RH. Identification of markers that distinguish monocyte-derived fibrocytes from monocytes, macrophages, and fibroblasts. *PLoS One*. 2009;4(10):e7475.
196. Madonna R, Massaro M, De Caterina R. Insulin potentiates cytokine-induced VCAM-1 expression in human endothelial cells. *Biochim. Biophys. Acta*. 2008;1782(9):511–6.
197. Zheng Y, Yang W, Aldape K, He J, Lu Z. Epidermal growth factor (EGF)-enhanced vascular cell adhesion molecule-1 (VCAM-1) expression promotes macrophage and glioblastoma cell interaction and tumor cell invasion. *J. Biol. Chem*. 2013;288(44):31488–31495.
198. Kim I, Moon S-O, Hoon Kim S, et al. VEGF Stimulates Expression of ICAM-1, VCAM-1 and E-Selectin through Nuclear Factor- $\kappa$  B Activation in Endothelial Cells as Manuscript M009705200. 2000;
199. Sheviakov, S.A.; Zakharov IM, Sheviakov SA, Zakharov IM. Effect of supernatant of erythroblastic island bone marrow cultures on erythropoiesis in vitro. 2012.
200. Dutta P, Hoyer FF, Grigoryeva LS, et al. Macrophages retain hematopoietic stem cells in the spleen via VCAM-1. *J. Exp. Med*. 2015;212(4):497–512.
201. Ulyanova T, Phelps SR, Papayannopoulou T. The macrophage contribution to stress erythropoiesis: When less is enough. *Blood*. 2016;128(13):1756–1765.
202. Satchwell TJ, Hawley BR, Bell AJ, Leticia Ribeiro M, Toye AM. The cytoskeletal binding domain of band 3 is required for multiprotein complex formation and retention during erythropoiesis. *Haematologica*. 2015;100(1):133–142.
203. Miller MR, Blystone SD. Reliable and inexpensive expression of large, tagged, exogenous proteins in murine bone marrow-derived macrophages using a second generation lentiviral system. *J. Biol. Methods*. 2015;2(3):23.
204. Kaplan G, Unkeless JC, Cohn ZA. Insertion and turnover of macrophage plasma membrane proteins. *Proc. Natl. Acad. Sci. U. S. A*. 1979;76(8):3824–8.
205. Leitinger B, McDowall A, Stanley P, Hogg N. The regulation of integrin function by  $\text{Ca}^{2+}$ . *Biochim. Biophys. Acta - Mol. Cell Res*. 2000;1498(2–3):91–98.
206. Brackenbury R, Rutishauser U, Edelman GM. Distinct calcium-independent and calcium-dependent adhesion systems of chicken embryo cells. *Proc. Natl. Acad. Sci*. 1981;78(1):387–391.
207. Armeanu S, Biihring H-J, Reuss-Borst M, Müller CA, Klein G. E-Cadherin Is Functionally Involved in the Maturation of the Erythroid Lineage.
208. Marschall ALJ, Single FN, Schlarmann K, et al. Functional knock down of VCAM1 in mice mediated by endoplasmatic reticulum retained intrabodies. *MAbs*. 2014;6(6):1394–401.
209. Sakamoto H, Zhang X-Q, Suenobu S, et al. Cell adhesion to ephrinb2 is induced by EphB4 independently of its kinase activity. *Biochem. Biophys. Res. Commun*. 2004;321(3):681–7.

210. Stein E, Lane AA, Cerretti DP, et al. Eph receptors discriminate specific ligand oligomers to determine alternative signaling complexes, attachment, and assembly responses. *Genes Dev.* 1998;12(5):667–678.
211. Peled A, Kollet O, Ponomaryov T, et al. The chemokine SDF-1 activates the integrins LFA-1, VLA-4, and VLA-5 on immature human CD34(+) cells: role in transendothelial/stromal migration and engraftment of NOD/SCID mice. *Blood.* 2000;95(11):3289–96.
212. Roseblatt M, Vuillet-Gaugler MH, Leroy C, Coulombel L. Coexpression of two fibronectin receptors, VLA-4 and VLA-5, by immature human erythroblastic precursor cells. *J. Clin. Invest.* 1991;87(1):6–11.
213. Thul PJ, Åkesson L, Wiking M, et al. A subcellular map of the human proteome. *Science (80-. ).* 2017;356(6340):eaal3321.
214. Human protein atlas.
215. Kampen KR, Scherpen FJG, Garcia-Manero G, et al. EphB1 Suppression in Acute Myelogenous Leukemia: Regulating the DNA Damage Control System. *Mol. Cancer Res.* 2015;13(6):982–992.
216. Burton NM, Bruce LJ. Modelling the structure of the red cell membraneThis paper is one of a selection of papers published in a Special Issue entitled CSBMCB 53rd Annual Meeting — Membrane Proteins in Health and Disease, and has undergone the Journal's usual peer review proces. *Biochem. Cell Biol.* 2011;89(2):200–215.
217. Rabilloud T. Membrane proteins and proteomics: Love is possible, but so difficult. *Electrophoresis.* 2009;30(SUPPL. 1):S174–S180.
218. Gautier EF, Ducamp S, Leduc M, et al. Comprehensive Proteomic Analysis of Human Erythropoiesis. *Cell Rep.* 2016;16(5):1470–1484.
219. Chu TTT, Sinha A, Malleret B, et al. Quantitative mass spectrometry of human reticulocytes reveal proteome-wide modifications during maturation. *Br. J. Haematol.* 2018;180(1):118–133.
220. Moura PL, Hawley BR, Mankelov TJ, et al. Non-muscle Myosin II drives vesicle loss during human reticulocyte maturation. *Haematologica.* 2018;haematol.2018.199083.
221. Pasquale EB. The Eph family of receptors. *Curr. Opin. Cell Biol.* 1997;9(5):608–615.
222. Zhou R. The Eph Family Receptors and Ligands. *Pharmacol. Ther.* 1998;77(3):151–181.
223. Eshghi S, Vogelezang MG, Hynes RO, Griffith LG, Lodish HF. Alpha4beta1 integrin and erythropoietin mediate temporally distinct steps in erythropoiesis: integrins in red cell development. *J. Cell Biol.* 2007;177(5):871–80.
224. Koolpe M, Burgess R, Dail M, Pasquale EB. EphB receptor-binding peptides identified by phage display enable design of an antagonist with ephrin-like

- affinity. *J. Biol. Chem.* 2005;280(17):17301–17311.
225. Wang S, Noberini R, Stebbins JL, et al. Targeted Delivery of Paclitaxel to EphA2-Expressing Cancer Cells. *Clin Cancer Res.* 1–10.
  226. Truitt L, Freywald T, DeCoteau J, Sharfe N, Freywald A. The EphB6 receptor cooperates with c-Cbl to regulate the behavior of breast cancer cells. *Cancer Res.* 2010;70(3):1141–1153.
  227. Janes PW, Griesshaber B, Atapattu L, et al. Eph receptor function is modulated by heterooligomerization of A and B type Eph receptors. *J. Cell Biol.* 2011;195(6):1033–1045.
  228. Matsuoka H, Obama H, Kelly ML, Matsui T, Nakamoto M. Biphasic functions of the kinase-defective Ephb6 receptor in cell adhesion and migration. *J. Biol. Chem.* 2005;280(32):29355–29363.
  229. Desai BN, Leitinger N. Purinergic and calcium signaling in macrophage function and plasticity. *Front. Immunol.* 2014;5(NOV):580.
  230. Leung K. 111In-Labeled-TNYLFSPNGPIARAW (TNYL-RAW)-polyethylene glycol-coated core-cross-linked polymeric micelle-Cy7. National Center for Biotechnology Information (US); 2004.
  231. Noberini R, Mitra S, Salvucci O, et al. PEGylation potentiates the effectiveness of an antagonistic peptide that targets the EphB4 receptor with nanomolar affinity. *PLoS One.* 2011;6(12):e28611.
  232. Beningo K a, Wang Y. Fc-receptor-mediated phagocytosis is regulated by mechanical properties of the target. *J. Cell Sci.* 2002;115(1):849–856.
  233. Solanas G, Cortina C, Sevillano M, Batlle E. Cleavage of E-cadherin by ADAM10 mediates epithelial cell sorting downstream of EphB signalling. *Nat. Cell Biol.* 2011;13(9):1100–1109.
  234. Lisabeth EM, Falivelli G, Pasquale EB. Eph receptor signaling and ephrins. *Cold Spring Harb. Perspect. Biol.* 2013;5(9):.
  235. Webb TE, Simon J, Krishek BJ, et al. Cloning and functional expression of a brain G-protein-coupled ATP receptor. *FEBS Lett.* 1993;324(2):219–225.
  236. Valera S, Hussy N, Evans RJ, et al. A new class of ligand-gated ion channel defined by P2X receptor for extracellular ATP. *Nature.* 1994;371(6497):516–519.
  237. Chu H, McKenna MM, Krump NA, et al. Reversible binding of hemoglobin to band 3 constitutes the molecular switch that mediates O<sub>2</sub> regulation of erythrocyte properties. *Blood.* 2016;128(23):2708–2716.
  238. Gokhin DS, Fowler VM. Feisty filaments: actin dynamics in the red blood cell membrane skeleton. *Curr Opin Hematol.* 2016;23(3):206–214.
  239. Lai KO, Chen Y, Po HM, et al. Identification of the Jak/Stat Proteins as Novel Downstream Targets of EphA4 Signaling in Muscle: Implications in the regulation of acetylcholinesterase expression. *J. Biol. Chem.* 2004;279(14):13383–13392.

240. Bourgin C, Murai KK, Richter M, Pasquale EB. The EphA4 receptor regulates dendritic spine remodeling by affecting beta1-integrin signaling pathways. *J. Cell Biol.* 2007;178(7):1295–307.
241. Warny M, Aboudola S, Robson SC, et al. P2Y6 Nucleotide Receptor Mediates Monocyte Interleukin-8 Production in Response to UDP or Lipopolysaccharide. *J. Biol. Chem.* 2001;276(28):26051–26056.
242. Suurväli J, Boudinot P, Kanellopoulos J, Rüütel Boudinot S. P2X4: A fast and sensitive purinergic receptor. *Biomed. J.* 2017;40(5):245–256.
243. Sikora J, Orlov SN, Furuya K, Grygorczyk R. Hemolysis is a primary ATP-release mechanism in human erythrocytes. *Blood.* 2014;124(13):2150–2157.
244. Melhorn MI, Brodsky AS, Estanislau J, et al. CR1-mediated ATP release by Human red blood cells promotes CR1 clustering and modulates the immune transfer process. *J. Biol. Chem.* 2013;288(43):31139–31153.
245. Zhao E, Xu H, Wang L, et al. Bone marrow and the control of immunity. *Cell. Mol. Immunol.* 2012;9(1):11–19.
246. Jacobsen RN, Forristal CE, Raggatt LJ, et al. Mobilization with granulocyte colony-stimulating factor blocks medullar erythropoiesis by depleting F4/80+VCAM1+CD169+ER-HR3+Ly6G+erythroid island macrophages in the mouse. *Exp. Hematol.* 2014;42(7):547–561.
247. Chamberlain JK, Lichtman MA. Marrow cell egress: specificity of the site of penetration into the sinus. *Blood.* 1978;52(5):959–68.
248. Mel HC, Prenant M, Mohandas N. Reticulocyte Motility and Form: Studies on Maturation and Classification.
249. Waugh RE, Sassi M. An in vitro model of erythroid egress in bone marrow. *Blood.* 1986;68(1):250–7.
250. Dabrowski Z, Szyguła Z, Misztal H. Do changes in bone marrow pressure contribute to the egress of cell from bone marrow? *Acta Physiol. Pol.* 32(6):729–36.
251. Swerlick RA, Eckman JR, Kumar A, Jeitler M, Wick TM. Alpha 4 beta 1-integrin expression on sickle reticulocytes: vascular cell adhesion molecule-1-dependent binding to endothelium. *Blood.* 1993;82(6):1891–9.
252. Barabino GA, McIntire L V, Eskin SG, Sears DA, Udden M. Endothelial cell interactions with sickle cell, sickle trait, mechanically injured, and normal erythrocytes under controlled flow. *Blood.* 1987;70(1):152–7.
253. Barabino GA, McIntire L V, Eskin SG, Sears DA, Udden M. Endothelial cell interactions with sickle cell, sickle trait, mechanically injured, and normal erythrocytes under controlled flow. *Blood.* 1987;70(1):152–7.
254. Agbani EO, van den Bosch MTJ, Brown E, et al. Coordinated Membrane Ballooning and Procoagulant Spreading in Human Platelets Clinical Perspective. *Circulation.* 2015;132(15):1414–1424.

255. Kido T, Morimoto Y, Yatera K, et al. The utility of electron microscopy in detecting asbestos fibers and particles in BALF in diffuse lung diseases. *BMC Pulm. Med.* 2017;17(1):71.
256. Using viscous suspension to measure cell motility in solution; swimming vs migration of cells. 2005;
257. Grabovsky V, Feigelson S, Chen C, et al. Subsecond induction of alpha4 integrin clustering by immobilized chemokines stimulates leukocyte tethering and rolling on endothelial vascular cell adhesion molecule 1 under flow conditions. *J. Exp. Med.* 2000;192(4):495–506.
258. Mankelow TJ, Griffiths RE, Trompeter S, et al. Autophagic vesicles on mature human reticulocytes explain phosphatidylserine-positive red cells in sickle cell disease. *Blood.* 2015;126(15):1831–1834.
259. Gu S, Fu WY, Fu AKY, et al. Identification of new EphA4 inhibitors by virtual screening of FDA-approved drugs. *Sci. Rep.* 2018;8(1):7377.
260. Noberini R, Koolpe M, Peddibhotla S, et al. Small molecules can selectively inhibit ephrin binding to the EphA4 and EphA2 receptors. *J. Biol. Chem.* 2008;283(43):29461–29472.
261. Sathyanarayana P, Menon MP, Bogacheva O, et al. Erythropoietin modulation of podocalyxin and a proposed erythroblast niche. *Blood.* 2007;110(2):509–18.
262. Fernández D, Horrillo A, Alquezar C, et al. Control of cell adhesion and migration by podocalyxin. Implication of Rac1 and Cdc42. *Biochem. Biophys. Res. Commun.* 2013;432(2):302–307.
263. Javan GT, Can I, Yeboah F, Lee Y, Soni S. Novel interactions between erythroblast macrophage protein and cell migration. *Blood Cells, Mol. Dis.* 2016;60:24–27.
264. Bauer A, Tronche F, Wessely O, et al. The glucocorticoid receptor is required for stress erythropoiesis. *Genes Dev.* 1999;13(22):2996–3002.
265. Jacobsen RN, Nowlan B, Brunck ME, et al. Fms-like tyrosine kinase 3 (Flt3) ligand depletes erythroid island macrophages and blocks medullar erythropoiesis in the mouse. *Exp. Hematol.* 2015;
266. Sadahira Y, Mori M, Kimoto T. Isolation and short-term culture of mouse splenic erythroblastic islands. *Cell Struct. Funct.* 1990;15(1):59–65.
267. Pradeep S, Huang J, Mora EM, et al. Erythropoietin Stimulates Tumor Growth via EphB4. *Cancer Cell.* 2015;28(5):610–622.
268. Torisawa Y, Mammoto T, Jiang E, et al. Modeling Hematopoiesis and Responses to Radiation Countermeasures in a Bone Marrow-on-a-Chip. *Tissue Eng. Part C Methods.* 2016;22(5):509–515.
269. Torisawa YS, Spina CS, Mammoto T, et al. Bone marrow-on-a-chip replicates hematopoietic niche physiology in vitro. *Nat. Methods.* 2014;11(6):663–669.
270. Sieber S, Wirth L, Cavak N, et al. Bone marrow-on-a-chip: Long-term culture of human haematopoietic stem cells in a three-dimensional microfluidic

- environment. *J. Tissue Eng. Regen. Med.* 2018;12(2):479–489.
271. Winkler IG, Sims NA, Pettit AR, et al. Bone marrow macrophages maintain hematopoietic stem cell (HSC) niches and their depletion mobilizes HSCs. *Blood.* 2010;116(23):4815–4828.
  272. Fraser ST, Midwinter RG, Coupland LA, et al. Heme oxygenase-1 deficiency alters erythroblastic island formation, steady-state erythropoiesis and red blood cell lifespan in mice. *Haematologica.* 2015;100(5):601–10.
  273. Kulkeaw K, Sugiyama D. Zebrafish erythropoiesis and the utility of fish as models of anemia. *Stem Cell Res. Ther.* 2012;3(6):55.
  274. Pishesha N, Thiru P, Shi J, et al. Transcriptional divergence and conservation of human and mouse erythropoiesis. *Proc. Natl. Acad. Sci.* 2014;111(11):4103–4108.
  275. Sankaran VG, Xu J, Ragoczy T, et al. Developmental and species-divergent globin switching are driven by BCL11A. *Nature.* 2009;460(7259):1093–1097.
  276. Braga P, Ricci D. Atomic Force Microscopy in Biomedical Research. 2011;736:508.
  277. Zeng G, Müller T, Meyer RL. Single-cell force spectroscopy of bacteria enabled by naturally derived proteins. *Langmuir.* 2014;30(14):4019–4025.
  278. Thie M, Röspel R, Dettmann W, et al. Interactions between trophoblast and uterine epithelium: Monitoring of adhesive forces. *Hum. Reprod.* 1998;13(11):3211–3219.
  279. Foster K, Lassailly F, Anjos-Afonso F, et al. Different motile behaviors of human hematopoietic stem versus progenitor cells at the osteoblastic niche. *Stem Cell Reports.* 2015;5(5):690–701.
  280. Prabhakarapandian B, Shen M-C, Nichols JB, et al. Synthetic tumor networks for screening drug delivery systems. *J. Control. Release.* 2015;201:49–55.
  281. Torisawa Y, Mammoto T, Jiang E, et al. Modeling Hematopoiesis and Responses to Radiation Countermeasures in a Bone Marrow-on-a-Chip. *Tissue Eng. Part C Methods.* 2016;22(5):509–515.
  282. Torisawa Y, Spina CS, Mammoto T, et al. Bone marrow-on-a-chip replicates hematopoietic niche physiology in vitro. *Nat. Methods.* 2014;11(6):663–669.
  283. Sieber S, Wirth L, Cavak N, et al. Bone marrow-on-a-chip: Long-term culture of human haematopoietic stem cells in a three-dimensional microfluidic environment. *J. Tissue Eng. Regen. Med.* 2018;12(2):479–489.

## 9 Chapter 9 – Appendices

Figure 9-1 Code for Tlescan analysis

```
1 var Title = getTitle();
2
3 run("Split Channels");
4 //run("Brightness/Contrast...");
5 setMinAndMax(4, 35);
6 selectWindow("C1-" + Title);
7 run("Duplicate...", " ");
8 run("16-bit");
9 run("Variance...", "radius=5");
10
11 //run("Subtract Background...", "rolling=3000 light slice");
12 //run("Subtract Background...", "rolling=50 light slice");
13 run("Threshold...");
14 waitForUser("Choose your threshold");
15
16 //Dialog.create("Threshold input");
17 //Dialog.addNumber("Lower", 0);
18 //Dialog.addNumber("Upper", 255);
19 //Dialog.show();
20 //var Lower = Dialog.getNumber();
21 //var upper = Dialog.getNumber();
22 //setThreshold(Lower, upper);
23 setOption("BlackBackground", false);
24 run("Convert to Mask");
25 run("Analyze Particles...", "size=4000-Infinity show=Outlines exclude clear include add");
26
27 ////COULD CLOSE THE BG-SUB WINDOW HERE?
28 close();
29 close();
30 ////
31
32 selectWindow("C1-" + Title);
33 name = getTitle();
34 dotIndex = indexOf(name, ".");
35 title = substring(name, 0, dotIndex);
36
37 var RoiNumber = roiManager("count");
38
39 for (i=RoiNumber; i>0; i--){
40     selectWindow("C1-" + Title);
41     roiManager("Select", i-1);
42     run("Select Bounding Box");
43     run("Scale... ", "x=3.50 y=3.50 centered");
44     run("Duplicate...", " ");
45
46     selectWindow("C1-" + Title);
47     name = getTitle();
48     dotIndex = indexOf(name, ".");
49     title = substring(name, 0, dotIndex);
50     run("Select None");
51
52     //Is this an island?
53     selectWindow("ROI");
54     // var island = newArray("Yes", "No");
55     // Dialog.create("Result");
56     // Dialog.addRadioButtonGroup("Is this a cell cluster?", island, 2, 1, "No");
57     // Dialog.show();
58     //var Opinion = Dialog.getRadioButton();
59     Opinion = getBoolean("Is this a cell cluster?");
60
61     //if not happy with results, redo threshold
62     if (Opinion == 0){
63         //save the no
64         setResult("Green?", i-1, "N/A");
65         setResult("Cell Number?", i-1, "N/A");
66         updateResults();
67         var ROIstackStatus = isOpen("ROIstack1");
68         close("ROI");
69         roiManager("delete");
70
71     } else {
72         selectWindow("C2-" + Title);
73         //run("Restore Selection");
74         roiManager("Select", i-1);
75         run("Select Bounding Box");
76         run("Scale... ", "x=3.50 y=3.50 centered");
77         run("Duplicate...", " ");
78         rename("ROIgreen");
79         //var island = newArray("Yes", "No");
80         //Dialog.create("Green");
81         //Dialog.addRadioButtonGroup("Is the center cell green", island, 2, 1, "No");
82         //Dialog.show();
83         //var GreenOpinion = Dialog.getRadioButton();
84         GreenOpinion = getBoolean("Is the center cell green?");
85
86         //save result somewhere
87         selectWindow("ROI");
88         Dialog.create("EInumber");
89         Dialog.addNumber("How many cells around the center cell?", 0);
90         Dialog.show();
91         var EInumber = Dialog.getNumber();
92         setResult("Green?", i-1, GreenOpinion);
93         setResult("Cell Number?", i-1, EInumber);
94         updateResults();
95         var ROIstackStatus = isOpen("ROIstack1");
96         close("ROI");
97         close("ROIgreen");
98     }
99 };
100 };
101
102 close("");
103
104 };
105
```

Figure 9-2 Code for Fibronectin analysis

```

1 macro "Sectioning count"{
2 var Title = getTitle();
3 getDimensions(w, h, nChannels, s, f);
4 var miniRed = NaN;
5 var miniGreen = NaN;
6 var miniBlue = NaN;
7 var maxiRed = NaN;
8 var maxiGreen = NaN;
9 var maxiBlue = NaN;
10 var lowerRed = NaN;
11 var lowerGreen = NaN;
12 var lowerBlue = NaN;
13 var upperRed = NaN;
14 var upperGreen = NaN;
15 var upperBlue = NaN;
16
17 //First image, what kind of image is it?
18 var Program = newArray("Test image", "New Image");
19 Dialog.create("Test or new image?");
20 Dialog.addRadioButtonGroup("What kind of image is this?", Program, 2, 1, "Test image");
21 Dialog.show();
22 var ProgramChoice = Dialog.getRadioButton();
23
24 //TESTING PHASE OF PROGRAM
25 while (ProgramChoice == "Test image") {
26     run("Z Project...", "projection=[Max Intensity]");
27     waitForUser("Create your selection");
28     setBackgroundColor(0, 0, 0);
29     run("Clear", "stack");
30     run("Split Channels");
31     var items = newArray();
32     for (i=1; i<=nImages; i++) {
33         selectImage(i);
34         items = Array.concat(items,getTitle());
35     }
36     //choose channel
37     Dialog.create("Choose image to work on");
38     Dialog.addRadioButtonGroup("Images open", items, nImages, 1, Title);
39     Dialog.show();
40     var ImageChoice = Dialog.getRadioButton();
41     selectWindow(ImageChoice);
42     //set brightness/contrast
43     run("Brightness/Contrast...");
44     waitForUser("Adjust the Brightness and Contrast");
45     var whichChannel = newArray("Red", "Green", "Blue");
46     Dialog.create("Which channel is it?");
47     Dialog.addRadioButtonGroup("Which channel is it?", whichChannel, 3, 1, "Red");
48     Dialog.show();
49     var channelChoice = Dialog.getRadioButton();
50     //get the min and max for all the channels and save them into new variables
51     getMinAndMax(min, max);
52     if (channelChoice == "Red") {
53         var miniRed = min;
54         var maxiRed = max;
55     }
56     else if (channelChoice == "Green") {
57         var miniGreen = min;
58         var maxiGreen = max;
59     }
60     else if (channelChoice == "Blue") {
61         var miniBlue = min;
62         var maxiBlue = max;
63     }
64     run("RGB Color");
65     run("Color Threshold...");
66     waitForUser("Choose your color threshold");
67     run("Analyze Particles...", "size=8.00-Infinity show=Outlines clear summarize");
68 //FIRST - See if want to redo color threshold
69 var happiness = newArray("Yes", "No");
70 Dialog.create("Result");
71 Dialog.addRadioButtonGroup("Are you happy with this result?", happiness, 2, 1, "Yes");
72 Dialog.show();
73 var Opinion = Dialog.getRadioButton();
74 //if not happy with results, redo threshold
75 while (Opinion == "No"){
76     selectWindow (Title);
77     close("\Others");
78     //close color threshold windows and start again
79     run("Z Project...", "projection=[Max Intensity]");
80     run("Restore Selection");
81     setBackgroundColor(0, 0, 0);
82     run("Clear", "stack");
83     run("Split Channels");
84     var items = newArray();
85     for (i=1; i<=nImages; i++) {
86         selectImage(i);
87         items = Array.concat(items,getTitle());
88     }
89     Dialog.create("Choose image to work on");
90     Dialog.addRadioButtonGroup("Images open", items, nImages, 1, Title);
91     Dialog.show();

```



```

92     var ImageChoice = Dialog.getRadioButton();
93     selectWindow(ImageChoice);
94     var whichChannel = newArray("Red", "Green", "Blue");
95     Dialog.create("Which channel is it?");
96     Dialog.addRadioButtonGroup("Which channel is it?", whichChannel, 3, 1, "Red");
97     Dialog.show();
98     var channelChoice = Dialog.getRadioButton();
99     //set the brightness/contrast already chosen previously
100    if (channelChoice == "Red") {
101        setMinAndMax(miniRed, maxiRed);
102    }
103    else if (channelChoice == "Green") {
104        setMinAndMax(miniGreen, maxiGreen);
105    }
106    else if (channelChoice == "Blue") {
107        setMinAndMax(miniBlue, maxiBlue);
108    }
109    run("RGB Color");
110    run("Color Threshold...");
111    waitForUser("Choose your color threshold");
112    run("Analyze Particles...", "size=8.00-Infinity show=Outlines clear summarize");
113    var happiness = newArray("Yes", "No");
114    Dialog.create("Result");
115    Dialog.addRadioButtonGroup("Are you happy with this result?", happiness, 2, 1, "Yes");
116    Dialog.show();
117    var Opinion = Dialog.getRadioButton();
118    }
119    //FIRST - if happy with the results, get the color threshold info for this channel and save it into a new variable
120    //getThreshold(lower, upper);
121    Dialog.create("Threshold input");
122    Dialog.addNumber("Lower", 0);
123    Dialog.addNumber("Upper", 255);
124    Dialog.show();
125    var lower = Dialog.getNumber();
126    var upper = Dialog.getNumber();
127    if (channelChoice == "Red") {
128        var lowerRed = lower;
129        var upperRed = upper;
130    }
131    else if (channelChoice == "Green") {
132        var lowerGreen = lower;
133        var upperGreen = upper;
134    }
135    else if (channelChoice == "Blue") {
136        var lowerBlue = lower;
137        var upperBlue = upper;
138    }
139    //move on to next channel - ask if need other channel
140    Dialog.create("Channel choice");
141    Dialog.addRadioButtonGroup("Move on to next image?", happiness, 2, 1, "Yes");
142    Dialog.show();
143    var channelChoice = Dialog.getRadioButton();
144    while (channelChoice == "No") {
145        //start again and choose new channel
146        selectWindow (Title);
147        close("\\Others");
148        //close color threshold windows and start again
149        run("Z Project...", "projection=[Max Intensity]");
150        run("Restore Selection");
151        setBackgroundColor(0, 0, 0);
152        run("Clear", "stack");
153        run("Split Channels");
154        var items = newArray();
155        for (i=1; i<=nImages; i++) {
156            selectImage(i);
157            items = Array.concat(items,getTitle());
158        }
159        Dialog.create("Choose image to work on");
160        Dialog.addRadioButtonGroup("Images open", items, nImages, 1, Title);
161        Dialog.show();
162        var ImageChoice = Dialog.getRadioButton();
163        selectWindow(ImageChoice);
164        run("Brightness/Contrast...");
165        waitForUser("Adjust the Brightness and Contrast");
166        var whichChannel = newArray("Red", "Green", "Blue");
167        Dialog.create("Which channel is it?");
168        Dialog.addRadioButtonGroup("Which channel is it?", whichChannel, 3, 1, "Red");
169        Dialog.show();
170        var channelChoice = Dialog.getRadioButton();
171        getMinAndMax(min, max);
172        if (channelChoice == "Red") {
173            var miniRed = min;
174            var maxiRed = max;
175        }
176        else if (channelChoice == "Green") {
177            var miniGreen = min;
178            var maxiGreen = max;
179        }
180        else if (channelChoice == "Blue") {
181            var miniBlue = min;

```

```

182     var maxiBlue = max;
183 }
184 run("RGB Color");
185 run("Color Threshold...");
186 waitForUser("Choose your color threshold");
187 run("Analyze Particles...", "size=8.00-Infinity show=Outlines clear summarize");
188 var happiness = newArray("Yes", "No");
189 Dialog.create("Result");
190 Dialog.addRadioButtonGroup("Are you happy with this result?", happiness, 2, 1, "Yes");
191 Dialog.show();
192 var Opinion = Dialog.getRadioButton();
193 //while not happy with results in other channels
194 while (Opinion == "No"){
195     selectWindow (Title);
196     close("\Others");
197     //close color threshold windows and start again
198     run("Z Project...", "projection=[Max Intensity]");
199     run("Restore Selection");
200     setBackgroundColor(0, 0, 0);
201     run("Clear", "stack");
202     run("Split Channels");
203     var items = newArray();
204     for (i=1; i<=nImages; i++) {
205         selectImage(i);
206         items = Array.concat(items,getTitle());
207     }
208     Dialog.create("Choose image to work on");
209     Dialog.addRadioButtonGroup("Images open", items, nImages, 1, Title);
210     Dialog.show();
211     var ImageChoice = Dialog.getRadioButton();
212     selectWindow(ImageChoice);
213     var whichChannel = newArray("Red", "Green", "Blue");
214     Dialog.create("Which channel is it?");
215     Dialog.addRadioButtonGroup("Which channel is it?", whichChannel, 3, 1, "Red");
216     Dialog.show();
217     var channelChoice = Dialog.getRadioButton();
218     //set the brightness/contrast already chosen previously
219     if (channelChoice == "Red") {
220         setMinAndMax(miniRed, maxiRed);
221     }
222     else if (channelChoice == "Green") {
223         setMinAndMax(miniGreen, maxiGreen);
224     }
225     else if (channelChoice == "Blue") {}
226         setMinAndMax(miniBlue, maxiBlue);
227     }
228     run("RGB Color");
229     run("Color Threshold...");
230     waitForUser("Choose your color threshold");
231     run("Analyze Particles...", "size=8.00-Infinity show=Outlines clear summarize");
232     var happiness = newArray("Yes", "No");
233     Dialog.create("Result");
234     Dialog.addRadioButtonGroup("Are you happy with this result?", happiness, 2, 1, "Yes");
235     Dialog.show();
236     var Opinion = Dialog.getRadioButton();
237 }
238 //get the color threshold info for this channel and save it into a new variable
239 Dialog.create("Threshold input");
240 Dialog.addNumber("Lower", 0);
241 Dialog.addNumber("Upper", 255);
242 Dialog.show();
243 var lower = Dialog.getNumber();
244 var upper = Dialog.getNumber();
245 if (channelChoice == "Red") {
246     var lowerRed = lower;
247     var upperRed = upper;
248 }
249 else if (channelChoice == "Green") {
250     var lowerGreen = lower;
251     var upperGreen = upper;
252 }
253 else if (channelChoice == "Blue") {
254     var lowerBlue = lower;
255     var upperBlue = upper;
256 }
257 Dialog.create("Channel choice");
258 Dialog.addRadioButtonGroup("Move on to next image?", happiness, 2, 1, "Yes");
259 Dialog.show();
260 var channelChoice = Dialog.getRadioButton();
261 }
262 while (nImages>0) {
263     selectImage(nImages);
264     close();
265 }
266 if (miniRed == NaN){
267     print ("Green: B/C min - " + miniGreen + " B/C max - " + maxiGreen + " Thresh low - " + lowerGreen + " Thresh high - " + upperGreen);
268     print (miniBlue + " " + maxiBlue + " " + lowerBlue + " " + upperBlue);}
269 else if (miniGreen == NaN){
270     print (miniRed + " " + maxiRed + " " + lowerRed + " " + upperRed);

```

```

271     print (miniBlue + " " + maxiBlue + " " + lowerBlue + " " + upperBlue);
272 }
273 else if (miniBlue == NaN){
274     print (miniRed + " " + maxiRed + " " + lowerRed + " " + upperRed);
275     print (miniGreen + " " + maxiGreen + " " + lowerGreen + " " + upperGreen);
276 }
277 else if ((miniRed == NaN) & (miniGreen == NaN)){
278     print (miniBlue + " " + maxiBlue + " " + lowerBlue + " " + upperBlue);
279 }
280 else if ((miniGreen == NaN) & (miniBlue == NaN)){
281     print (miniRed + " " + maxiRed + " " + lowerRed + " " + upperRed);
282 }
283 else if ((miniRed == NaN) & (miniBlue == NaN)){
284     print (miniGreen + " " + maxiGreen + " " + lowerGreen + " " + upperGreen);
285 }
286 else {
287     print ("Red - B/C min: " + miniRed + " B/C max: " + maxiRed + " Thresh low: " + lowerRed + " Thresh high: " + upperRed);
288     print ("Green - B/C min: " + miniGreen + " B/C max: " + maxiGreen + " Thresh low: " + lowerGreen + " Thresh high: " + upperGreen);
289     print ("Blue - B/C min: " + miniBlue + " B/C max: " + maxiBlue + " Thresh low: " + lowerBlue + " Thresh high: " + upperBlue);
290 }
291
292 waitForUser("Open a new image");
293 Dialog.create("Test or new image?");
294 Dialog.addRadioButtonGroup("What kind of image is this?", Program, 2, 1, "New Image");
295 Dialog.show();
296 var ProgramChoice = Dialog.getRadioButton();
297 }
298
299
300 //ANALYSIS STAGE
301 while (ProgramChoice == "New Image"){
302     var Title = getTitle();
303     getDimensions(w, h, nChannels, s, f);
304
305     run("Z Project...", "projection=[Max Intensity]");
306     waitForUser("Create your selection");
307     setBackgroundColor(0, 0, 0);
308     run("Clear", "stack");
309     run("Split Channels");
310     var items = newArray();
311     for (i=1; i<=nImages; i++) {
312         selectImage(i);
313         items = Array.concat(items,getTitle());
314     }
315     Dialog.create("Choose image to work on");
316     Dialog.addRadioButtonGroup("Images open", items, nImages, 1, Title);
317     Dialog.show();
318     var ImageChoice = Dialog.getRadioButton();
319     selectWindow(ImageChoice);
320     var whichChannel = newArray("Red", "Green", "Blue");
321     Dialog.create("Which channel is it?");
322     Dialog.addRadioButtonGroup("Which channel is it?", whichChannel, 3, 1, "Red");
323     Dialog.show();
324     var channelChoice = Dialog.getRadioButton();
325     //set brightness/contrast + threshold from test image
326     if (channelChoice == "Red") {}
327         setMinAndMax(miniRed, maxiRed);
328         run("RGB Color");
329         //threshold
330         // Color Thresholder 2.0.0-rc-6/1.49b
331         // Autogenerated macro, single images only!
332         min=newArray(3);
333         max=newArray(3);
334         filter=newArray(3);
335         a=getTitle();
336         run("HSB Stack");
337         run("Convert Stack to Images");
338         selectWindow("Hue");
339         rename("0");
340         selectWindow("Saturation");
341         rename("1");
342         selectWindow("Brightness");
343         rename("2");
344         min[0]=0;
345         max[0]=255;
346         filter[0]="stop";
347         min[1]=0;
348         max[1]=255;
349         filter[1]="stop";
350         min[2]=lowerRed;
351         max[2]=upperRed;
352         filter[2]="pass";
353         for (i=0;i<3;i++){
354             selectWindow(""+i);
355             setThreshold(min[i], max[i]);
356             run("Convert to Mask");
357             if (filter[i]=="stop") run("Invert");
358         }
359         selectWindow(2);
360         rename(Title + " " + channelChoice);

```

```

361     }
362     else if (channelChoice == "Green") {
363         setMinAndMax(miniGreen, maxiGreen);
364         run("RGB Color");
365         //threshold
366         // Color Thresholder 2.0.0-rc-6/1.49b
367         // Autogenerated macro, single images only!
368         min=newArray(3);
369         max=newArray(3);
370         filter=newArray(3);
371         a=getTitle();
372         run("HSB Stack");
373         run("Convert Stack to Images");
374         selectWindow("Hue");
375         rename("0");
376         selectWindow("Saturation");
377         rename("1");
378         selectWindow("Brightness");
379         rename("2");
380         min[0]=0;
381         max[0]=255;
382         filter[0]="stop";
383         min[1]=0;
384         max[1]=255;
385         filter[1]="stop";
386         min[2]=lowerGreen;
387         max[2]=upperGreen;
388         filter[2]="pass";
389         for (i=0;i<3;i++){
390             selectWindow(""+i);
391             setThreshold(min[i], max[i]);
392             run("Convert to Mask");
393             if (filter[i]=="stop") run("Invert");
394         }
395         selectWindow(2);
396         rename(Title + " " + channelChoice);
397     }
398     else if (channelChoice == "Blue") {
399         setMinAndMax(miniBlue, maxiBlue);
400         run("RGB Color");
401         //threshold
402         // Color Thresholder 2.0.0-rc-6/1.49b
403         // Autogenerated macro, single images only!
404         min=newArray(3);
405         max=newArray(3);
406         filter=newArray(3);
407         a=getTitle();
408         run("HSB Stack");
409         run("Convert Stack to Images");
410         selectWindow("Hue");
411         rename("0");
412         selectWindow("Saturation");
413         rename("1");
414         selectWindow("Brightness");
415         rename("2");
416         min[0]=0;
417         max[0]=255;
418         filter[0]="stop";
419         min[1]=0;
420         max[1]=255;
421         filter[1]="stop";
422         min[2]=lowerBlue;
423         max[2]=upperBlue;
424         filter[2]="pass";
425         for (i=0;i<3;i++){
426             selectWindow(""+i);
427             setThreshold(min[i], max[i]);
428             run("Convert to Mask");
429             if (filter[i]=="stop") run("Invert");
430         }
431         selectWindow(2);
432         rename(Title + " " + channelChoice);
433     }
434     run("Analyze Particles...", "size=8.00-Infinity show=Outlines clear summarize");
435
436
437     //do you want to do another channel?
438     Dialog.create("Channel choice");
439     Dialog.addRadioButtonGroup("Do you want to do another channel?", happiness, 2, 1, "Yes");
440     Dialog.show();
441     var channelChoice = Dialog.getRadioButton();
442     while (channelChoice == "Yes") {
443         //start again and choose new channel
444         selectWindow (Title);
445         close("\Others");
446         //close color threshold windows and start again
447         run("Z Project...", "projection=[Max Intensity]");
448         run("Restore Selection");
449         setBackgroundColor(0, 0, 0);
450         run("Clear", "stack");

```

```

451     run("Split Channels");
452     var items = newArray();
453     for (i=1; i<=nImages; i++) {
454         selectImage(i);
455         items = Array.concat(items,getTitle());
456     }
457     Dialog.create("Choose image to work on");
458     Dialog.addRadioButtonGroup("Images open", items, nImages, 1, Title);
459     Dialog.show();
460     var ImageChoice = Dialog.getRadioButton();
461     selectWindow(ImageChoice);
462     var whichChannel = newArray("Red", "Green", "Blue");
463     Dialog.create("Which channel is it?");
464     Dialog.addRadioButtonGroup("Which channel is it?", whichChannel, 3, 1, "Red");
465     Dialog.show();
466     var channelChoice = Dialog.getRadioButton();
467     //set brightness/contrast + threshold from test image
468     if (channelChoice == "Red") {
469         setMinAndMax(miniRed, maxiRed);
470         run("RGB Color");
471         //threshold
472         // Color Thresholder 2.0.0-rc-6/1.49b
473         // Autogenerated macro, single images only!
474         min=newArray(3);
475         max=newArray(3);
476         filter=newArray(3);
477         a=getTitle();
478         run("HSB Stack");
479         run("Convert Stack to Images");
480         selectWindow("Hue");
481         rename("0");
482         selectWindow("Saturation");
483         rename("1");
484         selectWindow("Brightness");
485         rename("2");
486         min[0]=0;
487         max[0]=255;
488         filter[0]="stop";
489         min[1]=0;
490         max[1]=255;
491         filter[1]="stop";
492         min[2]=lowerRed;
493         max[2]=upperRed;
494         filter[2]="pass";
495         for (i=0;i<3;i++){
496             selectWindow(""+i);
497             setThreshold(min[i], max[i]);
498             run("Convert to Mask");
499             if (filter[i]=="stop") run("Invert");
500         }
501         selectWindow(2);
502         rename(Title + " " + channelChoice);
503     }
504     else if (channelChoice == "Green") {
505         setMinAndMax(miniGreen, maxiGreen);
506         run("RGB Color");
507         //threshold
508         // Color Thresholder 2.0.0-rc-6/1.49b
509         // Autogenerated macro, single images only!
510         min=newArray(3);
511         max=newArray(3);
512         filter=newArray(3);
513         a=getTitle();
514         run("HSB Stack");
515         run("Convert Stack to Images");
516         selectWindow("Hue");
517         rename("0");
518         selectWindow("Saturation");
519         rename("1");
520         selectWindow("Brightness");
521         var greenTitle = Title + "Green";
522         rename(2);
523         min[0]=0;
524         max[0]=255;
525         filter[0]="stop";
526         min[1]=0;
527         max[1]=255;
528         filter[1]="stop";
529         min[2]=lowerGreen;
530         max[2]=upperGreen;
531         filter[2]="pass";
532         for (i=0;i<3;i++){
533             selectWindow(""+i);
534             setThreshold(min[i], max[i]);
535             run("Convert to Mask");
536             if (filter[i]=="stop") run("Invert");
537         }
538         selectWindow(2);
539         rename(Title + " " + channelChoice);
540     }

```

```

541 else if (channelChoice == "Blue") {
542     setMinAndMax(miniBlue, maxiBlue);
543     run("RGB Color");
544     //threshold
545     // Color Thresholder 2.0.0-rc-6/1.49b
546     // Autogenerated macro, single images only!
547     min=newArray(3);
548     max=newArray(3);
549     filter=newArray(3);
550     a=getTitle();
551     run("HSB Stack");
552     run("Convert Stack to Images");
553     selectWindow("Hue");
554     rename("0");
555     selectWindow("Saturation");
556     rename("1");
557     selectWindow("Brightness");
558     rename(2);
559     min[0]=0;
560     max[0]=255;
561     filter[0]="stop";
562     min[1]=0;
563     max[1]=255;
564     filter[1]="stop";
565     min[2]=lowerBlue;
566     max[2]=upperBlue;
567     filter[2]="pass";
568     for (i=0;i<3;i++){
569         selectWindow(""+i);
570         setThreshold(min[i], max[i]);
571         run("Convert to Mask");
572         if (filter[i]=="stop") run("Invert");
573     }
574     selectWindow(2);
575     rename(Title + " " + channelChoice);
576 }
577 run("Analyze Particles...", "size=8.00-Infinity show=Outlines clear summarize");
578 Dialog.create("Channel choice");
579 Dialog.addRadioButtonGroup("Do you want to do another channel?", happiness, 2, 1, "Yes");
580 Dialog.show();
581 var channelChoice = Dialog.getRadioButton();
582 }
583 while (nImages>0) {
584     selectImage(nImages);
585     close();
586 }
587 waitForUser("Open a new image");
588 Dialog.create("Test or new image?");
589 Dialog.addRadioButtonGroup("What kind of image is this?", Program, 2, 1, "New Image");
590 Dialog.show();
591 var ProgramChoice = Dialog.getRadioButton();
592 }
593 }

```

Supplementary Video 1 and 2 on CD

Timelapse movie of an isolated erythroblastic island captured using Olympus CellR wide-field imaging system using 63x lens.

Excel files: Medium\_All Data and High\_All Data (on CD)

All repeated samples of proteomics under medium (Medium\_All Data) FDR stringency (<0.05) and high stringency (High\_All Data) (<0.01). A1 and B1 are D6 samples, C1 and D1 are T0 samples, E1 and F1 are T72 samples and G1, H1 and I1 are reticulocyte samples.